

HYDROLOGICAL BEHAVIOUR THROUGH EXPERIMENTAL AND MODELLING APPROACHES. APPLICATION TO THE HAUTE-MENTUE CATCHMENT

THÈSE N° 3007 (2004)

PRÉSENTÉE À LA FACULTÉ ENVIRONNEMENT NATUREL, ARCHITECTURAL ET CONSTRUIT

Hydrologie et aménagements

SECTION DES SCIENCES ET INGÉNIERIE DE L'ENVIRONNEMENT

ÉCOLE POLYTECHNIQUE FÉDÉRALE DE LAUSANNE

POUR L'OBTENTION DU GRADE DE DOCTEUR ÈS SCIENCES

PAR

Daniela BALIN

licence en géographie de l'Université Al.I.Cuza, Iasi, Roumanie
et de nationalité roumaine

acceptée sur proposition du jury:

Prof. A. Musy, directeur de thèse
Prof. K. Beven, rapporteur
Prof. E. Parent, rapporteur
Prof. R. Schlaepfer, rapporteur

Lausanne, EPFL
2004

ABSTRACT

The present work is related to the recent research topics in hydrology devoted to the integration of field knowledge into the hydrological modelling.

The study catchment is the Haute-Mentue experimental basin (12.5 km²) located in western Switzerland, in the Plateau region.

In order to complete the existing knowledge about the hydrological behaviour of the study catchment, a field experimental approach has been conducted at two scales: catchment (environmental tracing) and local scale (TDR soil moisture measurements). The environmental tracing application has led to the same conclusion as previous researches: hydrological behaviour is strongly influenced by the catchment antecedent conditions and by the rainfall duration and intensity. The geology characteristics (moraine or molasse) explain the main differences in the hydrological behaviour that have been observed so far. As the environmental tracing does not allow easy identification of the mechanisms responsible for the runoff generation, TDR equipments have been installed on two hillslopes with different geological characteristics, which allowed monitoring of the soil moisture at different depths along the hillslope during two intensive campaigns in 2002 and 2003. Association of the environmental tracing and TDR technique has finally allowed precisising the conceptual model of two head sub-catchments of the Haute-Mentue catchment.

The second part of the research is devoted to the hydrological modelling. A simple conceptual model (TOPMODEL) has been considered as an appropriate representation of the hydrological processes on the Haute-Mentue catchment. In order to estimate TOPMODEL parameters and to take into account uncertainty associated with estimated parameters and model output, a Bayesian approach has been proposed and two Bayesian techniques have been compared: GLUE (Generalized Likelihood Uncertainty Estimation) and MCMC (Monte Carlo Markov Chains). The role of the statistical corrections on the resulting parameters and model output uncertainty has been assessed. In the last part of the present research, the Bayesian methodology has been extended to the case of multi-response calibration. Previous field acquired knowledge (i.e. soil storage saturation deficit, stream water silica and calcium concentrations) has been used to constrain parametrization of the classical and of a modified version of TOPMODEL. In both cases, multi-calibration led to trade-off behaviour of the efficiencies of the simulated responses. The total modelling uncertainty of the new introduced responses was considerably reduced at the expense of an increase in the total modelling uncertainty of the simulated discharges.

Key words: hydrological processes, TOPMODEL, Bayesian parameter estimation, uncertainty, multi-response calibration, GLUE, MCMC

RESUME

Cette étude s'inscrit dans le contexte des recherches actuelles en hydrologie qui visent à intégrer les connaissances acquises par l'approche expérimentale dans la modélisation hydrologique.

Le bassin-versant de la Haute-Mentue (12.5 km²), situé à l'ouest de la Suisse, dans la région du Plateau, constitue le terrain d'étude.

Afin de compléter les connaissances sur le comportement hydrologique de la région d'étude, une approche expérimentale a été menée à deux échelles: celle du bassin-versant (traçage environnemental) et celle du versant (mesures de teneur en eau par TDR). L'application du traçage environnemental a confirmé les résultats obtenus par les recherches précédentes: le comportement hydrologique est fortement influencé par les conditions antécédentes et par l'intensité et la durée de la pluie. Les particularités géologiques (moraine ou molasse) expliquent les principales différences du comportement hydrologique des sous-bassins versants de la Haute-Mentue. Le traçage environnemental ne permet pas une identification directe des mécanismes responsables de la génération des crues. Dans ce contexte, des équipements TDR ont été installés sur deux sites ayant des caractéristiques géologiques différentes ce qui a permis un suivi temporel de l'humidité des sols à plusieurs profondeurs durant 2 campagnes de terrain intensives en 2002 et 2003. L'association des deux techniques (traçage environnemental et TDR) a contribué à une meilleure représentation du modèle conceptuel de deux sous-bassins versants de la Haute-Mentue.

La deuxième partie de ce travail a été destinée à la modélisation hydrologique. Un modèle conceptuel simple (TOPMODEL) a été considéré comme une représentation appropriée des principaux processus hydrologiques identifiés pour le bassin-versant de la Haute-Mentue. Une approche Bayésienne a été proposée pour estimer les paramètres de TOPMODEL et quantifier l'incertitude des paramètres et celle des résultats du modèle. Deux techniques bayésiennes ont été comparées: GLUE (Generalized Likelihood Uncertainty Estimation) et MCMC (Monte Carlo Markov Chains). Le rôle des corrections statistiques sur l'incertitude des paramètres et des résultats du modèle a été étudié. Dans la dernière partie de cette recherche, la méthodologie bayésienne a été appliquée pour le cas de la calibration multi-réponse. Les données de terrain acquises précédemment (i.e. déficit à saturation des sols, concentration en calcium et silice de l'écoulement) ont été utilisées pour réduire les paramétrisations de deux versions de TOPMODEL. Dans les deux cas, la procédure multi-calibration a mis en évidence un compromis entre les efficacités des réponses simulées. L'incertitude des nouvelles réponses introduites dans la calibration a été considérablement réduite aux dépens d'une incertitude plus grande des débits simulés.

Mots-clés: processus hydrologiques, TOPMODEL, estimation des paramètres, approche Bayésienne, incertitude, calibration multi-réponses, GLUE, MCMC

ACKNOWLEDGMENTS

I would like to sincerely thank PROFESSOR André MUSY for having accepted me in his “LABORATORY”, for the confidence, all the technical support, the humanity he showed me all these years long and for having invited in his institution the right professors at the right time!

I am particularly grateful to Prof. Eric PARENT for the precious “green notebook” which contains notes about the Bayesian theory that he taught me with such a great passion and pedagogical talent.

I thank Prof. Keith BEVEN for the attention and advice he gave me in the beginning and for the valuable comments at the end of my work.

I also thank all the members of the jury: Prof. Mermoud, Prof Musy, Prof. Beven, Prof. Parent, Prof. Schlaepfer, who read the thesis report and expressed their useful opinions and comments.

I thank Prof. Andras Bardossy for having helped me in the beginning of the thesis to start with the Bayesian approach.

This thesis was supported by the Swiss National Foundation (project ESPACE), and EPFL, which are kindly thanked here.

Before going any further I must thank, Christophe Joerin for his helping “hands” all these years, for having opened my eyes to this small but so cheered by him “Haute-Mentue” catchment, for all the discussions we had about this endless topic “where the Mentue water comes from?”. I thank him as well for having read and corrected the draft dissertation. Speaking of Haute-Mentue catchment, I want to thank Ion Iorgulescu for having read and corrected my manuscript and for his precious comments and suggestions especially at the end of my thesis.

Many thanks to my “field” colleagues without whom this work would have been impossible to accomplish:

- Alex Amiguet for his practical advice and his field experience from which I benefited so much,
- Bernard Sperandio for his kindness, seriousness and for being available when I needed,
- Elena Rossel and Karine Vernez-Thomas for their precious collaboration,
- François Etter for his love of the Haute-Mentue and for everything I learned from him from the professional and personal points of view,
- and of course, Mario Fazzoletti.

I want to thank Siham Karaoui for her technical and scientific collaboration, her courage and her enthusiasm.

A thought of gratefulness goes out to my former or present colleagues who studied with me at the post-graduate level:

- to Stéphane who took the time to explain some of the insights of the engineering hydrology, to show me those little but so useful tricks of the MSOffice, and who encouraged me to progress with my thesis even before it began,
- to Dominique, to whom I certainly took several weeks from his thesis time to discuss on different ecological or political world affairs,
- to John, who found time on his so busy personal and professional agenda to help me and to answer to my questions...

Three years might seem to be a long period but it finally seemed so short because of such a great HYDRAM team and the family atmosphere built by its former and current players: Cécile, Benoît, Markus, Colin, Séverine, Christophe “the modeller”, Cathy, Gorana, Bettina, Richard, Kirsten, Flavio, Eric, Anne, Imed, Frédérique, Alain, Alexandre, Christine, Marc, Abdel, Yasser, Nassima, Gilles, Danrong, Jacques, Faten, Roland, Nicolas, Pierre-André, Jean-Marc, Konrad....and, I will also mention here Liliana, Marius and of course Natalya.

Thanks go out to Michèle and Marie for having encouraged me when I needed it, for their understanding, their warming words and their professionalism!

And now, as everyone imagines, from the beginning until the end, this work would have not been possible without the huge helping hand of Jean, to whom I am sincerely grateful - my husband, my home, field and scientific collaborator, my technical advisor, my trainer, and my support through the difficult moments!

I am grateful to my family in Focsani / Romania, to my mother, my father, and my sister and to my newer family in Maramures / Romania for having accepted my professional choices, away from home, meaning so few hours spent together and for all their encouragements. I am also grateful to my Lausanne “family”, represented by Fam. Moldovan, Fam. Cosinschi, Fam. Petrescu, Fam. Jimenez, Fam. Styger who helped and encouraged me constantly in good and in difficult moments.

Last but not least, I want to thank Professor Sergiu Arfire from Focsani / Romania, who was the initial instigator behind my studies, and all my professors and further colleagues at the Geography Faculty of the “Al.I.Cuza” University, Iasi / Romania and particularly, Professor Emeritus Ion Harjoaba who oriented me towards hydrology.

Lausanne, Switzerland,

May, 2004

Hydrological behaviour through experimental and modelling approaches. Application to the Haute-Mentue catchment

Table of Contents

Abstract.....	i
Résumé.....	ii
Acknowledgments.....	iii

1. Introduction

1.1. Objective and context of the research.....	1
1.2. State of art: hydrological processes and corresponding mechanisms involved in runoff generation.....	1
1.3. State of art: Hydrological modelling (hydrological models, model calibration, uncertainty).....	4
1.4. Research presentation.....	6
1.5. References.....	8

2. Presentation of the Haute-Mentue catchment

2.1 Geographical localization.....	12
2.2 Physical characteristics.....	12
2.2.1 Geology.....	13
2.2.2 Morphology.....	19
2.2.3 Pedology.....	20
2.2.4 Vegetation and Land use.....	23
2.2.5 Climatology.....	24
2.3 Catchment instrumentation.....	26
2.4 References.....	29

3. Study of hydrological behaviour through experimental approaches

3.1. Hydrological behaviour at the catchment scale.....	32
3.1.1 Hydrograph analysis.....	32

3.1.2 Environmental tracing.....	39
3.2. Hydrological behaviour at the hillslope scale.....	52
3.2.1. Time Domain Reflectometry (TDR) principles.....	52
3.2.2. Implementation of a TDR system on the Haute-Mentue catchment- field sites description.....	55
3.2.3. Soil moisture temporal variability.....	58
3.2.4. Soil water regime.....	63
3.3. Synthesis of the hydrological processes and conceptual model for the Haute-Mentue catchment.....	76
3.4. References.....	82

4. Hydrological modelling

4.1. Conceptual rainfall-runoff models.....	86
4.1.1 Topmodel concepts.....	86
4.1.1 Modified version of Topmodel in order to include shallow storm flow.....	89
4.2. Parameter estimation: the case of single-response calibration.....	91
4.2.1 The bayesian method (likelihood formulation, prior and posterior distribution)...	92
4.2.2 GLUE (Generalized Likelihood Uncertainty Estimation) methodology.....	95
4.2.3 Monte Carlo Markov Chain (MCMC) methods.....	98
4.3. Conclusions.....	110
4.4. References.....	111

5. Integrating additional information in conceptual rainfall-runoff modelling

5.1. Augmenting information in conceptual hydrological models; internal variables.....	116
5.1.1 Local saturation deficit as an internal variable: field estimation and TOPMODEL concept.....	117
5.1.2 Linking hydrological models with water quality models; use of chemical information as soft data to constrain a hydrological model- brief review.....	120
5.2. Parameter estimation: the case of multi-response calibration.....	122
5.2.1 The bayesian method (likelihood formulation, prior and posterior distribution).	123
5.2.2 GLUE (Generalized Likelihood Uncertainty Estimation) methodology.....	124
5.2.3 MCMC -Monte Carlo Markov Chain methods.....	125
5.3. Multi-response calibration of the Haute-Mentue catchment with GLUE and MCMC Bayesian approaches.....	129
5.3.1 Integrating catchment saturation deficit field estimates in rainfall-runoff modelling: classical version of TOPMODEL.....	130
5.3.2 Integrating tracing information in rainfall-runoff modelling: modified version of TOPMODEL.....	148
5.4. Conclusions.....	160
5.5. References.....	161

6. Conclusions and perspectives.....165

7. Annexes	175
Annex I – Haute-Mentue catchment topographical map and permanent equipment.....	176
Annex II – Mineral soils conditioned by limited age: Cambisoils.....	177
Annex III – Haute –Mentue Catchment (photos: examples of preferential flow).....	180
Annex IV – CODEAU – hydrological data treatment computer program.....	181
Annex Va – LABVIEW implementation of TOPMODEL.....	182
Annex Vb – LABVIEW implementation of GLUE methodology.....	183
Annex Vc – LABVIEW implementation of MCMC methodology.....	184
Annex Vd – LABVIEW implementation of GLUE multi-calibrating methodology.....	185
Annex VI – MCMC methodology with L1 statistical likelihood function.....	186
Annex VII – MCMC methodology with L2 statistical likelihood function.....	187
Annex VIII – MCMC methodology with L3 statistical likelihood function.....	188
Annex IXa – Ruzillon catchment: Single and 3-response calibrating methodology with L3 statistical likelihood function.....	189
Annex IXb – Esserts catchment: Single and 3-response calibrating methodology with L3 statistical likelihood function.....	190
 Curriculum Vitae	 191
Publications	192

1. Introduction

1.1 Objectives and context of the research

The present study is in line with the last years' researches at the Hydrology and Land Improvement Laboratory from Swiss Federal Institute of Technology (Lausanne-Switzerland) concerning the modelling of the hydrological behaviour of the Haute-Mentue, a small catchment in the Swiss Plateau.

In a more general context, this work intends to insert itself in the frame of the hydrological studies which try to take advantage of the advances acquired in the experimental field and to integrate this knowledge into the hydrological modelling in order to get not only a close representation of the modelled time series but also a better one of the hydrological processes involved in the runoff generation.

The main objectives of this work are:

- ❑ Identification of the main hydrological processes responsible for runoff generation on the Haute-Mentue catchment using a field experimental approach;
- ❑ Development of a Bayesian methodology to integrate the above field experimental knowledge into the hydrological modelling;

1.2 State of art: hydrological processes and correspondent mechanisms involved in runoff generation

Hydrological processes have been intensively studied the last decades and important progresses have been done in understanding the catchment hydrological behaviour. Many experiments have been carried out on a large variety of catchments in the whole world. Intensive point, hillslope and catchment monitoring and coupling with environmental and dye tracing have allowed progresses in understanding the main factors controlling the hydrological response.

A brief review of the most important hydrological processes exists in many literature references (see further references in the text below). For the Haute-Mentue catchment, reviews of the same topic can be found by Jordan (1992), Iorgulescu (1997) and Joerin (2000).

The first important theory concerning this subject appeared in the beginning of the last century with the works of Horton (1933) which considered the flood hydrograph is formed essentially by the “infiltration excess surface runoff”. This would have been possible as the rainfall intensities exceeded the soil infiltration capacity, a space constant catchment characteristic. Infiltration would occur when the rainfall intensities would be smaller than the soil infiltration capacity, which would allow recharge of the deep groundwater. Since this theory, many other mechanisms have been proposed to explain the flood hydrographs.

Dunne (1978) considered that the subsurface flow is an important component of the flood hydrograph. In his concept, the overland flow occurs when the rainfall new water falls on surfaces that have already reached saturation conditions (i.e. groundwater rise at the ground surface). In these conditions, exfiltration of the groundwater (“return flow”) occurs and a mixing between new and old water forms the “saturation overland flow”.

As the hydrological scientific community realized that the subsurface flow is an important component of the flood hydrograph, several studies in the years 70's accorded attention to this subject in order to identify different mechanisms responsible for the subsurface flow generation. A distinction is generally made to separate between a superficial (or shallow) subsurface flow and a deep subsurface flow. In order to explain the rapid contribution of the subsurface flow to the stream several preferential mechanisms have been proposed such as: macropores and structural cracks networks that provide preferential paths through which water may be rapidly transmitted (Beven and Germann (1982)); lateral flow at the soil horizons textural discordances or the soil/bedrock interface. Two kinds of lateral flow have been described in the scientific literature:

- The classical one has been called “throughflow” (Kirkby and Chorley (1967)), interflow” (Betson et al. (1968)), subsurface storm flow etc, and this can occur where the upper soil horizons are underlain by an impermeable soil layer. In this case the lateral soil conductivity is much more important than the horizontal one and this causes infiltrated water to flow laterally at the impermeable-permeable interface.
- The second type of lateral flow has been long time ignored and is now commonly referred to as funnelled flow (Kung (1990)). Funnelled flow is a category of flow phenomena referring to the situation in which a capillary barrier develops above a coarse layer which underlies a relatively fine texture (Walter et al. (2000)).

Rapid recharge of the groundwater has been also explained by the presence of:

- vertical macropores and cracks that support rapid transport of the water to the groundwater table,
- finger phenomena that are produced by the wetting-front instability.
- another mechanism that has been proposed by Hewlett and Hibbert (1967) considered that the deep subsurface flow could feed the stream water during the floods by the intermediate of a “piston-flow” that generates a “translatory flow”; during the rainfall event, the hillslope would receive a pressure wave that would push the deep water component before even that the rain new water reach it.
- Sklash and Farvolden (1979) proposed a new mechanisms to explain the deep flow component called “groundwater ridging” which consider that as the saturation deficit

in regions closed to the stream are smaller than on the hillslopes, this determines higher hydraulic gradients near the stream and thus delivers easily groundwater to the stream.

One concept that was considered as a real revolution in the field of hydrology was those of variable contributing area developed in the years '65 by Hewlett and Hibbert (1967), which observed no overland flow coming from the whole Coweeta catchment in USA. They proposed the concept of variable contributive area to explain the observed hydrograph, meaning that the catchment area contributing to the streamflow changes temporally during a rainfall event. Dunne and Black (1970) and Dunne and Black (1970) reported that extension or shrinking of the contributing areas are determined by several factors such as the antecedent soil moisture and the rainfall characteristics.

In order to achieve this knowledge, a variety of experimental techniques have been used by the hydrological scientific community. Environmental tracing is one of the most employed techniques that was used in different parts of the world in order to identify the main flood components participating to the floods. Tracers have proven to be a powerful tool in hydrologic research and the use of tracers has been one of the most productive in terms of providing new insight to hydrologic processes. Stable isotopes of oxygen and hydrogen have been used extensively in hydrologic investigations in order to determine residence times and streamflow generation processes (Fritz et al. (1976), Sklash et al. (1976), Kennedy et al. (1986), Rodhe (1984), Lindström and Rodhe (1986), Pearce et al. (1986), Sklash et al. (1986), Turner et al. (1987)). On the Haute-Mentue catchment, oxygen-18 has been used in the years '80 and beginning of '90 in order to investigate the contribution of old and new waters to the flood generation (Jordan (1992), Iorgulescu (1997)). The use of the water isotopes is limited as it allows essentially identification of the temporal origin of the water (new water and pre-existing or old water) but it doesn't easily allow identification of the geographical pathways that the water takes in order to reach the streams. That is why, later, the water isotopes have been combined with other natural tracers such as silica, chloride (Neal et al. (1988)), bromide or other physical and chemical characteristics (e.g. temperature, specific conductance and alkalinity) in order to better precise the hydrological processes responsible for the runoff generation (Hooper et al. (1990), Christophersen et al. (1990)). Concerning the use of the environmental tracing, it should be mentioned that the assumptions that have been validated for one environment might not be applicable to another environment (Peters (1994)). A brief review of the main achievements obtained using the environmental tracing applied at the scale of the Haute Mentue catchment as a case study is given in Iorgulescu (1997). For the Haute-Mentue catchment, calcium and silica have been applied in order to perform hydrograph separation and to identify the main flow pathways during the rainfall-runoff events (Iorgulescu (1997) and Joerin (2000)).

Nevertheless the application of environmental tracing doesn't allow the identification of the mechanisms responsible for flows through hill slopes (Elsenbeer and Lack (1996)). In order to identify both runoff generation mechanisms and water pathways during flood events it is suitable to combine hydro-chemical approach with other types of measurements (Jenkins et al. (1995)). The same conclusion has been evidenced by Joerin (2000) which has associated environmental tracing and some other local techniques (rainfall simulator, TDR, dye tracing) in order to build the conceptual model of a small Swiss catchment.

Nowadays, an important theoretical and practical knowledge has been accumulated concerning the main mechanisms and the hydrological processes within the catchment, thus integration of this kind of experimental information during the hydrological modelling could be very useful in the modelling approach.

Instead of the fact that this approach may seem very promising for the improvement of the hydrological models, in practice there are few attempts to use the experimental results in the hydrological modelling. Indeed, there are few publications on this subject, which insist rather on the validation of hydrological models by using the environmental tracing (Robson et al. (1992), Lamb et al. (1998), Guntner et al. (1999), Seibert and McDonnell (2002)).

Hence, among the present challenges in hydrology, one is those of including all the available field information in the hydrological modelling in order to get better simulation results and to reduce model and parameter uncertainty.

1.3 State of art: Hydrological modelling (hydrological models, model calibration, uncertainty)

In hydrological modelling, conceptual (i) and physically based (ii) hydrological models are used.

(i) Conceptual models use generally semi-empirical equations that have a physical basis. Their model parameters could not be estimated from field data alone but they have to be calibrated (Refsgaard and Storm (1996)). Different kinds of conceptual models have been used through the world, the most known being: Sacramento model in USA, the Tank model used in Japan, the HBV model used in Scandinavian countries or TOPMODEL (Beven and Kirkby (1979)) developed in England.

(ii) A physically based hydrological model may be defined as a model, which uses physical laws and equations to describe the hydrological processes. In the same context of the physical laws describing hydrological processes and in order to simplify resolution of too complex physical equations, one can work with simpler hypothesis and then we can speak of semi-physical hydrological models. One example in that sense is TOPMODEL while a fully physically based hydrological model is represented by SHETRAN (Abbot et al. (1986)).

Another classification is based on, in one hand, lumped models and in other hand, distributed models upon the consideration or not of the spatial variability of the input data or of the geometrical characteristics of a catchment. Between these two categories, semi-distributed models (such as TOPMODEL) take into account the spatial variability by the intermediate of similar classes of hydrological behaviour.

Refsgaard and Storm (1996) divide the hydrological models into three categories: empirical models; lumped, conceptual models and distributed physically based models.

Models calibration and uncertainty

Calibration means adjustment of the model parameters such as the difference between the observed and the simulated responses be as small as possible. This could be done manually (trial and error method) or automatically by searching an optimal value of a given criterion (often called objective function), which describes the fit between observed and simulated data. Different methods exist to search for this optimal value: direct search methods such as Rosenbrock optimisation method (Rosenbrock (1960)), Simplex method (Nelder and Mead (1965)). These methods found rapidly their limits as often, the surface response of the parameters are multi modal with many local optima. Complex searching methods have thus been developed in the idea of finding the global optimum. The most used is the Shuffled

Complex Evolution (SCE-UA) algorithm, a combination of simplex and genetic algorithms (Duan et al. (1992)). Recently, another global optimisation algorithm gained importance i.e. simulated annealing whose principle comes from the physical processes of heating and cooling of a solid. In the years '90, Beven (1993) introduced the notion of equifinality to express the fact that there is not only one single set of parameters that lead to an optimum but several sets of parameters lead to equivalent performances. Since that, the uncertainty associated with the estimated model parameters became a very important issue in order to assess the accuracy of a given parameter set. For operational purposes, the uncertainty became very important to assess the accuracy of the model-simulated outputs. The calibration of the hydrological modelling became often associated with the uncertainty.

Refsgaard and Storm (1996) consider that there are four main sources of uncertainty coming from:

- ❑ random or systematic errors in input data (i.e. precipitation, temperature)
- ❑ random or systematic errors in the recorded data (water level records, raining curves and discharge data, groundwater levels, soil moisture levels);
- ❑ errors due to non-optimal parameters values;
- ❑ errors due to the non-optimal model structure.

In order to account for the uncertainty associated with model parameters and model outputs different statistical methods have been used. The most well known are Monte Carlo methods and the Bayesian methods such as GLUE (Generalized Likelihood Uncertainty Estimation) and MCMC (Monte-Carlo Markov Chains). The principles of these methods are largely presented in chapter IV.

The parameterisation of the hydrological processes in order to assess the model uncertainty is the present great challenge in the hydrological modelling. If parameterisation of the simple conceptual hydrological models was done using essentially different optimisation algorithms and Monte Carlo techniques, parameterisation of the physically based hydrological models still encounters many difficulties due to their complexity and their great number of parameters. Theoretically, all the parameters in the physically based hydrological models can be measured on field. Hence, the problem that arises is the representativity of field data given their spatial and temporal variability. Another problem related to this subject concerns the scale and how to bridge the gap between plot scale and model scale. Using additional data in hydrological modelling was rather seldom considered in order to reduce uncertainties of the results. This approach was adopted for simpler models by using a Monte Carlo approach within a Bayesian framework (Lamb et al. (1997)). The Monte Carlo approach is difficult when considering the physically based hydrological models because of the large number of parameters involved and because of the great amount of computing time and only few researches were carried out in that sense. There are few alternatives concerning parameterisation of the physically based hydrological models and in general these consider sensitivity analysis rather than parameter estimation. Even less work was done when considering the uncertainty of the output of the physically based hydrological models. The works of Ewen and Parkin (1996) are to be mentioned in this context. They proposed defining the mean, the outer and lower bounds of some of the most important input parameters and after that, they run the models several times and superposed the total output results choosing the upper and the lower bounds of the simulations ensemble as being a quantification of the uncertainty. Christiaens and Feyen (1999) and Soutter (1996) used a Latin Hypercube Simulation approach in order to make

sensitivity and uncertainty analysis of a complex physically based hydrological model. The results of a multi-site parameter estimation technique (Iorgulescu (1997)) as an application of the “conjunction of information states” Bayesian theory (Tarantola (1987)), may open interesting perspectives for parameter estimation for complex physically based hydrological models.

In this context, in which the uncertainty became such an important issue of the hydrological modelling, the ways to reduce the uncertainty of the output simulations became an important research topic in hydrology. Further more, it seems now like we are crossing a decisive period in hydrological modeling where there is not sufficient anymore to consider the catchment as a black box whose main role be to reproduce more or less correctly the discharge at the outlet. Where the water comes from and which are the main pathways that the water takes until reaching the stream become questions to be answered at least as much important as the question of well reproducing the discharge at the outlet.

The present work deals with these two topics: how to reduce model prediction uncertainty and how to make use of the field knowledge in order to ensure that calibrated parameters don't only reproduce discharge adequately during calibration periods but are also able to do so for validation periods or are able to reproduce other internal fluxes as well. A Bayesian methodology has been proposed in order to reach these objectives.

1.4 Research content presentation

The present work tries to link experimental and modelling approaches in order to improve both model predictions and their confidence. The experimental results helped confirm and improve some of the conceptual models concerning the hydrological behaviour of the Haute-Mentue subcatchments. At the same time, field data contributed to reduce model predictions uncertainty as well as estimated parameter uncertainty.

Chapter 2 introduces briefly the Haute-Mentue catchment in terms of geographical localization, geological and geomorphological conditions, land use and climatic environment. The catchment's regular and new installed instrumentation for appropriate experiments is presented.

Chapter 3 is presenting the study of the hydrological behaviour of the Haute-Mentue catchment through an experimental approach. This experimental approach has been initiated since the 90's with the aim the improvement of understanding of the hydrological processes responsible for the floods generation. After the model of Joerin (2000), this work evidences the importance of associating field measurements at different scales for the understanding of the catchments' hydrological behaviour. The results of two intensive field campaigns of environmental tracing are presented together with those given by local soil moisture measurements.

Chapter 4 is devoted to the hydrological modelling and introduces the main concepts related to the Bayesian calibration of a simple, semi-distributed conceptual model (TOPMODEL). Classical and modified versions of TOPMODEL are presented and two Bayesian techniques (GLUE and Monte Carlo Markov Chains) to estimate model parameters are introduced and compared.

Chapter 5 explores the ability of the modified version of TOPMODEL to simulate several hydrological responses in the same time. Experimental data such as soil moisture saturation deficit (estimated from TDR local measurements) and discharge calcium and silica concentrations are used to constrain uncertainty of both TOPMODEL estimated parameters and simulated outputs. In order to constrain model predictions uncertainty two Bayesian “multi-response” calibrating methodologies (GLUE and Monte Carlo Markov Chains) are presented and the results compared.

The conclusion and the main perspectives of the present work are presented in **Chapter 6** and the annexes are grouped together in **Chapter 7**.

An overview of the present research is presented in *Figure 1-1*.

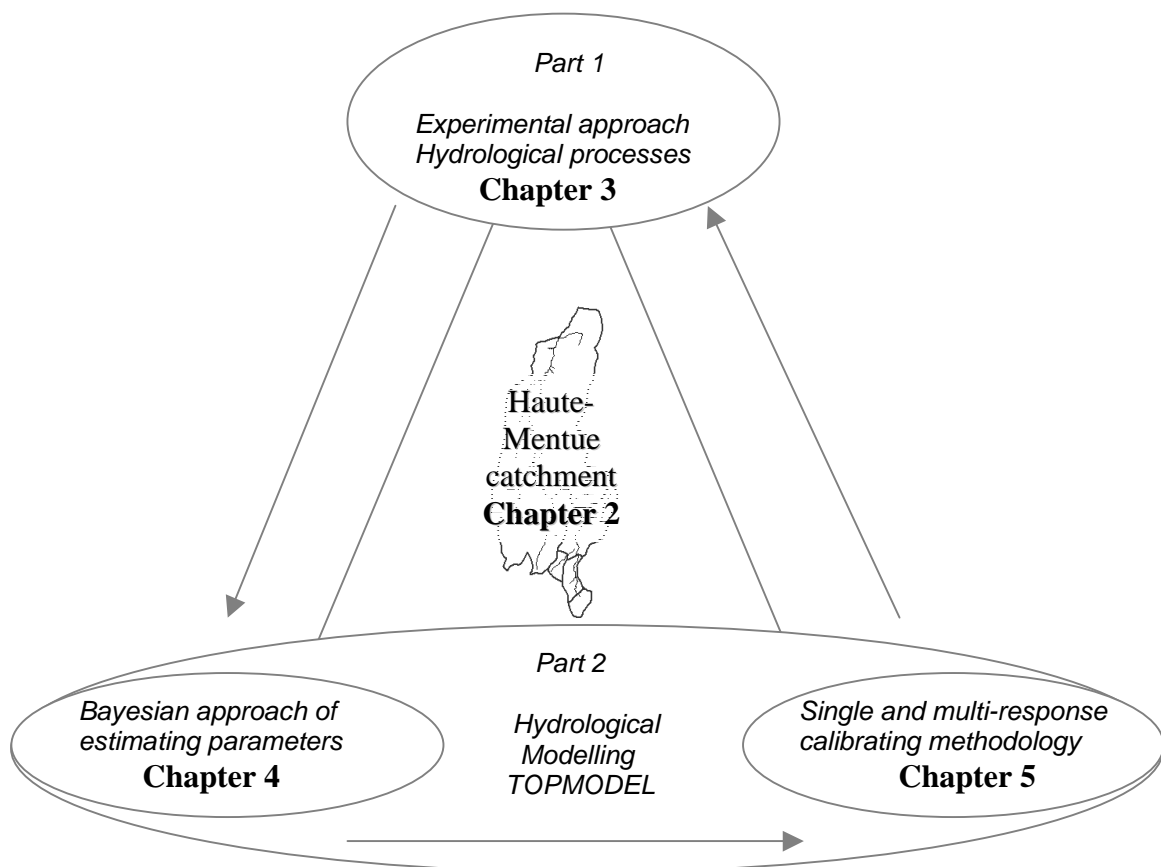


Figure 1-1 Schematic overview of the present research structure

Key words: hydrological processes, TOPMODEL, Bayesian parameter estimation, uncertainty, multi-response calibration, GLUE, Monte Carlo Markov Chain

1.5 References

- Abbot, M. B., J. C. Bathurst, J. A. Cunge, P. E. O'Connell and J. Rasmussen (1986). "An introduction to the European Hydrological System-Système Hydrologiques Européen, "SHE", 1. History and philosophy of a physically based modelling system; 2. Structure of a physically based distributed modelling system." *Journal of Hydrology* 87: 45-77.
- Betson, R. P., J. P. Marius and R. T. Joyce (1968). "Detection of saturated interflow in soils with piezometers." *Soil Sci. Soc. Am. Proc.* 32: 602-604.
- Beven, K. and M. J. Kirkby (1979). "A physically based variable contributing area model of basin hydrology." *Hydrol.Sci.Bull.* 24(1): 43-69.
- Beven, K. J. (1993). "Prophecy, reality and uncertainty in distributed hydrological modelling." *Advances in Water Ressources* 16: 41-51.
- Beven, K. J. and P. Germann (1982). "Macropores and water flow in soils." *Water Resources Research* 18: 1311-1325.
- Christophersen, N., C. Neal, R. P. Hooper, R. D. Vogt and S. Andersen (1990). "Modelling streamwater chemistry as a mixture of soilwater end-members- A step towards second-generation acidification models." *Journal of Hydrology* 116(1-4): 307-320.
- Duan, Q. Y., S. Sorooshian and V. K. Gupta (1992). "Effective and efficient global optimization for conceptual rainfall-runoff models." *Water Resources Research* 28(4): 1015-1031.
- Dunne, T. (1978). "Field studies of hillslope flow processes". *Hillslope hydrology*. M. J. Kirkby. New York, Wiley: 227-293.
- Dunne, T. and R. D. Black (1970). "An experimental investigation of runoff prediction in permeable soils." *Water Resources Research* 6: 478-490.
- Dunne, T. and R. D. Black (1970). "Partial areas contributions to storm runoff in a small New England watershed." *Water Resources Research* 6(5): 1296-1311.
- Elsenbeer, H. and A. Lack (1996). "Hydrometric and hydrochemical evidence for fast flowpaths at La Cuenca, Western Amazonia." *Journal of Hydrology* 180(1-4): 237-250.
- Fritz, P., J. A. Cherry, K. V. Weyer and M. G. Sklash (1976). "Runoff analysis using environmental isotope and major ions". *Interpretation of Environmental Isotope and Hydrochemical Data in Groundwater Hydrology*. Vienna, IAEA: 111-130.
- Guntner, A., S. Uhlenbrook, J. Seibert and C. Leibundgut (1999). "Multi-criterial validation of TOPMODEL in a mountainous catchment." *Hydrological Processes* 13(11): 1603-1620.
- Hewlett, J. D. and A. R. Hibbert (1967). "Factors affecting the response of small watersheds to precipitation in humid areas". *International Symposium on Forest Hydrology*, Oxford, Pergamon.
- Hooper, R. P., N. Christophersen and N. E. Peters (1990). "Modeling streamwater chemistry as a mixture of soilwater end-members-An application to Panola Mountain catchment, Georgia, USA." *Journal of Hydrology* 116(1-4): 321-343.
- Horton, R. E. (1933). "The role of infiltration in the hydrologic cycle." *Trans. of Am. Geophys. Union* 14: 446-460.
- Iorgulescu, I. (1997). "Analyse du comportement hydrologique par une approche intégrée à l'échelle du bassin versant. Application au bassin versant de la Haute-Mentue." Thesis EPFL, No.1613. Lausanne.
- Jenkins, A., W. T. Sloan and B. J. Cosby (1995). "Stream chemistry in the middle hills and high mountains of the Himalayas, Nepal." *Journal of Hydrology* 166(1-2): 61-79.

- Joerin, C. (2000). *"Etude des processus hydrologiques par l'application du traçage environnemental. Association à des mesures effectuées à l'échelle locale et analyse d'incertitude"*. Thesis EPFL, No.2165. Lausanne.
- Jordan, J. P. (1992). *"Identification et modélisation des processus de génération des crues; Application au bassin-versant de la Haute-Mentue"*. Thesis No.1014, EPFL. Lausanne.
- Kennedy, V. C., C. Kendall, G. W. Zellweger, T. A. Wynman and R. J. Avanzino (1986). *"Determination of the components of stormflow using water chemistry and environmental isotopes, Mat tole River basin, California."* Journal of Hydrology 84: 107-140.
- Kirkby, M. J. and R. J. Chorley (1967). *"Throughflow, overland flow and erosion."* Bull.Int.Assoc.Sci.Hydrol 12: 5-21.
- Kung, K. J. S. (1990). *"Preferential flow in a sandy vadoze zone, 2, Mechanisms and implications."* Geoderma 46: 59-71.
- Lamb, R., K. Beven and S. Myrabo (1997). *"Discharge and water table predictions using a generalized TOPMODEL formulation."* Hydrological Processes 11(9): 1145-1167.
- Lamb, R., K. Beven and S. Myrabo (1998). *"Use of spatially distributed water table observations to constrain uncertainty in a rainfall-runoff model."* Advances in Water Ressources 22(4): 305-317.
- Lindström, G. and A. Rodhe (1986). *"Modelling water exchange and transit times in till basins using oxygen-18."* Nordic Hydrology 17(4/5): 325-334.
- Neal, C., N. Christophersen, R. Neale, C. J. Smith, P. G. Whitehead and R. Reynolds (1988). *"Chloride in precipitation and stream water for the upland catchment of the River Severn, mid Wales; some consequences for hydrochemical models."* Hydrological Processes 2: 155-165.
- Nelder, J. A. and R. Mead (1965). *"A simplex method for function minimization."* The Computer Journal 7: 308-313.
- Pearce, A. J., M. K. Stewart and M. G. Sklash (1986). *"Storm runoff generation in humid catchments-1. Where does the water come from?"* Water Resources Research 22: 1263-1272.
- Peters, N. E. (1994). *"Hydrologic studies"*. Biogeochemistry of small catchments, A tool for Environmental Research. B. Moldan and J. Cerny, Wiley. 51.
- Refsgaard, J. C. and B. Storm (1996). *"Construction, calibration and validation of hydrological models"*. Distributed hydrological modelling. B. A. Abbot and J. C. Refsgaard. Dordrecht, Kluwer Academic Publisher.
- Robson, A., K. Beven and C. Neal (1992). *"Towards identifying sources of subsurface flow: a comparison of components identified by a physically based runoff model and those determined by chemical mixing techniques."* Hydrological Processes 6: 199-214.
- Rodhe, A. (1984). *"Groundwater contribution to streamflow in Swedish forested till soil as estimated by oxygen-18."* Isotope Hydrology. Vienna, IAEA: 55-66.
- Rosenbrock, H. A. (1960). *"An automatic method for finding the greatest or the least value of a function."* The Computer Journal 3: 175-184.
- Seibert, J. and J. McDonnell (2002). *"On the dialog between experimentalist and modeler in catchment hydrology: Use of soft data for multicriteria model validation."* Water Resources Research 38(11): 1241.
- Sklash, M. G. and R. N. Farvolden (1979). *"The role of groundwater in storm runoff."* Journal of Hydrology 43(46-65).
- Sklash, M. G., R. N. Farvolden and P. Fritz (1976). *"A conceptual model of watershed response to rainfall, developed through the use of oxygen-18 as a natural tracer."* Can.J.Earth Sci. 13: 271-283.

-
- Sklash, M. G., M. K. Stewart and A. J. Pearce (1986). "*Storm runoff generation in humid catchments. A case study of hill slope and low-order stream response.*" *Water Resources Research* 22(1273-1282).
- Soutter, M. (1996). "*Prédiction stochastique à l'échelle régionale des risques de contamination des eaux souterraines par des pesticides*". Thesis No.1487, EPFL. Lausanne.
- Tarantola, A. (1987). "*Inverse problem theory*". Amsterdam, Elsevier.
- Turner, J. V., D. K. MacPherson and R. A. Stokes (1987). "*The mechanisms of catchment flow processes using natural variations in deuterium and oxygen-18.*" *Journal of Hydrology* 94(143-162).
- Walter, M. T., J. S. Kim, T. S. Steenhuis, J. Y. Parlange, A. Heilig, R. D. Braddock, J. S. Selker and J. Boll (2000). "*Funneled flow mechanisms in a sloping layered soil: Laboratory investigations.*" *Water Resources Research* 36(4): 841-849.

2. Presentation of the Haute-Mentue catchment

Abstract

This chapter introduces the study region and presents its main physical characteristics such as geographical localization, geology, morphology, pedology as well as climatology, and land use. The study area is located in the Plateau region, in the western part of Switzerland. The present characteristics are determined by the geological evolution and the climatic factors. The gentle morphology, with altitudes between 800-900 m, is a direct consequence of local lithology represented by molassic sandstones and clayey moraine. Moderate temperate climatic conditions with annual precipitations of about 1200 mm and potential evapotranspiration of about 600 mm determine important annual runoff values. Vegetation is represented essentially by spruce forests, consequence of the intensive past beech exploitation and of the recent plantations. The study region is represented by the Haute-Mentue catchment, which is, since 1988, the experimental catchment of the Hydrology and Land Improvement Laboratory at the Swiss Federal School of Technology from Lausanne.

2.1 Geographical localization

The study region is represented by the Haute-Mentue experimental catchment, situated in the southwest of Switzerland, 15 km north of Lausanne, in the canton of Vaud. This catchment belongs to the Swiss Plateau, which lies between the Jura (at west) and the Alps mountains (at east). The Haute-Mentue forms the upper part of the Mentue River, which is a tributary of the Neuchatel Lake (Figure 2-1). The study catchment has an area of 12.5 km² and is limited by the Talent basin in the west, by those of Broye in the east (ANNEX I). The most intensive studied region includes the upper part of the Haute-Mentue catchment called Corbassière (2 km²) and its main subcatchments: Esserts (0.33 km²), Bois-Vuacoz (0.24 km²) and Ruzillon (0.18 km²).

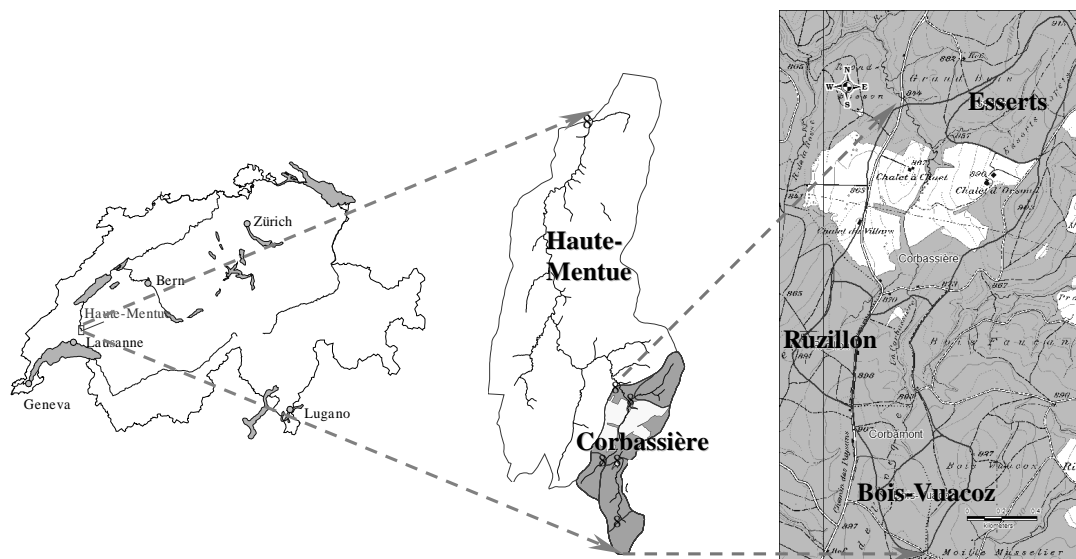


Figure 2-1 Geographical localization of the Haute-Mentue catchment

The present research is devoted to the study of the hydrological behavior of this catchment. A brief introduction will be further made concerning its main geographical characteristics.

2.2 Physical characteristics

The hydrological behaviour of a given catchment depends on the multiple interactions that have been taken place over the past recent (days), medium (years), and long (geological) time scales between the main internal (geological) and external (weathering)

factors (climatology and meteorology). These interactions occur at the interface between the lithosphere and the atmosphere and determine the characteristics of terrestrial morphology, of the catchments' hydrology, of the soils and of the type of land use. Beside these, the actual catchment hydrology is influenced by the many other interactions that take place between the geomorphologic factors, the soil characteristics and the vegetation particularities (Figure 2-2).

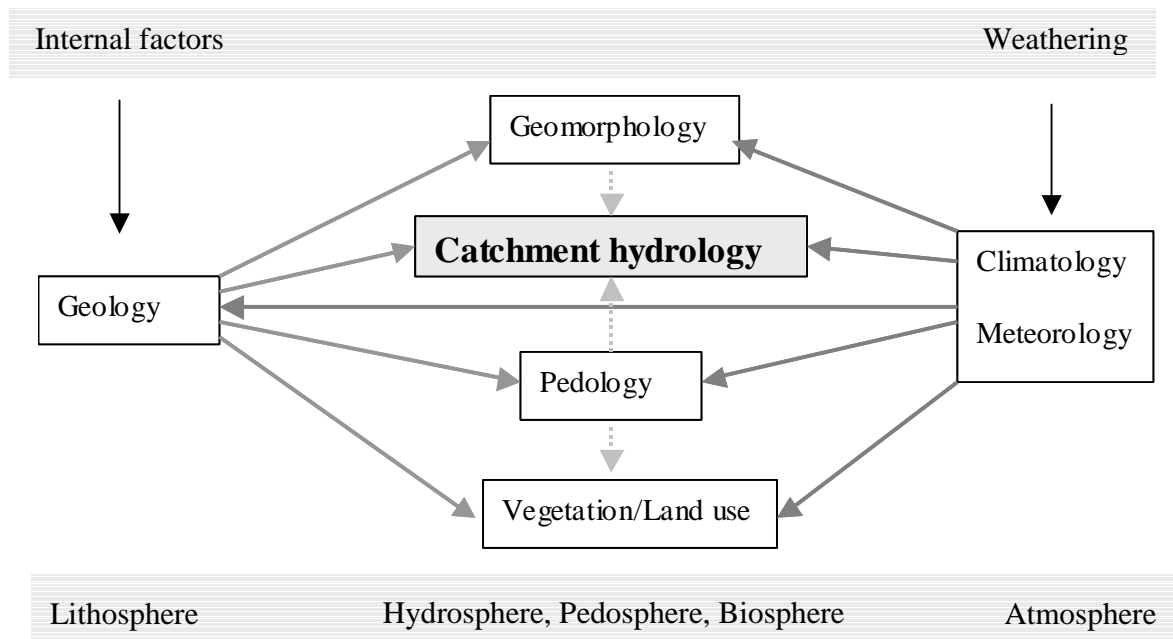


Figure 2-2 Overview of the main interactions that determine the catchment hydrology

In order to understand the Haute-Mentue catchment hydrological behavior first, a brief presentation of the main factors that contribute to explain it will be given below.

2.2.1 Geology

The Haute-Mentue belongs to the Alpine foreland, which is a contact region between the Jura and the Alps folded structures (Figure 2-3). More precisely, the study region belongs to the gently dipping part of the Swiss Molasse basin.

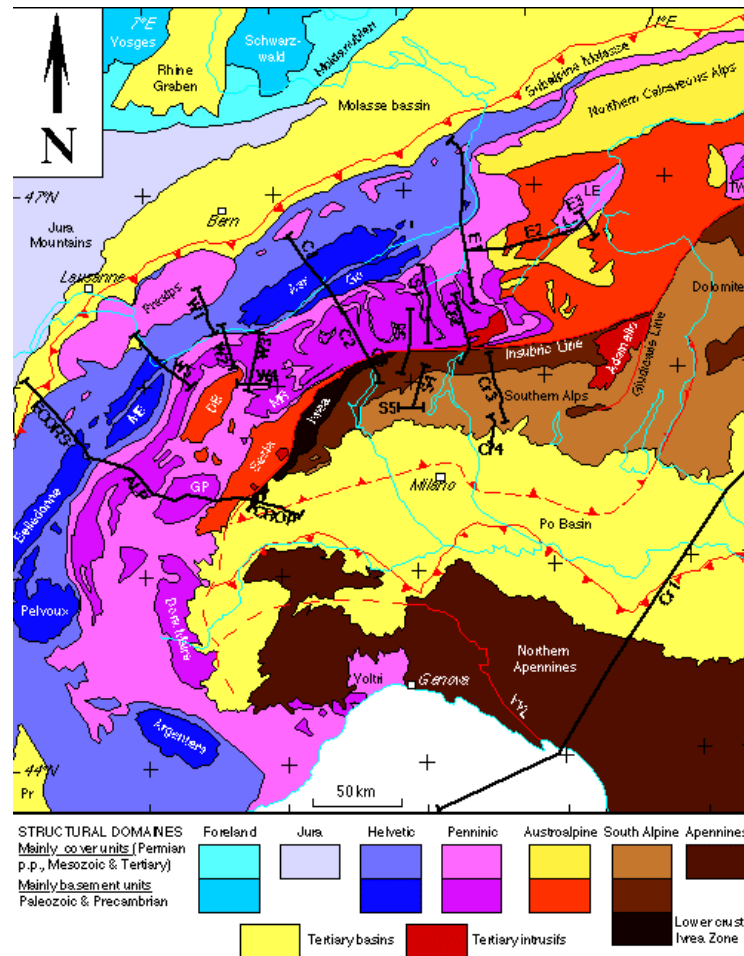


Figure 2-3 Tectonic map of the alpine orogene and foreland regions (taken from http://www-sst.unil.ch/research/seismic/w_alps.htm)

This was formed by a complex sedimentation process during the Miocene period. The STRATIGRAPHY is represented by alternating sedimentary strata with different characteristics, the most important being the aquitanian lower freshwater molasse and the burdigalian upper seawater molasse. During the quaternary period the region was influenced by the alpine glaciation when important morainic formations covered partially or totally the molassic ones. In the present, the region is affected by weathering processes.

The aquitanian LITHOLOGY is formed by alternating thick sandstone and marl layers while the burdigalian is represented essentially by compact sandstone (with depths more than 200 m on the top of Jorat) (Bersier (1938)). These formations are often covered by quaternary morainic deposits, which are generally very clayey and hence very slow permeable. The lithological composition of the moraine is very variable and generally the zones marked as moraine on the geological map are only relative. One important characteristic is the presence of ancient wetlands with peaty deposits in different stages of evolution located in the central parts, along the streams (Figure 2-4).

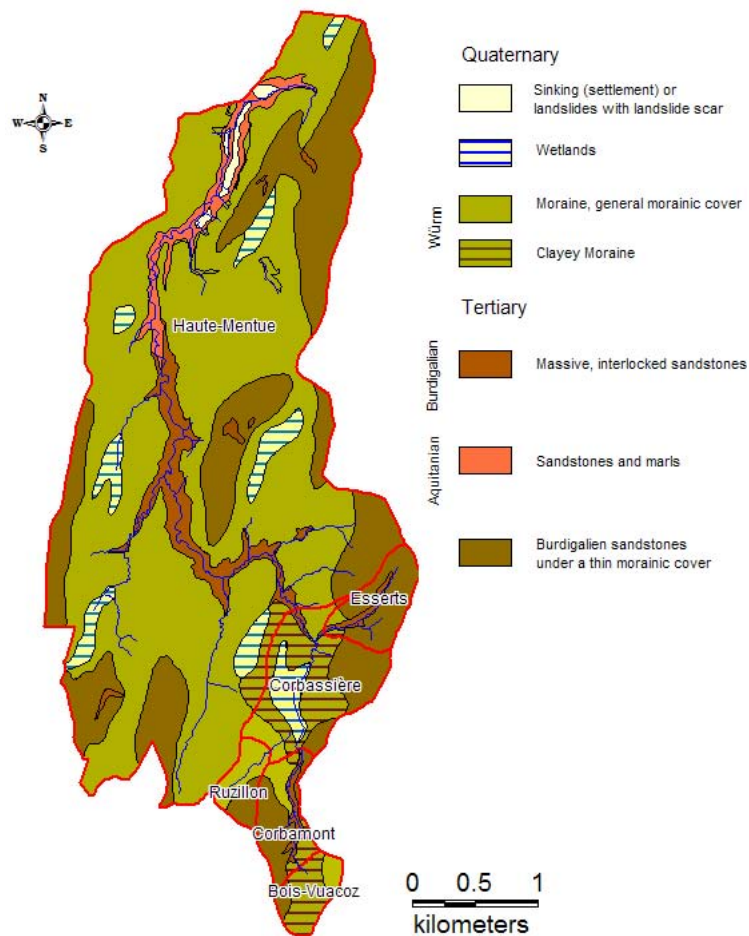


Figure 2-4 Geological map of the Haute-Mentue catchment (after Geological Atlas of Switzerland, 1952, 1:25 000, Sheet Jorat, n° 1223)

Tectonically, the region is situated in the non-folded part of the molassic basin (Figure 2-5), with large anticlines and synclines having gentle slopes (2° - 5°) and being oriented SSW-NNW. The Haute-Mentue catchment is located on the southeastern side of the Mormont anticline, with strata having a monoclinical structure.

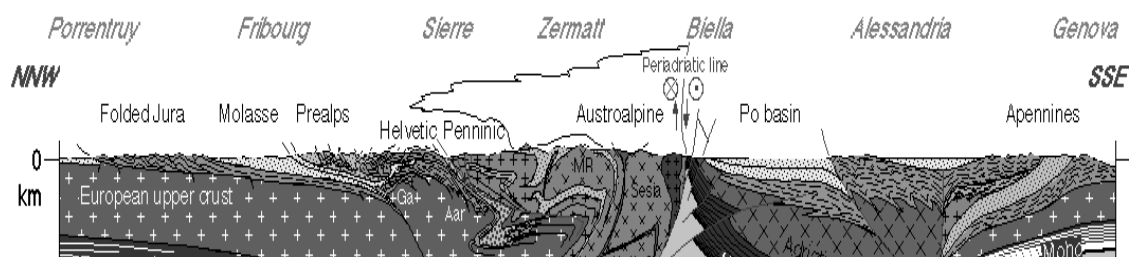


Figure 2-5 Geological cross section through the alpine domain (taken from http://www-sst.unil.ch/research/seismic/w_alps.htm)

The 40 m troll geo-electrical study of the region done by Zwahlen (1981) confirmed the geological map indications and showed a quite uniform lithological distribution of the Corbassière catchment. Apparent electrical resistivities greater than 100 ohm-m, on the most part of Bois Vuacoz, on the central and southern of the Ruzillon and on the southern part of the Esserts and Corbassière catchment, indicate the presence of the burdigalian sandstone, outcropping or slightly covered by morainic deposits.

The apparent resistivities in the size range of 70-100 ohm-m (in the center and the north of Corbassière as well as in the north of Ruzillon basin) give evidence of the thick clayey morainic deposits (up to 10 m), with low permeability.

The 9 m geo-electrical study of Zwahlen (1981) seems to be much more difficult to interpret because of the important variations of the apparent resistivity due to the climatic seasonal variations. Electrical resistivities greater than 200 ohm-m, located in the south, west and north-west of Bois Vuacoz, in south of Ruzillon and Corbassière catchments and in the north of Esserts, show more or less drained porous zones, infiltration favorable, giving strong evidence of the altered permeable burdigalian strata. In the north of Ruzillon and in the central and northern parts of Corbassière, electrical resistivities less than 100 ohm-m indicate clayey morainic quaternary formations with infiltration conditions very unfavorable.

The 9 m / 40 m electrical resistivities ratio is very important for determining the relationship between the subsurface and the deeper formations thus defining the hydrological behavior across the lithological formations. Ratio values less than 1 indicate subsurface formations of low permeability while ratios greater than 1 give evidence of more permeable subsurface formations. In the Esserts catchment, ratios greater than 2 show very permeable and well drained sub-superficial formations.

In order to further investigate the geological characteristics of the Haute-Mentue catchment, a 3D electrical resistivity tomography was done during the 2003 summer by the Geophysical Institute of the University of Lausanne, Switzerland. Two sites have been chosen for their geological and morphological characteristics: one is located in the southern part of the Corbassière catchment, in a region covered essentially by morainic deposits (Ruzillon sub-catchment) and the other one is located in an other head catchment covered essentially by molassic altered sandstones deposits (Esserts sub-catchment). The study fields cover a surface of about 2x400 m² situated along Ruzillon and Esserts streams. Figure 2-6 and Figure 2-7 represent the results of the 3D electrical resistivity tomography as horizontal cross-sections (a) and vertical (b) 2D profiles for Ruzillon and respective Esserts experimental sites.

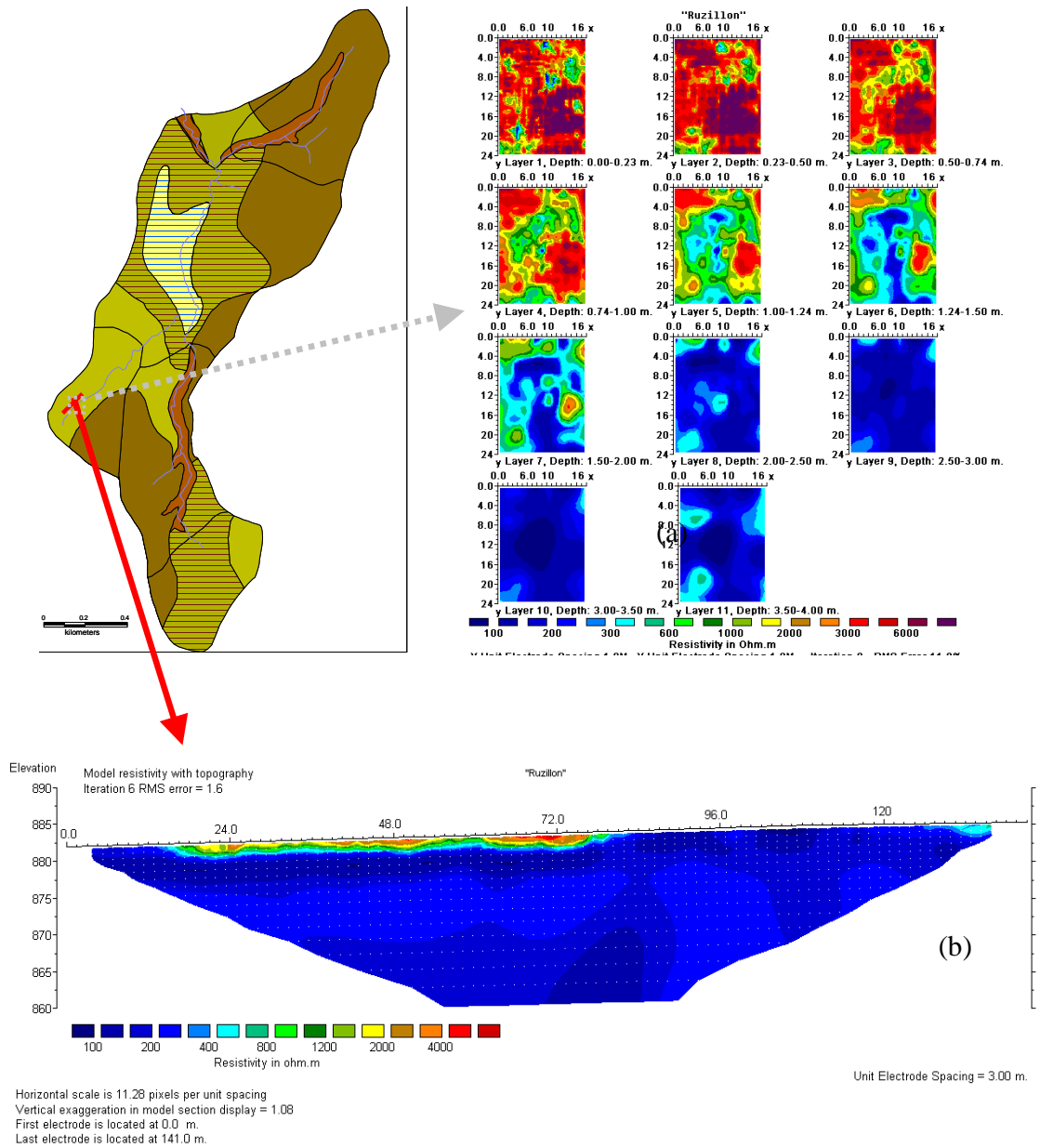


Figure 2-6 Ruzillon site: 3D resistivity tomography (a) and resistivity cross-section (b) (obtained from the Geophysical Institute from Lausanne)

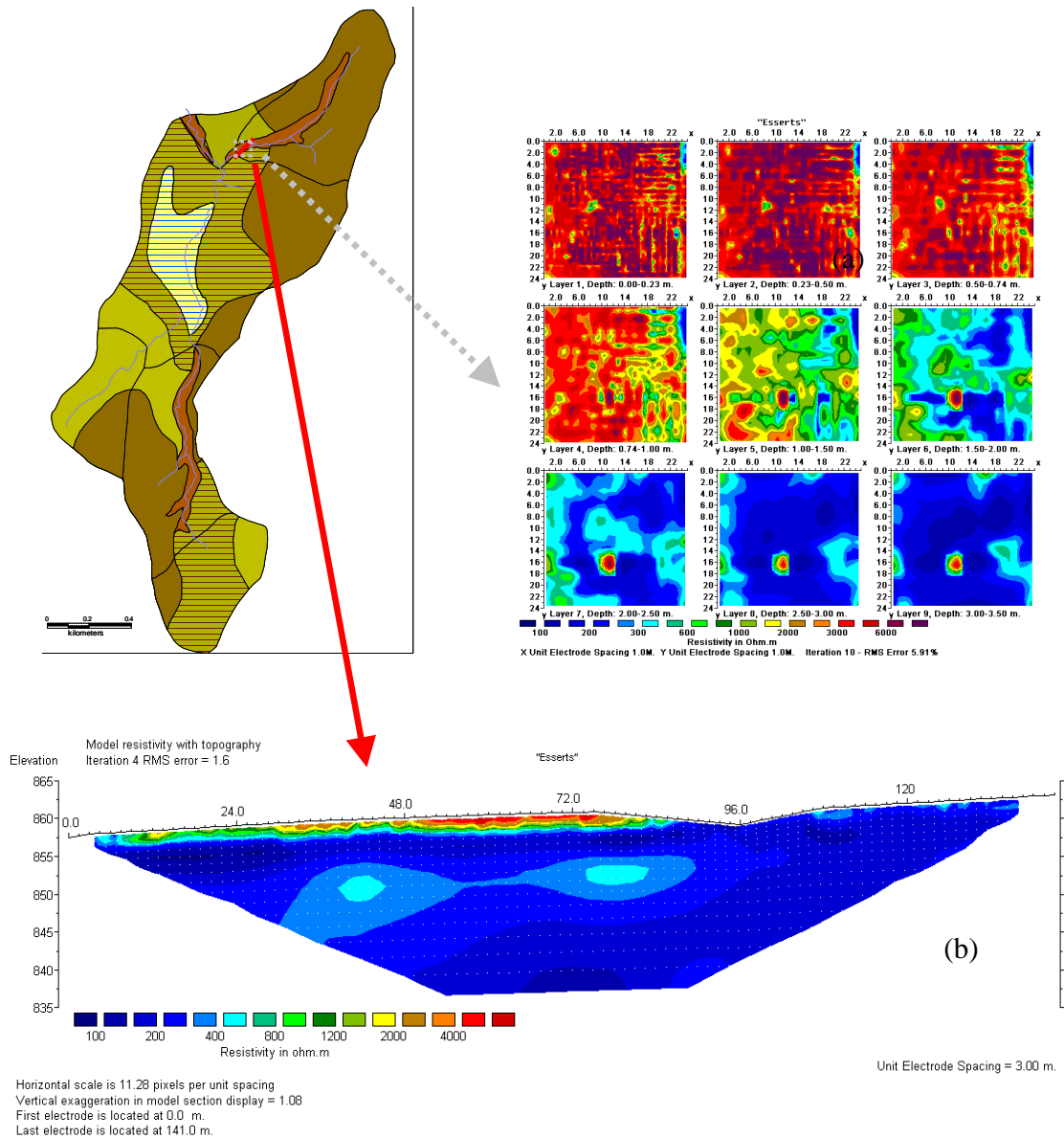


Figure 2-7 Esserts site: 3D resistivity tomography (a) and resistivity cross-section (b) (obtained from the Geophysical Institute from Lausanne)

As these soil electrical resistivity tomographies were done in very dry conditions, the high values observed for the upper part of the soils (up to 1 m depth) are easily explained. The lower parts of the soils profiles show lower values of the electrical resistivity (100 ohm.m) for the Ruzillon site starting with 1.5 m depth while for Esserts site, the resistivity values are higher (150-200 ohm.m) for depths greater than 2 m. Zwahlen (1981) showed that the difference between molassic and morainic deposits is not easy to distinguish because of the close resistivity values of the two formations but he also indicated that in general, values lower than 100 ohm.m can be attributed to the moraine while values greater than 100 ohm.m could be associated with burdigalian molassic

deposits. The recent application of the geophysical techniques confirmed the findings of Zwahlen i.e. morainic deposits seem to be more representative for the Ruzillon site while molassic ones seem to develop more extensively at the Esserts site.

2.2.2 Morphology

In this work, only the morphological characteristics of the upper part of the Haute-Mentue catchment will be further analyzed. Details on the morphometry and morphology of the whole catchment can be found in Higy (2000), Jordan (1992), Iorgulescu (1997) and Joerin (2000).

A comparative analysis between the MORPHOLOGY of the Corbassière sub-catchments shows some similar characteristics: uniform morphology with hills and valleys oriented N-NW, modeled in the miocene molassic and quaternary formations. Figure 2-8 (left) shows the spatial distribution of the altitudes on the Corbassière catchment as given by the DEM (Digital Elevation Model) at the scale 1:25000 and Figure 2-8 (center) present the hypsometric map resulted from the same DEM model.

Catchment MORPHOMETRY indicates small altitudinal amplitude (83 m between the top of Jorat at 927 m and 844 m at the basin outlet) and thus low relief energy for the Corbassière catchment.

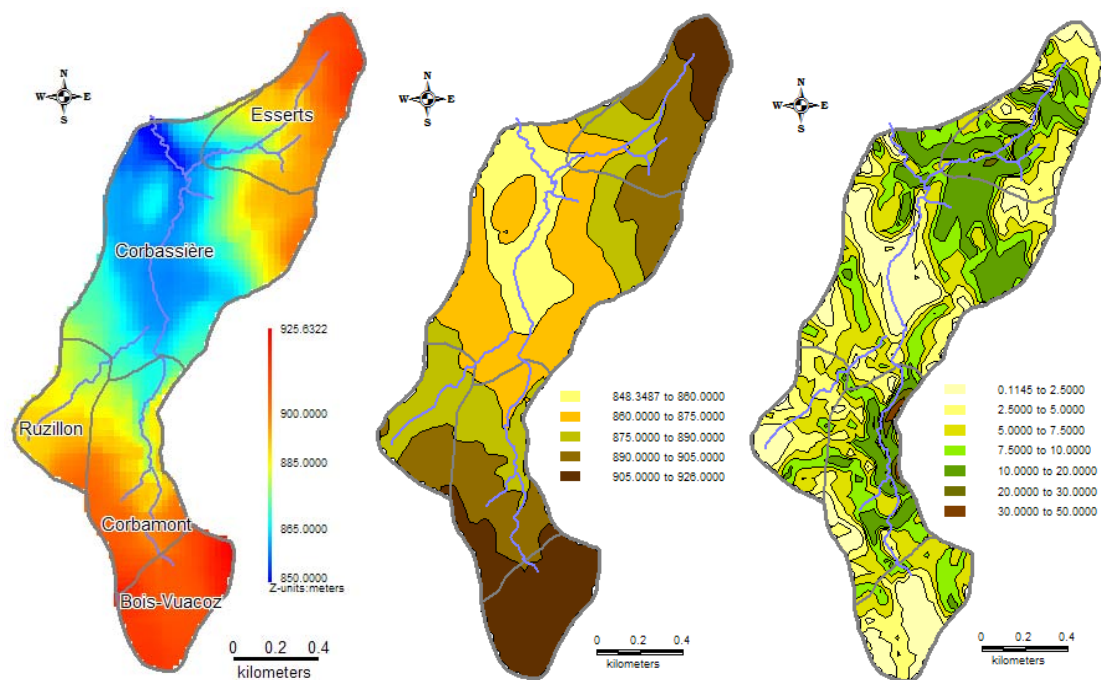


Figure 2-8 Corbassière catchment: DEM (1:25 000) (left), hypsometric map (center) and slopes map (right)

The relief horizontal and vertical fragmentation points out the Esserts catchment which has a clearly higher value than the other basins, this having important implications on its hydrological behavior.

Catchment	H _{max}	H _{min}	Vertical fragmentation	Horizontal fragmentation
Bois-Vuacoz	927 m	900 m	27 m	1.2 km/km ²
Ruzillon	905 m	870 m	35 m	2.72 km/km ²
Esserts	919 m	857 m	62 m	3.65 km/km ²
Corbassière	927 m	844 m	83 m	2.97 km/km ²

Table 2-1 Minimum and maximum altitudes; vertical and horizontal relief fragmentation

The slopes vary between 0-9% for the upper hillslopes on Bois Vuacoz, Ruzillon and central part of Corbassière. Slopes ranging between 15-30% are more characteristic for the Corbassière and Esserts catchments (Figure 2-8- right).

Other morphometric characteristics are briefly presented in the table below and have been partially taken from Higy (2000):

	Haute-Mentue	Corbassière	Esserts	Bois-Vuacoz	Ruzillon
Surface [km ²]	12.5	1.95	0.33	0.24	0.18
Catchment length [km]	6.65	2.63	1.02	0.57	0.63
Catchment width [km]	1.88	0.74	0.33	0.40	0.30
Main stream length [km]	7.25	2.8	0.84	0.31	0.61
Stream network length [km]	30.0	6.73	1.11	0.31	0.61

Table 2-2 Morphometric characteristics of the Haute-Mentue catchment

The geomorphology shows absence of real fluvial forms especially of a real alluvial plain on the Corbassière watershed. The relation between the geological structure and the valleys orientation could be responsible for the formation of structural forms (i.e. obsequent and subsequent streams sectors), which could explain some morphological and hydrological particularities of the concerned watersheds.

At the regional scale, the Corbassière catchment appears to be somehow raised in comparison with the neighboring Talent (at west) and Broye (at east) watersheds. This situation is explained by a higher relief energy of the neighboring rivers and thus by their higher morphologic potential to the detriment of the upper Mentue catchment.

2.2.3 Pedology

The current soil characteristics are a consequence of the geologic and climatic evolution in time. For the Corbassière catchment, the class and the type of the soils can be mainly explained by the parent rock types: molassic sandstone and clayey morainic formations. The characteristics of the soil subtypes can be explained by the hillslope topography, climate and by the vegetation conditions.

The pedology of the Corbassière catchment is essentially represented by the class of brown soils, not very well developed and with different vertical profiles according to what the parent rock is altered sandstone or clayey moraine. The brown soils are the equivalent of the FAO cambisols (acid brown soils) and have intermediary position

between the incipient soils (lithomorphic soils, rankers) and the more developed podzolic soils (Annex II). The diagnostic horizon is B, which is depleted in carbonates but enhanced in silt relatively to the substratum.

A short synthesis of the pedological researches done by Reber (1993) on the Corbassière catchment is presented below. On the eastern part of Bois Vuacoz catchment, on the central parts of Ruzillon and Corbassière as well as on the central northern part of Esserts catchment, the brown soils appear on clayey morainic deposits, the solum profile being represented by the following horizons and textures:

Horizons	Texture	Depth (cm)
A	SI _{sa} - SI _{organic}	0-50
B (g)	SI _{sa} compact	50-70
C (g)	SA _{si} - SA _{si} compact	70-90
C	moraine	> 90

* where SI = silt, SA = sand, SI_{sa} = silty sand, SA_{si} = sandy silt

Table 2-3 Typical soil textural profile on morainic parent material

On the ecological-physiographical soils map of Vaud canton (Haeberli (1971)), these soils are considered as having a normal to moderate drainage, moderate depth and silt to silt-sand textures. Sometimes, one can notice the presence of gravels of morainic origin and one can also notice the presence of a pseudogley horizon (g) between 50-70 cm.

On the most part of Esserts catchment and partially in Corbassière and Bois Vuacoz catchment, the brown soil profile (horizons and related texture) is presented as follows:

Horizons	Texture	Depth (cm)
A	SI _{sa} - SI _{organic}	0-50
B	SA - SA _{si}	50 -90
C	SA	90 - 120
M	sandstone	> 120

Table 2-4 Typical soil textural profile on molassic parent materials

These soils have developed on the altered molassic sandstone materials and generally have a silty-sandy texture. They are generally normally drained and they have practically no gravels at all.

Depending on the substratum and on the morphological characteristics, other subsidiary soil classes appear. The most important are the hydromorphic soils. Temporary and permanent saturation conditions have influenced the formation of the hydromorphic mineral soils such as pseudogley, gley and stagnogley with generally very low hydraulic conductivities.

The pseudogley soils with a clayey horizon appear mostly on the upper parts of Ruzillon, in the central and western part of Bois Vuacoz, along the main stream in Corbassière catchment and locally in the Esserts basin:

Horizons	Texture	Depth (cm)
A1	SI _{sa organic}	0- 25
A2 (g)	SI	25 - 50
B (g)	SI - SA	50 - 140
C (g)	SA - SA _{si}	140 - 170
M		> 170

Table 2-5 Typical soil textural profile for pseudogley soils

In the lower parts of the catchments, along the Corbassière stream, moderately organic hydromorphic soils have typically the following solum structure and texture:

Horizons	Texture	Depth (cm)
An	-	0-50
Gr	SI _{sa}	50-100
Gr	SA _{si}	100-120
M	moraine	>120

Table 2-6 Typical soil textural profile for moderately organic hydromorphic soils

In the central part of the Haute-Mentue catchment, the permanent water logging has produced peaty soils, which have been intensively drained.

The spatial distribution of the main types of soil textures can be seen in the soil texture map realized by Reber (1993) and given below:

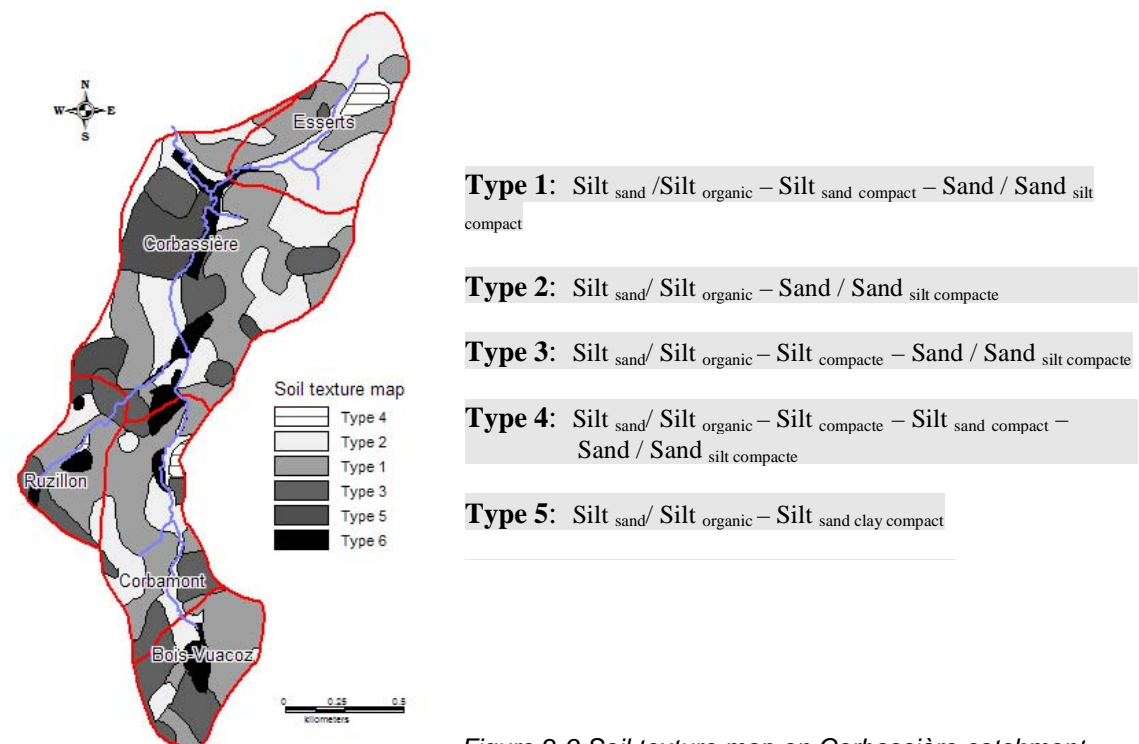


Figure 2-9 Soil texture map on Corbassière catchment

The texture map indicates essentially the presence of the two kind of texture whose spatial distribution is closely related to the lithological substratum characteristics. The soils have the same generally silty and sandy texture the difference consisting in the occurrence of a silty compact horizon for the soils with a morainic substratum.

Soil properties are also influenced by morphometric characteristics such as slope and orientation. Concerning the soil depth, the same study (Reber (1993)) showed that Bois Vuacoz catchment presents the deepest soils (> 120 cm) while Corbassière has the thinnest soil cover (30 - 60 cm). In Esserts and Ruzillon, both deep and thin soils are present: deep soils in the upper part of the hill-slopes and thin soils on the lower parts of the watersheds.

2.2.4 Vegetation and Land use

The vegetation of the Haute-Mentue catchment is determined by the temperate climatic conditions and is represented essentially by forests (55%) and pastures and agricultural fields (43%). Urban regions are limited (two villages and roads) to 2% of the catchment surface. Regarding the Corbassière catchment, the forest covers almost 80% of the total surface. This is essentially formed by: common spruce (most part in plantations) and fir-trees at which one can add on the upper slopes, beeches and in the valley, and other humid regions: maples and ash-trees.

The present vegetation characteristics can be explained by different factors. Clot et al. (1993) published a guide to the vegetation in the northern region of Lausanne including the upper part of the Haute-Mentue catchment. Several ecological gradients can explain the present characteristics of the vegetation such as: climatic gradient, hydrological and chemical gradients. In conformity with the climatic and altitudinal gradients, the natural vegetation is represented by broad-leaved trees such as beeches (*Fagus sylvatica*) in association with fir-trees (*Abies alba*), and rarely, oak (*Quercus robur*) (Figure 2-10A). The long forest exploitation of the beeches (as wood fuel) and later the silviculture interests explain why nowadays most of the present forest is formed by spruce (*Picea abies*) and fir-tree (*Abies alba*) (Figure 2-10B). Different local factors interfere and determine the vegetation characteristics. Topography and water availability determine greatly the vegetation particularities in the head catchments where the groundwater level is very close to the surface and where the stream form. These are the so-called “mouilles” influenced by the morainic cover and concave topography where ash-trees (*Fraxinus excelsior*) and alders (*Alnus glutinosa*) are found together with plants such as: *Crepis paludosa*, *Lysimachia vulgaris* (Figure 2-10F). Along the streams, the hydric conditions allow *Fraxinus* wood to develop accompanied by stream speedwells (*Veronica officinalis*), *Ranunculus* (*Ranunculus aconitifolius*) and large-flowers bittercress (*Cardamina amara*) (Figure 2-10E). The last years, parts of the Esserts and Ruzillon forests have been cut and replaced with spruce plantations (Figure 2-10D) or pastures (Figure 2-10C).

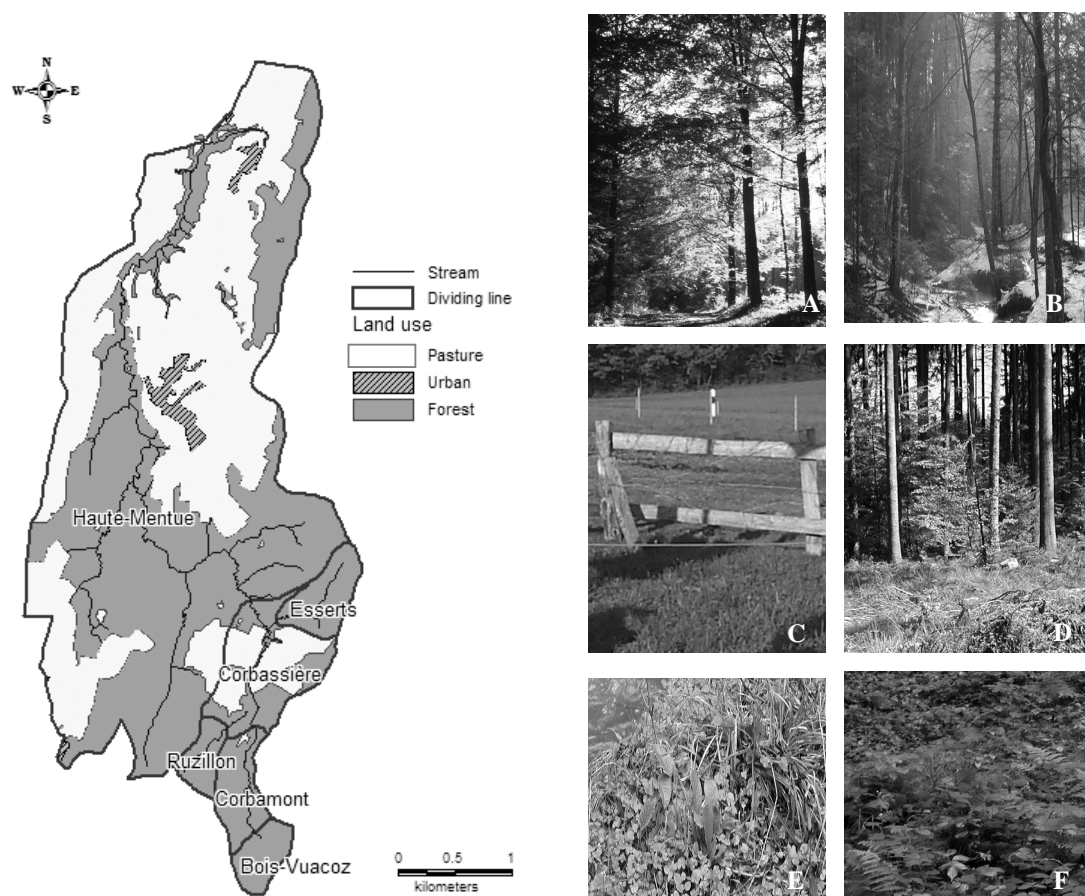


Figure 2-10 Land use map of the Haute-Mentue catchment

2.2.5 Climatology

The climate of the Haute-Mentue catchment is humid-temperate with a continental tendency. The mean annual temperature is about 7°C.

The table below presents the maximum and minimum instantaneous temperature values for the last 3 years registered at Chalet du Villars station in order to give an idea of the annual temperature amplitudes.

Year	Max Temperature	Min temperature	Amplitude
2001	28°C (26 June)	-8.5°C (2 February)	36.5°C
2002	31°C (23 June)	-7°C (21 February)	38°C
2003	37°C (13 August)	-12°C (13 January)	49°C

The mean multi-annual precipitation is about 1200 mm and they are generally most important during the autumn period. During the summer period, important storms could also occur. The potential evapo-transpiration has been estimated by using the Penman-Monteith formula, which is given below (2.1):

$$ET_p = \frac{R_n \cdot \Delta + \frac{\rho \cdot c_p \cdot \delta e}{r_a}}{\lambda \left[\Delta + \gamma \left(1 + \frac{r_c}{r_a} \right) \right]} \quad (2.1)$$

where ET_p [mm/s] is the potential evapotranspiration, R_n [W/m^2] the net radiation, Δ [$kPa/^\circ C$] the slope of the vapor pressure curve at the mean air temperature, ρ [kg/m^3] is the air volumic mass, c_p [$kJ/kg/^\circ C$] is the thermic capacity of the humid air, δe [kPa] is the difference between the saturated vapour pressure e_s [kPa] and the effective vapor pressure in the air e_a [kPa], r_a [s/m] is the aerodynamic resistance, and r_c [s/m] is the canopy resistance. Details of the way to compute the different components of the above formula are given in Higy (2000).

We preferred this formula to the well-known Penman formula as the values obtained from the latter were much more exaggerated compared with previous estimations of the potential evapo-transpiration on the Haute-Mentue catchment. The potential evapo-transpiration depends on multiple factors such as temperature and radiative budget, which determine its seasonal variation. As an average, the annual potential evapo-transpiration has been estimated at about 600 mm.

Figure 2-11 presents the meteorological context for the years 2002 (left) and 2003 (right), as hydro-meteorological data from these periods have been used for further analysis in this work. For the year 2002, a total of 1400 mm of precipitation has been recorded while the potential evapo-transpiration was estimated at 450 mm. For the year 2003, the total precipitation was about 1000 mm while the total evapo-transpiration has been estimated at 690 mm.

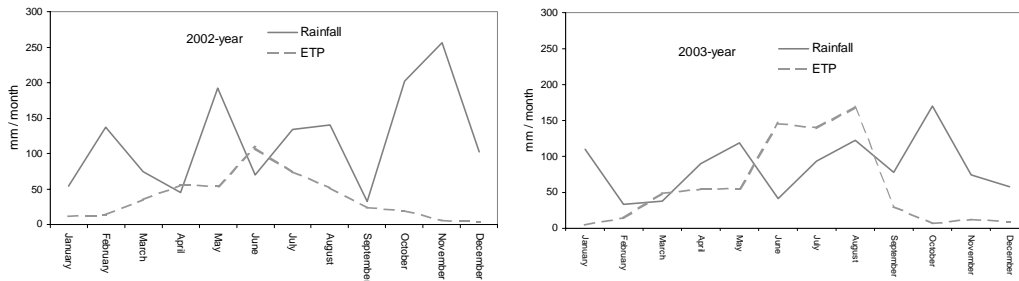


Figure 2-11 Monthly precipitation and potential evapo-transpiration at the Chalet du Villars station during 2002 (left) and 2003 (right)

Figure 2-11 (right) shows that for the year 2003, particular meteorological conditions occurred. The water balance has been in deficit for almost the whole summer season, which produced a pronounced continental tendency rather than moderate temperate climatic conditions. Under these circumstances, the soil water reserves have been intensively used. Compared with the previous year, these reserves reestablished slowly during the autumn period as only a limited amount of precipitation has fallen.

2.3 Catchment instrumentation

The main discharge data that have been used in this work have been provided by the already existing runoff gages: Corbassière, Esserts, Bois-Vuacoz and Ruzillon (Figure 2-12). Most of these stations are operational beginning with 1996 and measurements are taken automatically at 5 minutes time step. Details about the type of weirs in the actual configuration can be found in Joerin (2000). Figure 2-12 presents some of the permanent instruments that are installed on the Corbassière catchment. All runoff gages are equipped with a pressure transducer sonde for measuring the water level and with a recent HYDROMADD[®] data acquisition system, from which the data is retrieved every 2 weeks on mobile memory cards.

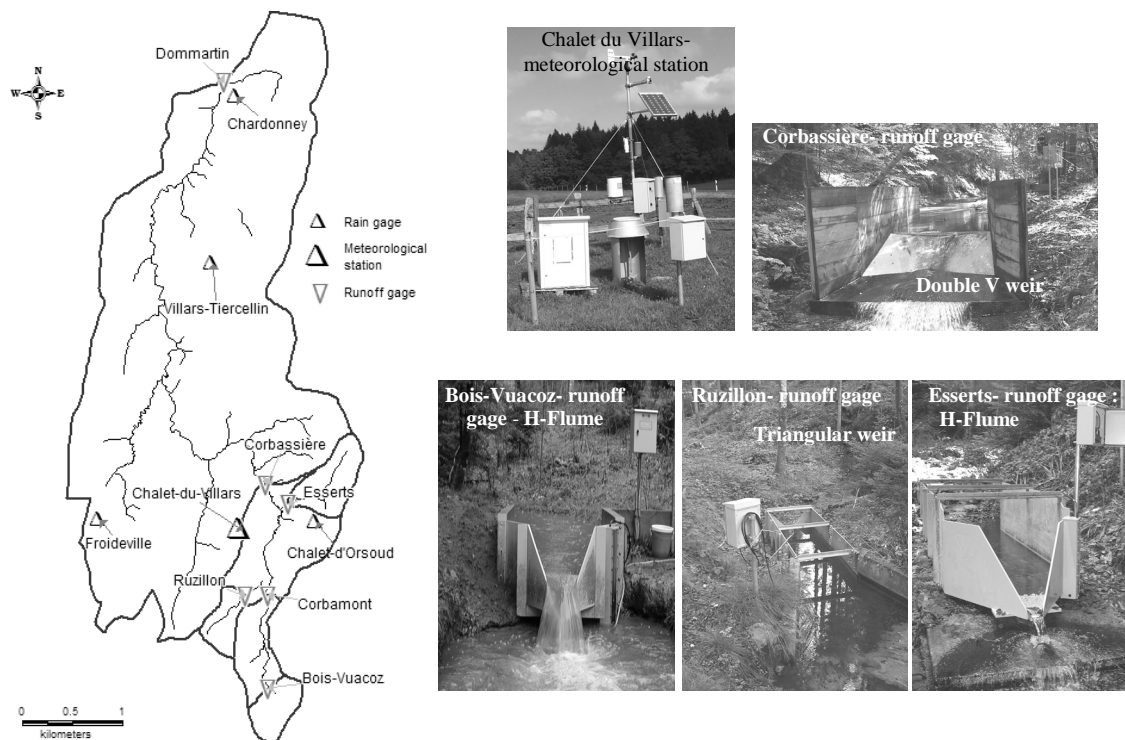


Figure 2-12 Haute-Mentue catchment: permanent equipments

The meteorological data is collected at the meteorological station (Chalet du Villars) at every 15 minutes time interval and they are retrieved every 2 weeks on the same type of mobile memory as for the water level data. A network of five pluviometers (tipping-bucket rain gauges) is operating on the whole Haute-Mentue catchment in order to better capture the spatial variability of the precipitations.

Appropriate rating curves have been used to transform the water level in discharge data and appropriate formulas are also used to transform counting of the pluviometers to rainfall intensities. These transforms have been done with the CODEAU® computer program (EPFL-HYDRAM et al. (1996)) developed at HYDRAM Laboratory in order to handle and control hydro-meteorological data. More information on this computer program can be found in ANNEX IV.

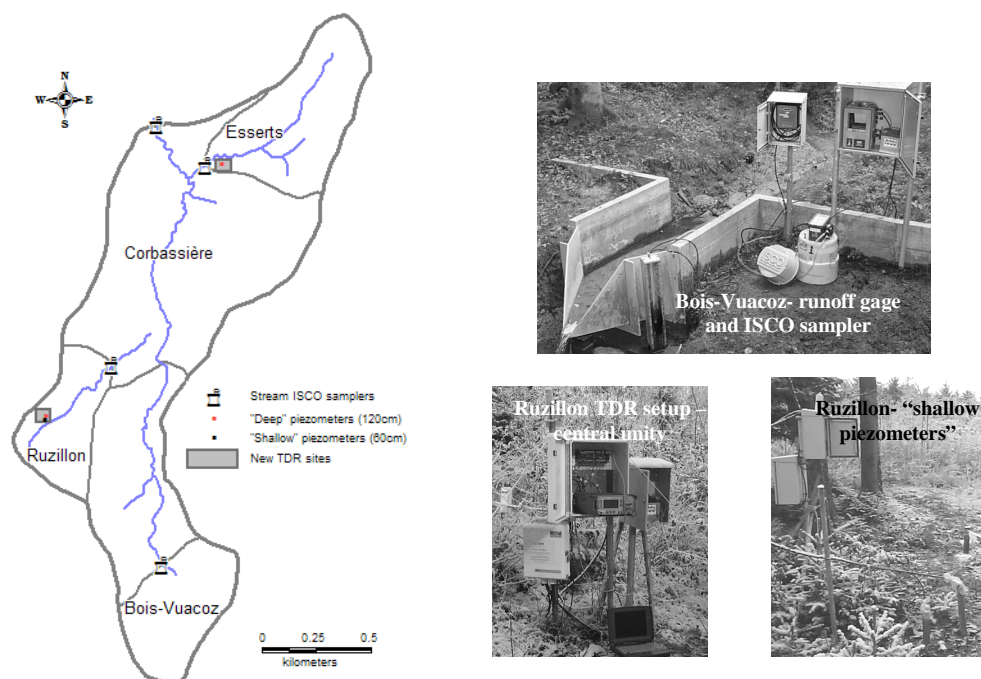


Figure 2-13 Corbassière catchment: temporary equipments

Beside the permanent instruments, new equipments have been installed temporally during several intensive filed campaigns (Figure 2-13). These concern:

- the TDR (Time Domain Reflectometry) set-up for measuring and monitoring the soil moisture humidity at several depths along the hillslope on two geologically representative sites of the Corbassière catchment (further details on this type of equipment can be found in Chapter 3, Section 2).
- the ISCO samplers used in order to collect stream water samples at several locations (Corbassière, Esserts, Ruzillon and Bois-Vuacoz outlets) in order to be further analyzed for different chemical species.
- Shallow piezometers installed in autumn 2002 in order to test the hypothesis of possible superficial perched temporary water tables on the Ruzillon site.

Table 2-7 presents the available set of hydro-meteorological data collected on the Corbassière catchment during 2001-2003 period.

	2001												2002												2003											
	1	2	3	4	5	6	7	8	9	10	11	12	1	2	3	4	5	6	7	8	9	10	11	12	1	2	3	4	5	6	7	8	9	10	11	12
Runoff	Permanent equipment																																			
Corbassière																																				
Esserts																																				
Bois-Vuacoz																																				
Ruzillon																																				
Rainfall																																				
Ch.Villars																																				
Ch.Orsoud																																				
Froideville																																				
Other meteorological parameters																																				
Temperature																																				
Relative humidity																																				
Global radiation																																				
Wind (direction, speed)																																				
ISCO- stream sampling	Temporary equipment																																			
Corbassière																																				
Esserts																																				
Bois-Vuacoz																																				
Ruzillon																																				
Soil moisture -TDR																																				
Ruzillon																																				
Esserts																																				
"Shallow" piezometers																																				
Ruzillon																																				

Table 2-7 Available field data series during 2001-2003 period

For the environmental tracing application, water sampling was necessary and was done by using ISCO samplers. For this work, only the stream water was sampled during two intensive field campaigns conducted in autumn 2001 and in April-December 2002. We decided not to continue with sampling of the rainfall water, as previous researches done during 1993-1998 showed stable low concentrations of rainfall in calcium and silica. Furthermore, we didn't sample the soil water either, as the few samples that we would have achieved during our study period would have asked for a lot of efforts without reducing the great uncertainty in determining the chemical definition of the soil water (Joerin et al. (2002)). On the contrary, in order to have spatial information of the chemical composition of the groundwater, we have sampled the streams during the 2002 summer period when in absence of important rainfall, most of the water in the streams is supposed to come from the groundwater sources. Concerning the sampling methodology, we adopted the same as those proposed by Joerin (2000): we used a volume proportional water sampling method instead of a time proportional sampling one. In order for us to better sample the flood events, water samples were taken by the ISCO equipment each fixed volume of water that passed through a given runoff gage. These volumes are station dependent and they have been proposed by Joerin (2000) function of the specific discharges at each of the four runoff gages on the Corbassière catchment.

2.4 References

- Bersier (1938). "*Recherches sur la géologie et la stratigraphie du Jorat*." Mem.Soc. Vaud.Sc.Nat. 6(3).
- Clot, F., P. Kissling and A. C. Plumettaz Clot (1993). "*Petit guide botanique dans les forêts lausannoises*". Lausanne, Service des forêts, domaines et vignobles.
- EPFL-HYDRAM, B+C Ingénieur SA and AIC Association d'ingénieurs conseils SA (1996). "*CODEAU, Logiciel de traitement de données hydrologiques*". Lausanne.
- Haeberli, R. (1971). "*Carte écologique-physiographique des sols du canton de Vaud*". Lausanne, Office Cantonal Vaudois de l'Urbanisme.
- Higy, C. (2000). "*Modélisations conceptuelles et à base physique des processus hydrologiques: Application au bassin versant de la Haute-Mentue*". Thesis EPFL, No.2148. Lausanne.
- Iorgulescu, I. (1997). "*Analyse du comportement hydrologique par une approche intégrée à l'échelle du bassin versant. Application au bassin versant de la Haute-Mentue*". Thesis EPFL, No.1613. Lausanne.
- Joerin, C. (2000). "*Etude des processus hydrologiques par l'application du traçage environnemental. Association à des mesures effectuées à l'échelle locale et analyse d'incertitude*". Thesis EPFL, No.2165. Lausanne.
- Joerin, C., K. J. Beven, I. Iorgulescu and A. Musy (2002). "Uncertainty in hydrograph separations based on geochemical mixing models." *Journal of Hydrology* 255(1-4): 90-106.
- Jordan, J. P. (1992). "*Identification et modélisation des processus de génération des crues; Application au bassin-versant de la Haute-Mentue*". Thesis No.1014, EPFL. Lausanne.
- Reber, O. (1993). "*Rôle de la couverture pédologique dans la réponse hydrologique*". Diploma work, Dpt. GR, Lausanne, EPFL.
- Zwahlen, F. (1981). "*Contribution à l'étude hydrologique du bassin de la Mentue*". Faculté des Sciences. Lausanne, Université de Lausanne: 130.

3. Study of hydrological behaviour through experimental approaches

Abstract

This chapter presents the experimental work that was performed on the Haute-Mentue catchment. Since 2001, the experimental set-up allows for studying the hydrological response at two different spatial scales. First, an analysis of the hydrological response at the catchment scale was performed by mean of environmental tracing. This allowed identification of two types of hydrological behaviour mainly explained by the geological conditions: (i) rapid catchment responses, low baseflow and high flood peaks composed essentially by soil water for head catchments covered by morainic deposits; (ii) slower responses to the rainfall input, higher baseflows, smaller ratio between peak and base discharge, flood runoff composed essentially by groundwater and soil water for head catchments covered essentially by molassic deposits. Two other experiments have been conducted at the hillslope scale, by using the TDR method in order to monitor soil moisture variations at different depths along two typical topographical profiles on both morainic and molassic deposits. These experiments helped better identifying the mechanisms explaining the two different hydrological behaviours. The results, both at the catchment and the hillslope scales, led to a general conceptual model of the Haute-Mentue head catchments function of the local geology, antecedent conditions and rainfall characteristics.

Key words: hydrograph separation, environmental tracing, hydrological processes, TDR

3.1 Hydrological behaviour at the catchment scale

A first introspection into the hydrological behaviour of a given catchment can be realized using the observed hydrograph characteristics. In absence of other type of information, graphical hydrograph separation, no matter how empirical it might be, could prove a useful method to define, in an approximate way, the general response of the catchment to a specific rainfall input. This chapter will analyse comparatively, the observed hydrographs of the Corbassière catchment and its main sub-catchments during several events in 2001-2002. Although that allowed general interesting remarks about the spatial variability of the hydrologic response, this analysis will particularly serve to characterize the hydro-meteorological context for events for which chemical or soil moisture data are available.

3.1.1 Hydrograph analysis

The hydrograph analysis allowed a first study of the Haute-Mentue catchment reaction following a rainfall event. Several rainfall-runoff events have been chosen in order to study the hydrometric response of the Corbassière catchment as well as of its main sub-catchments: Ruzillon (0.18 km²), Bois-Vuacoz (0.24 km²) and Esserts (0.24 km²). The rainfall-runoff events have been analysed using CODEAU[®] hydrological data computer program (EPFL-HYDRAM et al. (1996)) (Annex IV). A set of 17 rainfall-runoff events, that occurred in autumn 2001 and during 2002, have been analysed and characterized in terms of:

- total rainfall (P), measured at the meteorological station for all the events and at two other pluviometers (Chalet d'Orsoud and Froideville) for the storm events [mm].
- maximum rainfall hourly intensity (I_{\max}) for all events and maximum rainfall intensity at 10' time step for the storm events ($I_{\max-10'}$) [mmh⁻¹].
- rainfall structure (histogram plot of the rainfall event for which each column represents 1 hour time step),
- evapo-transpiration (ETP) for the 10 days previous the considered even, as given by the Pennman-Monteith formula [mm];
- 10 day antecedent rainfall index (ARI), which is the total precipitation that occurred 10 days previous to the considered event [mm],
- total runoff during the event (LET) [mm],
- rapid direct runoff (LER) as computed by CODEAU computer program with a graphical method based on the exponential low that governs the flood recession with the [mm].

Figure 3-1 represents the measured discharges for the four cathments during the period 1 April 2002 -10 January 2003. With numbered black arrows, the rainfall-runoff events for which either chemical information or local soil moisture data are available are identified.

In order to characterize the different rainfall-runoff events we considered the following thresholds:

- dry antecedent conditions when the ARI index is less then 30 mm;

- ❑ humid (wet) antecedent conditions for ARI index larger then 30 mm;
- ❑ low rainfall intensities when the hourly rainfall intensity is smaller than 7mm/h;
- ❑ high rainfall intensities for hourly rainfall intensities larger then 7mm/h.

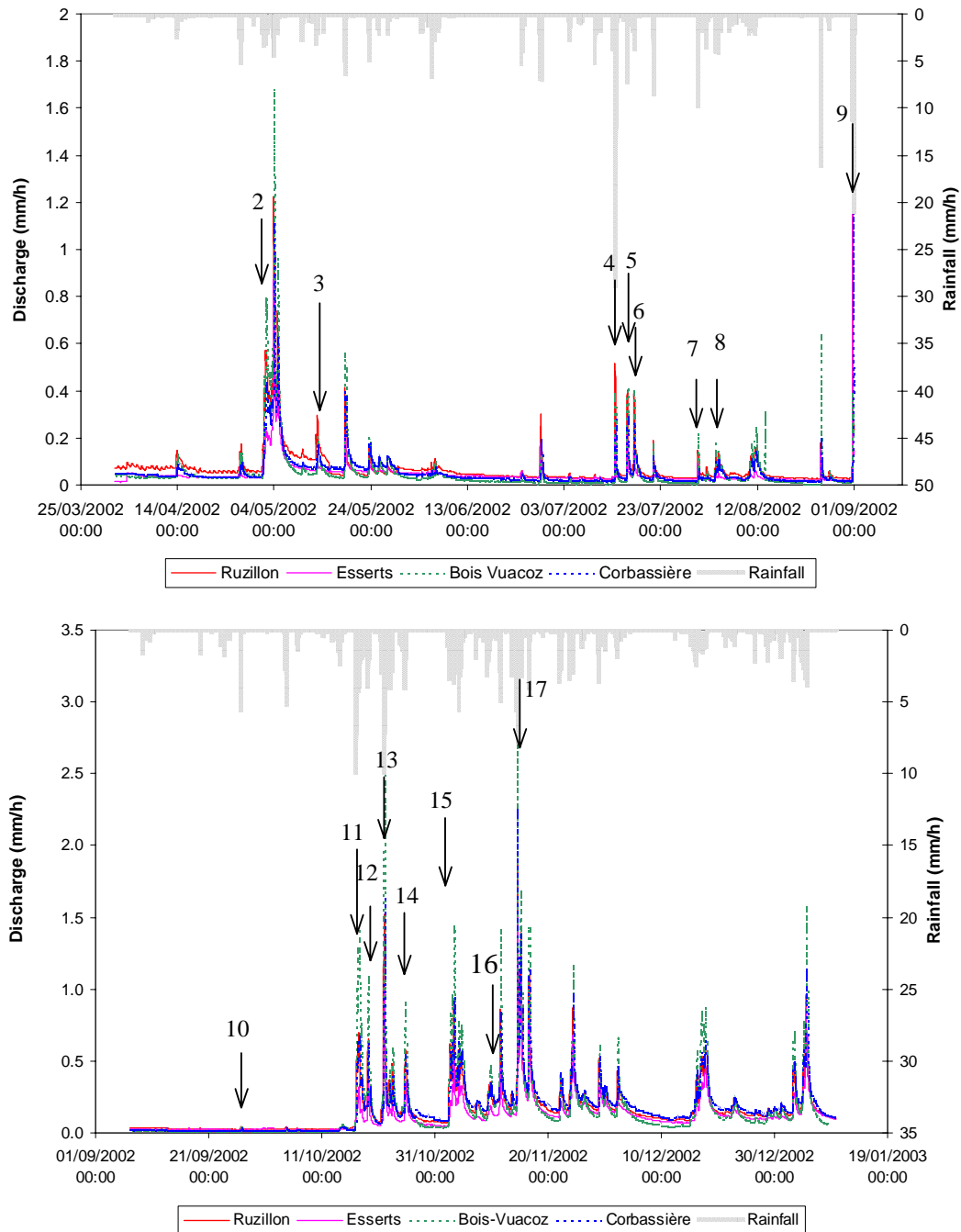


Figure 3-1 Observed discharge for the study catchments during April-September 2002 (top) and September 2002-January 2003 (down)

The *first* studied *event* was chosen in autumn 2001 (not in the above charts) and it represents the response of the four catchments after dry antecedent conditions (the ARI index is only 12 mm rainfall for the last 10 days previous to this event). The catchment response was, in the beginning of the event, very slow and the discharges were important only in the second part of the rainfall event when rainfall intensities were greater. Maximum peak discharges were important and varied between 17 times the initial base flow for Bois-Vuacoz and 9 times for Esserts.

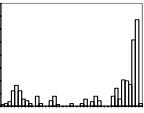
Event 1 08.11.2001	Total rainfall [mm]	Imax [mm/h]	Rainfall structure	ETP [mm]	ARI [mm]	LET [mm]	LER [mm]	Qmax [mm/h]	Qbase [mm/h]
Bois-Vuacoz	31.6	6.74		7.2	12	5	2.2	1.14	0.06
Ruzillon						3.17	1.08	0.54	0.045
Esserts						1.74	0.42	0.18	0.02
Corbassière						3.41	1.29	0.53	0.045

Table 3-1 Hydro-meteorological context: 8 November 2001

Event number 2 distinguishes by the duration of the rainfall, more than 80 hours, and the low rainfall intensities (less than 5mm/h). These rainfall characteristics determined an important increase of the discharges for all considered catchments. The ratios between peak discharges and base flow before the events vary between 15 for Ruzillon to 60 for Bois Vuacoz catchment.

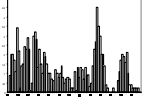
Event 2 02.05.2002	Total rainfall [mm]	Imax [mm/h]	Rainfall structure	ETP [mm]	ARI [mm]	LET [mm]	LER [mm]	Qmax [mm/h]	Qbase [mm/h]
Bois-Vuacoz	108	4.5		20	22	51.2	38.7	2.4	0.04
Ruzillon						46.5	32.0	0.9	0.06
Esserts						27.0	17.0	0.9	0.03
Corbassière						37.0	25.3	1.2	0.04

Table 3-2 Hydro-meteorological context between 02-05 May 2002

Event number 3 corresponds to the 16.05.2002 00:00 - 21.05.2002 09:00 period. Some less than 30 mm of rainfall occurred with an hourly maxima of 6.4 mm/h with moderate antecedent conditions. For this event, Bois-Vuacoz catchment evidences with an important rapid runoff (almost 3 mm) and Esserts catchment with the response the least important (about 0.5 mm).

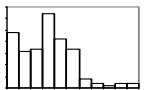
Event 3 16- 21.05.2002	Total rainfall [mm]	Imax [mm/h]	Rainfall structure	ETP [mm]	ARI [mm]	LET [mm]	LER [mm]	Qmax [mm/h]	Qbase [mm/h]
Ruzillon	27.6	6.4		17	22	3	1.42	0.4	0.04
BoisVuacoz						5.26	2.89	0.6	0.03
Esserts						1.59	0.46	0.2	0.05
Corbassière						3.18	1.29	0.4	0.07

Table 3-3 Hydro-meteorological context between 16-21 May 2002

Event number 4 was the first storm that has been sampled for the environmental tracing, with the most part of the rain concentrated in a single time step with high variability of the rainfall intensities from one pluviometer to another (29 mm/h recorded by the Chalet de Villars pluviometer, 37mm/h recorded for the Froideville pluviometer and only 18 mm/h for Chalet d'Orsoud pluviometer). Differences are even more pronounced when one considers the 10' average rainfall intensity, which varied between 100 mm/h for Froideville pluviometer and 40 mm/h for Chalet d'Orsoud pluviometer. The attribution of a given pluviometer to a catchment was made on the basis of the distance criterion. The event occurred in a dry summer period and the catchments discharges increase is comparable for all considered basins. The ratio between peak and low discharges varies nevertheless between 10 for Esserts and 50 for Bois-Vuacoz catchments.


Event 4 13- 14.07.2002	Pluvio- meter	P [mm]	Imax 60' [mm/h]	Imax 10' [mm/h]	Rainfall structure	ETP [mm]	ARI [mm]	LET [mm]	LER [mm]	Qmax [mm/h]	Qbase [mm/h]
Ruzillon	Froideville	41	37	100			28	1	0.67	0.5	0.03
BoisVuacoz	Froideville	41	37	100				0.65	0.47	0.4	0.008
Esserts	Ch.Orsoud	17	16	40				0.44	0.31	0.20	0.02
Corbassière	Ch.Villars	32	29	82				0.73	0.44	0.3	0.02

Table 3-4 Hydro-meteorological context between 13-14 July 2002

Event numbers 5 and 6 are very similar in terms of total rainfall (about 18 mm) and antecedent conditions (moderate to wet), with comparable responses of the four considered catchments. Bois-Vuacoz has the most important direct runoff for the two events while Esserts has comparatively the smallest contribution of the direct runoff to the total streamflow discharge.

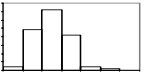
Event 5 15-17.07. 2002	Total rainfall [mm]	Maximum intensity [mm/h]	Rainfall structure	ETP [mm]	ARI [mm]	LET [mm]	LER [mm]	Qmax [mm/h]	Qbase [mm/h]
Ruzillon	17.2	7.2		23	52	2	1.12	0.4	0.04
BoisVuacoz						2.05	1.39	0.4	0.01
Esserts						0.80	0.38	0.2	0.03
Corbassière						1.60	0.93	0.3	0.02

Table 3-5 Hydro-meteorological context between 15-17 July 2002

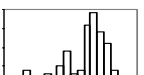
Event 6 17-19.07. 2002	Total rainfall [mm]	Maximum intensity [mm/h]	Rainfall structure	ETP [mm]	ARI [mm]	LET [mm]	LER [mm]	Qmax [mm/h]	Qbase [mm/h]
Ruzillon	18.2	3.80		21	65	2.67	0.88	0.4	0.06
BoisVuacoz						2.94	1.46	0.4	0.04
Esserts						1.31	0.43	0.15	0.04
Corbassière						2.21	0.75	0.26	0.04

Table 3-6 Hydro-meteorological context between 17-19 July 2002

Event number 7 is characterized by a small quantity of rainfall fallen in a short time with a rather high intensity (maximum intensity at 10 minutes time step is about 30 mm/h). The dry antecedent conditions determined a small but rapid increase of the observed discharges. The increase of the peak discharges varied between 3 times the initial baseflow for Esserts catchment and 10 times the initial base-flow for Bois-Vuacoz

catchment. This seems to be determined by the very dry antecedent conditions: the ETP equals 31 mm for the previous 10 days and only 15 mm of rainfall have fallen during the same reference period.

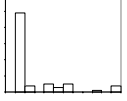
Event 7 30.07.2002	Pluvio meter	P mm	Max. Int. 60' [mm]	Max. Int. 10' [mm]	Rainfall structure	ETP [mm]	ARI [mm]	LET [mm]	LER [mm]	Qmax [mm/h]	Qbase [mm/h]
Bois-Vuacoz	Froideville	21	16	56		31	15	0.54	0.38	0.21	0.015
Ruzillon	Froideville	21	16	56				0.72	0.35	0.12	0.02
Esserts	Ch.Orsoud	15	12	40				0.21	0.09	0.075	0.02
Corbassière	Meteo. St.	14	10	32				0.48	0.24	0.075	0.018

Table 3-7 Hydro-meteorological context between 30-31 July 2002

Event number 8 occurred in the beginning of August 2002 and it was chosen for the dry antecedent conditions and the low rainfall intensities. Very small increase of the discharges is to be noticed for all the catchments.

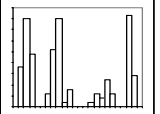
Event 8 03.08.2002	P [mm]	Imax [mm/h]	Rainfall structure	ETP [mm]	ARI [mm]	LET [mm]	LER [mm]	Qmax [mm/h]	Qbase [mm/h]
Bois-Vuacoz	27.6	4		24	24	3.53	1.85	0.21	0.015
Ruzillon						3.64	1.50	0.14	0.04
Esserts						1.54	0.40	0.08	0.02
Corbassière						3.22	1.46	0.11	0.02

Table 3-8 Hydro-meteorological context between 03-08 August 2002

The event number 9 is the second storm event that has been sampled for the environmental tracing at least in one catchment. Its duration is very small and rainfall intensities are very high and almost concentrated in 2 time steps. The response of the four catchments is very quick and the direct flow is very important even if the event occurred after a relatively dry antecedent period (21 mm of rainfall for the 10 preceding days).

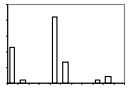
Event 9 31.08.- 03.09. 2002	Pluvio meter	P [mm]	Max. Int. 60' [mm/h]	Max. Int. 10' [mm/h]	Rainfall structure	ETP [mm]	ARI [mm]	LET [mm]	LER [mm]	Qmax [mm/h]	Qbase [mm/h]
Ruzillon	Froideville	32	18	41		15	21	2.91	2.12	1.2	0.03
BoisVuacoz	Froideville	32	18	41				11.7	8.88	3.9	0.015
Esserts	Ch.Orsoud	63	35	80				2.98	2.51	1.2	0.02
Corbassière	Meteo St.	43	21	47				4.78	4.78	2.09	0.02

Table 3-9 Hydro-meteorological context between 31 August -03 September 2002

Event number 10 was chosen to illustrate the stream response to a small rainfall event with low intensities and in dry antecedent conditions. The changes in the observed discharge are very small and the discharges' increases very progressive.

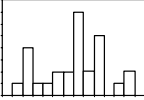
Event 10 06.10.2002	P [mm]	Imax [mm/h]	Rainfall structure	ETP [mm]	ARI [mm]	LET [mm]	LER [mm]	Qmax [mm/h]	Qbase [mm/h]
Bois-Vuacoz	6	1.5		8	16.8	0.5	0.11	0.03	0.015
Ruzillon						0.6	0.07	0.04	0.02
Esserts						0.22	0.01	0.03	0.02
Corbassière						0.46	0.06	0.025	0.015

Table 3-10 Hydro-meteorological context between 06 -07 October 2002

Event number 11 occurs after a long period without any important precipitation. The rainfall intensity is high (10 mm/h) and the total rainfall is important (almost 70 mm of precipitation in 2 days). The general behaviour of the four catchments produces important direct flows for all catchments but Esserts, which reacts more slowly to this strong rainfall input.

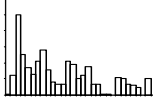
Event 11 16-18.10. 2002	Total rainfall [mm]	P [mm/h]	Rainfall structure	ETP [mm]	ARI [mm]	LET [mm]	LER [mm]	Qmax [mm/h]	Qbase [mm/h]
Ruzillon	70	10.0		5	16	12.5	7.91	0.7	0.04
BoisVuacoz						22.6	15.3	1.2	0.018
Esserts						5.77	3.47	0.25	0.02
Corbassière						13.0	8.05	0.65	0.03

Table 3-11 Hydro-meteorological context between 16 -18 October 2002

Events 12, 13, 14 are represented by moderate total precipitation with moderate hourly intensities which are occurring in a typical autumnal context with frontal precipitations and longer durations. The antecedent conditions are wet and thus the direct runoff flows are important for all considered catchments.

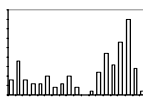
Event 12 18-21.10. 2002	Total rainfall [mm]	Maximum intensity [mm/h]	Rainfall structure	ETP [mm]	ARI [mm]	LET [mm]	LER [mm]	Qmax [mm/h]	Qbase [mm/h]
Ruzillon	21.6	4.0		5	86	6.13	1.66	0.65	0.17
BoisVuacoz						10.6	3.64	1.1	0.24
Esserts						3.36	1.0	0.35	0.08
Corbassière						6.55	1.87	0.63	0.17

Table 3-12 Hydro-meteorological context between 18 -21 October 2002

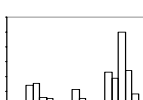
Event 13 21-22.10. 2002	Total rainfall [mm]	Maximum intensity [mm/h]	Rainfall structure	ETP [mm]	ARI [mm]	LET [mm]	LER [mm]	Qmax [mm/h]	Qbase [mm/h]
Ruzillon	38.8	10.0		5	106	9.61	4.5	1.52	0.08
BoisVuacoz						12.1	5.48	2.5	0.06
Esserts						5.65	2.50	0.98	0.05
Corbassière						8.24	3.0	1.65	0.07

Table 3-13 Hydro-meteorological context between 21 -22 October 2002

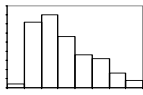
Event 14 25-29.10. 2002	Total rainfall [mm]	Maximum intensity [mm/h]	Rainfall structure	ETP [mm]	ARI [mm]	LET [mm]	LER [mm]	Qmax [mm/h]	Qbase [mm/h]
Ruzillon	22.6	4.0		4	155	9.06	2.68	0.58	0.17
BoisVuacoz						11.2	4.55	0.92	0.15
Esserts						5.17	1.52	0.35	0.085
Corbassière						7.0	1.91	0.56	0.15

Table 3-14 Hydro-meteorological context between 25 -29 October 2002

Event number 15 describes the last sampled event for the environmental tracing in 2002-year. Important precipitations (70 mm) are occurring and the stream responses are very important even if previous to this event only 30 mm of rainfall has fallen. One can explain the important direct runoff flows that have been computed by the very low evapo-transpiration at this period of the year.

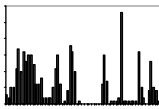
Event 15 02-07.11 2002	Total rainfall [mm]	P [mm/h]	Rainfall structure	ETP [mm]	ARI [mm]	LET [mm]	LER [mm]	Qmax [mm/h]	Qbase [mm/h]
Ruzillon	71.8	5.6		8	31	30.4	17	0.9	0.07
BoisVuacoz						41.5	27	1.43	0.04
Esserts						17.5	7.5	0.52	0.04
Corbassière						32.5	17.0	0.92	0.08

Table 3-15 Hydro-meteorological context between 02 -07 November 2002

Event number 16 is presented to illustrate the stream response to small rainfall event with low intensities in wet antecedent conditions. Hydrograph analysis reveals that all considered streams react quickly even to small rainfall inputs and the peak discharges are between 2-5 times the observed base flow before the considered event.

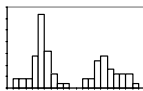
Event 16 09-10. 11. 2002	Total rainfall [mm]	P [mm/h]	Rainfall structure	ETP [mm]	ARI [mm]	LET [mm]	LER [mm]	Qmax [mm/h]	Qbase [mm/h]
Bois-Vuacoz	15	3.2		3	81	8.0	3.5	0.48	0.09
Ruzillon						6.5	2.0	0.36	0.12
Esserts						3.7	0.7	0.18	0.08
Corbassière						6.5	2.0	0.36	0.15

Table 3-16 Hydro-meteorological context between 09 -10 November 2002

The last analysed event occurred towards mid-November 2002, in wet antecedent conditions and characterises itself by an important volume and moderate to high rainfall intensities. All considered streams reacted promptly to this input precipitation, the peak discharge being between 12 times (Corbassière, Esserts, Ruzillon) and 23 times (Bois Vuacoz) greater than the measured baseflow before the considered event.

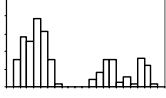
Event 17 14-15.11. 2002	Total rainfall [mm]	P [mm/h]	Rainfall structure	ETP	ARI [mm]	LET [mm]	LER [mm]	Qmax	Qbase
Bois-Vuacoz	48	8		2	63	31.15	19.70	3.22	0.13
Ruzillon						24.0	13.6	2.02	0.16
Esserts						19.0	9.62	1.55	0.12
Corbassière						25.0	12.2	2.35	0.2

Table 3-17 Hydro-meteorological context between 14 -15 November 2002

A brief synthesis of this hydrometric analysis reveals, even in the absence of other kind of information, a first pattern of the hydrological behaviour of the study catchments:

- ❑ Bois Vuacoz catchment is reacting very quickly even to the smallest rainfall inputs and even in dry antecedent conditions. This catchment response is probably motivated by geological conditions: impermeable morainic clayey deposits with low hydraulic conductivities that are covering almost 90% of the total basin surface.
- ❑ Esserts catchment behaviour is completely different in the sense that its response is very late to appear and the increase of the discharge is limited even for the big rainfall events. Geological conditions might also explain these differences: only some more than 5% of the basin surface is covered by morainic formations. The rest is represented by molassic deposits formed by sandstone and altered sandstones with better hydraulical properties.
- ❑ The hydrographs of Corbassière and Ruzillon catchments have intermediary characteristics between those presented for Bois Vuacoz and Esserts. From the geological point of view the proportion of morainic deposits vary between 60 for Ruzillon and 55 % for the Corbassière catchment.

3.1.2 Environmental tracing

The environmental tracing is one of the keys to understanding the hydrological processes that occur at the catchment scale. Peters (1994) considered that of “all of the methods used to understand hydrologic processes in small catchments, the use of tracers has been one of the most productive in terms of providing most of the new insight to hydrologic processes”. Many applications have been conducted in different parts of the world and on different catchments concerning application of the environmental tracing.

On the Haute-Mentue catchment the environmental tracing has become a routine tool to study the hydrological behaviour and the hydrological processes that occur at the catchment scale. Application of the environmental tracing on the Haute-Mentue catchment has made the subject of several PhD theses at HYDRAM Laboratory (Jordan (1992), Iorgulescu (1997), Joerin (2000)) and that is why the details of this application will not be presented here. Jordan (1992) was the first to apply the environmental tracing on the Haute Mentue catchment. He used Oxygen-18 to separate the flood hydrograph in two components: new and old water and demonstrated that the general conditions

imposed by the use of such model weren't completely fulfilled. Indeed, he noticed that the groundwater couldn't be characterized by a unique tracer concentration, as the O18 concentration of the water in the upper part of the soil profile was different from those of the lower layers. Following these conclusions, Iorgulescu (1997) has definitely shown that the use of a two components chemical models was not appropriate for the Haute-Mentue catchment. Based on an EMMA (*End Member Mixing Analysis*) approach (Christophersen et al. (1990)), and in order to distinguish between the soil and the groundwater component, he developed a three components chemical mixing model using calcium and silica as tracers. The chemical model has been further integrated in a computer program: AIDH[®] (*Analyse d'Incertitude des Décompositions des Hydrogrammes*) (Joerin et al. (2002)), which is able to perform hydrograph separation and to analyse the hydrograph separation uncertainty.

Chemical mixing model definition

The EMMA model (Christophersen et al. (1990)) was used to separate hydrographs into three components based on concentrations of two chemical tracers: calcium and silica. Iorgulescu (1997), after a detailed analysis of the environmental tracers on the Haute-Mentue catchment, concluded that calcium and silica could be used as tracers to identify three runoff components.

The concentration of the two tracers is clearly different for the three components:

- rainwater is completely depleted in calcium and silica,
- groundwater is considerably enriched in calcium because of the contact with the carbonated bedrock and also in silica.
- soil water is the most difficult component to define: the calcium content is much lower than those of the groundwater but silica concentrations are spatially and temporally highly variable and the median values are only a little lower than those of the groundwater.

Definition of the three end-members has been done by using all the samples collected on the Haute-Mentue catchment during 1998-2002 (Joerin et al. (2002)). We used in this work model 3 of Joerin (2000): the rainwater and soil water definitions were constant for all considered periods and for all the catchments while the chemical definition of the groundwater was considered unique for each considered catchment and it was defined by the calcium and silica concentrations measures in the stream water at low discharges (Figure 3-2).

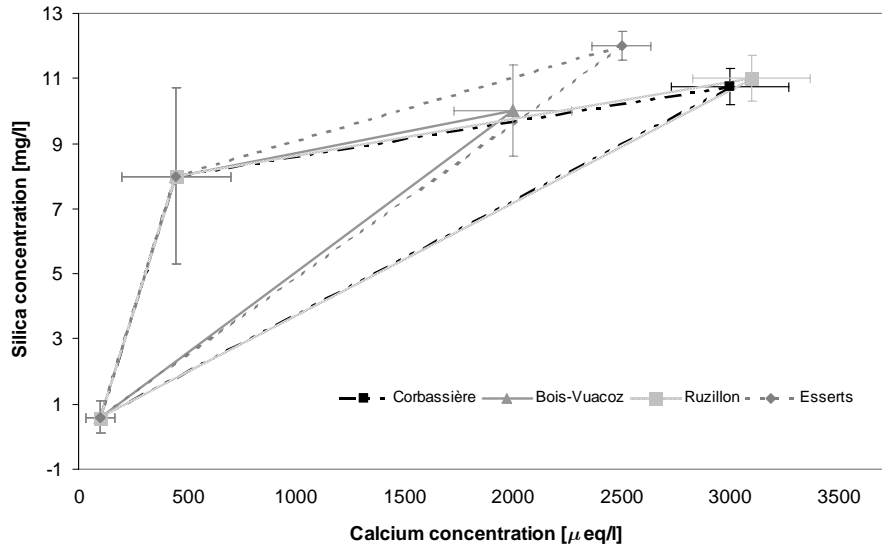


Figure 3-2 Chemical triangles defining the three end-members of the EMMA chemical mixing model for the Haute-Mentue catchment

In order to separate the flood hydrograph, the following mass balance system equations must be solved at each time step where chemical information is available:

$$\begin{cases} 1 = X_{\text{groundwater}} + X_{\text{soil}} + X_{\text{rainfall}} \\ C_{\text{Ca-stream}} = X_{\text{groundwater}} \cdot C_{\text{Ca-groundwater}} + X_{\text{soil}} \cdot C_{\text{Ca-soil}} + X_{\text{rainfall}} \cdot C_{\text{Ca-rainfall}} \\ C_{\text{Si-stream}} = X_{\text{groundwater}} \cdot C_{\text{Si-groundwater}} + X_{\text{soil}} \cdot C_{\text{Si-soil}} + X_{\text{rainfall}} \cdot C_{\text{Si-rainfall}} \end{cases} \quad (3.1)$$

where:

$$X_{\text{groundwater}} = \frac{Q_{\text{groundwater}}}{Q_{\text{total}}}; X_{\text{soil}} = \frac{Q_{\text{soil}}}{Q_{\text{total}}}; X_{\text{rainfall}} = \frac{Q_{\text{rainfall}}}{Q_{\text{total}}},$$

$Q_{\text{groundwater}}$, Q_{soil} , Q_{rainfall} represent the groundwater, soil and rainfall contributions to the total discharge Q_{total} ;

$C_{\text{Ca-groundwater}}$, $C_{\text{Ca-soil}}$, $C_{\text{Ca-rainfall}}$ represent the concentrations in calcium of the three end-members: groundwater, soil and rainfall and $C_{\text{Ca-stream}}$ is the measured calcium concentration in the stream;

$C_{\text{Si-groundwater}}$, $C_{\text{Si-soil}}$, $C_{\text{Si-rainfall}}$ represent the concentrations in silica of the three end-members: groundwater, soil and rainfall and $C_{\text{Si-stream}}$ is the measured silica concentration in the stream;

Here, we used the AIDH model of Joerin et al. (2002) in order to separate the hydrograph into its three components. We performed a Monte Carlo sampling from the observed calcium and silica distributions of the groundwater, soil water and rainfall in order to make use of the uncertainty that characterize the chemical definition of these three end-members. This statistical uncertainty is then propagated on the model output resulting in uncertainty bounds of the computed model components. Joerin (2000) studied in detail the uncertainty associated with decomposition of hydrographs and the interested reader can consult this reference. Although we considered the uncertainty of the chemical definition of the end-members, we used here only the median of the resulting hydrograph separations for further analysis.

In the next part of this chapter we will analyse some of the sampled events during 2001-2002 period in order to analyse the hydrological behaviour of Corbassière catchment.

Hydrograph separation – Spatial variability

During the period between mid-October and mid-December 2001, dry meteorological conditions explain why only a single important rainfall-runoff event occurred. The meteorological context for this event is presented in Table 3-1.

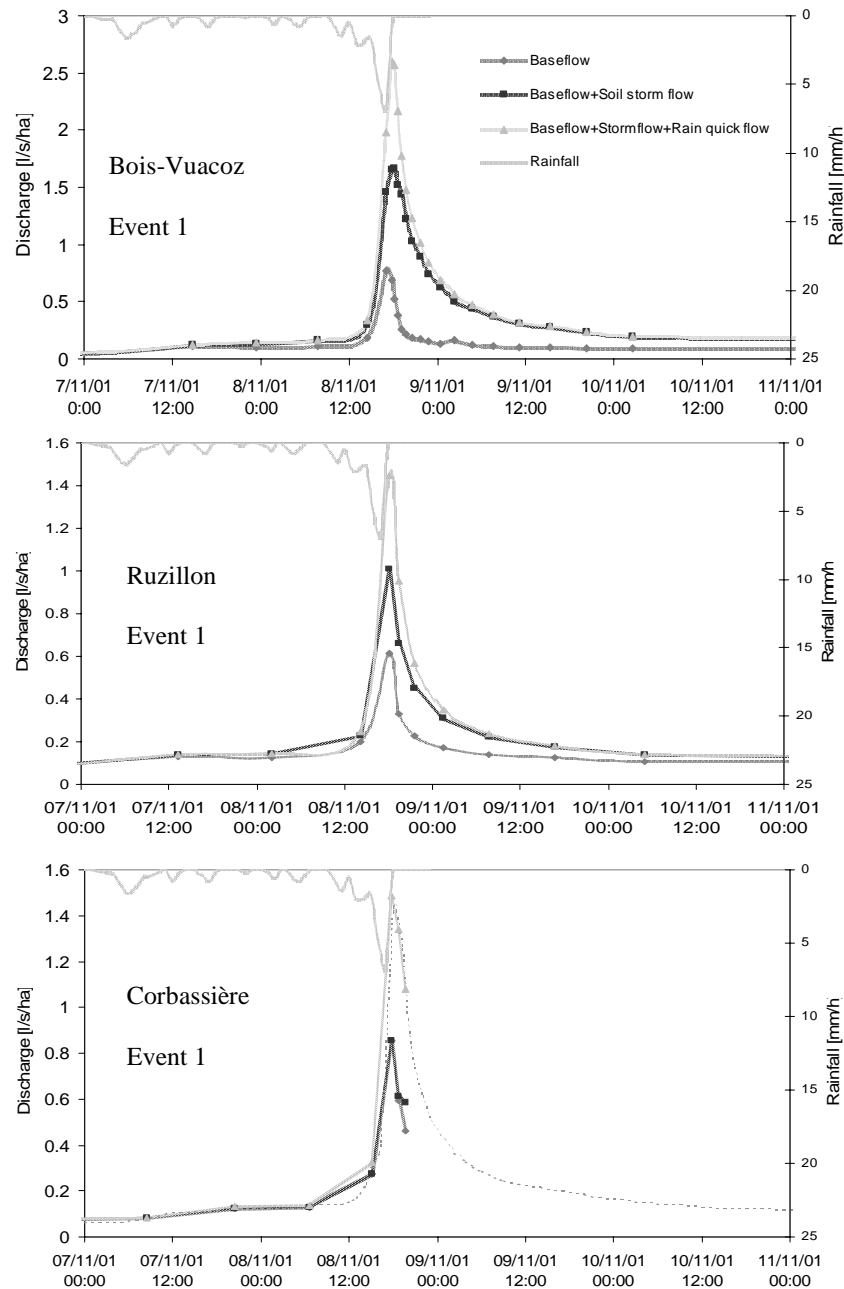


Figure 3-3 Hydrograph separation using calcium and silica tracers for Bois-Vuacoz, Ruzillon and Corbassière catchments (dark grey- groundwater component, black - soil water component; light grey- rain water component)

Figure 3-3 shows the results of the hydrograph decomposition for three sampled catchments. Comparison of these decompositions indicates that even after dry antecedent conditions (12 mm of rainfall for the 10 days preceding the considered event) the soil component is slowly growing and finally significantly contributing to the total runoff at least for Bois-Vuacoz and Ruzillon catchments. Conversely, the total runoff of Corbassière catchment is formed essentially by the groundwater flow and by the rainfall water. These results are confirming those presented by Joerin (2000) and Talamba (1999)

who concluded that the total discharge at Bois-Vuacoz catchment is essentially represented by water coming essentially through the soil horizons even in dry antecedent conditions.

Further hydrograph decompositions are presented for Bois-Vuacoz, Ruzillon, Esserts and Corbassière catchments during the year 2002.

BOIS-VUACOZ CATCHMENT

Figure 3-4, Figure 3-5 and Figure 3-6 present the decompositions of the flood hydrographs for Bois-Vuacoz catchment during some sampled events in spring, summer and autumn of the year 2002.

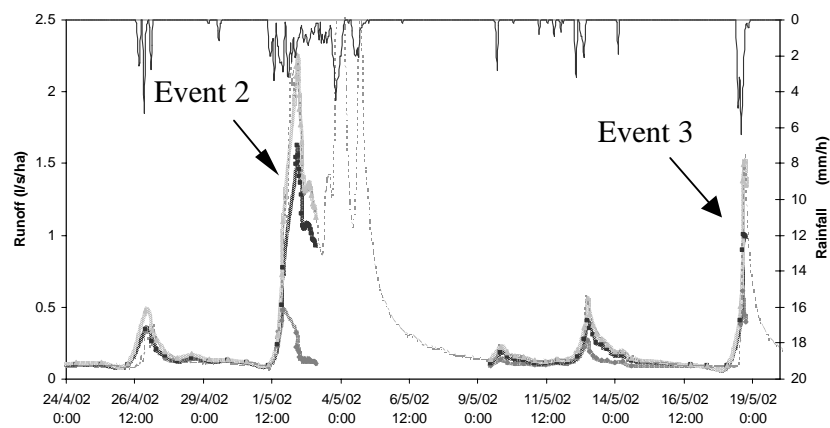


Figure 3-4 Hydrograph decomposition for Bois-Vuacoz catchment during April-May 2002 (dark grey - groundwater component, black - soil water component; light grey- rain water component)

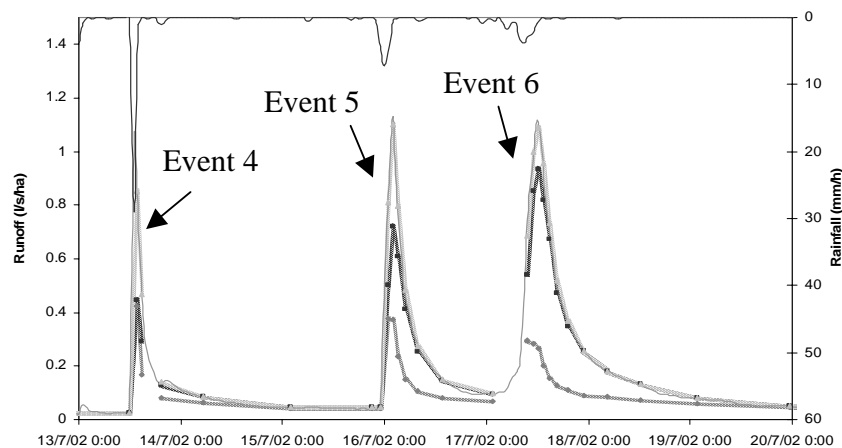


Figure 3-5 Hydrograph decomposition at Bois-Vuacoz catchment in July 2002 (dark grey - groundwater component, black - soil water component; light grey- rain water component)

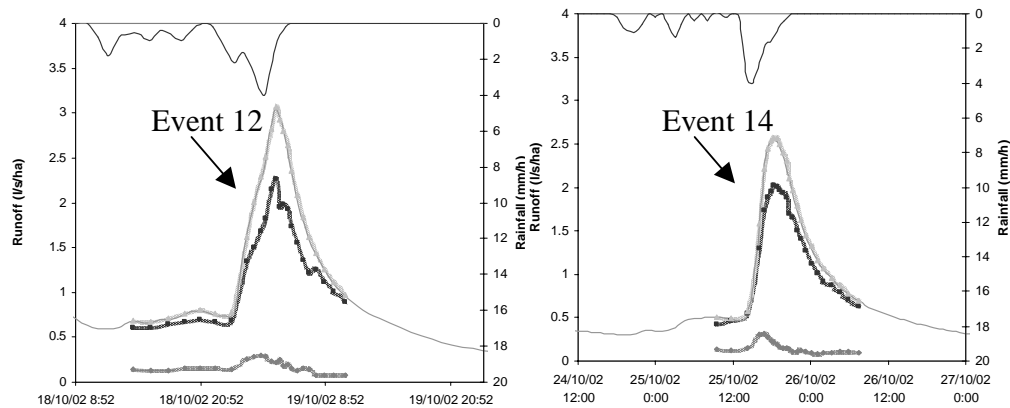


Figure 3-6 Hydrograph decomposition at Bois-Vuacoz catchment in October 2002 (dark grey - groundwater component, black - soil water component; light grey- rain water component)

As previously discussed, the hydrological behavior of the Bois-Vuacoz catchment is distinguished from the other studied catchments in that the most important component contributing to the floods is represented by the soil water (Figure 3-4, Figure 3-5 Events 5,6 and Figure 3-6). This is valid for all considered events but one. The exception here is represented by the 13-14 July event (Figure 3-5-Event 4) where strong rainfall intensities of 30 mm/h occurred in a small lapse of time. Hydrograph decomposition evidences that the resulting discharge was formed essentially by rainfall water and groundwater.

ESSERTS CATCHMENT

Hydrograph analysis for Esserts catchment indicates that this catchment is reacting differently from Bois-Vuacoz catchment at least after dry antecedent conditions. Indeed, the events of 16-17 July 2002 (Figure 3-8, Event 5) and 16-17 October 2002 (Figure 3-9, Event 11) occur after long periods without important precipitation. The soil storage must be very low and the soil water component is less contributing to the total discharge. For periods with wetter antecedent conditions one can see that the soil water component is contributing significantly to the total discharge and this behaviour approaches those of Bois-Vuacoz catchment (Figure 3-7- Events 2,3; Figure 3-8-Event 6, Figure 3-9-Events 12,13). The same observation as for Bois-Vuacoz catchment is to be made for small duration strong rainfall intensities events (13-14 July 2002), which determine total hydrograph to be separated into almost two components: rainfall water and groundwater (Figure 3-8-Event 4).

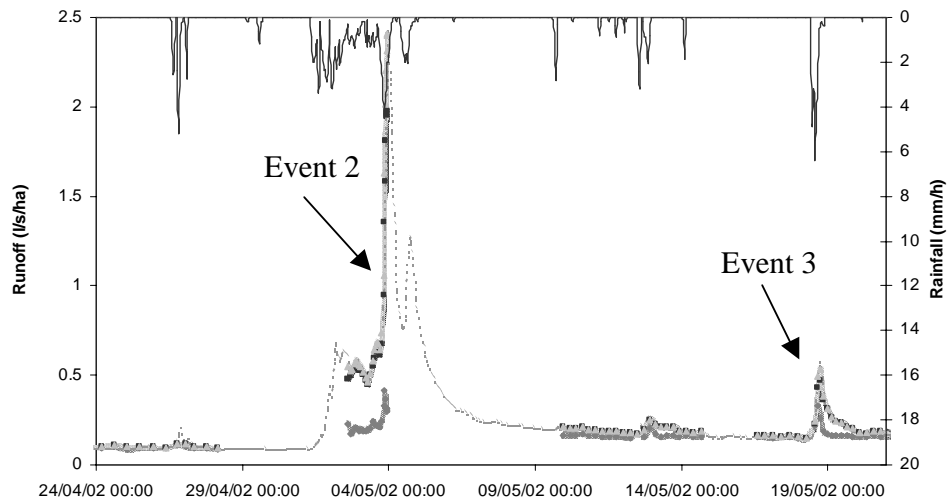


Figure 3-7 Hydrograph decomposition for Esserts catchment in April-May 2002 (grey colour- groundwater component, black colour- soil water component; light grey- rain water component)

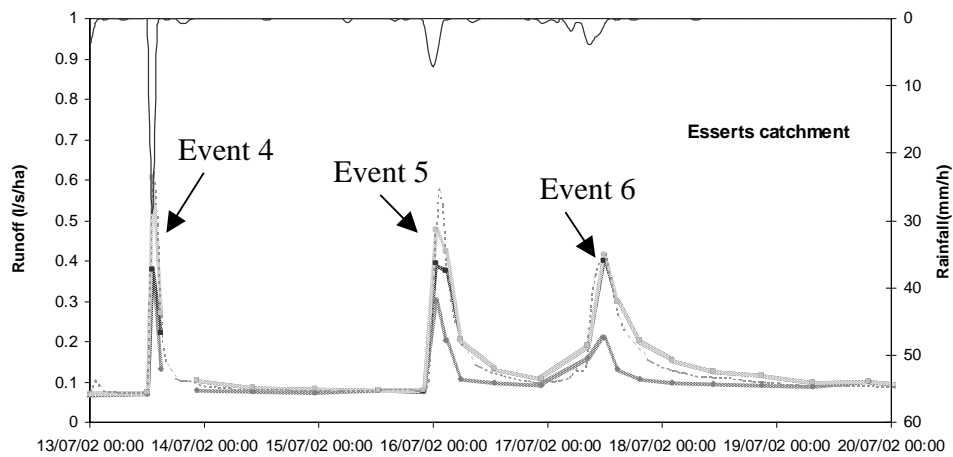


Figure 3-8 Esserts catchment: hydrograph decomposition in July 2002 (dark grey - groundwater component, black - soil water component; light grey- rain water component)

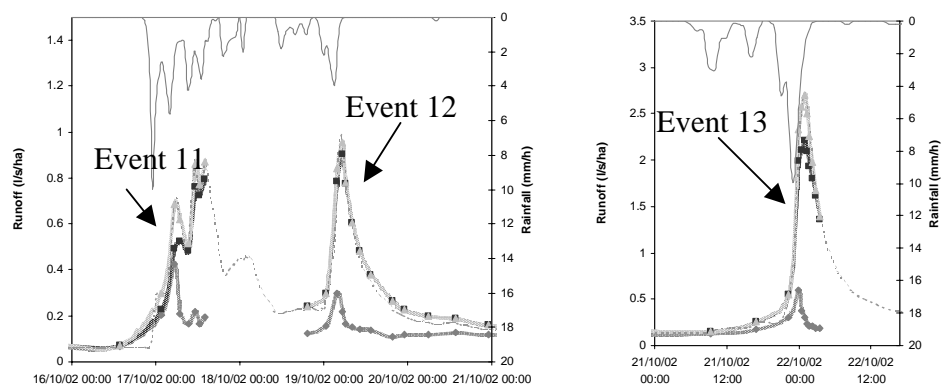


Figure 3-9 Esserts catchment: hydrograph decomposition in autumn 2002 (dark grey - groundwater component, black - soil water component; light grey- rain water component)

RUZILLON CATCHMENT

Figure 3-10 (Events 11, 12, 14 and 15) represents hydrograph decomposition for Ruzillon catchment for the autumn 2002 period. Unfortunately, the sampler that was installed previously on this site failed and chemical data is not available for the spring-summer period. Analysis of the hydrological behaviour of this catchment shows similarity with Bois-Vuacoz catchment in the sense that even after long periods without important precipitation, a strong contribution of the soil water to the total discharge is observed. The soil water component becomes quickly the most important one contributing to the flood for periods with wet antecedent conditions and rainfall intensities from small to moderate.

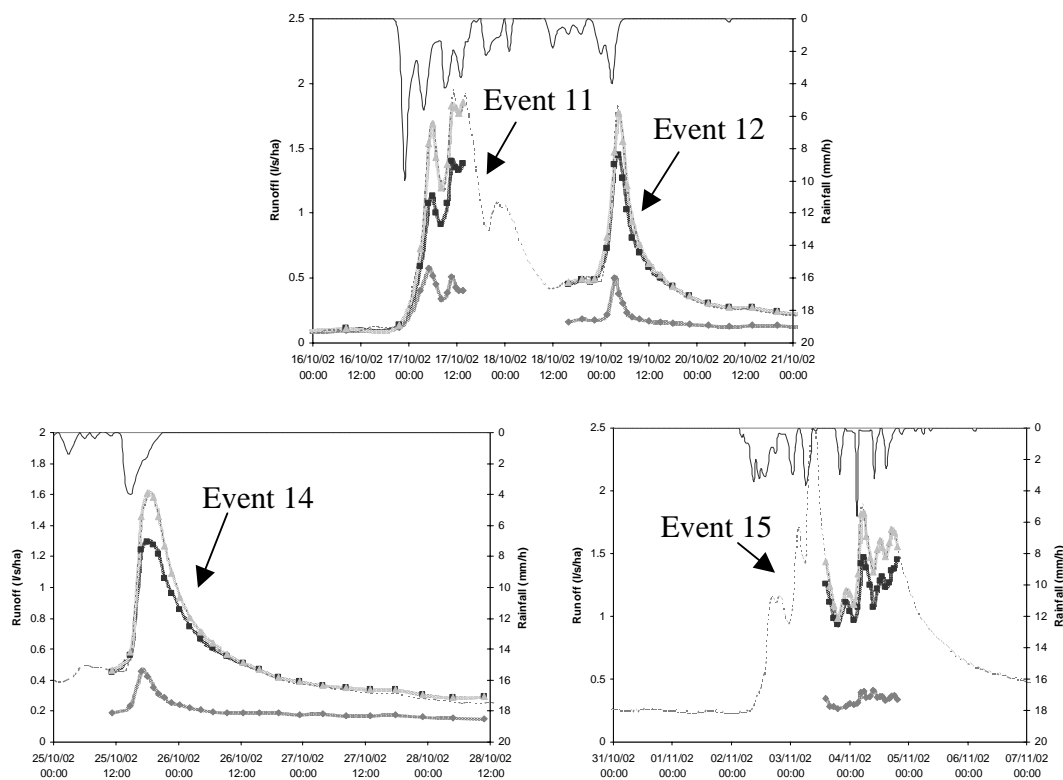


Figure 3-10 Ruzillon catchment: Hydrograph decomposition in autumn 2002 (dark grey - groundwater component, black - soil water component; light grey- rain water component)

CORBASSIERE CATCHMENT

Corbassière catchment presents a particular hydrological behaviour as revealed by the environmental tracing approach. Iorgulescu (1997), Joerin (2000) and Talamba (1999) showed that for this catchment the soil component is the least important component of the total discharge. In presence of wet antecedent conditions, this component's contribution increases but remains less important than those of the groundwater or the rainwater

(Figure 3-12, Events 11 and 12). The wetter the antecedent conditions, the more important the contribution of the soil water to the total discharge becomes (Figure 3-12-Event 14). A particular rainfall event occurred in 31 August 2002 with strong intensities (> 40 mm/h 10' average maximum intensity) determining a discharge of almost 6 l/s/ha at the Corbassière outlet. Chemical data available for the first part of this event show that under such conditions the total discharge was essentially composed of water coming from the direct rainfall and the groundwater (Figure 3-11, Event 9). This behaviour was also evidenced for the other catchments.

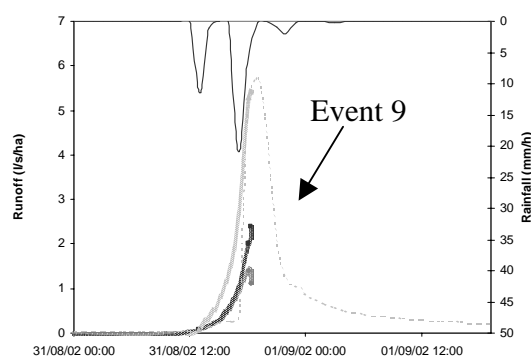


Figure 3-11 Corbassière catchment: storm hydrograph decomposition in Summer 2002 (dark grey - groundwater component, black - soil water component; light grey- rain water component)

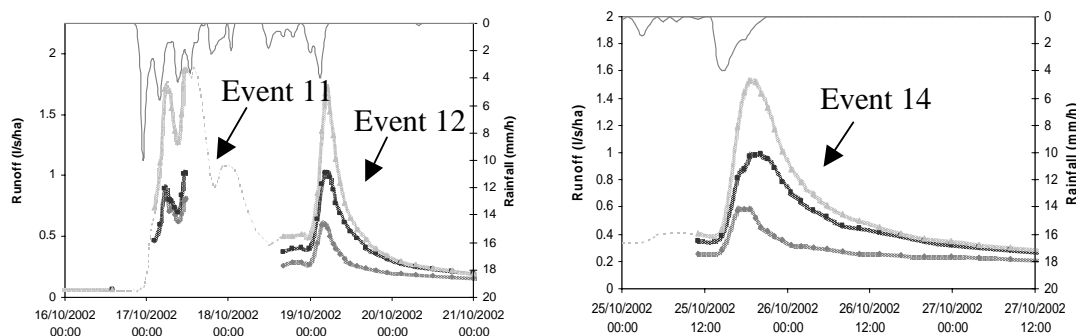


Figure 3-12 Corbassière catchment: hydrograph decomposition in Autumn 2002 (dark grey - groundwater component, black - soil water component; light grey- rain water component)

Environmental tracing on the Haute –Mentue catchment: comments

Table 3-18 presents a synthesis grouping the AIDH computed contribution of the three components to the peak discharge for the sampled events during the period comprised between Autumn 2001 – Autumn 2002 for all considered catchments.

No.event	P [mm]	ETP [mm]	API [mm]	Antecedent conditions	Bois Vuacoz			Esserts			Ruzillon			Corbassière		
					24 ha			33 ha			18 ha			195 ha		
					Rain	Soil	Gw	Rain	Soil	Gw	Rain	Soil	Gw	Rain	Soil	Gw
1	31.6	7	12	dry	36	37	26	-	-	-	30	27	42	42	0	58
11-a	33	5	16	dry	-	-	-	28	9	62	33	36	30	48	0	52
3	30	17	22	dry	35	36	30	12	39	48	-	-	-	38	0	62
5	17	23	52	dry	35	32	34	18	20	63	-	-	-	-	-	-
11-b	70	5	64	wet	-	-	-	11	63	25	26	51	24	45	11	43
6	18	21	65	wet	14	61	24	3	46	50	-	-	-	-	-	-
2-b	108	20	80	wet	28	62	10	5	61	35	-	-	-	41	21	39
12	22	5	86	wet	26	67	7	6	72	23	18	60	21	40	26	33
13	39	5	106	wet	-	-	-	18	70	11	-	-	-	-	-	-
14	23	4	155	wet	22	71	7	-	-	-	19	54	26	36	25	38
Sampled storm events in summer 2002																
4	17-41	25	28	dry	48	3	50	38	0	63	-	-	-	-	-	-
9	32-63	15	21	dry	-	-	-	-	-	-	-	-	-	56	23	21

Table 3-18 Synthesis of the hydrograph decomposition for the Haute-Mentue main subcatchments for the events sampled in 2001-2002 (letters a and b refer at the first and respective second part of a multi-peak rainfall-runoff event)

To summarize the table above, one can see that different hydrological behaviours were observed for the three small head catchments (Bois Vuacoz, Esserts and Ruzillon) and the main catchment (Corbassière).

One obvious characteristic is that the soil component contributes significantly to the total streamflow discharge in the small head catchments. This is especially true for the humid periods when the soil water components reaches over 50% of the peak observed flows. After dry antecedent conditions, the soil water component is lower but remains one of the most important sources to the total discharge for the BOIS-VUACOZ and RUZILLON catchments. Both of these catchments are characterized by specific geographical conditions, which explain partially their hydrological behavior: geological formations such as quaternary morainic deposits (87% and 63% of the total surface of Bois-Vuacoz and respective Ruzillon catchments) with bad hydraulical conditions; soil types with a variable texture and layered horizons with different characteristics which influence superficial infiltration and laterally flow over different textural discordances; rich vegetation which influenced formation of an important macropores network which favour rapid delivery of the soil water to streams during wet periods.

For the ESSERTS catchment, the soil water component in dry conditions is the least important component of the streamflow. This is greatly determined by the different morphometry of this catchment with steeper slopes and incised stream channel. It seems that these conditions are a direct consequence of the geological conditions: tertiary molassic deposits (94% of the catchment surface) with thick altered sandstones that support better deep infiltration of the water and favours a deep circulation of the water at the contact with the bedrock. The morphometrical characteristics seem influenced by the stream channel orientation relative to the geological structure. Indeed, the river flows in an opposite strata direction which determines an obsequent valley with symmetric steeper hillslopes. The presence of the altered sandstone deposits contributes also by sustaining a higher baseflow than observed for the other catchments.

The CORBASSIÈRE catchment exhibits a completely different hydrological behaviour. In this catchment, the soil water component is by far the least important component that contributes to the total flow. Several hypotheses have been proposed to explain this particular characteristic. Joerin (2000) used a statistical regression approach to model the soil contribution to the total streamflow discharge. It suggested that the relative contribution of the soil water component to the total discharge is best explained by the meteorological variables (total rainfall and the antecedent precipitation index), catchment area and a geological recession constant. The statistical negative coefficient obtained for the catchment area dependent variable, confirm field observations that indicates that soil water contribution to the total discharge is varying inversely proportional with the catchment area. Several factors could explain this situation:

- geological evolution: almost 55% of the catchment area is formed by ancient wet regions that have been underlain by quaternary morainic impermeable deposits which don't favour infiltration and deep circulation of the groundwater;
- land-use: 20% of the Corbassière catchment is covered by cultures which are superposed on the ancient wet zones that have partially been drained; this means that direct rainfall precipitation that occurs at the soil surface is rapidly drained to the Corbassière stream.
- scale factor: Joerin (2000) proposed the hypothesis that this behaviour could be explained by a scale effect but the small number of available catchments doesn't allow for further confirmation or generalization.

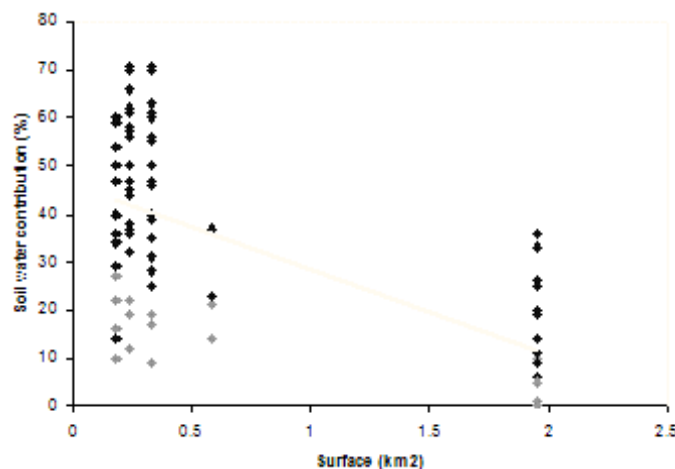


Figure 3-13 Correlation between the soil water contributions to the discharge and the catchment's discharges

Figure 3-13 presents the available data with the soil water contribution to the peak flows evaluated with the EMMA approach for several rainfall-runoff events during the 1993, 1998 and 2002 years. The light grey points correspond to dry and moderate antecedent conditions while the dark grey points correspond to wet antecedent conditions. Each column of points corresponds to one specific catchment whose area is figured on X-axis. The size of the statistical sample is not sufficient to make a statistical analysis between the soil water contribution to the flow and the catchment surfaces; nevertheless, the

general trend confirms our observation: the soil water contribution to the total discharge is diminishing with the catchment areas.

In conclusion, among the small-considered head catchments,

- the Bois Vuacoz is reacting more quickly than the others and systematically one can see that the soil component is rapidly increasing, becoming the most important flow components even after dry antecedent periods.
- the Esserts catchment shows slowly variation of the soil component after dry antecedent periods, the groundwater being most part of time the most important flow component. Esserts catchment is covered essentially by altered molassic tertiary deposits, which facilitate infiltration of the water.
- the Ruzillon catchment exhibits intermediary characteristics between the Ruzillon and Esserts catchments. This behaviour has been already reported by Talamba (1999) and Joerin (2000) and is due to the geological and lithological conditions of the Haute-Mentue head catchments. Recent quaternary morainic deposits cover large areas in Bois Vuacoz and Ruzillon catchments, which influence the hydrological properties of the soils.

The present results concerning the environmental tracing application for the Corbassière catchment complete and confirm those obtained previously by Iorgulescu (1997) and Joerin (2000). It seems that one major factor able to explain the main characteristics of the hydrological behaviour for the three analysed head catchments would be the geological one. The lithology (morainic or molassic) influenced the soil texture characteristics, and this will further influence the state of the soil initial humidity conditions before a given rainfall-runoff event. In our opinion, the lithological and the soil textural differences explain the main differences in the hydrological behaviour that have been observed for the head catchments.

In order to validate this hypothesis, a new experiment has been envisaged and finally conducted on two chosen sites with different lithological characteristics: one in Ruzillon catchment, in a region covered by morainic deposits and the second in Esserts catchment, where molassic formations are predominant.

We hope that this experiment will also contribute to a better understanding of the hydrological mechanisms that are responsible for the runoff generation at the hillslope scale and that it will help identification of main subsurface processes (lateral flow at the soil organic/mineral and/or at the soil/bedrock interfaces? (Joerin et al.), macropore flow?, perched water?) that might explain the important observed soil water contribution to the flood runoff.

Details of this new experiment and the main conclusions are presented here further.

3.2 Hydrological behaviour at the hillslope scale

Application of the environmental tracing brought important knowledge and helped improve understanding of the main characteristics of the hydrological behaviour on the Haute Mentue catchment. The environmental tracing is particularly important because it allows the study of hydrological processes at the catchment scale. Nevertheless its application does not allow the identification of the mechanisms responsible for flows through hill slopes. In fact, the hydrograph decomposition identifies the origin of flows but the mechanisms responsible for the stream flow generation cannot be determined from it (Elsenbeer and Lack (1996)). Indeed, water following different pathways can present the same tracer concentration or a mechanism can involve different kinds of water (chemical characteristics) (McDonnell (1990)). More generally, because of the equifinality problem (Buttle, 1994) it is not possible to identify the combination of hydrological processes from the application of only one observation method (Ambroise, 1998). Then in order to identify the water pathways and the mechanisms, which are at the origin of flood formation, it is necessary to associate hydrochemical observations to other types of measurements (Jenkins et al., 1994). Joerin (2000) concluded in his work that association of several techniques could be very useful in studying the hydrological behaviour of the Haute-Mentue catchment. Here, we used soil moisture local measurements in order to better understand the hydrological behaviour for two representative hillslopes on the Haute-Mentue catchment. Joerin (2000) has already used the TDR technique on the Bois-Vuacoz catchment with the aim (i) of studying the spatial variability of the near-surface soil moisture and (ii) of assessing the role of the micro topography in explaining observed patterns of the soil moisture spatial variability.

3.2.1 Time Domain Reflectometry (TDR) principles

TIME-DOMAIN REFLECTOMETRY is a testing and measurement technique that has found increasing usefulness in testing transmission lines, cables, connectors, and other wideband systems or components. Basically, time-domain reflectometry is an extension of an earlier technique in which reflections from an electrical pulse were monitored to locate faults and to determine the characteristics of power transmission lines. The technique used in time-domain reflectometry consists of feeding an impulse of energy into the system and then observing that energy as it is reflected by the system at the point of insertion. By analyzing the magnitude, deviation, and shape of the reflected waveform, one can determine the nature of the impedance variation in the transmission system. Also, since distance is related to time and the amplitude of the reflected step is directly related to impedance, the comparison indicates the distance to the fault as well as the nature of the fault. Jones et al. (2002) give a detailed presentation of the principles of this method and the main applications for the measuring of the soil water content. Water content is inferred from the dielectric permittivity of the medium, whereas electrical conductivity is inferred from TDR signal attenuation. The same authors considered that the main advantages of TDR over other soil water content measurement methods are:

- minimal calibration requirements —in many cases soil-specific calibration is not needed;

- lack of radiation hazard compared with neutron probe or gamma-attenuation techniques;
- high spatial and temporal resolution
- simplicity in operation, the method being able to provide continuous measurements through automation and multiplexing.

TDR – PRINCIPLES OF THE METHOD

A TDR system allows retrieving of the dielectric constant of the soil from the travel time analysis of an electromagnetic signal through a cable system including a rod probe. The relative dielectric constant ϵ_r of soil surrounding the probe is a function of the propagation velocity ($v = 2l / t$) according to:

$$\epsilon_r = \left(\frac{c}{v} \right)^2 = \left(\frac{ct}{2l} \right)^2 \quad (3.2)$$

where c is the light speed, t is the travel time of the electromagnetic signal to traverse the length (l) of the system (down and back – $2l$). The travel time is computed based on the apparent or electromagnetic length of a probe, which appears on a LCD Tektronix screen by changes in the waveform.

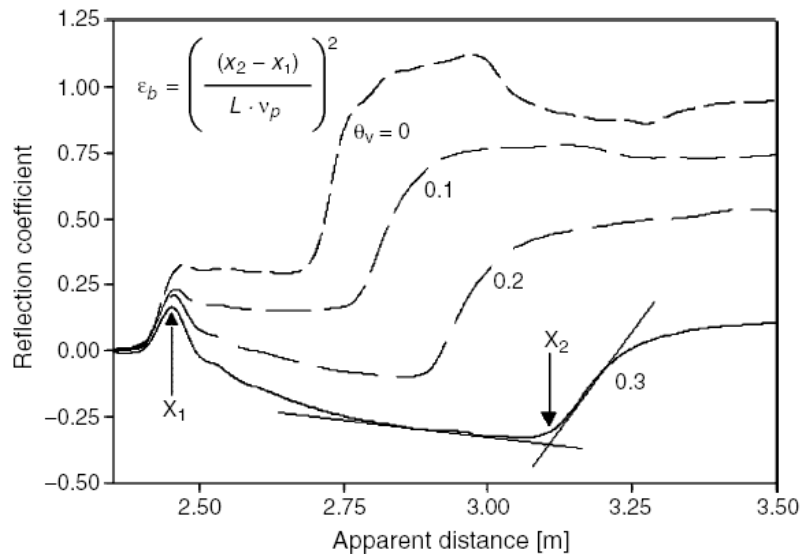


Figure 3-14 TDR signal displayed by Tektronix and apparent length determination (taken from Jones et al. (2002))

As precised in Jones et al. (2002), x_1 marks the entry of the signal probe and x_2 the reflection in the end of the probe (Figure 3-14). The apparent probe length ($x_2 - x_1$) increases as the water content increases, as the dielectric constant is greater for wetter media because of reduced propagation velocities of the electromagnetic signal through this kind of medium. The relationship between the apparent length and the relative dielectric constant is given below:

$$\varepsilon_r = \left(\frac{x_2 - x_1}{v_p l} \right)^2 \quad (3.3)$$

where the V_p is the relative propagation velocity usually chosen by the user at 0.99.

$$\text{Most generally we can write: } \varepsilon_r = \left(\frac{l_a}{l} \right)^2 \cdot \left(\frac{\alpha}{v_p} \right)^2 \quad (3.4)$$

where α is a calibration constant (generally close to 1).

The relative dielectric constant of the water is $\varepsilon_s = 81$ (at 20 °C) while the relative dielectric constant of the other soil components is much smaller (mineral soil $\varepsilon_s = 3$ to 5, ice $\varepsilon_i = 4$ and air $\varepsilon_a = 1$) and this property rends the technique almost insensitive to the soil texture and allows good retrieving of the soil water content. Nevertheless, several factors could affect the measurement of the dielectric constant such as porosity, volumetric density and temperature. In order to estimate the soil water content (θ) from the soil relative dielectric constant (ε_r) we used the formula presented in Topp et al. (1980):

$$\theta = -5.3 \times 10^{-2} + 2.92 \times 10^{-2} \cdot \varepsilon_r - 5.5 \times 10^{-4} \cdot \varepsilon_r^2 + 4.3 \times 10^{-6} \cdot \varepsilon_r^3 \quad (3.5)$$

This equation gives an appropriate description for soil water contents lower than 0.5 cm^3/cm^3 , which covers the most usual range of variation for the mineral soils. For clayey and high organic soil the relationship is to be used only with care.

Other relationships have been proposed to evaluate the soil water content from the dielectric constant such as Roth et al. (1990) which takes into account dielectric constants for the three water phases (liquid- ε_w , solid- ε_s and air- ε_a), the soil porosity (n), volume fractions for the three phases water constituents ($1-n$, θ , $n-\theta$), and a constant factor depending on the medium geometry in relation to the axial direction of the waveguide (β):

$$\varepsilon_r = \left[\theta \varepsilon_w^\beta + (1-n) \varepsilon_s^\beta + (n-\theta) \varepsilon_a^\beta \right]^{1/\beta} \quad (3.6)$$

This relationship was used by Joerin (2000) in order to study the spatial distribution of the soil moisture on the Bois-Vuacoz catchment but he concluded that a previous comparison of the two soil water content estimation methods gave similar results.

In this work, a comparison was also done between the two methods and we finally decided to work with the Topp formula because of the similar results and the much simpler equation.

3.2.2 Implementation of a TDR system on the Haute-Mentue catchment – field sites description

Based on the conclusions given by the environmental tracing approach, the TDR equipment was installed on two different sites in order to monitor the soil water content variation with the depth and along a typical hillslopes on the Haute-Mentue catchment. The two sites were chosen to represent the main hydro-geological conditions of the study catchment and they have been chosen in order to study the influence of lithology on the hillslope hydrological behaviour:

- Ruzillon site: morainic deposits with gentle slopes and clayey soil conditions;
- Esserts site: molassic deposits with steeper slopes and more permeable soil conditions.

The localization of the two sites is indicated in Figure 2-13. In order to monitor the relationship between soil moisture at different locations along the hillslope for each field location, three measurements plots noted with: “Near-Stream”, “Mid-Slope” and “Upper-Slope” were defined.

The geological map (Figure 2-4) shows that the most of the Ruzillon catchment is covered by morainic formations, which together with climatic conditions led to the formation of pseudogley soils (Reber (1993)). The hydromorphic characteristics seem influenced by the existence of different discontinuities that might have either a geological or a pedological nature. These soil types are spread on gentle slopes on a morainic substrate, with low hydraulic conductivities. The soil profile of such a typical morainic hillslope is given Table 3-19.

Depth [cm]	Horizon	Texture
0-10	Organic+A ₁	Silt-sandy, Organic silt
15-25	Transition Organic - Mineral A/B	Silt sandy -organic
20-50	B Silt	Silt, Silt sandy compact
50-120	B Silt-sandy + oxidation spots, stony at the bottom part	Sandy Silt
>120	C	Morainic deposits

Table 3-19 Soil profile characteristics at Ruzillon TDR site

The Esserts catchment is characterized by the presence of well-drained soils without hydromorphic spots until 100 cm, with the bedrock formed by the burdigalien weathered molasse. The typical soil profile is given below:

Profondeur [cm]	Horizon	Texture
0-25	A Organic	Silt sandy, Organic silt
25-50	A Mineral	Silt sandy
50-70	B	Silt sandy
70-100	Transition B/C	Sandy, Sandy silt
>100	C	Molasse

Table 3-20 Soil profile characteristics at Esserts TDR site

The sites noted: « Upper-Slope » are located about 12 m on the hill slope away from the streams, « Mid-Slopes » at about 10 m away from the streams and « Near-Stream » are within 2 m from the considered streams (Figure 3-16). The notations “upper” and “middle” are relative to the stream position and don’t refer to the total length of the hillslope which is about 80 m for the Ruzillon site and 100 m for the Esserts site. The tables below are presenting the textural profiles of the two TDR field sites. These locations have been chosen in the aim of monitoring the soil moisture regime changes at different distances along the hillslope as well as the spatial repartition of the potential contributive areas.

Depth	Texture			Depth	Texture		
[cm]	Sand %	Silt %	Clay %	[cm]	Sand %	Silt %	Clay %
Upper-Slope				Upper Slope			
0-10	55.2	32.5	12.3	0-10	57.2	29.7	13.2
15-25	54.6	31.9	13.5	15-25	55.8	29.8	14.4
30-45	61.8	26.5	11.7	30-45	53.6	32.3	14.1
45-55	69.9	22.4	7.6	45-55	57.1	29.4	13.5
Mid-Slope				Mid-Slope			
0-15	54.0	32.1	13.9	0-15	56.6	29.1	14.4
15-25	50.3	32.6	17.1	15-25	57.0	28.1	15.0
30-45	51.6	32.1	16.3	30-45	56.1	30.3	13.6
45-55	59.6	27.9	12.5	45-55	55.0	30.7	14.2
55-65	51.0	33.5	15.5	55-65	53.2	32.2	14.6
60-70	54.4	31.1	14.5				
70-75	59.3	28.8	12.0				
Near-Stream							
15-25	63.1	26.1	10.8				
30-45	67.7	22.5	9.7				
45-55	72.7	19.0	8.3				

Table 3-21 Texture profiles at Ruzillon (a) and Esserts (b)

A comparison between the textural profiles of the two sites shows texture variation for the Ruzillon site which is common to the soils developed on morainic formations while the textural profile at the Esserts site is much more uniform with small depth variation which is common for soils developed on altered molassic deposits.

TDR – EQUIPEMENT AND EXPERIMENT SETUP

The measuring configuration was possible through the multiplexing facility of the TDR equipment. Three-second level multiplexers are connected to the central unit through a first level multiplexer. The TDR system includes a cable tester Tektronix 1502 B commanded by a Campbell Scientific data-logger (CR10 and CR21X types), four multiplexors (SMX50 type) and several pairs of rods (Figure 3-15). The rods have a length of 10 cm and were inserted vertically into the soils and the TDR measurements were obtained automatically by programming the data loggers and thus hourly measurements are available for the study period. The program that was implemented (Software PC208e, Campbell Scientific) in order to run the system automatically as well

as the calibration procedures are given in Karaoui (2002). The two data-loggers have been programmed to work on an hourly basis. The general scheme of the implemented system is presented in Figure 3-16 and more details can be found in Karaoui (2002).

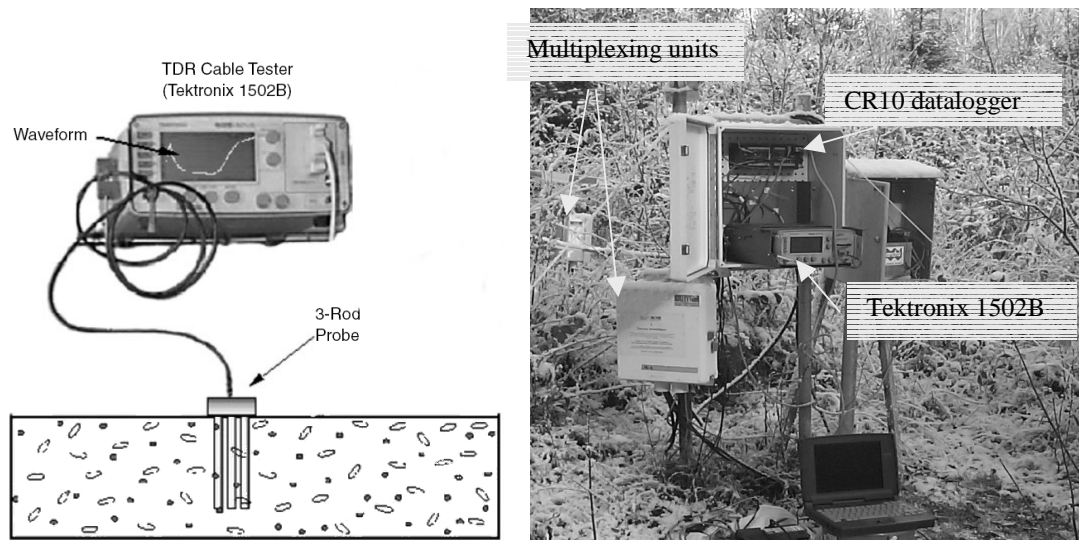


Figure 3-15 TDR equipment (a) and field set-up (b)

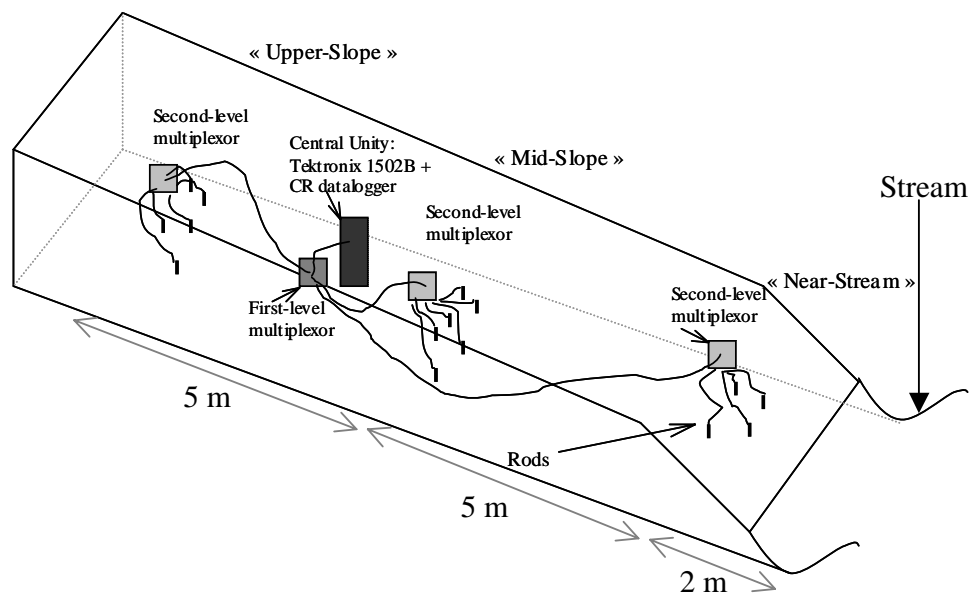


Figure 3-16 Field implementation of the TDR equipment

3.2.3 Soil moisture temporal variability

Two intensive field campaigns have been organized in order to install the TDR systems and to monitor the soil moisture at different depths at the two sites Ruzillon and Esserts in during Mid-July 2002 -January 2003 (A) and June –December 2003 (B).

A. 2002 Intensive field campaign

RUZILLON SITE: Figure 3-17, Figure 3-18 and Figure 3-19 present the temporal dynamics of the soil moisture at Ruzillon for the three sites: “Upper-Slope”, “Mid-Slope” and “Near-Stream”. Dynamics of the soil moisture at the Ruzillon site shows two different regimes of the soil moisture over the study period. The two “Upper-Slope” and “Mid-slope” sites exhibit the same general behaviour during the study period (Figure 3-17) and (Figure 3-18 top). In the summer period, the soil water content is lower and long recessions can be observed for periods without important precipitation. Even if the soil storage is considerably reduced, the soil profiles react quickly after important storm events such as those that occurred on 31 August 2002. In September, with little precipitation (32 mm) and estimated potential evapotranspiration that almost equals the total rainfall for the month (23 mm), the soil moisture is slowly decreasing for the entire soil profile. The transition period from the dry to the wet season (second part of October) is rapid and the soil profile water content varies during almost the entire wet period (November-December) between the soil field capacities and the soil saturation. The high soil moistures values measured even for the soil horizons close to the surface are confirmed by the water table in a 60 cm deep piezometer installed on the site beginning with 2 November 2002 (Figure 3-18 down).

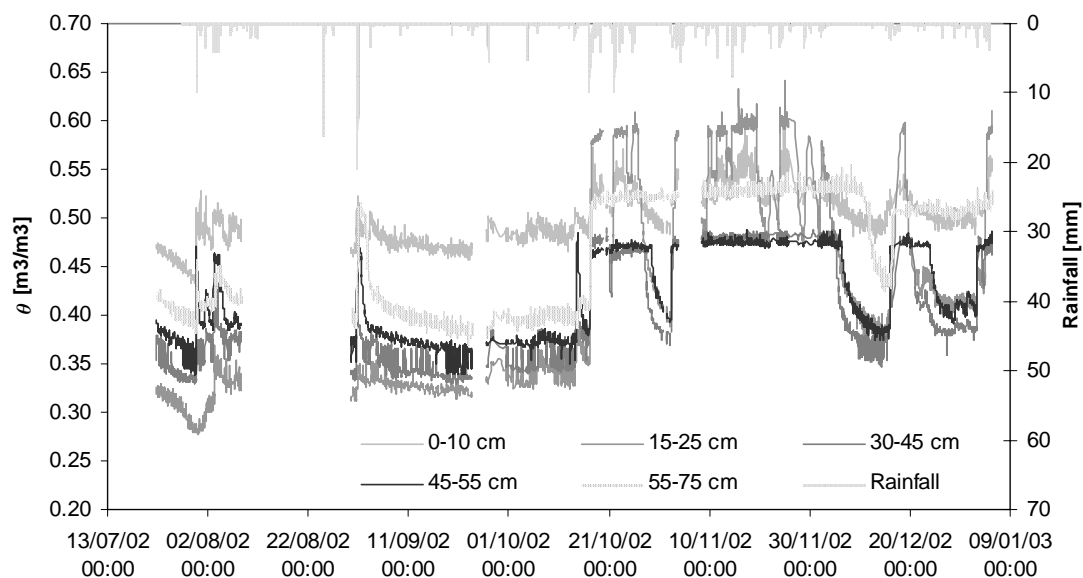


Figure 3-17 Ruzillon: Upper-Slope site - Soil moisture time evolution during July 2002 –January 2003 period

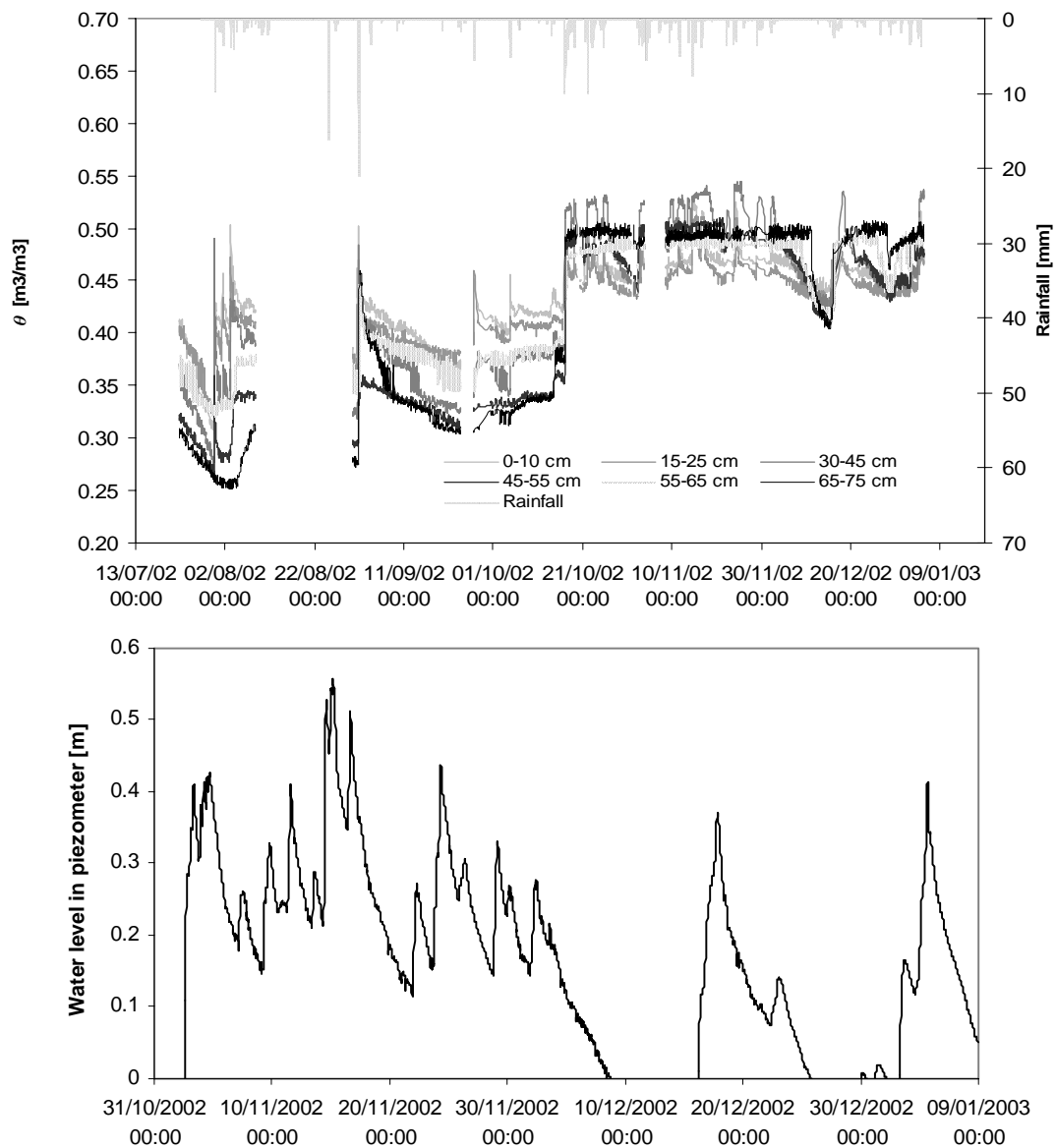


Figure 3-18 Ruzillon site: “Mid-slope” – soil moisture time evolution (top) and water level in a 60 cm shallow piezometer (down)

The site “Near-Stream” shows a different behaviour typical for the lower part of a hillslope (Figure 3-19). For the summer period, soil moisture values are higher than those observed for the two other sites but this soil profile doesn’t reach saturation conditions for the upper soil horizons even during the wet period (October-December 2002). The lower soil horizons, close to the sandstone bedrock are reaching saturation very quickly. Even if only the soil moisture information doesn’t allow for further interpretation concerning the water circulation, the plot below suggest that a very rapid drainage occurs

for the upper soil horizons which would explain why saturation conditions have been never reached during the study period.

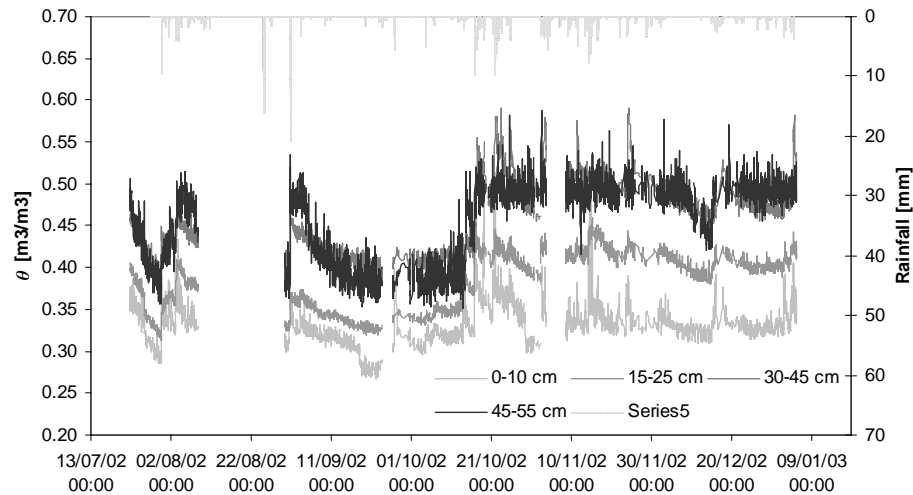


Figure 3-19 Ruzillon site: “Near-Stream” site – soil moisture time evolution

ESSERTS: The same kind of analysis has been conducted for the Esserts site for the “Upper” and the “Mid-Slope” field plots. Because of a technical failure, no data has been recorded for the “Near-Stream” field site. The available time series of the soil moisture cover October 2002 - beginning of January 2003 period as the available CR21X datalogger needed longer time to be updated. Because of the same technical problems, the data series recorded with this datalogger are in general much more noisier than those recorded at Ruzillon site with the CR10 datalogger. In these circumstances, as the soil moisture readings were noisy for this site, we performed a moving average filtering over 20 time steps in order to maintain the main trend of the observed data and to remove the background noise.

A simple appreciation of the two graphs (Figure 3-20 and Figure 3-21) indicates that the difference between the dry (first part of October) and the wet period (November to December) is much less pronounced for the Esserts site. The transition period seems longer and only the upper soil horizons respond more rapidly to the rainfall input. The lower soil horizons respond very slowly and only in wet conditions and after important rainfall is an increase in the soil moisture observed for the lower soil horizons. For this site, over the whole study period, saturation of the entire soil profile was not observed.

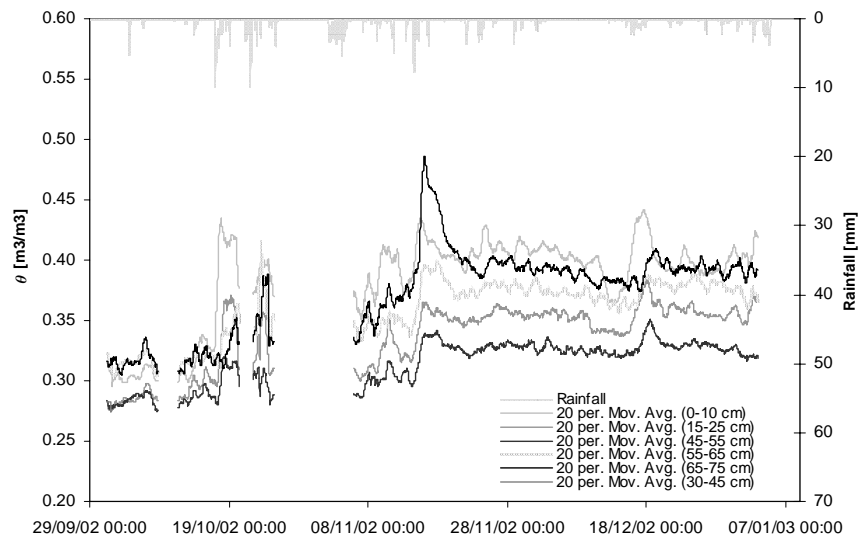


Figure 3-20 Esserts site: “Upper-Slope” – soil moisture time evolution

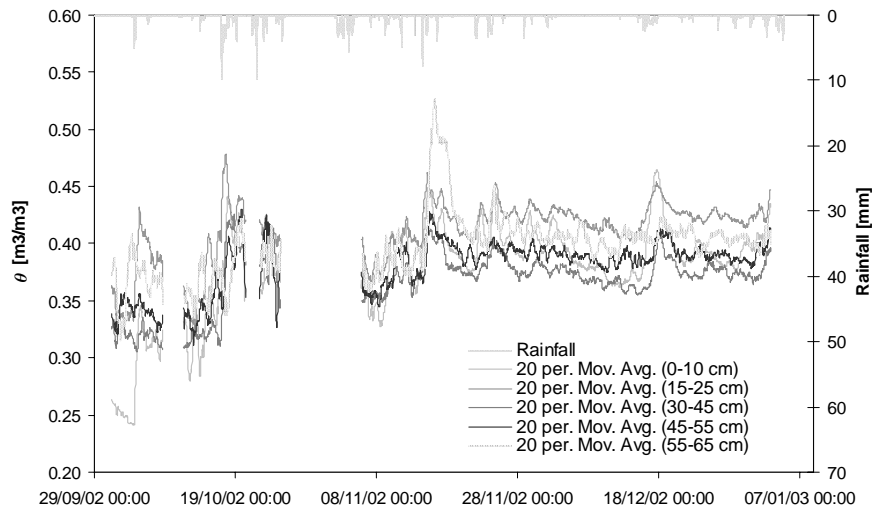


Figure 3-21 Esserts site: “Mid-Slope” – soil moisture time evolution

B. 2003 Intensive Field-Campaign

RUZILLON SITE: Soil moisture measurements are available only for the Ruzillon site as the TDR Esserts set-up failed.

The analysis of the 2003 period reveals that the dynamics of the soil water are strongly influenced by the exceptional meteorological conditions that characterized this year. Figure 3-22 and Figure 3-23 show, for the “Mid-Slope” and “Upper-Slope”, that the soil moisture registered a steady decrease during all the summer period, with very low levels (soil moisture between $0.2 \text{ m}^3/\text{m}^3$ for the upper soil horizons and $0.35 \text{ m}^3/\text{m}^3$ for the lower ones) towards mid-July and beginning of August. The great values of soil deficit

are also explained by the high values of potential evapotranspiration (145 mm, 140 and 170 mm for June, July and respectively August) compared with the medium precipitation input (41 mm, 93 mm, 122 mm). These meteorological conditions explain the soil moisture temporal trend for the autumn period. Indeed, the soil storage increases very slowly during the autumn period, this being essentially determined by the small quantity of precipitation that has fallen. Practically, until the end of the year, the groundwater level did not reach the upper soil horizons. The lower soil horizons (65-75 cm) didn't reflect any of the rainfall events that occurred between the beginning of September and mid-October 2003 and the recharge of the groundwater was very slow.

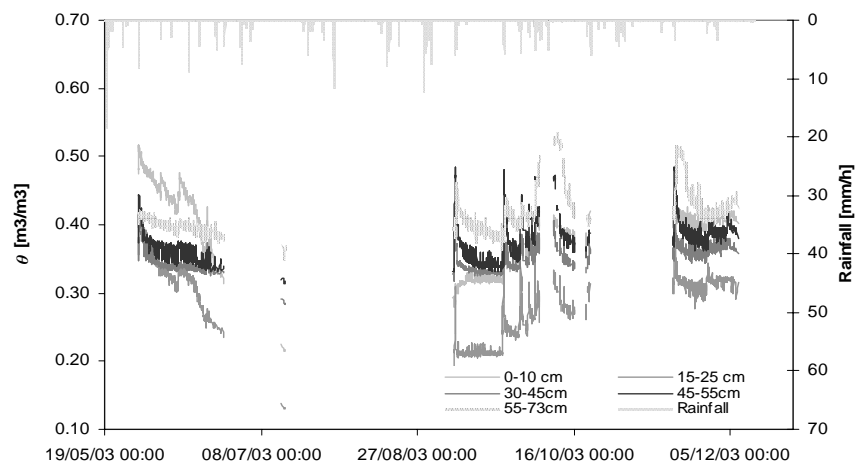


Figure 3-22 “Upper-Slope”: Ruzillon site soil moisture dynamic during May-December 2003 period

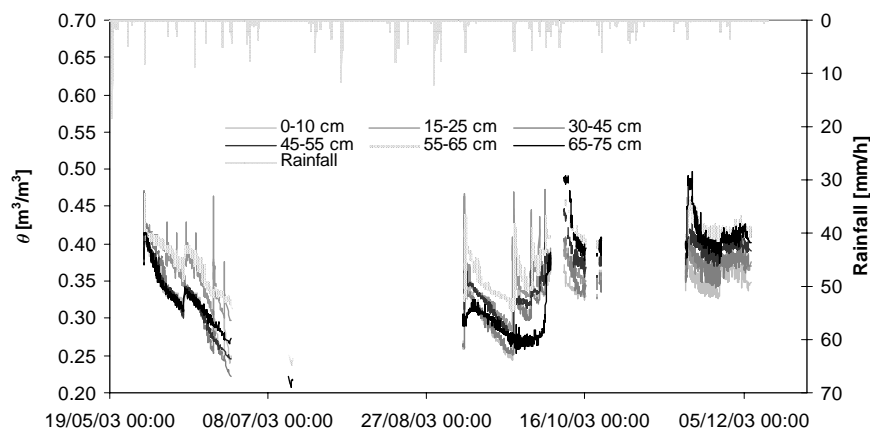


Figure 3-23 Ruzillon site – “Mid-Slope”: soil moisture dynamic during May-December 2003 period

The soil moisture dynamic for the “Near-Stream” site exhibits almost the same characteristics as presented before for the 2002 year, but much more attenuated (Figure 3-24). The long summer “recession” is also present but it seems that the soil storage is much less influenced by the lack of precipitation. The lower profiles placed at the contact with the bedrock have greater soil moisture values than the upper ones and this is the general characteristic of the soil moisture profile for the down slope location. For the

autumn period we retrieve the same behavior such as those observed for the previous year. The lower part of the soil profile has soil moisture close to the saturation and thus reacts very quickly to the rainfall input.

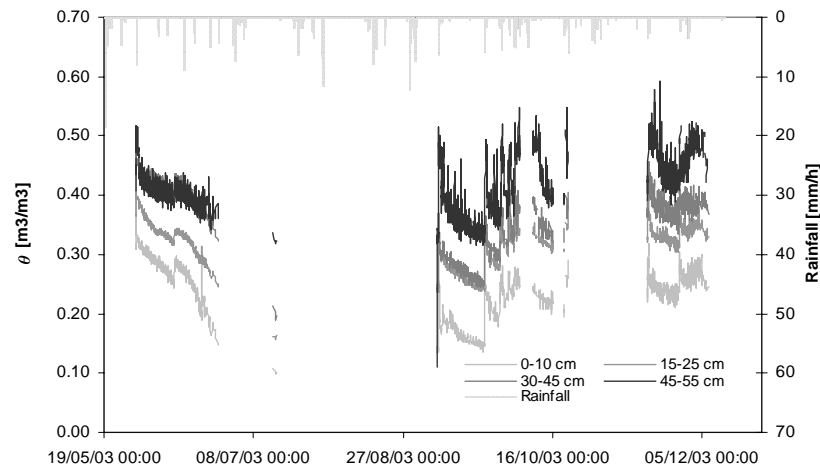


Figure 3-24 “Near-Stream” Ruzillon site: Soil moisture dynamic during May-December 2003 period

These field observations confirm the hypothesis of a variable contributing area: while the “Upper-Slope” site rarely reaches saturated conditions, the part of the catchment, which is promptly active following a rainfall event is the closest one to the stream. Comparison between 2002 and 2003 soil moisture dynamics indicate that the contributive area is not stable and varies in space depending on the antecedent conditions and the magnitude of the rainfall events. For the autumn 2002, one could see that contributive areas included the “Near-Stream” and the “Mid-Slope” sites where saturated conditions have been observed during the second part of the autumn period.

In order to better understand the hydrological behaviour of the studied hillslopes and to realize a conceptualisation of the processes that occur at this scale, we will further analyse some of the rainfall-runoff events that occurred during the study period under different antecedent conditions and different rainfall amount and intensities.

3.2.4 Soil water regime

The water regime for the two experimental sites (Ruzillon and Esserts) was studied with the help of the TDR set-up. Soil moisture changes have been computed at different depths and for different rainfall-runoff events with different antecedent conditions and rainfall intensities.

The results of these analyses will be presented below. In order to better identify the hydrological processes, that occur at the hillslope scale we have chosen several events during the 2002-year to reflect the main meteorological context in which representative hydrological processes take place. For this analysis we used only data coming from the “Mid-Slope” and “Near-Stream” plots. Four cases will be further analysed function of the

dry antecedent condition (defined by the ARI index – total amount of rainfall within the last 10 days previous a considered event) and the hourly rainfall intensity:

- dry antecedent conditions (ARI < 30 mm) and low rainfall intensities ($I_{\max} < 7$ mm/h);
- dry antecedent conditions (ARI < 30 mm) and high rainfall intensities ($I_{\max} > 7$ mm/h);
- wet antecedent conditions (ARI > 30 mm) and low rainfall intensities ($I_{\max} < 7$ mm/h);
- wet antecedent conditions (ARI > 30 mm) and moderate to high rainfall intensities ($I_{\max} > 7$ mm/h).

a) Dry antecedent conditions and low rainfall intensities

This analysis will be made in parallel for the two catchments. As the available data are not corresponding different rainfall-runoff events were used to illustrate the soil water regime for Ruzillon and Esserts sites during dry antecedent conditions and low rainfall intensities.

RUZILLON SITE: The event that occurred during 3 – 4 August 2002 (see Table 3-8) is representative for these conditions, as a total rainfall of 27 mm has been recorded with a maximum hourly intensity of 4.8 mm/h. The antecedent conditions could be considered as dry, as only 25 mm of precipitations have been recorded for the 10 days preceding the considered event. The total potential evaporation has been estimated at 24 mm for the same period for which the ARI index has been computed. The flood hydrograph at the catchment outlet shows an increase of the total discharge from 1.7 to 7.7 l/s.

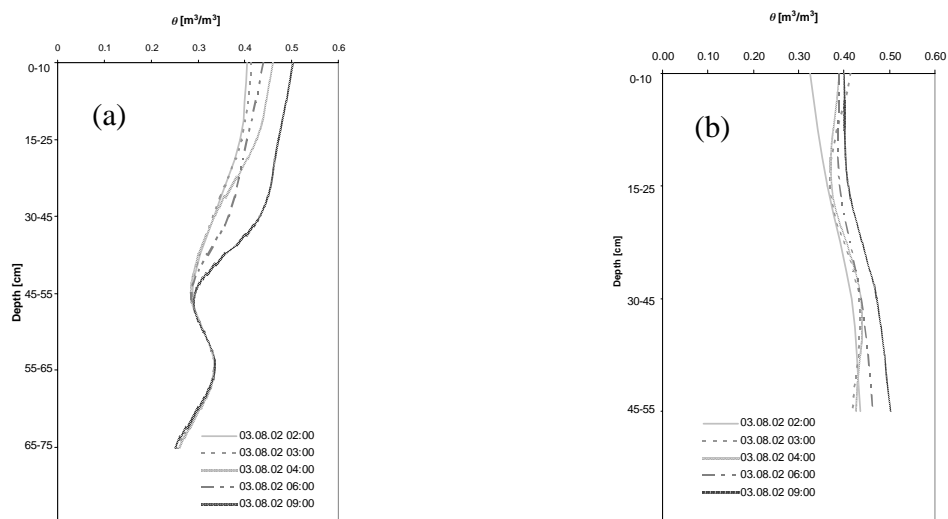


Figure 3-25 Ruzillon site - Soil moisture profiles before, during and after a rainfall even; “Mid-Slope” site (a) and “Near-Stream” site (b)

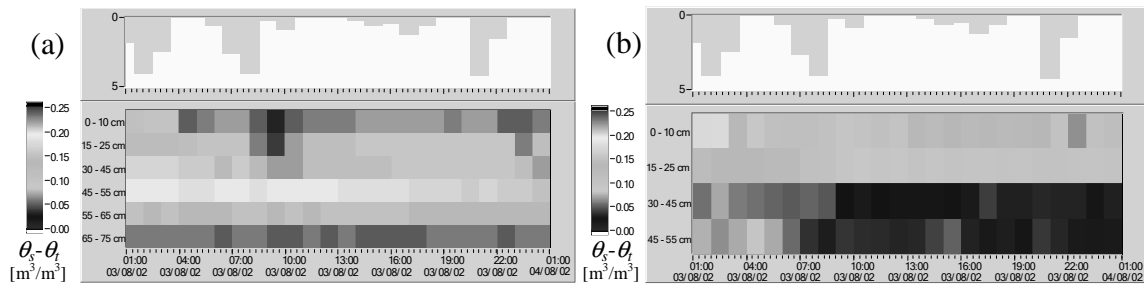


Figure 3-26 Ruzillon site - Soil moisture changes (difference between saturated and current soil moisture) over 2-4 August 2002 period; “Mid-Slope” site (a) and “Near-Stream” site (b)

Figure 3-25 (a and b) shows the typical soil moisture profiles for this event for the Ruzillon site both “Mid-Slope” and “Near-Stream” field plots. Figure 3-26 represents the soil moisture changes over the study period for both field plots as well. Soil moisture changes are given by the difference between the soil moisture at saturation (θ_s) and the current measured value at different depths (θ_t).

MID-SLOPE site: Before the rainfall event, the soil profile is dry with small values of the soil moisture for the deeper soil horizons. The rainfall event explains the infiltration that occurs in the upper soil horizons but because of the small quantity and intensity this is not affecting the deeper soil horizons.

NEAR-STREAM site plot evidences two parts of the soil profile: the upper one which is well drained and which favours infiltration of the rain water to the deeper soil horizons, which are wetter and thus saturate very easily. The soil profiles that have been represented in Figure 3-26 show that low rainfall intensities generate infiltration of the water for the upper soil profiles, which is finally drained to the deeper horizons.

ESSERTS – MID-SLOPE SITE: Because of the different length of the TDR series at Esserts site, we have chosen an event that occurred in the beginning of October 2002 to represent the hillslope response to small rain inputs in dry antecedent conditions. This one is described in Table 3-10. Analysis of the hydrograph at the catchment outlet indicates that the input rainfall had no important impact on the discharge, which increased insignificantly from 1.7 to 2.6 l/s. This could also be explained by the high interception of the vegetation because of the small rainfall intensities.

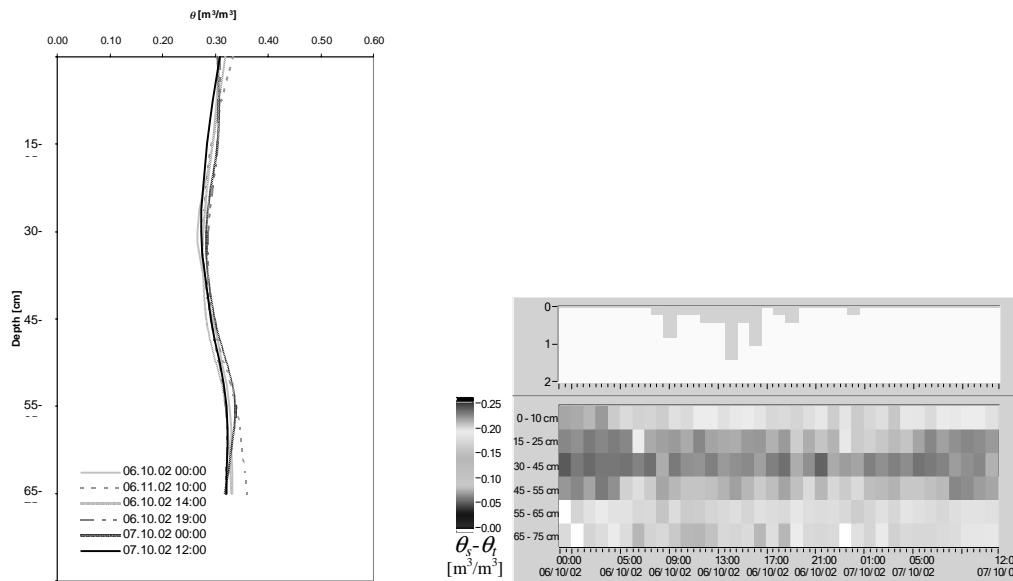


Figure 3-27 Soil moisture profile (left) and soil moisture changes (right) for Esserts “Mid-Slope” profile during 6-7 October 2002 period

Figure 3-27(left) shows that the input precipitation had minimum impact on the entire profile of the soil moisture. The same information is also deduced from Figure 3-27(right) where the time changes in the deficit to saturation of each soil horizon are represented.

No TDR data are available for the Esserts “Near-Stream” site but direct observations indicate that only the river closest part of the riparian zone is active during this kind of event.

b) Dry antecedent conditions and high rainfall intensities

RUZILLON: In order to represent the hydrological behaviour at the hillslope scale for the Ruzillon site we have chosen three cases:

- ❑ 30-31 July 2002 storm event (Table 3-7): 20 mm of precipitation occurred on a small lapse of time and maximum rainfall intensity for a 10' time step reached 56 mm/h;
- ❑ 31 August 2002 storm event when an important quantity of rainfall has been registered at the Chalet de Villars meteorological station and at different pluviometers on the Corbassière catchment (Table 3-9): for Ruzillon catchment, a total of 32 mm of rainfall were recorded with a maximum intensity for a 10' time step of 41mm/h;
- ❑ beginning of the 16-18 October event, which occurred after a long period without important precipitation (Table 3-11) with hourly rainfall intensities of 10 mm/h.

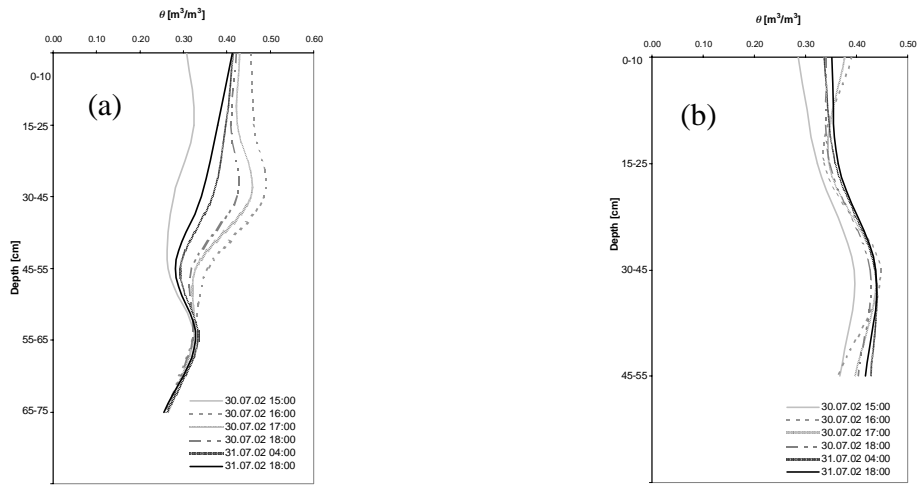


Figure 3-28 Ruzillon site - Soil moisture profiles before, during and after the 30-31 July 2002 rainfall event; “Mid-Slope” (a) and “Near-Stream” (b) sites

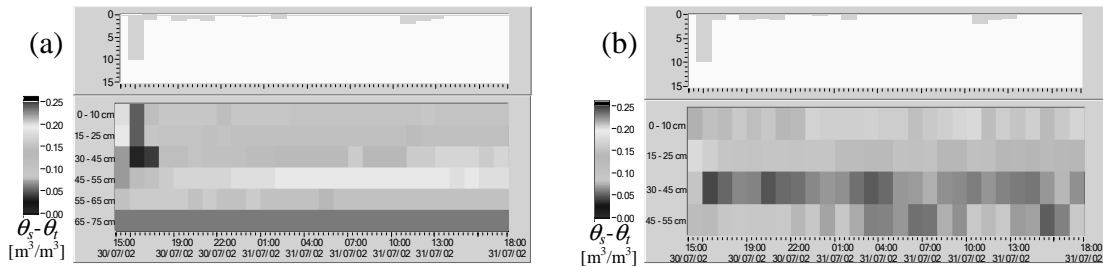


Figure 3-29 Soil moisture changes (difference between saturated and current soil moisture) over 30-31 July 2002 period; “Mid-Slope” (a) and “Near-Stream” (b) sites

Figure 3-28 shows, for Ruzillon site, the soil moisture profiles for the initial state, during the wetting period and after the rainfall event has ceased. The high rainfall intensities produced a rapid increase of the soil moisture but only in the upper part of the soil profile. The time changes of the deficit to saturation are represented in Figure 3-29. This event generated a temporary perched water table but for a very short period of time. Part of this perched water has drained to the deeper soil horizons. A water balance computation is necessary to know if part of this water fed the “Near-Stream” riparian zone as lateral flow. The “Near-Stream” site shows changes in the soil moisture of the deeper horizons without nevertheless reaching saturation.

Another example to illustrate this kind of event is presented below. The storm event that occurred in the end of August 2002 produced a flood hydrograph for the Ruzillon site of more than 70 l/s. The main characteristics of this event have been presented in Table 3-9. Figure 3-30 presents the soil moisture profiles corresponding to different moments of the rainfall-runoff event: initial state, wetting period and draining period.

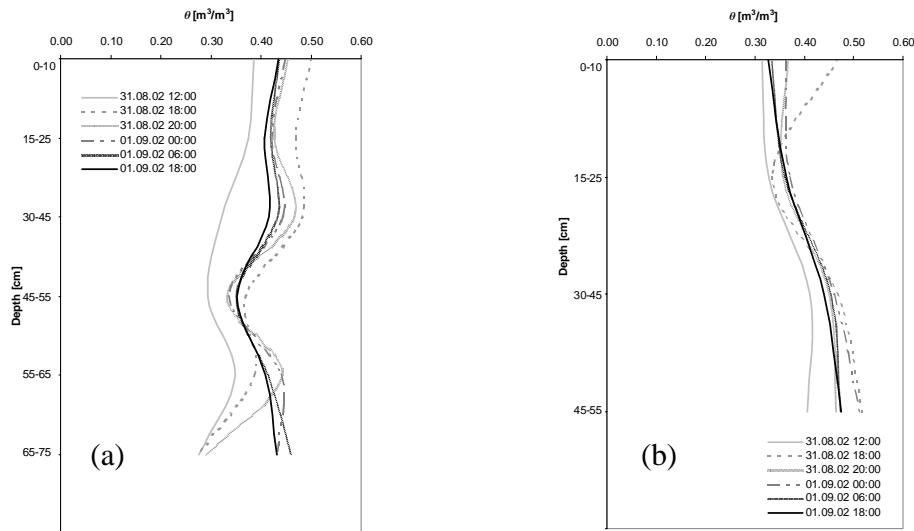


Figure 3-30 Ruzillon site - Soil moisture profiles before, during and after the 31 August -01 September 2002 rainfall event; “Mid-Slope” (a) and “Near-Stream” (b) sites

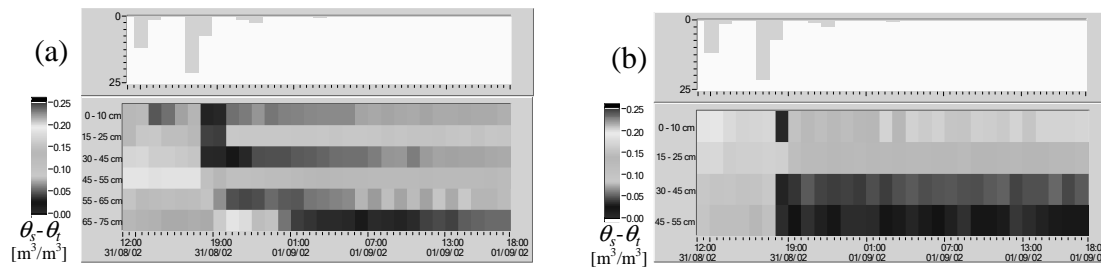


Figure 3-31 Ruzillon site - Soil moisture changes (difference between saturated and current soil moisture) over 31 August – 1 September 2002 period; “Mid-Slope” (a) and “Near-Stream” (b) sites

Figure 3-30 and Figure 3-31 indicate that the important rainfall intensities produced a brutal change in the soil moisture for the upper soil horizon while these changes have been less important for the deeper soil horizons. After the rain has ceased the tendency in the soil moisture changes has changed, the upper soil horizons drained while the deeper ones have been recharged. Analysis of the soil moisture profiles at the “Near-Stream” site indicates that the deeper soil horizons, which are in contact with the sandstone bedrock reached saturation conditions very quickly. Analysis of the soil moisture changes confirms the affirmations above: one can notice that a short time perched water level is observed for the upper horizons (0-45 cm depth) while later, after infiltration, the deeper soil horizons had greater soil moisture values than the upper ones. For the Near Stream, site one can notice that a saturated horizon had appeared at the interface with the rock substrata soon after the rainfall event has ceased.

The last rainfall-runoff event presented in this case corresponds to the transition period toward wet autumn conditions. The entire event has been presented Table 3-11. At the difference of the preceding examples, this one occurs on rather intermediate antecedent conditions because of the lower values of the ETP.

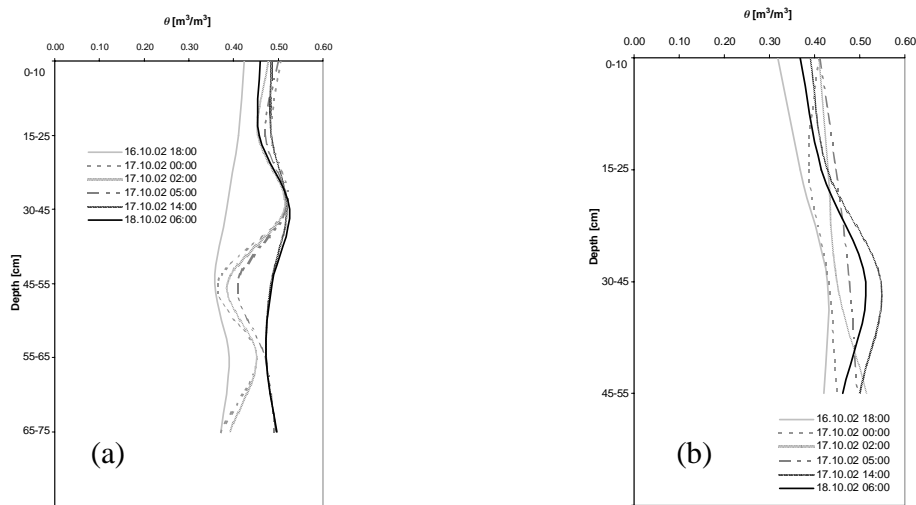


Figure 3-32 Ruzillon site - Soil moisture profiles before, during and after the 16-18 October 2002 rainfall event; “Mid-Slope” (a) and “Near-Stream” (b) sites

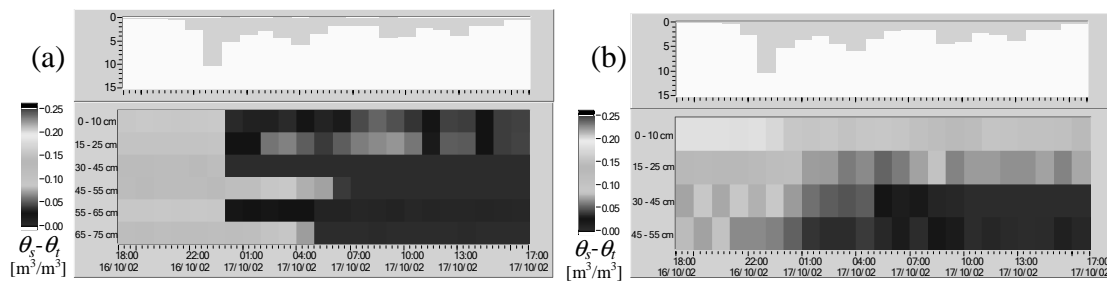


Figure 3-33 Ruzillon site - Soil moisture changes (difference between saturated and current soil moisture) over the 16-18 October 2002 period; “Mid-Slope” (a) and “Near-Stream” (b) sites

Figure 3-32 and Figure 3-33 indicate that soon after the beginning of the rainfall event, the soil moisture has very quickly increased reaching saturation in the upper soil horizons (0-45 cm). As previously noticed, the soil moisture changes are very slow to appear. As the rainfall continues, infiltration and drainage to the deeper soil horizons, of the perched water occurs. After the rain has ceased, one can observe that the soil horizon above 45-55 cm reached saturation. The temporal evolution of the soil moisture absolute values for the Near Stream site indicates that saturation occurs from the bottom and reaches progressively the 30-45 cm soil horizon.

ESSERTS: In order to study the reaction of the second field site to a strong storm the 16-17 October event was chosen. The meteorological context has been presented earlier in Table 3-11. The hydrograph analysis indicates that discharge has increased from 1.8 l/s to 23 l/s and further consideration of the tracing information (Figure 3-9, Event 11) indicates that most part of the discharge in the beginning of the event is represented by the groundwater flow.

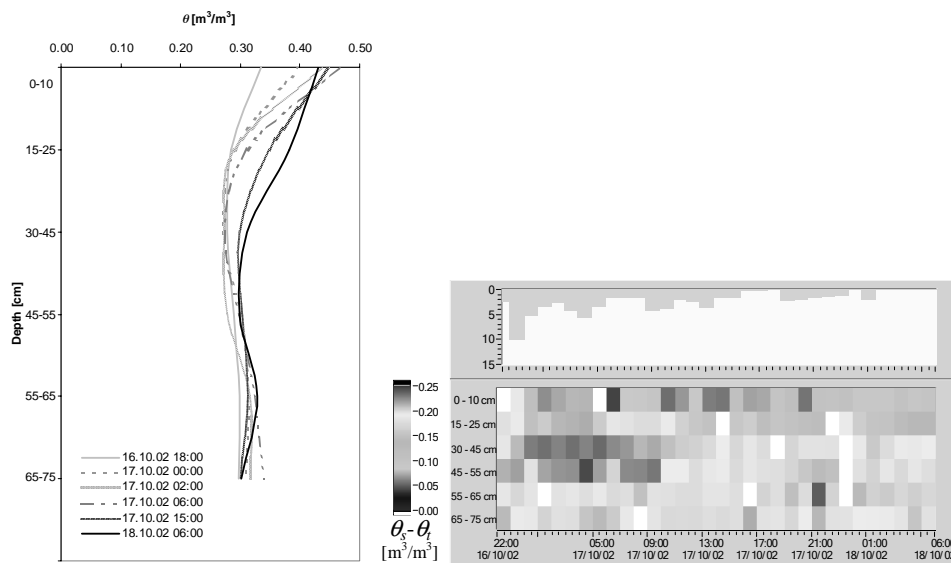


Figure 3-34 Soil moisture profile (left) and soil moisture changes (right) for Esserts “Mid-Slope” profile during 16-18 October 2002 period (White colour represents missing data)

Figure 3-34 presents the soil moisture profiles during the considered event as well as the soil moisture saturation deficit time changes during the same event. In comparison with what was observed for Ruzillon site, only the upper part of the soil profile is influenced by the rainfall event. Infiltration is the most important process that occurs and that explains slow change with the time of the saturation deficits for the entire profile.

c) Wet antecedent conditions and low rainfall intensities

In order to study the hydrological behaviour of the considered sites in this meteorological context the 2 November 2002 event for the Ruzillon site and the 9 November 2002 event for the Esserts site were chosen.

RUZILLON: The 2 November 2002 event has been presented in Table 3-15. Flood hydrograph indicates that the discharge increased from 4 l/s before the rainfall event, to more than 45 l/s to the peak flow.

The soil moisture profile shows that this time, the wet upper soil horizons change slowly towards greater values of soil moisture and the saturation is occurring from the bottom. Indeed the groundwater is recharged, and the water table reaches progressively the upper soil horizons (Figure 3-35 and Figure 3-36). The “Near-Stream” site exhibits the same behaviour as previously shown. From the beginning of the event, the soil profile is saturated at the interface with the bedrock and saturation progresses toward the upper part of the soil profile.

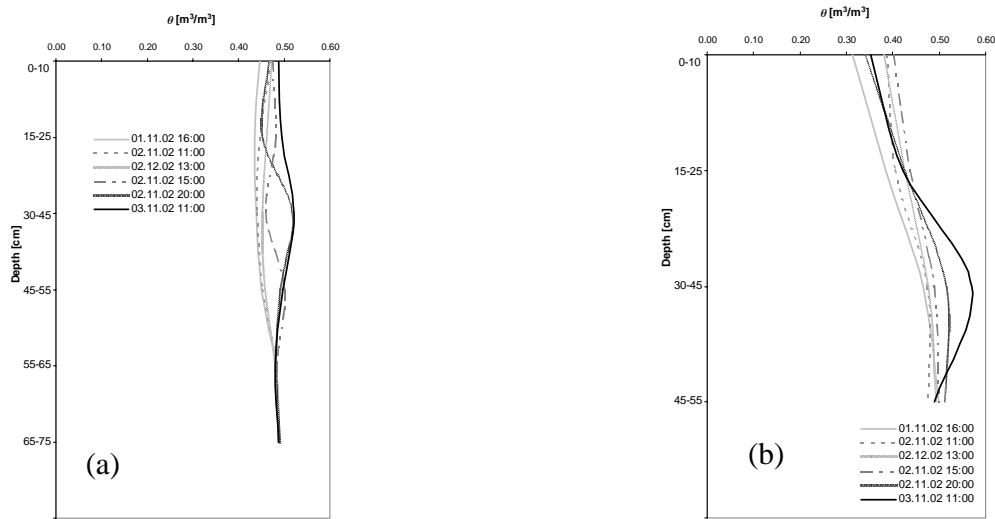


Figure 3-35 Ruzillon site - Soil moisture profiles before, during and after the 02 - 03 November 2002 rainfall event; “Mid-Slope” (a) and “Near-Stream” (b) sites

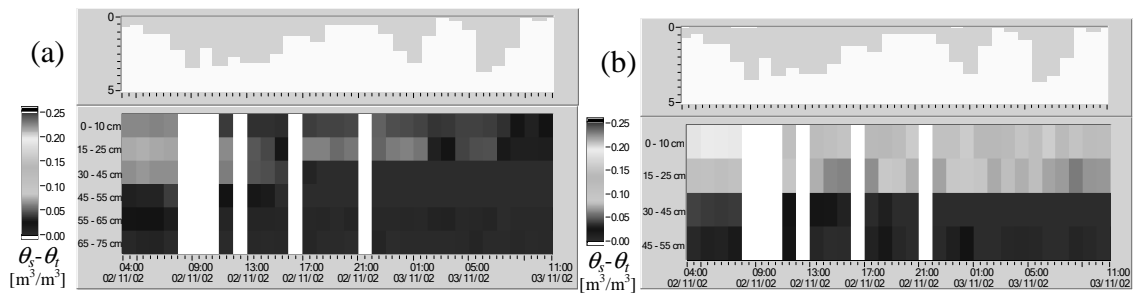


Figure 3-36 Ruzillon site - Soil moisture changes (difference between saturated and current soil moisture) over the 02-03 November 2002 period; “Mid-Slope” (a) and “Near-Stream” (b) sites (White colour represents missing data)

ESSERTS: The rainfall-runoff event from 9 November 2002 meteorological context is presented in Table 3-16. During the whole period, infiltration of the rainfall water is the most important process that occurs at this site (see Figure 3-37). This contributes to the slowly change toward wetter humidity conditions of the deeper soil horizons.

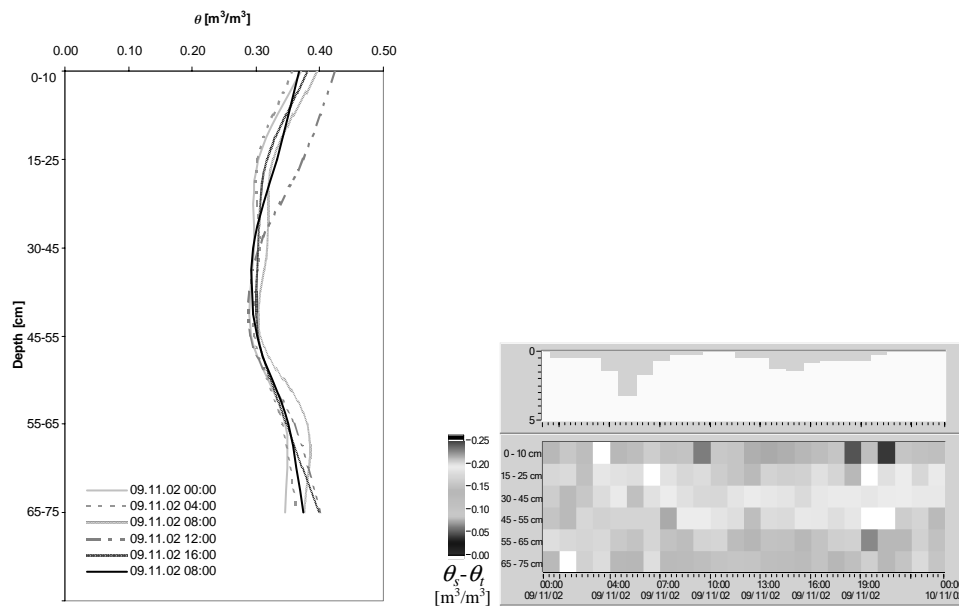


Figure 3-37 Soil moisture profile (left) and soil moisture changes (right) for Esserts “Mid-Slope” profile during 09-11 November 2002 period (White colour represents missing data)

d) Wet antecedent conditions and moderate to high rainfall intensities

The soil moisture response to high precipitation input was analysed considering the event from 14-15 November 2002 for both field sites. The meteorological context is presented in Table 3-17.

RUZILLON: During the considered event, Ruzillon total discharge increased from 9 l/s to almost 100 l/s at the peak (14 November 2002 at 14 hour). The analysis of Figure 3-38 and Figure 3-39 shows that for wet antecedent conditions, when the soil profile is almost entirely saturated, rapid infiltration occurs through the upper soil horizons which lead to rapid groundwater rising and saturation of the entire soil profile. The groundwater reached almost the ground surface and exfiltration of the groundwater could have been possible for a small lapse of time in the morning of 15 November 2002. As the topsoil of the “Near-Stream” site has well-drained soil horizons it seems that down slope, the possible exfiltrated groundwater from the “Mid-Slope” site reinfiltreated quickly and recharged the local groundwater, which fed the stream runoff.

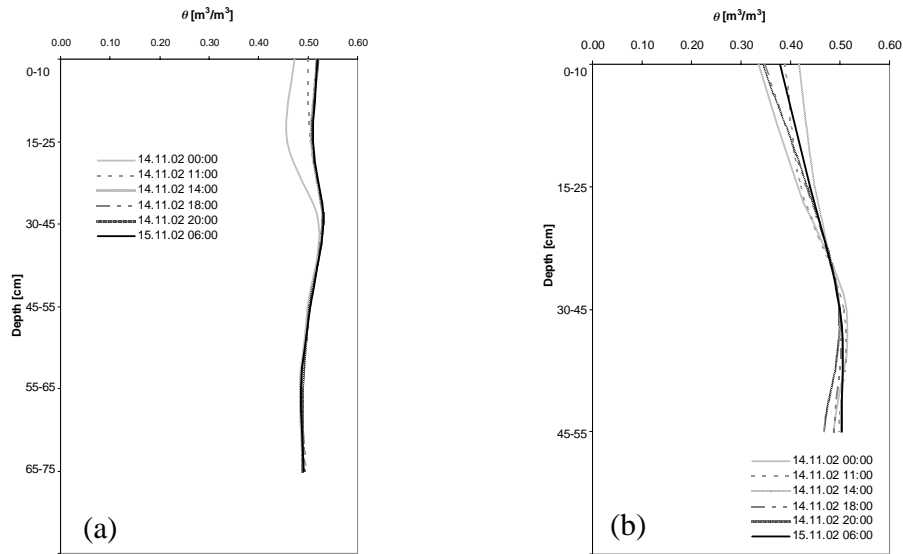


Figure 3-38 Ruzillon site: Soil moisture profiles before, during and after the 14 - 15 November 2002 rainfall event; “Mid-Slope” (a) and “Near-Stream” (b) sites

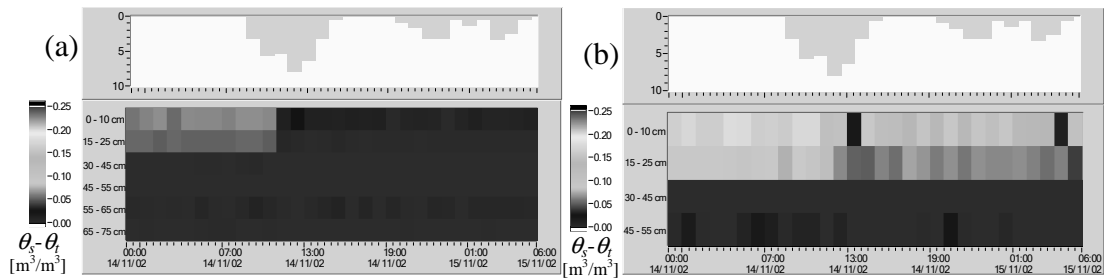


Figure 3-39 Ruzillon site: Soil moisture changes (difference between saturated and current soil moisture) over the 14-15 November 2002 period; “Mid-Slope” (a) and “Near-Stream” (b) sites

ESSERTS: We considered the same event for the Esserts Mid-Slope site. Figure 3-40 shows the soil moisture profiles and the soil moisture changes in time. Analysis of these figures indicates that even in presence of wet antecedent conditions, the infiltration remains the most important process that occurs at this site. Only long time draining conditions determine elevation of the groundwater table closer to the soil surface. Periodical observation of the groundwater table (in a 1.2 m deep piezometer) at this site evidenced that only rarely this reaches the bottom soil horizons (65-75cm).

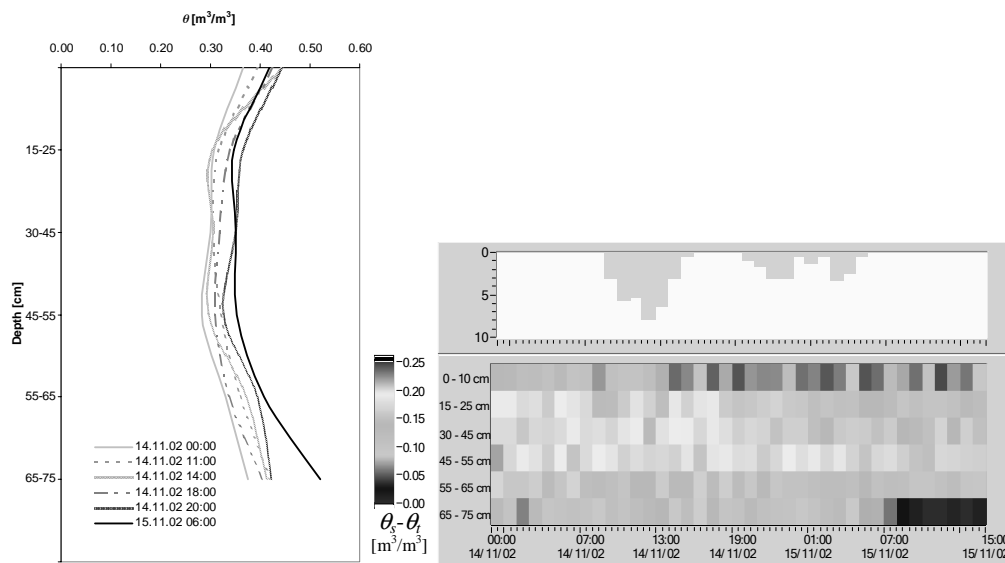


Figure 3-40 Soil moisture profile (left) and soil moisture changes (right) for Esserts “Mid-Slope” profile during 14-15 November 2002 period

A brief synthesis including the main observations made during the individual analysis of the above rainfall-runoff events is presented below in Table 3-22 and Table 3-23. Two working hypothesis will be made concerning the soil water flow through the soils:

- unsaturated soil: water flows vertically through the soil matrix;
- saturated soil: water flows laterally.

Ruzillon	“Mid-Slope”	“Near-Stream”
Geology	Moraine	Molasse
Soil Texture	<ul style="list-style-type: none"> - Rapid textural variations within the soil profile; - General silty texture (15-17% clay and 50% sand) with sandy horizons between 45-55 cm and 70-75 cm (12% clay and 60 % sand); - Presence of gravels starting at about 70 cm depth; 	<ul style="list-style-type: none"> - Uniform texture profile; - General sandy texture (8-9% clay and 70% sand) with the sandstone at about 60 cm depth;
DRY/LOW	<ul style="list-style-type: none"> - Wetting front and vertical infiltration in superficial soil horizons without saturation; 	<ul style="list-style-type: none"> - Wetting front and vertical infiltration through the entire soil profile;
DRY/HIGH	<ul style="list-style-type: none"> - Wetting front and rapid infiltration until the 45-55 cm soil horizon is reached; - Water accumulation above this horizon and rapid soil saturation; - Initiation of lateral flow 	<ul style="list-style-type: none"> - Rapid vertical infiltration of the rain water; - Possible lateral flow from the upslope; - Lateral flow to the stream;

	above the considered horizon; - Drainage of water to the lower soil horizons;	
WET/LOW	- Rapid infiltration of the rainwater because of the more homogeneous and wetter soil moisture profile; - Groundwater rise close to the ground surface;	- Rapid vertical infiltration; - Lateral flow to the stream;
WET/HIGH	- Complete saturation of the soil profile; - Lateral flow downslope;	- Rapid vertical infiltration; - Lateral flow to the stream

Table 3-22 Ruzillon site: soil texture and synthesis of the soil moisture monitoring

The second case, (DRY/HIGH - dry antecedent conditions and high rainfall intensities) needs further discussion concerning the soil moisture response to the rainfall input. The three analysed rainfall-runoff events show that under important rainfall intensities, the wetting front seems to be retarded above the 45-55 cm soil horizon. The texture profile at the “Mid-Slope” site shows a sandier layer (10% sand more than above and under/beneath ones), which might explain this behaviour. In fact, in dry conditions, the unsaturated hydraulic conductivity of the clayer soil horizons may be greater than that of sandier ones. A layer of sandier unsaturated soil in a finer texture may retard downward movement of infiltrating water owing to its lower unsaturated hydraulic conductivity (Fetter (1994)). As the TDR data indicated, retardation of the wetting front for a longer period could produce saturation of the superficial soils and could initiate lateral flow downslope. The textural variations of the brown soils developed on morainic deposits (silty over sandy textures or vice-versa) seem to generate preferential flow at the soil texture discordances. This was also evidenced by (Joerin et al.), who have noted preferential flow at the organic/mineral soil interface through a dye tracing experiment on the Bois-Vuacoz catchment.

Under wet antecedent conditions, this phenomenon is not anymore observed, uniform vertical infiltration occurring through the soil profile and recharging the groundwater.

Esserts	“Mid-Slope”
Geology	Molasse
Soil Texture	- Uniform soil texture profile; - General sandy-silty texture (13-14% clay and 55% sand);
DRY/LOW	- Wetting front and vertical infiltration in superficial soil horizons without saturation;
DRY/HIGH	- Wetting front and infiltration;
WET/LOW	- Wetting front and infiltration of the rainwater;
WET/HIGH	- Wetting front and infiltration of the rainwater; - Groundwater rise; - Initiation of a deep lateral flow downslope (70 cm -1 m depth);

Table 3-23 Esserts site: soil texture and synthesis of the soil moisture monitoring

3.3 Synthesis of the hydrological processes and conceptual model for the Haute-Mentue catchment

In this chapter two different approaches have been considered in order to identify the hydrological behaviour of the Haute-Mentue catchment. Association of the environmental tracing and the soil moisture monitoring results allowed development of a general conceptual model for the Ruzillon and Esserts head sub-catchments.

The two different experimental approaches that have been presented before, together with all previous experiments that have been done the last decade on the Haute-Mentue catchment allow nowadays a general conceptualisation of the hydrological processes responsible for the runoff generation on this catchment. The association of measurements is particularly profitable to retrieve the most important characteristics able to explain hydrological processes that occur at different scale. This methodology has been proposed by Joerin (2000) and the results have been rather promising. He used the environmental tracing for the Bois-Vuacoz subcatchment and compared the results with those given by a dye tracing experiment done on a typical hill slope in the same catchment. He found that the important contribution of the soil water observed thanks to hydrograph separation corroborated well with the indication that rapid displacement of the water could be possible at the organic / mineral interface of the soil profile such as proven by the sulforhodamin dye that was injected at this interface prior to a rainy period in October 1999. He concluded that this behaviour is typical for Bois-Vuacoz catchment, which is covered essentially by morainic impermeable deposits, favouring the rapid displacement of the water above these impermeable horizons. In order to explain the rapid displacement of the soil water to the stream he suggested the hypothesis that this could be explained by an important network of connected macropores that would be activated during wet conditions.

In this research, an associative approach in order to identify the most important patterns that could explain the hydrological behaviour of Ruzillon and Esserts catchments was also used. We focussed on four distinct cases in order to underline the different hydrological processes that are characteristic for different meteorological contexts: dry antecedent conditions and low rainfall intensities (DRY/LOW), dry antecedent conditions and high rainfall intensities (DRY/HIGH), wet antecedent conditions and low rainfall intensities (WET/LOW) and finally wet antecedent conditions and moderate to high rainfall intensities (WET/HIGH). The thresholds that have been used to distinguish between DRY and WET antecedent conditions or LOW and HIGH rainfall intensities are the same with those presented previously at page 61.

No.event	P [mm]	Antecedent conditions	Rainfall intensity	Ruzillon 18 ha			Esserts 33 ha		
				Rain	Soil	Gw	Rain	Soil	Gw
1	32	DRY	LOW	30	27	42	-	-	-
3	30	DRY	LOW	-	-	-	12	39	48
5	17	DRY	LOW	-	-	-	18	20	63
11-a	33	DRY	HIGH	33	36	30	28	9	62
11-b	70	WET	LOW	26	51	24	11	63	25
12	22	WET	LOW	18	60	21	6	72	23
14	23	WET	LOW	19	54	26	-	-	-
13	39	WET	HIGH	-	-	-	18	70	11

Table 3-24 Environmental tracing results: selected events for Ruzillon and Esserts catchments

Table 3-24 synthetises the results of the environmental tracing for the two catchments Ruzillon and Esserts during several rainfall-runoff events that have been classified upon the above methodology. The main conclusions are:

- For dry antecedent conditions and low rainfall intensities the most important component contributing to the streamflow is represented by the groundwater component for both catchments.
- Under dry antecedent conditions and high rainfall intensities, the Esserts streamflow is formed essentially by rainwater and groundwater while Ruzillon catchments shows equal contributions of the three components. Unfortunately, the event chosen to represents this case is not the most representative one. Another event that has been sampled at Bois-Vuacoz catchment and that belongs clearly to this case study shows that under strong rainfall intensities, the streamflow is essentially formed by groundwater and rainfall components.
- Under wet antecedent conditions and low rainfall intensities, the hydrological behaviour of the two catchments seems similar: the soil water becomes the most important component of the total streamflow.
- The last case, groups only one sampled event for the Esserts catchment and shows that the soil water remains the most important component that feeds the stream.

Table 3-25 presents the water balance results for each of the three plots (“Upper-Slope”, “Mid-Slope” and “Near-Stream”) of the two experimental sites (Ruzillon and Esserts). Total rainfall, potential evapotranspiration (such as estimated with the Penman-Monteith formula) and changes in soil moisture for the entire soil profiles have been computed and reported. Nevertheless, the computed values reported here are only orientative and include a high uncertainty due to both soil moisture and rainfall measurement errors. Question marks have been used to express doubt about the computed soil storage change computed values. A simple water balance formula (between the initial state of the soil profile before the rainfall event and two hours after the rain has ceased) was here used.

$$P + Q_{upslope} = ETP \pm \Delta S + Q_{downslope} \quad (3.7)$$

where

P is the total rainfall [mm];

$Q_{upslope}$ is the lateral flow coming from the upslope [mm];

ETP is the real evapotranspiration as given by the Penman formula [mm]

ΔS is are the soil profile soil moisture changes [mm]

$Q_{downslope}$ is the draining downslope lateral flow [mm];

No information was available about possible lateral flow from the upslope ($Q_{upslope}$) at the “Upper-Slope” site.

Site	No. Event	Antecedent conditions	Rainfall intensity	P	ETP	Δ Soil-Storage	Δ Soil-Storage	Δ Soil-Storage	Downslope lateral flow possible?	Downslope lateral flow possible?	Downslope lateral flow possible?
				[mm]	[mm]	"Upper-Slope"	"Mid-Slope"	"Near - Stream"	"Upper-Slope"	"Mid-Slope"	"Near-Stream"
						[mm]	[mm]	[mm]			
Ruzillon	8	DRY	LOW	28	0.5	28	28	24	no	no	yes
	7	DRY	HIGH	21	0.5	21	42?	20	no	?	yes
	9	DRY	HIGH	32-63	0.5	38?	65?	31	?	?	yes
	11	DRY	HIGH	70	0.2	82?	60	30	?	yes	yes
	15	WET	LOW	48	0.2	64?	39	27	?	yes	yes
	17	WET	HIGH	48	0.2	10	18	9	yes	yes	yes
Esserts	10	DRY	LOW	6	0.2		7			no	
	11	DRY	HIGH	70	0.2		62			?	
	16	WET	LOW	15	0.2		20?			?	
	17	WET	HIGH	48	0.2		40			yes	

Table 3-25 Soil water balance estimation for the TDR field sites during different antecedent conditions and rainfall intensities

Based on these soil moisture changes estimations and on our field experience (field visits during some of the mentioned events) we tried to indicate in the last three columns of the Table 3-25 whether lateral flow occurred or not for the considered soil profile. For the Ruzillon site, lateral flow occurrence seems to be related to the catchment antecedent conditions and to the rainfall characteristics. The lateral flow and thus the contributive area extends as the antecedent conditions are wetter and as rainfall intensity increases. For the Esserts site, based rather on direct field observations than soil moisture field measurements one can say that lateral flow at the “Mid-Slope” site didn’t occur until the antecedent conditions were wet and rainfall intensities important, the contributing area being mainly limited to the down-slope part of the hillslope.

Table 3-26 represents a synthesis of the main processes that could explain the hydrological behaviour of the two considered catchments.

Ruzillon					
Case	Catchment	Hillslope			
		“Mid-Slope”		“Near-Stream”	
	Soil water-predominant?	Lateral flow possible?	Hydrological processes	Lateral flow possible?	Hydrological processes
DRY/ LOW	no	no	<input type="checkbox"/> Infiltration	yes	<input type="checkbox"/> Infiltration <input type="checkbox"/> Return flow
DRY/ HIGH	no	yes	<input type="checkbox"/> Storm Subsurface flow-SSM (interflow and/or funneled flow) <input type="checkbox"/> <i>Hortonian overland flow-HOF</i>	yes	<input type="checkbox"/> Infiltration <input type="checkbox"/> Return flow <input type="checkbox"/> Translatory flow
WET/ LOW	yes	yes	<input type="checkbox"/> Infiltration <input type="checkbox"/> Groundwater rise	yes	<input type="checkbox"/> Infiltration <input type="checkbox"/> Return flow
WET / HIGH	yes	yes	<input type="checkbox"/> Return flow <input type="checkbox"/> <i>Macropore flow-MF</i> <input type="checkbox"/> <i>Saturation overland flow-OSF</i>	yes	<input type="checkbox"/> Return flow <input type="checkbox"/> <i>Saturation overland flow-OSF</i>

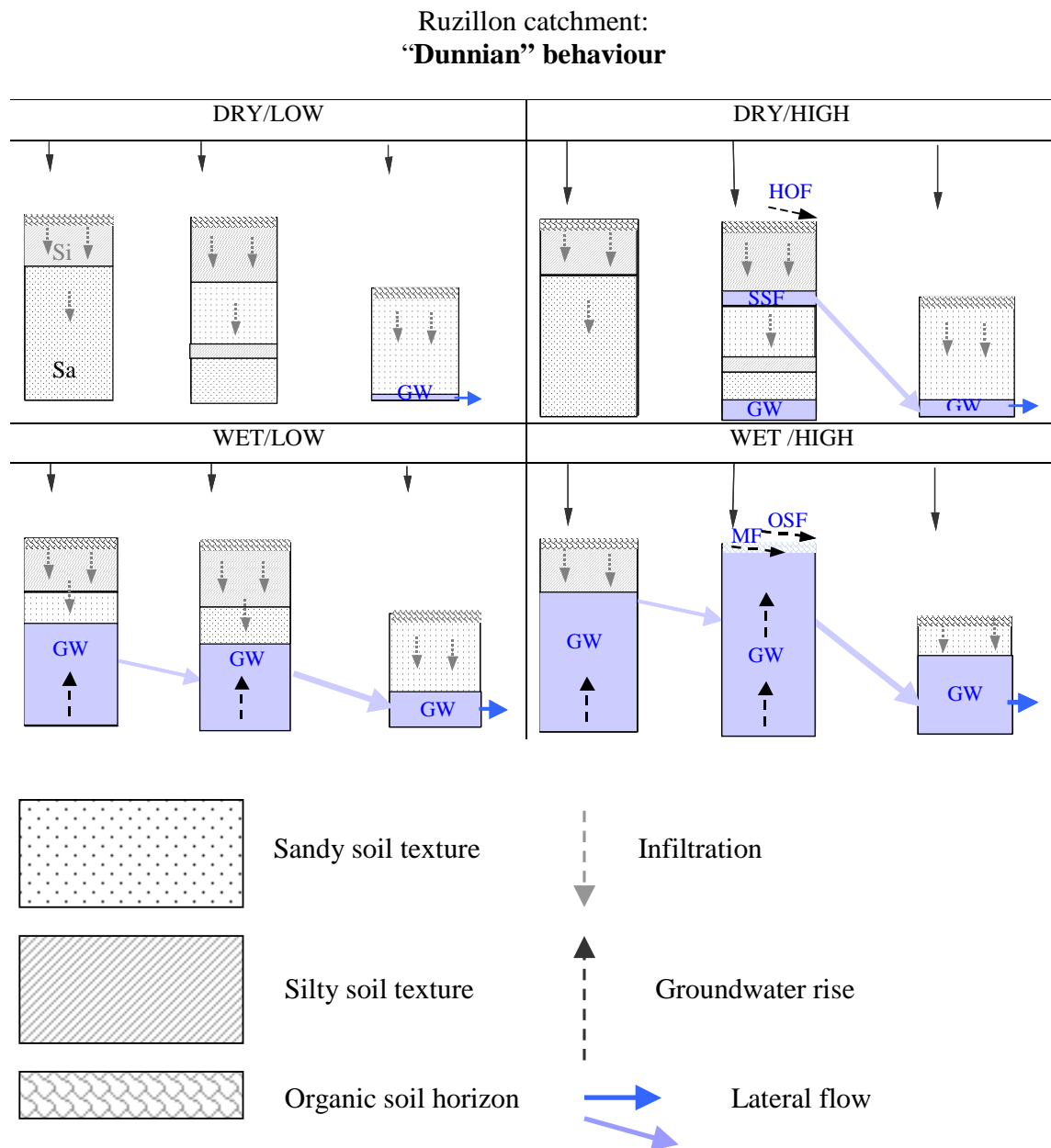
Esserts					
Case	Catchment	Hillslope			
		“Mid-Slope”		“Near-Stream”	
	Soil water-predominant?	Lateral flow possible?	Hydrological processes	Lateral flow possible?	Hydrological processes
DRY/ LOW	no	no	<input type="checkbox"/> Infiltration	yes	<input type="checkbox"/> Infiltration <input type="checkbox"/> Return flow
DRY/ HIGH	no	no	<input type="checkbox"/> Infiltration	yes	<input type="checkbox"/> Infiltration <input type="checkbox"/> Return flow <input type="checkbox"/> Translatory flow
WET/ LOW	yes	no	<input type="checkbox"/> Infiltration <input type="checkbox"/> Slow groundwater rise	yes	<input type="checkbox"/> Infiltration <input type="checkbox"/> Return flow
WET / HIGH	yes	yes	<input type="checkbox"/> Infiltration <input type="checkbox"/> Groundwater rise <input type="checkbox"/> Deep interflow	yes	<input type="checkbox"/> Return flow <input type="checkbox"/> <i>Saturation overland flow-OSF</i>

Table 3-26 Ruzillon catchment (top) and Esserts catchment (down): Synthesis of the main hydrological processes that might occur at the field plot scale based on environmental tracing, TDR data (normal font) and on direct observations and on previous experiments (italic font)

It is difficult to consider that one single type of hydrological processes or mechanisms would be responsible to generate floods on the Haute-Mentue catchment. Several processes seem to occur as a function of the meteorological conditions (rainfall amount, intensity and duration, evapo-transpiration) and other physical factors (vegetation, soil textures and initial soil storage deficits). The main hydrological processes that explain a

certain flood event change with the time during a single rainfall event as the catchment conditions changes.

In Table 3-27 a graphical synthesis of the hydrological functioning of the two hillslopes under the four meteorological cases is depicted based on Table 3-26 and on the soil texture characteristics of the two field sites.



Esserts catchment:
“Hewlettian” behaviour

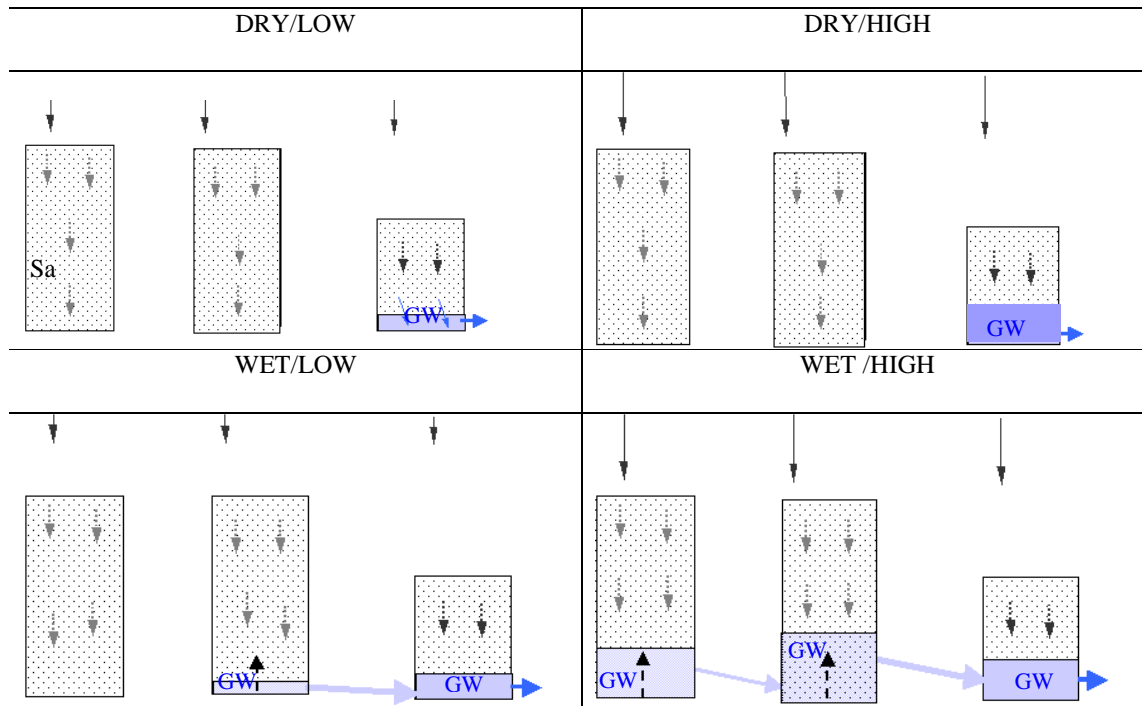


Table 3-27 Conceptual model of the main hydrological processes on the morainic and molassic hillslopes based on TDR field experiments (Si- Silt soil texture; Sa- Sandy soil texture; GW- groundwater, SSF- subsurface storm flow, MF-macropore flow, OSF- saturation overland flow, HOF Hortonian overland flow)

Comparisons between the representative processes at the two sites underline the main geological properties of the two catchments: morainic deposits and soils with various textural changes for Ruzillon and molassic altered sandstone deposits with soils having uniform texture. It may be considered that:

- Ruzillon catchment has a general “Dunnian” behavior with gentle hillslopes that saturate quickly and generate return flow and saturation overland flow during the wet conditions and temporary perched lateral flow (interflow/funnelled flow) during intensive storm events in dry antecedent conditions (Table 3-27 top).
- Esserts catchment has typical “Hewlettian” behaviour with steeper slopes and permeable soils with a high infiltration capacity that favors infiltration even during wet conditions or high rainfall intensity (Table 3-27 down).

A first conclusion that imposes is that in front of such complex reality, the development of a hydrological model (conceptual or physically based) to represent the time evolution

of the observed discharge is rather delicate and it reflects a compromise between the main different processes that explain the hydrological behaviour of a given catchment.

Based on the conclusions of the experimental work, the second part will be dedicated to the application of different versions of a simple conceptual model in order to test its applicability in the Haute-Mentue catchments. Further, the experimental information (tracing information and local estimates of the soil storage saturation deficits) will be used as additional information to constrain the conceptual model parameters and output predictions.

3.4 References

- Christophersen, N., C. Neal, R. P. Hooper, R. D. Vogt and S. Andersen (1990). "*Modelling streamwater chemistry as a mixture of soilwater end-members - a step towards second generation acidification models.*" *Journal of Hydrology* 116: 307-320.
- Elsenbeer, H. and A. Lack (1996). "*Hydrometric and hydrochemical evidence for fast flowpaths at La Cuenca, Western Amazonia.*" *Journal of Hydrology* 180(1-4): 237-250.
- EPFL-HYDRAM, B+C Ingénieur SA and AIC Association d'ingénieurs conseils SA (1996). "*CODEAU, Logiciel de traitement de données hydrologiques*". Lausanne.
- Fetter, C. W. (1994). "*Applied hydrogeology*". New Jersey, Prentice Hall.
- Iorgulescu, I. (1997). "*Analyse du comportement hydrologique par une approche intégrée à l'échelle du bassin versant. Application au bassin versant de la Haute-Mentue.*" Thesis EPFL, No.1613. Lausanne.
- Joerin, C. (2000). "*Etude des processus hydrologiques par l'application du traçage environnemental. Association à des mesures effectuées à l'échelle locale et analyse d'incertitude*". Thesis EPFL, No.2165. Lausanne.
- Joerin, C., K. Beven, A. Musy and D. Talamba (accepted). "*Study of hydrological processes by the combination of environmental tracing and hill slope measurements: application on the Haute-Mentue catchment.*" *Hydrological Processes* accepted.
- Joerin, C., K. J. Beven, I. Iorgulescu and A. Musy (2002). "*Uncertainty in hydrograph separations based on geochemical mixing models.*" *Journal of Hydrology* 255(1-4): 90-106.
- Jones, S. B., M. Wraith and D. Or (2002). "*Time Domain Reflectometry measurement principles and applications.*" *Hydrological Processes* 16: 141-153.
- Jordan, J. P. (1992). "*Identification et modélisation des processus de génération des crues; Application au bassin-versant de la Haute-Mentue*". Thesis No.1014, EPFL. Lausanne.

- Karaoui, S. (2002). *"Etude du comportement hydrologique par association de mesures à l'échelle globale (traçage) et locale (TDR)"*. Lausanne, EPFL.
- McDonnell, J. (1990). "A rationale for old water discharge through macropores in a steep, humid catchment." *Water Resources Research* 26: 2821-2832.
- Peters, N. E. (1994). *"Biogeochemistry of Small Catchments"*, Wiley.
- Reber, O. (1993). *"Rôle de la couverture pédologique dans la réponse hydrologique"*. Diploma work, Dpt. GR, Lausanne, EPFL.
- Roth, K., R. Schulin, H. Fluhler and W. Attinger (1990). "Calibration of time domain reflectometry for water content measurement using a composite dielectric approach." *Water Resources Research* 26(10): 2267-2273.
- Talamba, D. (1999). *"Study of the hydrological processes by a comparative approach at the catchment scale: Application to the Haute-Mentue catchment"*. Lausanne, EPFL.
- Topp, G. C., J. L. Davis and A. P. Annan (1980). "Electromagnetic determination of the soil water content: measurements in coaxial transmission lines." *Water Resources Research* 16: 574-582.

4. Hydrological modelling

Abstract

This chapter is devoted to the conceptual hydrological modeling. The TOPMODEL conceptual hydrological model is briefly presented together with a modified version in order to include a storm flow component. The principles of the Bayesian methodology are introduced and further two Bayesian methodologies to estimate model parameters are compared. The first one is GLUE (Generalized Likelihood Uncertainty Estimation), which was used in order to estimate both parameters' and model output uncertainty. The second one is the MCMC (Monte Carlo Markov Chain) methodology. The chapter investigates the effects of the statistical corrections on the uncertainty estimation. Detailed presentation of the two Bayesian methods in terms of likelihood function and searching algorithm are provided. Application of these two methods has been done through one case study concerning a small head catchment of the Haute-Mentue watershed. TOPMODEL as well as GLUE and MCMC methodologies have been implemented in LABVIEW, a graphical programming environment, which offers many facilities for the user interface and real time modifications.

Key words:

Conceptual model, TOPMODEL, model calibration, Bayesian approach, GLUE, MCMC methodology

4.1 Conceptual rainfall-runoff models

Predicting the catchment discharge under a given meteorological context is one of the main aims in hydrology. Efforts have been concentrated towards developing different models to predict catchment discharges. Two kinds of hydrological models: conceptual hydrological and physically based hydrological models are considered for assessing the rainfall-runoff processes. The first category represents the catchment as a grey box with several connected reservoirs, the main processes that occur in a catchment being described by empirical relations with a presumed physical basis. The model output is obtained by routing the rainfall through these reservoirs and using generally simple relations including a variable number of parameters. These parameters are estimated during a calibration process by comparing the model output with the observed discharges. Several calibration methods of hydrological models are used. In this chapter, two of them will be discussed. The calibrated parameters are often without a physical meaning and often they could not be successfully used out of calibration periods.

Physically based hydrological models are complex representations of the reality, they are distributed at the grid scale and they are based on partial differential equations to describe the processes that occur at the grid scale. Contrary to the conceptual models, the *physically based models* (PBM) are supposed to work directly with values measured on the field. Nevertheless, these models need a huge number of parameters and it becomes quickly impossible to work only with field-measured values. Furthermore, field measurements are usually done at a local scale and hence one important topic is how to transpose this local information to the grid scale. They use equations of small scale physics at larger scales with the assumption that the change of scales can be accommodated by the use of “effective” parameter values (Beven (1996)). Most of the PBM models work with field measured parameters, effective parameters and a variable number of calibrated parameters.

Which models to choose in order to better represent the catchment hydrological response? It depends on the final aim of the modeler. There is matter to think twice about this choice because it will influence the whole approach to follow in order to reach the fixed aim. Observations made by Engeland (2002)) show that the bigger the catchment area is, the more the results obtained with the two kind of models tend to be comparable. For large catchments it becomes difficult to define the effective parameters and the use of the physical equations at the grid scale becomes less appropriate (Blöschl and Sivapalan (1995)).

A lot of scientific literature (Beven (1989), Sorooshian (1991), Refsgaard and Storm (1996), Higby (2000)) etc. can be consulted on this topic.

4.1.1 TOPMODEL concepts

For this study we've chosen to work with TOPMODEL, which can be considered as a semi-physically based model. TOPMODEL has been developed by (Beven and Kirkby (1979)) and it was intended to be more like a collection of modeling concepts than a model in a classical way of thinking. The main concepts related to TOPMODEL are the hydrological similarity concept (a) and those of variable contributing area (b). This model has been the object of an

important number of scientific publications. Here only the main features and concepts of TOPMODEL will be presented.

a) The originality of TOPMODEL is that it uses the hydrological similarity concept, which it makes possible the introduction of the spatial topographic characteristics in a semi-distributed way. Instead of working at the grid scale, TOPMODEL uses classes of similar topographical characteristics as given by the topographical index distribution. For a point i , the topographic index (IT_i) has been defined by Beven and Kirkby (1979) and it is given by the upslope drained area per unit contour length (a_i) divided by the local slope angle ($\tan \beta_i$):

$$IT_i = \ln \frac{a_i}{\tan \beta_i} \quad (4.1)$$

All the grids, which have the same topographical index, are considered to respond in the same way from the hydrological point of view. TOPMODEL is thus working with classes of equal values of topographical index taking into account the catchment spatial variability in a simple and efficient way.

b) The topographical index is further exploited in order to estimate the proportion of the catchment, which is saturated. According to the model concept, only a proportion is contributing to the total discharge (variable contributing area concept) and this is calculated by relating the mean physical catchment characteristics (such as depth to the groundwater table or groundwater zone saturation deficit) to the local ones. The version that we work with uses the deficit at saturation as main characteristic of the catchment. Its spatial distribution is obtained through a relationship between the local and the mean catchment values of the saturation deficit. Classic TOPMODEL identifies two sources that form the stream water: the overland flow occurring on saturated variables contributing surfaces and the subsurface flow.

A detailed presentation of the TOPMODEL including the model hypotheses and model equations can be found in Higy (2000) and Beven (2001). Here below only the main equations used for computing subsurface flow, vertical drainage, actual evapo-transpiration as well as computation of local deficit and of the saturated contributing areas are reminded.

The subsurface flow is given, at each time step, by the following formula:

$$Q_b = Q_o \cdot \exp(-D_{average} / m) \text{ where } Q_o = A \cdot T_0 \cdot \exp(-\lambda) \quad (4.2)$$

and

Q_b is the subsurface flow;

$D_{average}$ is the mean catchment saturation deficit;

m is a parameter showing the decreasing of the saturated transmissivity with the depth;

T_0 is a model parameter representing the surface saturated transmissivity;

A is catchment area;

λ is the mean catchment value of the topographic index.

The local saturation deficit is computed by relating it to the mean value of the catchment:

$$D_i = D_{average} + m \cdot \left(\lambda - \ln \left(\frac{a_i}{\tan \beta_i} \right) \right) \quad (4.3)$$

D_i is the local saturation deficit;

$D_{average}$ is the mean catchment saturation deficit;

λ is the mean catchment value of the topographic index,

$\ln \left(\frac{a_i}{\tan \beta_i} \right)$ are the local values of the topographic index.

The vertical drainage for each class of topographic index is computed as follows:

$$q_{vi} = \frac{SUZ_i}{T_d \cdot D_i} \quad (4.4)$$

q_{vi} is the vertical drainage to the saturated zone;

SUZ_i is the local storage of the unsaturated zone;

T_d is the delay time per unit saturation deficit;

D_i is the local saturation deficit.

Topographical index classes for which the local saturation deficit is zero or less than zero are saturated zones and determine the extent of the contributing areas. At the event scale, the saturated zones are varying depending on the local and the mean catchment deficits, which introduce the second TOPMODEL concept, those of variable contributing areas.

Actual evapo-transpiration depletes only the upper root reservoir and is computed by using a simple relationship between the saturation deficits at the time t and the maximum allowed deficit for the root store.

$$E_{a,t} = E_{p,t} \cdot \left(1 - \frac{S_{rzt}}{S_{rzm\max}} \right) \quad (4.5)$$

where:

$E_{a,t}$ is the actual evapo-transpiration at time t ,

$E_{p,t}$ is the potential evapo-transpiration at time t ;

S_{rzt} is the root store deficit at time t ;

$S_{rzm\max}$ is the root store zone maximum deficit;

4.1.2 Modified version of TOPMODEL in order to include shallow storm flow

As shown previously, the classical TOPMODEL simulates two main components contributing to the floods: (i) the quick flow given by the overland flow and (ii) the subsurface flow.

The use of tracers and of the environmental tracing on the Haute-Mentue catchment shown clearly that for this catchment the discharge is essentially computed by water coming from three stores: groundwater, soil and surface. As one aim of the intended study is to link the chemical information to the hydrological one, the first thing to take care of is to ensure, as much as possible, a proper definition of the components defined by the environmental tracing and by the hydrological model. This is a sensible step because care is needed in order to compare the components given by two approaches.

First, the environmental tracing was used to separate the stream flow in three components based on an EMMA approach (Christophersen et al. (1990)). This considers that the water into the stream is a mixing of several chemically distinct waters coming from several distinct end-members. The end-members chemical definition is thought constant or varying slowly over the time. This seems to be a strong hypothesis at least for the groundwater end-member. Scanlon et al. (2001) has shown that for the South Fork Brokenback Run (SFBR) catchment, the groundwater content in silica is changing with the general antecedent conditions: the greater the saturation deficit for the saturated zone is, the greater the content in silica of the groundwater is. The studies done before took into consideration this aspect by defining the end-members not by unique values but by distributions based on observed concentrations measured on the field. The choice of the end-members has been presented and argued by works of Iorgulescu (1997) and Joerin (2000). As shown in Chapter 3, the tracers we used are the *calcium* and the *silica* and the end-members for the Haute-Mentue catchment are: groundwater - enriched in both calcium and silica, soil water - enriched in silica but depleted in calcium because of the contact with decarbonated soil matrix and the rain water - depleted both in calcium and silica. They allow identification of geographical pathways for mixed old and new waters. The results of the application of the environmental tracing for the Haute-Mentue catchment are presented in Chapter 3.

Classical TOPMODEL identifies the overland and the subsurface component contributing to the total discharge. The quick component is generated by rainfall falling on saturated areas and producing a rapid delivery of the waters to the stream via macropores flow, overland flow or displacement of the old water. The subsurface flow represents a mixture of different proportions of new and old waters.

In order to have a link between components identified by TOPMODEL and EMMA approach, model modification was necessary. This is not an easy task since it is requiring new parameters added to the existing ones which increases model complexity and model parameters indentifiability. A compromise has to be done in order to approximate the model components to those identified by the chemical approach. In this sense, we've chosen to work with a version of TOPMODEL, which simulates the quick flow component, a deep groundwater component and a shallow subsurface component contributing to the stream flow.

We have chosen to work with this model in respect to the main hypothesis concerning the hydrological behaviour on the Haute-Mentue catchment. Works of Iorgulescu (1997), Joerin (2000), and Balin (see Chapter 3) identified several behaviours for the experimental sub catchments. For humid periods, rapid rising of the groundwater table can be observed for almost all the catchments covered by morainic deposits. This corresponds also with important volumes of the soil water contributing to the stream discharge. For these periods one can

assume that the soil water is a mixing between the new water and diluted groundwater. This behaviour is reproduced generally by the TOPMODEL version we worked with and whose developments have been stated by Boyer et al. (1996). The second kind of behaviour during wet periods concerns the formation of the perched water table over impervious or over soil texture discordances. In this case the storm flow appearing in the upper soils horizons would be formed essentially by new water. During the rainfall event soil moisture deficit uniformization is occurring through the unsaturated zone and the groundwater reaches the storm flow zone. This kind of behaviour is represented, for example, by a version of TOPMODEL developed by Scanlon et al. (2000). As this type of behavior is a secondary one and it doesn't last for long time periods, we considered that the classical version of TOPMODEL and the version proposed by Boyer et al. (1996) are appropriate simplified representations of the main hydrological processes that have been observed on the Haute-Mentue catchment.

“Groundwater rise” version of TOPMODEL

This version uses classic TOPMODEL equations and it separates the subsurface flow in two components depending on the mean catchment saturation deficit compared to an upper allowed separation deficit. Further complexity could be allowed by introducing a new parameter to separate between the macropore zone and the soil zone. Comparing with classical TOPMODEL, this version is introducing between 1 and 3 supplementary hydrological parameters. This operation is not without consequences when considering the model calibration and the parameters identification. To discern eventual over-parameterization of the model, study of the correlations between the parameters should be considered.

This version is based on the same principles and the same reservoirs as classical TOPMODEL and it has been used by Boyer et al. (1996) in order to simulate the DOC concentration in the Deer Creek river. The root zone is defined by two parameters: the initial and the maximum store deficit. The vertical drainage to the saturated zone is described by the same equation like in classical Topmodel (4.4). The flow through the saturated zone is separated in subsurface shallow flow and deep flow upon that the mean catchment saturation deficit is less or greater than an upper limit of the soil reservoir. This upper deficit limit is given by two model parameters:

- the drainable porosity (n);
- the upper depth of the stormflow reservoir (Z_{upper});

In case that the mean catchment deficit (D_{moy}) is greater than an upper deficit ($n \cdot Z_{upper}$) than the upper stormflow (Q_{upper}) is given by:

$$Q_{upper} = Q_b \cdot \left(\frac{Z_{upper} \cdot n - D_{moy}}{Z_{tot} \cdot n - D_{moy}} \right) \quad (4.6)$$

where

Q_b is the simulated total groundwater flow (m);

Z_{tot} is the total depth of the saturated zone (m);

Otherwise the upper stormflow is zero and the baseflow is routed only through the deep groundwater reservoir. In the version used by Boyer et al. (1996) the upper soil reservoir was

characterized by constant values of the drainable porosity and of the depth of the upper reservoir. In our version, these parameters were allowed to vary and were introduced as two supplementary model parameters.

This TOPMODEL version simulates rise of the groundwater flow and partition between the upper and the deep subsurface reservoirs.

As already stated, after comparing with the general conceptual model given by application of the environmental tracing, we considered that this TOPMODEL version approaches the general functioning of the catchment as indicated by the experimental approach.

4.2 Parameter estimation: the case of single response calibration

One of the issues of conceptual rainfall-runoff modeling was the development of the different calibration approaches in order to estimate the model parameters. While the first methods to estimate parameters were done manually, the hydrologists had quickly realized that for complex models this calibration is a very demanding task and could simply be inappropriate for models, which require a large number of parameters. With the development of computer power, different automatic calibration methodologies have been developed which generally aim to find a unique set of parameters for a given objective criterion describing the fit between the observed and the simulated records. For the interested reader many references, Refsgaard and Storm (1996), Sorooshian (1991), Gupta and Sorooshian (1985), Sorooshian and Gupta (1983; Duan et al. (1993) exist on this subject. The experience accumulated over the past decennia shows clearly that the use of different fitting criteria lead to different sets of optimum parameters and this issue was an important constraint for the practitioners and the hydrologist working in the applied field of hydrology. Moreover, depending on the model complexity, the calibrated optimum sets of parameters are difficult to use in validation, for periods completely different than those used for calibration (Beven et al. (2001)). In this context it became important to specify which is the uncertainty associated with a given “optimum” set of parameters. This contributed to the development of new methodologies of calibration of the hydrological models, which are the stochastic ones such as the Bayesian estimation techniques. The Generalized Likelihood Uncertainty Estimation (GLUE) of Beven and Binley (1992) became one of the most familiar and well-known methodology to estimate parameters and their uncertainty as well as uncertainty of the hydrological model outputs. Parallel to this approach, other Bayesian methodologies have been used in order to estimate parameters uncertainty such as Monte Carlo Markov Chain (MCMC) estimation techniques used by Kuczera and Parent (1998).

This chapter will introduce and will compare two kinds of bayesian estimation techniques that we used to estimate parameters for different version of TOPMODEL. These are the GLUE and the Monte Carlo Markov Chain methodologies. Both of them are stochastic techniques as they are based on use of random numbers and of probabilities.

4.2.1 The bayesian method principles: likelihood formulation, prior and posterior distribution

The main characteristics of the Bayesian methods consist in the fact that they are using a probability model to fit a set of data and they summarize the results (estimated model parameters and predictions for new observations) by probability distributions. Gelman et al. (2000) consider that the Bayesian methodology can be divided into three steps:

- (i): set a probability model by choosing in conformity with the knowledge we have, a prior probability distribution for all unknown quantities (model parameters in our case);
- (ii) condition on the observed data by choosing a likelihood function and then computing the posterior distribution of the unknown quantities (e.g. model parameters);
- (iii) evaluate the fit of the model and the consequences of the resulting posterior probability distributions on the model outputs.

Thus Bayesian theory is built on three probability concepts: the prior distribution (1), the likelihood function (2), the posterior distribution and through Bayes theorem (3).

1. The prior distribution $p(\theta)$

It is one of the most controversial topics between the frequentists and the Bayesians statisticians because prior distributions are subjective probabilities, i.e. distributions that should be interpreted as decisional bets, not frequencies limits. The Bayesian approach considers the model parameters as random variables to which one can associate a certain subjective probability. The knowledge of the model parameters before using the observed data (or measurements) is given by the prior probability density function of the parameters. From the Bayesian point of view, the width of the prior distribution represents rather the range of values consistent with our perception than a parameter variability range.

Function of the amount of information, the prior distribution, could be non-informative or informative. Vague knowledge about the parameters could be represented by a non-informative prior distribution such as a bounded uniform distribution:

$$p(\theta) \propto \text{constant} \quad (4.7)$$

Another example of non-informative prior used in the following work is the case of an unknown variance parameter. In this case one can specify a prior distribution for the variance parameter. Usually a uniform distribution is chosen on $(-\infty, +\infty)$ for $\ln(\sigma)$ which means that $p(\ln(\sigma)) \propto \text{constant}$.

Transformation from $p(\ln(\sigma))$ to $p(\sigma)$ leads to a non informative prior distribution for $p(\sigma)$ on $(0, +\infty)$:

$$p(\sigma) = p(\ln(\sigma)) \left| \frac{\partial \ln(\sigma)}{\partial \sigma} \right| = \text{constant} \cdot \frac{1}{\sigma} \propto \sigma^{-1} \quad (4.8)$$

In this case, this prior distribution it is said to be improper because it leads to an infinite integral over the range $(0, +\infty)$ and thus it does not integrate to 1 as the sum of probabilities should do.

More knowledge of the parameters before the data are used can be expressed as informative prior distributions such as different standard probability distributions.

2. The likelihood function $L(\theta), p(Y | \theta)$

The likelihood function summarizes all the information about the parameters available from the data. The common notation for the likelihood function is $L(\theta)$ and this is found by evaluating the probability density function $p(y | \theta)$ at the observed data (y). As the data are fixed, the likelihood is a function of the parameters θ only. For multiple independent y_i , the likelihood function is given by the product of individual probability density functions evaluated at individual observations.

Note: The likelihood function can be also interpreted as a conditional probability ($p(y | \theta)$) and it should be read like the “probability of y given θ “. The classical approach to defining conditional probabilities is via joint distribution. A well-known formula is used:

$$p(y | \theta) = \frac{p(y, \theta)}{p(\theta)} \quad (4.9)$$

where:

- $p(y, \theta)$ is the joint probability distribution of y and θ (which is given by $p(y \cap \theta)$);
- $p(\theta)$ is the prior distribution.

3. The posterior distribution and the Bayes' theorem ($p(\theta | Y)$)

If the likelihood function $p(y | \theta)$ gives information of the data y conditioned on the model parameters θ , the conditional distribution of the model parameters θ given the observed data y is called posterior distribution $p(\theta | y)$ and represents the update of the prior distribution $p(\theta)$ with the likelihood function $p(y | \theta)$.

Applying the conditional probabilities properties one can write:

$$1. \ p(\theta | y) = \frac{p(\theta, y)}{p(y)} \quad (4.10)$$

$$2. \ p(y | \theta) = \frac{p(y, \theta)}{p(\theta)} \quad (4.11)$$

$$3. \ p(\theta, y) = p(y, \theta) \quad (4.12)$$

From (4.10), (4.11) and (4.12) one can derive the expression of the posterior distribution of the model parameters conditioned on the observed data, which is well known as the Bayes' rule:

$$p(\theta | y) = \frac{p(y | \theta) \cdot p(\theta)}{p(y)} \quad (4.13)$$

$p(y)$ can be considered as a probability of the evidence which is a constant and in this case the Bayes rule can be rewritten as:

$$p(\theta | y) \propto p(y | \theta) \cdot p(\theta) \Leftrightarrow \text{posterior} \propto \text{likelihood} \cdot \text{prior} \quad (4.14)$$

In the context of hydrological modeling, the Bayes' rule can be used to estimate model parameters and parameters uncertainty. In order to do that one should have knowledge about the model parameters (θ) prior information $p(\theta)$ and about the form of the likelihood function $p(Y|\theta)$ in order to compute the posterior distribution of the model parameters conditioned on the observed data $p(\theta|Y)$.

A general conceptual rainfall-runoff model (Figure 4-1) can be transposed into a Bayesian framework by introducing a model for the errors. To sum it up, the general aim of a conceptual model is to reproduce the discharges at the catchment's outlet (Y) by using input data such as measured rainfall, potential evapotranspiration (P , PET) and model parameters (θ). This is usually done by estimating the model parameters such as the difference between observed and simulated discharges, or model error (ϵ), be as small as possible. In other words, and in a Bayesian approach, the main aim of a hydrological model is to estimate parameters given the observed discharges at the catchment's outlet $p(\theta | Y)$.

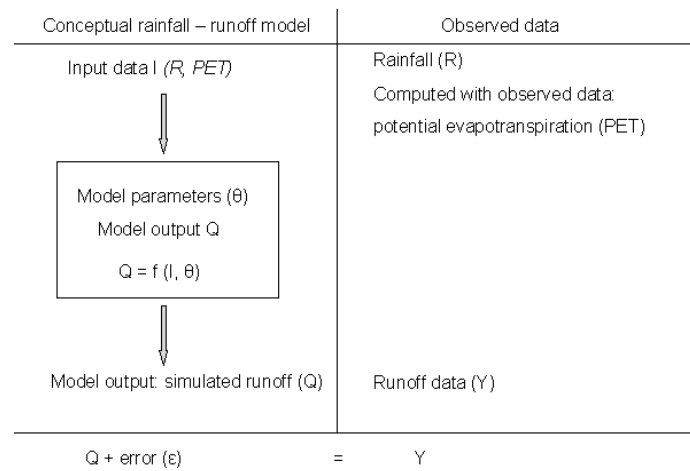


Figure 4-1. Conceptual hydrological model – conceptual scheme

The further chapter introduces two Bayesian methods to estimate parameters of a hydrological model. The first is GLUE methodology developed by Beven and Binley (1992) and the second one is a Monte Carlo Markov Chain methodology presented by Kuczera and Parent (1998). Both methods belong to the class of the Bayesian techniques of estimating parameters and both include two steps in their implementation:

- 1) choice of the simulation error modeling strategy;
- 2) choice of the sampling strategy to estimate model parameters.

4.2.2 GLUE methodology

The GLUE methodology is largely used in different fields of the environmental modeling in order to estimate model parameters and their uncertainty i.e. hydraulic applications (Aronica et al. (1998)), erosion modeling (Brazier et al. (2000)), groundwater modeling (Christensen (2004)), land-surface atmosphere modeling (Franks and Beven (1997)), atmospheric deposition (Page et al. (2003)), regionalization studies (Engeland and Gottschalk (2002)), flood frequency modeling (Blazkova and Beven (2002)), rainfall modeling (Cameron et al. (2000)) and runoff-rainfall modeling (Franks et al. (1998), Blazkova et al. (2002), Lamb et al. (1998)). The starting point was the observation that different calibration strategies lead to different sets of optimum parameters and one of the main goals of the GLUE methodology was to take into account the uncertainty associated with model parameters estimation. Another important point of the GLUE methodology was the concept of equifinality meaning that in the parameter space one cannot speak of optimum parameter set because often calibration of the hydrological models leads to multiple sets of parameters that give acceptable simulations. More than that, application of the GLUE methodology showed that equally likely performing parameters may be found in different regions of the parameter response surface, which makes difficult the use of traditional calibration techniques.

Generalized likelihood function

The first step in implementing GLUE concept is related to the choice of a likelihood function. Beven and Binley (1992) work with the so-called “Generalized Likelihood Function“. As indicated by its name, this likelihood function is a generalized one and does not make explicit assumptions about the structure and the nature of the errors associated with model simulations. Several choices can be made for the “Generalized Likelihood function”:

$$\text{- Nash-Sutcliffe criterion Nash and Sutcliffe (1970): } NS = 1 - \frac{\sum_t (Q_{obs} - Q_{sim})^2}{\sum_t (Q_{obs} - Q_{obs-average})^2} \quad (4.15)$$

$$\text{- sum of squared residuals over all the time steps: } SSR = \sum_t (Q_{obs} - Q_{sim})^2 \quad (4.16)$$

$$\text{- sum of squared log residuals over all the time steps: } SSLR = \sum_t (\ln(Q_{obs}) - \ln(Q_{sim}))^2 \quad (4.17)$$

$$\text{- sum of the absolute errors over all the time steps: } SAE = \sum_t |Q_{obs} - Q_{sim}| \quad (4.18)$$

It is worth mentioning that the likelihood function is used more like a likelihood measure that gives information of the departure of simulated data compared to observed data.

Recently different forms of likelihood measures have been presented in a general review of the GLUE methodology (Beven and Freer (2001) in environmental systems (Table 4-1).

Based on inverse error variance (Beven and Binley, 1992)	$L[M(\Theta Y_T, Z_T)] = (\sigma_e^2)^{-N}$
Based on Nash and Sutcliffe criterion (Freer et al., 1996)	$L[M(\Theta Y_T, Z_T)] = (1 - \sigma_e^2 / \sigma_o^2)^N, \sigma_e^2 < \sigma_o^2$
Based on exponential transformation of error variance (Freer et al., 1996)	$L[M(\Theta Y_T, Z_T)] = \exp(-N\sigma_e^2)$

Table 4-1. Example of likelihood measures for GLUE methodology- after Beven and Freer (2001), where σ_e^2, σ_o^2 are the error variance and the variance of the observations, $M(\Theta | Y_T, Z_T)$ indicates the i th model conditioned on input data Y_T and observations Z_T

Importance sampling algorithm

The second step in implementing the GLUE concept is related to the sampling methodology to estimate model parameters. Importance sampling is used in the GLUE methodology.

Importance sampling belongs to the class of Monte Carlo sampling methods that are used to approximate posterior parameters' distributions. These methods have been developed in order to overcome the problem of sampling uniformly over regions of low interest and hence to improve the overall efficiency of the Monte Carlo sampling Tanner (1992). As mentioned in Kuczera and Parent (1998), the idea behind this method is to sample from weighted probability distribution that approximates the posterior probability distribution. Three steps characterize the Monte Carlo importance-sampling algorithm used by GLUE:

1. sample parameters from the uniform prior parameter distributions and compute the likelihood measures;
2. evaluate the importance weights $w_i(\theta)$ and then normalize the importance weights

such as their sum is 1: $p_i(\theta) = \frac{w_i(\theta)}{\sum_1^N w_i(\theta)}$; in this case the weights are the generalized

likelihood for the simulated sample of θ .

3. update the posterior parameter distributions and weight the model predictions by the importance weights in order to compute their posterior distributions.

Case study

An application example is presented further with the classical version of TOPMODEL rainfall-runoff model. The model was applied for a small basin, Bois-Vuacoz (area of 0.24 km²) on the Haute-Mentue catchment during a humid period in autumn 2002. The model input data is represented by the rainfall provided by a close meteorological station and the potential evapotranspiration that has been computed with the Pennman –Monteith formula (Equation 2.1 in Chapter 2).

Prior distribution of the four parameters have been chosen uniform on feasible ranges defined in Table 4-2:

Parameter	Minimum value	Maximum value	Prior distribution
m [m]	0.001	0.1	uniform
lnT0 [m ² /h]	0.001	10	uniform
SRmax [m]	0.0001	0.1	uniform
SRinit [-]	0	1	uniform

Table 4-2. Prior distribution for TOPMODEL parameters

The likelihood measure used in this example was the Nash-Sutcliffe criterion (4.15), which can be rewritten as:

$$L(\theta | Y) = 1 - \frac{\sigma_i^2}{\sigma_{obs}^2}$$

The likelihood measures were rescaled with the formula below (GLUE- computer program, Help contents):

$$w_i = \frac{L_i - L_{\min}}{L_{\max} - L_{\min}} \quad (4.19)$$

where

L_i is the Nash-Sutcliffe criterion for a i set of parameter;

L_{\min} is the minimum Nash-Sutcliffe criterion;

L_{\max} is the maximum Nash-Sutcliffe criterion.

No threshold was used in order to compute likelihood weights and thus the entire Monte Carlo sample was used to compute the weights to assign to the runoff predicted by the sampled sets of parameters.

Figure 4-2 presents the scatter plots of the likelihood measure for three of the most sensitive parameters: m - the groundwater scale depth parameter, $lnT0$ - the saturated transmissivity at the soil surface and $Srmax$ - the maximum capacity of the root zone. The results suggest that for all the parameters but m , the parameter response surface is spread over almost all the feasible range and that multiple sets of the parameters are likely to give equal results in terms of likelihood measure. These results confirm the equifinality concept developed by Beven (2000) that lead to large uncertainty in the model discharge predictions (Figure 4-3) and which diminishes the predictive power of the model. These uncertainties are more important for high discharge peaks rendering the model unusable for prediction purposes.

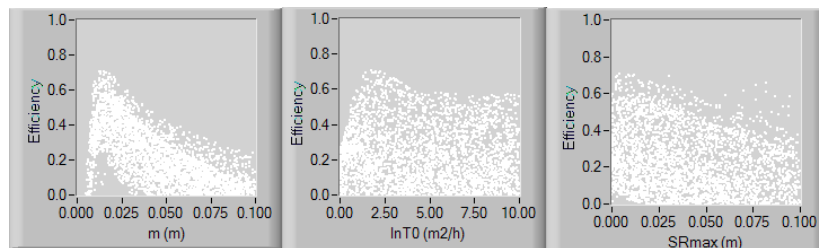


Figure 4-2. TOPMODEL and GLUE: Efficiency versus sampled parameters from the posterior distributions

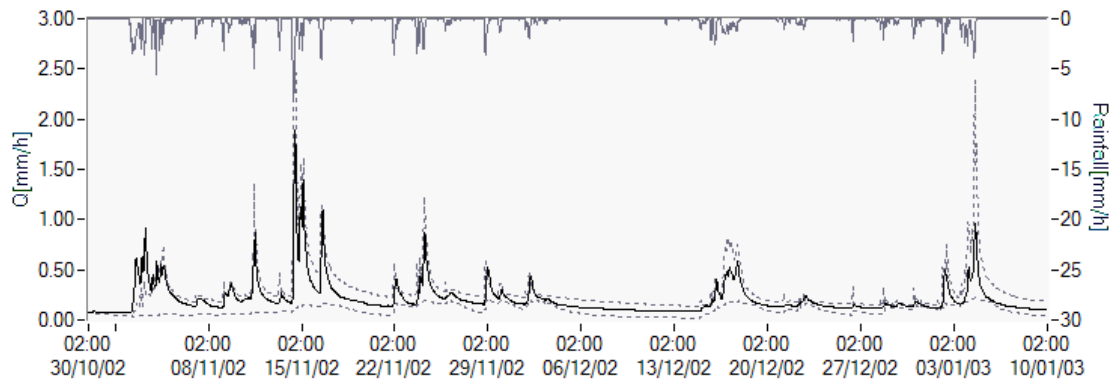


Figure 4-3. TOPMODEL and GLUE methodology- Observed discharge and simulated uncertainty bounds at 90%

4.2.3 Monte Carlo Markov Chain methods

The GLUE methodology produces estimates of the uncertainty associated with model predictions but it finds its limits for models with a big number of parameters because of the huge required number of simulations. In this case, an alternative could be the Monte Carlo Markov Chain methods. The MCMC methods are increasingly used for estimating parameters in different applications such as medicine, economy, biology, different environmental fields etc. but they are less frequently used in the hydrological field. Nevertheless, the last few years several papers appeared which used the MCMC methods on hydrological model parameter estimation (Overney (1997), Kuczera and Parent (1998)).

The beginning of the MCMC method is connected to the Metropolis algorithm used for the first time in statistical physics and due to Metropolis et al. (1953), which aimed to simulate the evolution of a solid in a heat bath towards equilibrium. As a statistical tool, the MCMC methods belong to the class of Bayesian methods to sample from a distribution known up to a constant. This is generally the case of posterior distribution. A Markov chain is a sequence of random values whose probabilities at a time interval depend upon the value iterated at the previous time. Consider a stochastic process (X) which is in state i at time t : $X(t) = i$ and note the probability $P_{ij}(t+1)$ as the probability that this stochastic process be in state j at time $t+1$ given that it is in state i at time t :

$$P_{ij}(t+1) = P\{X(t+1) = j \mid X(t) = i\} \quad (4.20)$$

A Markov chain is a stochastic process in which the conditional distribution at any future time $t+1$ for the given past states and the present state is independent of the past states and depends only on the present state (Sen and Stoffa (1995)).

The controlling factor in a Markov chain is the transition probability that can be seen as a conditional probability for the system to go to a particular new state, given the current state of the system. A positive and a homogeneous Markov Chain converges towards a limiting probability distribution which is independent of the initial state and which, in Bayesian terms, corresponds to a posterior probability density function.

As the GLUE methodology, the implementation of the Monte Carlo Markov Chain method supposes two steps:

- choice of the simulation error modeling strategy;
- choice of the sampling strategy to estimate model parameters

Simulation error modelling strategy: Statistical likelihood function

The first step before implementing the MCMC methodology is the choice of the likelihood function. In this work, we have chosen to work with a statistical likelihood approach. The simulation errors have been modeled by a normal law that means that between the observed and predicted values the following relation can be stated:

$$Y = Q + \varepsilon, \text{ where } \varepsilon = N(0, \sigma^2) \quad (4.21)$$

As Q is a function of observed input data (I) and model parameters (θ) one can say that

$$Y = f(I, \theta) + \varepsilon \quad (4.22)$$

In terms of likelihood function this means that the conditional probability of the observed data given the model parameters can be described, for a single observation, by a normal distribution:

$$L(\theta) = \frac{1}{\sqrt{2\pi} \cdot \sigma} \exp\left(-\frac{1}{2\sigma^2} (Y_i - Q_i)^2\right) \quad (4.23)$$

The likelihood function for n observations, independent and identically distributed IID is given by the product of individual probability distributions:

$$L(\theta) = \frac{1}{(\sqrt{2\pi})^n \cdot \sigma^n} \exp\left(-\frac{1}{2\sigma^2} \sum_{i=1}^n (Y_i - Q_i)^2\right) \quad (4.24)$$

In order to be able to use this likelihood function, the required statistical hypothesis such as constancy of the variance and time independence of the residuals (ε) should be respected. In respect to this, exploratory analysis of the modelling errors is required and when important departures from these hypothesis are observed, it is important to correct the data by using different techniques such as Box – Cox transformations (Box and Cox (1964), Kuczera (1983)).

Sampling methodology: the Metropolis algorithm

As already mentioned, the origins of the Metropolis algorithm can be found in physical statistics and mechanical physics. Due to the complexity of the macroscopic system it was necessary to use statistics instead of determinism to describe a physical system. Statistics describe a system by using a probability distribution. The Metropolis algorithm proposed towards 1953 by Metropolis N. et al. was intended to simulate the evolution of a system in a heat bath towards thermal equilibrium and since the works of Kirkpatrick et al. (1983) it was used in a wide range of applications.

As a Monte Carlo method, the Metropolis algorithm generates samples by using a Markov chain that converges to a given probability posterior distribution. The Metropolis algorithm includes three steps: (1) generation of new samples from the previous generated ones (jump specification), (2) acceptance of the new generated parameters set (acceptance rule) and (3) monitoring of the convergence of the algorithm.

1) Generation of new parameters by jump specification step

The jump specification is needed to build a Markov chain in order to sample new candidates starting from the previous ones. Several methods exist and a brief review of them is given in Torre et al. (2001). The jump specification is needed to sample from fixed multivariate probabilities distributions and this can be done by using a random or a forced walk algorithm. For the random walk, each candidate is sampled around the last sampled ones without specification of a special direction of movement. The sampling can be done by using any symmetric probability distribution (which means that $p(\theta_{old} | \theta_{new}) = (p(\theta_{new} | \theta_{old}))$ centred on the last accepted candidates ($\theta_{new} | \theta_{old} = N(\theta_{old}, s \cdot I)$ where θ_{new} and θ_{old} are the candidate and respective the last vectors of accepted parameters, s is a variance scaling factor and I is the identity matrix). The jump distribution isn't correlated, every direction of movement having the same weight or the same probability (Figure 4-4-a).

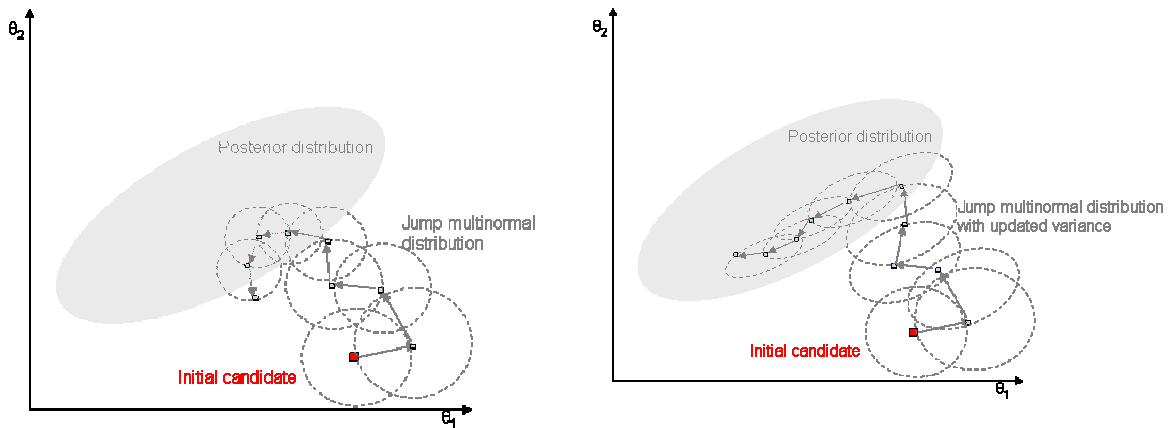


Figure 4-4. Jump distribution: random walk algorithm (a) and forced walk algorithm (b)

In the forced walk algorithm, the candidates are drawn in the same way as for the random walk but with a preferential direction (Figure 4-4-b). This is given by the variance-covariance matrix V of the last n iterations of the chain. In this case, one can write $\theta_{new} | \theta_{old} = N(\theta_{old}, s \cdot V)$ where θ_{new} and θ_{old} are the candidate and respective the last vectors of accepted parameters, s is a variance scaling factor and V is the variance-covariance matrix of the parameters generated over the last n iterations of the chain.

For both jump distributions, the variance of the jump distribution can be periodically tuned by a scaling factor s to speed convergence of the algorithm. Gelman et al. (2000) suggested that the strength of the jump be adjusted according to the observed acceptance ratio after a fixed number of iterations and that the initial scaling factor of the jump distribution should be equal to $2.4/\sqrt{d}$ where d is the number of parameters. Ideally, this scaling factor should be adjusted in such way that the acceptance ratio (the number of accepted sets of parameters reported to

the total number of generated sets of parameters) vary around 0.23 (for $d > 5$) and 0.43 for $d = 1$ (Torre et al. (2001)).

2) Acceptance /rejection of the new generated parameters step: Acceptance rule

The second part of the Metropolis algorithm is given by the acceptance-rejection of the last generated set of parameters. This step is the central point of the Metropolis algorithm. First, one has to compute the ratio of the posterior probabilities densities function between the last accepted and the candidate vectors of parameters:

$$r = \frac{p(\theta_{new} | Y)}{p(\theta_{old} | Y)} \quad (4.25)$$

where θ_{new} and θ_{old} are the candidate (new) and respective the last accepted (old) vectors of parameters.

The candidate vector of parameters is added or not to the previous Markov chain based on the following rule known as the Metropolis rule:

- if $r > 1$ than set $\theta^{i+1} = \theta_{new}$, the candidate set of parameters is accepted with probability 1.
- if $r < 1$ than u is generated randomly from the uniform distribution $[0,1]$:
 - if $r > u$ than set $\theta^{i+1} = \theta_{new}$, the candidate set of parameters is accepted,
 - otherwise set $\theta^{i+1} = \theta_{old}$ the candidate set of parameters is rejected and we keep the last vector set of parameters.

The transition probability (P_{ij}) for a parameter to be in a state j at $t+1$ given that it is at state i at the time t is influenced by both generation and acceptance probabilities:

$$P_{ij} = G_{ij} \cdot A_{ij} \quad (4.26)$$

where G_{ij} is called generation probability (jump probability) and A_{ij} is called the acceptance probability and is given by the Metropolis acceptance rule.

Special cases of the Metropolis algorithm

a) The Metropolis algorithm it is a special case of the more general **Metropolis-Hastings algorithm** Hastings (1970). The only difference consists in specifying the jump distributions. The Metropolis - Hastings algorithm allows using of asymmetric jumping distributions which imposes an update of the acceptance rule to:

$$r = \frac{p(\theta_{new} | Y) \cdot p(\theta_{old} | \theta_{new})}{p(\theta_{old} | Y) \cdot (p(\theta_{new} | \theta_{old}))} \quad (4.27)$$

where for asymmetric distributions $p(\theta_{old} | \theta_{new})$ ($p(\theta_{new} | \theta_{old})$).

b) The **Gibbs algorithm** introduced in the context of image processing by Geman and Geman (1984) represents another special case of the Metropolis algorithm. Given the parameter vector $(\theta_1, \theta_2, \dots, \theta_n)$, the Gibbs algorithm samples a parameter value at once conditional on all

the other values, which are kept fixed so the Gibbs algorithm works with univariate conditional distributions.

A simple example to illustrate this algorithm is given below (from Walsh (2000)):

Consider a bivariate parameter vector (θ_1, θ_2) ;

- to compute the posterior marginal distributions $p(\theta_1)$ and $p(\theta_2)$ consider the conditional distributions $p(\theta_1|\theta_2)$ and $p(\theta_2|\theta_1)$;
- the sampler starts with some initial values for θ_{2-0} and generates θ_{1-0} from the conditional distribution $p(\theta_1|\theta_2 = \theta_{2-0})$;
- then the sampler uses θ_{1-0} to generate a new value for θ_{2-1} and for the iteration i the sampler proceeds as follows:

$$\theta_{1-i} = p(\theta_1|\theta_2 = \theta_{2-(i-1)}) \text{ and } \theta_{2-i} = p(\theta_2|\theta_1 = \theta_{1-(i-1)})$$

When more than two variables are involved, the generalization of the above algorithm becomes:

$$\theta_i^{(k)} = p(\theta^{(k)} | \theta_i^{(1)}, \dots, \theta^{(k-1)} = \theta^{(k-1)}, \theta_{i-1}^{(k+1)} = \theta_{i-1}^{(k+1)}, \dots, \theta^{(n)} = \theta_{i-1}^{(n)}) \quad (4.28)$$

The Gibbs sampler is a special case of the Metropolis algorithm for which all the candidates are accepted, the acceptance ratio r being equal to 1.

c) **Gibbs within Metropolis-Hastings** represents another special case of the Metropolis algorithm. More attention will be accorded to this algorithm, as it was this one that we used later in order to estimate parameters of different versions of TOPMODEL. This algorithm is a hybrid between Metropolis-Hastings and Gibbs algorithms. The acceptance rule is given by the Metropolis-Hastings rule while generation of new parameters is made by using both Metropolis and Gibbs methods. This choice was motivated by the use of the gaussian statistical likelihood function with unknown model variance. In our application, the model variance was considered as a new parameter added to the hydrological model parameters. Thus, the parameters' vector contains a hydrological parameter sub-vector (θ) and a noisy statistical parameter sub-vector (ψ) that includes the model variance (σ^2) and different autoregressive parameters (AR).

If only the model variance is considered as a noisy parameter, the Bayes' formula gives the posterior distribution of the parameters given the observed data:

$$(\theta, \sigma^2 | Y) \propto L(\theta, \sigma^2) \cdot p(\theta, \sigma^2) \quad (4.29)$$

which means that

$$(\theta, \sigma^2 | Y) \propto \frac{1}{(\sqrt{2\pi})^n \cdot \sigma^n} \cdot \exp \left(-\frac{1}{2} \cdot \frac{\sum_{i=1}^n (Y - Q(\theta))^2}{\sigma^2} \right) \cdot p(\theta, \sigma^2) \quad (4.30)$$

This is equivalent to:

$$(\theta, \sigma^2 | Y) \propto \frac{1}{(\sqrt{2\pi})^n \cdot \sigma^{2\left(\frac{n}{2}\right)}} \cdot \exp\left(-\frac{1}{2} \cdot \frac{\sum_{i=1}^n (Y - Q(\theta))^2}{\sigma^2}\right) \cdot p(\theta, \sigma^2) \quad (4.31)$$

$$\text{We note } S = \frac{\sum_{i=1}^n (Y - Q(\theta))^2}{2} \quad (4.32)$$

and we replace (4.32) in the equation above:

$$(\theta, \sigma^2 | Y) \propto \frac{1}{\sigma^{2\left(\frac{n}{2}\right)}} \cdot \exp\left(-S \cdot \frac{1}{\sigma^2}\right) \cdot p(\theta, \sigma^2) \quad (4.33)$$

If we note $z = \frac{1}{\sigma^2}$ (4.34), the posterior marginal distribution of the model variance (σ^2) conditioned on the observed data (Y) and model hydrological parameters (θ) the equation above becomes:

$$(\sigma^2 | Y, \theta) \propto z^{\frac{n}{2}} \cdot \exp(-S \cdot z) \quad (4.35)$$

which is a Gamma distribution with parameters $\frac{n}{2}$ and S .

We use this as a conditional distribution in order to sample the model variance parameter given previously fixed sampled hydrological parameters. This is called Gibbs within Metropolis-Hastings algorithm as we use both a multivariate normal jump specification for generating hydrological parameters and the Gibbs sampler in order to sample the variance model parameter. The acceptance rule is given by the Metropolis-Hastings rule (4.27), which becomes:

$$r = \frac{p(\theta_{new}, z_{new} | Y) \cdot p(\theta_{old}, z_{old} | \theta_{new}, z_{new})}{p(\theta_{old}, z_{old} | Y) \cdot p(\theta_{new}, z_{new} | \theta_{old}, z_{old})} \quad (4.36)$$

Replacing the posterior distributions by their equivalents and considering that the prior distributions for the hydrological parameters have been chosen uniform and that the prior distribution for the transformed variance (z) it is a non informative one (equal to $\frac{1}{z}$) the equation above becomes:

$$r = \frac{L(Y | \theta_{new}, z_{new}) \cdot p(z_{new}) \cdot p(z_{old} | z_{new})}{L(Y | \theta_{old}, z_{old}) \cdot p(z_{old}) \cdot p(z_{new} | z_{old})} \quad (4.37)$$

After introducing the corresponding equations and after replacing z with $\frac{1}{\sigma^2}$ the final form of the acceptance ratio becomes:

$$r = \exp\left[\left(\frac{1}{\sigma_{old}^2} + \frac{1}{\sigma_{new}^2}\right) \cdot (S_{old} - S_{new})\right] \cdot \left(\frac{S_{new}}{S_{old}}\right)^{\frac{n}{2}} \quad (4.38)$$

3) Monitoring convergence of the algorithm

A keynote of MCMC method implementation is the length of the sampled Markov chain that will influence the convergence of the chain towards the posterior limiting distribution. Usually the first part of the chain that corresponds to the burn-in period is removed and analyses are done on the second part, which should correspond to the well-mixed part of the chain supposed to represent the limiting posterior distribution after convergence. For our analysis, the first three quarters of the chain were thrown out and only the last quarter was used for further analysis. In order to determine if the sampled chain has reached a stationary limiting distribution, a convergence test has been applied. Several tests exist for studying convergence of a Markov chain (Gelman et al. (2000)). They are based on two different approaches: one kind establishes a diagnostic based on a single chain and the second kind on the base of several independent chains with different starting points in the parameter space. Both methods verify that the last part of the iterated chains belongs to the same statistical population since they are supposed to converge all towards the same target distribution. A list of the different techniques used to establish algorithm convergence is given in Cowles and Carlin (1996).

In this work, the Geweke test (Geweke (1992)) has been applied in order to check for convergence. This test is based on the assumption that the resulting chains can be seen as time series, which can be analysed by spectral density methods. According to this test, the last quarter of the chain was split in two samples: the first 15% of the chain and the last 50% of the chain. If the sampled chain had reached stationarity than the mean of the two samples should be the same. In order to check this, a simple z-score test has been further applied:

$$z = \frac{\mu_1 - \mu_2}{\sqrt{\frac{S(0)_1}{n_1} + \frac{S(0)_2}{n_2}}} \quad (4.39)$$

where

μ_1 and μ_2 are the means of the two separated chains;

$S(0)_1$ and $S(0)_2$ are the standard errors of the two separated chains as given by the spectral density estimation at the frequency 0.

n_1 and n_2 are the number of points in the two separated chains.

If the Metropolis chain has converged, this score should follow a standard normal distribution $N(0,1)$. Generally, a value larger than 2 indicates that the mean of the chain is not stationary, it is still drifting and thus the chain needs a longer burn-in period.

Case study

The following example shows applications of the Metropolis algorithm with a statistical approach for modelling the simulation errors. The classical version of TOPMODEL was used for this application and it was applied to the same small head-basin of the Haute-Mentue catchment. The study period was the same as for the GLUE application: October 2002-January 2003. This period was split in two sub-periods: a calibration period (7 October- 21 November 2002) and a validation one (22 November 2002-18 January 2003).

The model hydrological parameters to be estimated are: m the groundwater zone scale depth, $\ln T0$ – the saturated transmissivity at the soil surface, S_{rmax} – the maximum capacity of the root reservoir and S_{ro} – the initial capacity of the root reservoir.

To sample from parameters posterior distribution the Metropolis algorithm was used and we considered a statistical model for the simulation errors (4.24).

12500 iterations have been done (Figure 4-5 a, b, c) from which the first 75% has been discarded (Figure 4-5 d) in order to ensure that we sample from the posterior distributions of the model parameters. A thinning factor of 2 was applied to the retained chain in order to reduce dependence of the parameters within their posterior distributions. The Geweke test has been applied in order to test convergence of the algorithm. Figure 4-5d shows the first 15% and the last 50% of the remaining chain for m parameter. The results of the Geweke test indicate convergence of the algorithm (z score less than 1).

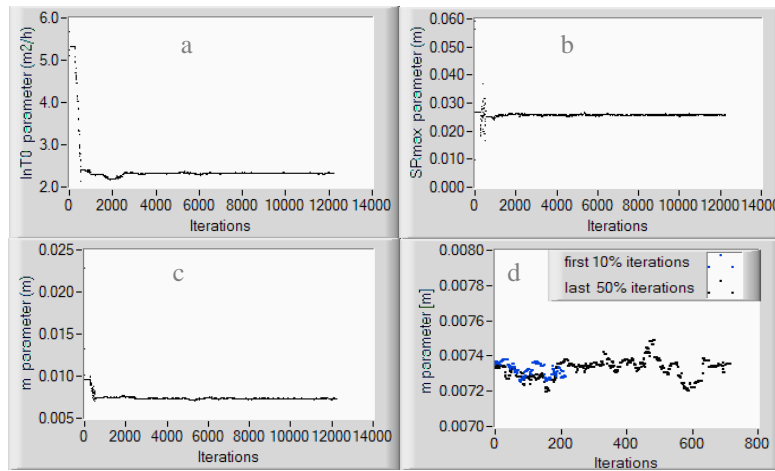


Figure 4-5 Gibbs within Metropolis algorithm: parameter trace (a, b, c) and convergence Geweke test results for m parameter (d)

The parameter prior distributions were the same as in the GLUE methodology (see Table 4-2). The simulation errors have been modelled by a normal model, which means that the likelihood function is given by (4.24).

The model variance has been introduced as a new statistical parameter added to the 4 hydrological ones and its prior distribution was considered uniform on the range $(0, +\infty)$. The Gibbs within Metropolis algorithm has been used in order to sample from the parameter posterior distribution. In order to speed convergence of the algorithm a forced walk algorithm has been used as jumping distribution for the hydrological parameters. The variance scaling parameter has been updated every 500 iterations. In order to sample feasible values of the variance parameter we applied a Gibbs within Metropolis algorithm. We sampled the inverse of model variance from its posterior conditional distribution, which is a Gamma distribution

with parameters $\frac{n}{2}$ and S where n is the number of observations and $S = \frac{1}{2} \sum_{i=1}^n (Y - Q(\theta))^2$.

The Figure 4-6 presents the posterior distribution of the hydrological parameters as well as of the model variance. The form of the posterior distributions depends essentially on the selected likelihood function as the prior distributions were chosen uniform on feasible ranges. Figure 4-7a plots the model residuals ($r = Q_{\text{observed}} - Q_{\text{simulated}}$ [l/s]) versus the simulated runoff. One can see that one of the statistical hypotheses of residual variance constancy is not respected, as the residuals are greater with greater runoff values. The second diagnosis plot (Figure 4-7b) indicates large departure from the hypotheses of time independence of the modelled residuals.

These results might influence the quality of the results and hence the quality of the estimated uncertainty of the predicted response. The propagation of the uncertainty of the parameters on the predicted discharges is presented in Figure 4-8. One can see that in comparison with the same plot given by the GLUE methodology the uncertainty is smaller but still important in order to use it for predictive purposes. Moreover in order to produce reliable estimates of the model parameters and of the predictive uncertainty, further corrections of the discharge data appear to be necessary in order that the statistical hypotheses be accomplished. The observed discharges find themselves within the simulated uncertainty bounds at 90%, which indicates that the model structure is acceptable, and that it captures the most important features of the hydrological processes for this catchment and this period.

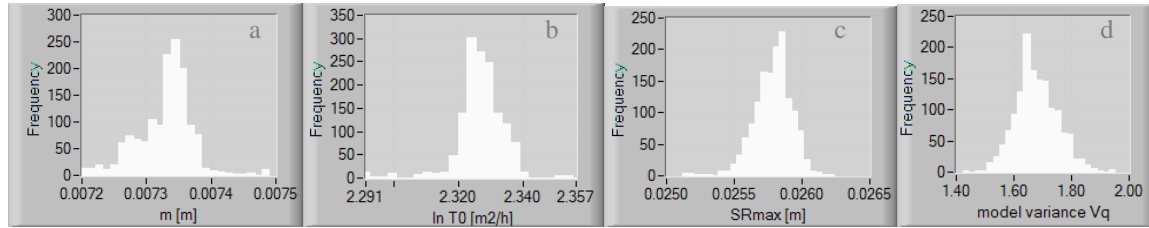


Figure 4-6. TOPMODEL and MCMC methodology with statistical likelihood without Log and AR corrections: posterior distributions of hydrological parameters (a, b, c) and statistical parameter (d)

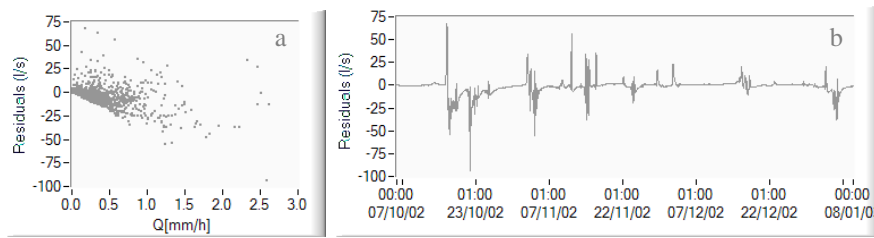


Figure 4-7. TOPMODEL and MCMC methodology with statistical likelihood without Log and AR corrections: model residuals against predicted runoff (a) and against time (b)

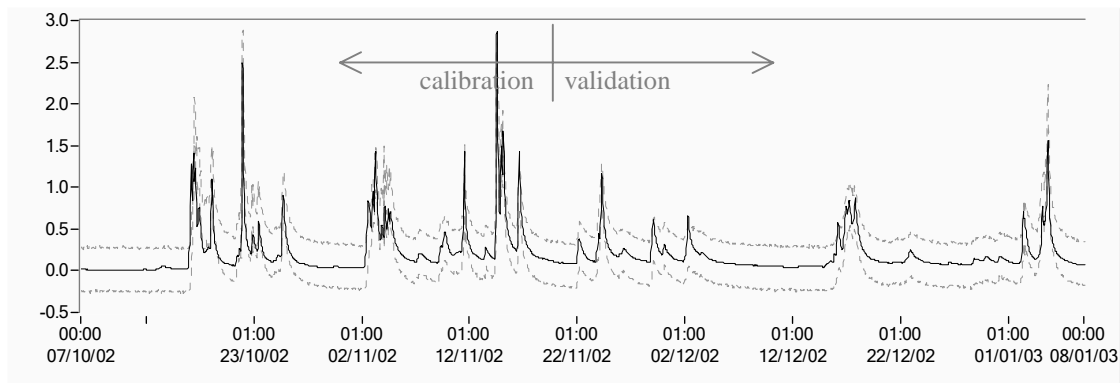


Figure 4-8 TOPMODEL and MCMC methodology with statistical likelihood without Log and AR corrections: observed discharge and simulated uncertainty bounds at 90%

In order to correct for inadvertences of the statistical hypothesis further step was to transform the discharge data by using the Box-Cox transformations (Kuczera (1983)). In order to stabilize the residuals variance we worked we log transformed discharge data (Q), which corresponds to the following Box-Cox transformations:

$$q = \frac{(Q+k)^\lambda - 1}{\lambda} \quad \text{for } \lambda \neq 0 \quad (4.40)$$

$$q = \log(Q + k) \text{ for } \lambda = 0; \quad (4.41)$$

In this work the Box-Cox parameters were: $\lambda = 0$ and $k = 0.0001$ and the corresponding likelihood function becomes:

$$L(\theta) = \frac{1}{(\sqrt{2\pi})^n \cdot \sigma_{\log}^n} \exp\left(-\frac{1}{2\sigma_{\log}^2} \sum_{i=1}^n (q_{obs_i} - q_{sim_i})^2\right) \quad (4.42)$$

where q is defined above and σ_{\log} is the standard deviation of the log transformed model.

The results of these transformations are presented below. The posterior distributions of the model parameters are slightly different shaped and their mode and variance are also slightly different that those obtained in the model without any corrections (Figure 4-9).

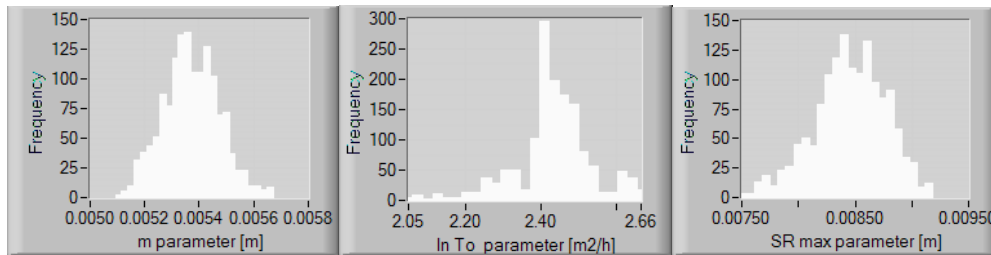


Figure 4-9. TOPMODEL and MCMC methodology with statistical likelihood with Log and without AR corrections: Marginal posterior distribution for m , $\ln T_0$ and SR

The parameters uncertainty determined the following uncertainty limits for the predicted discharge (Figure 4-10):

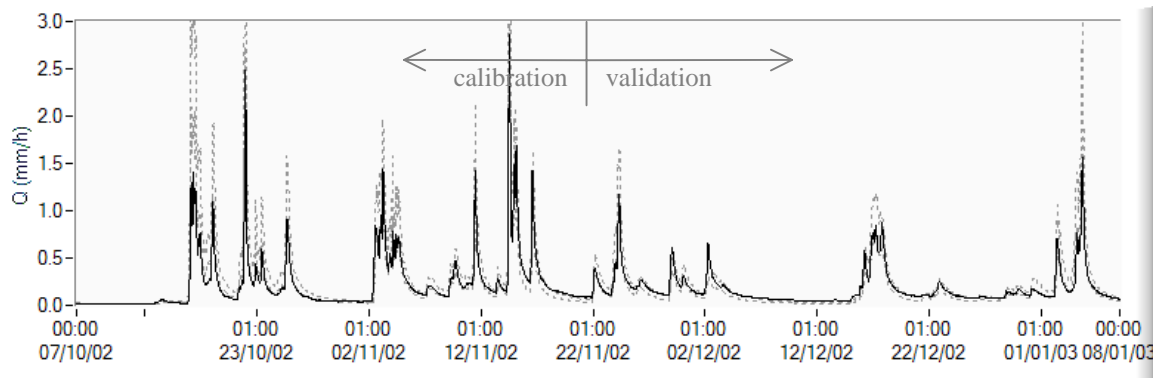


Figure 4-10 . TOPMODEL and MCMC methodology with statistical likelihood with Log and without AR corrections: Observed discharge and simulated uncertainty bounds at 90%

The observed discharges are within the simulated uncertainty bounds and the uncertainty is smaller in comparison with previous cases, which increases the predictive power of the proposed model. Nevertheless, the model fails to reproduce the observed discharge in the beginning of the simulated period as well as the peaks discharge.

The model variance posterior distribution is given in the Figure 4-11a and residuals diagnostic plots are presented in Figure 4-11b, c. The residuals are given by the following formula: $r = q_{obs} - q_{sim}$ [log (1/s)] where $q = \log(Q + k)$ with $k = 0.0001$.

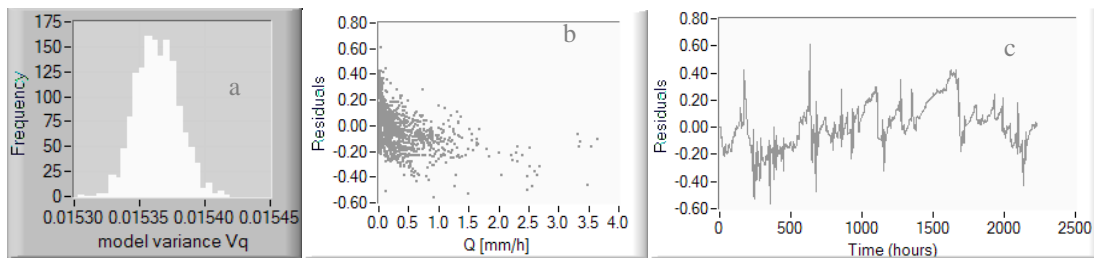


Figure 4-11 TOPMODEL and MCMC methodology with statistical likelihood with Log and without AR corrections: a) Posterior distribution of the model variance (in mm) and b) model residuals against predicted runoff and c) against time (in hours).

These plots indicate that model residuals are less dependent on the discharge predicted values but they are still significantly time dependent. To remove this dependency an autoregressive model should be applied.

The last part of this study case includes both kinds of corrections: Box-Cox transformation of the discharge data and autoregressive model with order 1. These corrections have been applied in order to ensure that the statistical hypotheses demanded by the normal assumption of the statistical likelihood model are accomplished. The parameter posterior distributions of the hydrological parameters are presented in Figure 4-12 and those of the statistical parameters in Figure 4-13. The resulting uncertainty on the predicted discharge is presented in Figure 4-14.

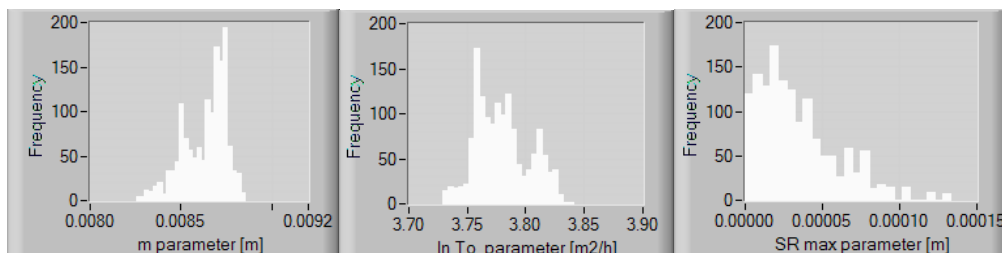


Figure 4-12 TOPMODEL and MCMC methodology with statistical likelihood with Log and AR corrections: posterior distribution of the hydrological parameters

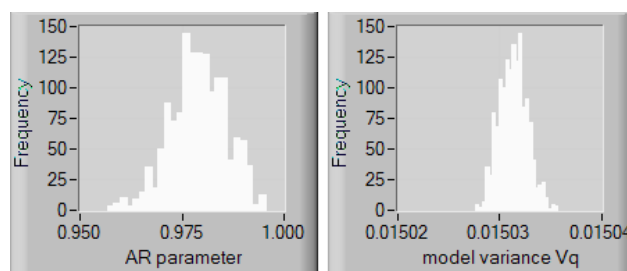


Figure 4-13 TOPMODEL and MCMC methodology with statistical likelihood with Log and AR corrections: posterior distribution of the statistical parameters

We note that the autoregressive parameter has values closed to 1 and thus it accounts/corrects for a major part of the model structure error. The resulting model variance is small compared with previous examples, which determines very narrow uncertainty bounds and thus high confidence and high predictive power for further predictions.

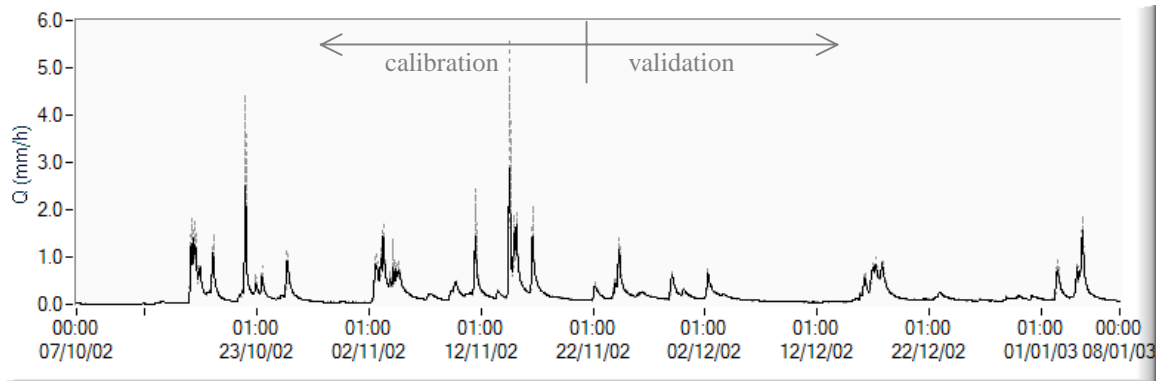


Figure 4-14 TOPMODEL and MCMC methodology with statistical likelihood with Log and AR corrections: Observed discharge and simulated uncertainty bounds at 90%

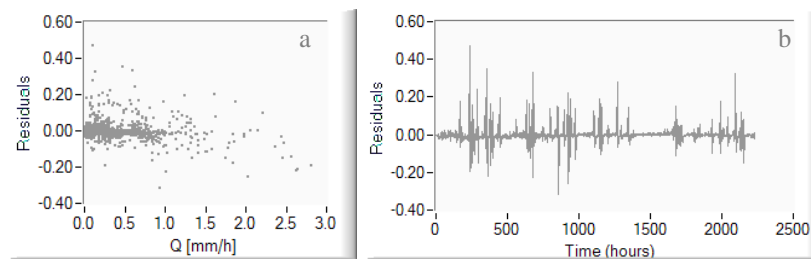


Figure 4-15 TOPMODEL and MCMC with statistical likelihood with Log and AR corrections: model residual against predicted runoff (a) and against time (b)

The residuals have been computed with the formula: $r = (q_{obs_t} - q_{sim_t}) - AR(q_{obs_{t-1}} - q_{sim_{t-1}})$ where q_{obs} is the log-transformed observed discharge and q_{sim} is the log-transformed simulated discharge and AR is an autoregressive parameter. The model residuals indicate no important departure for the constancy of the variance assumption (Figure 4-15a) and show improvement for the time independence assumption (Figure 4-15b). Departures for the last assumptions are however noticed for the peak discharges which might indicate that another form of the Box-Cox transformation should be more appropriate than the simple log transformation of the discharge data.

The main results of the application of the MCMC methodology with the classical version of TOPMODEL concerning the posterior distributions of both hydrological and statistical parameters are resumed in Table 4-3.

	MCMC model without Log transform and without autoregressive (AR) parameter	MCMC model with Log transform and without autoregressive (AR) parameter	MCMC model with Log transform and with autoregressive (AR) parameter
Hydrological parameters			
m [m]	0.0073 ± 0.00004	0.0054 ± 0.0001	0.0086 ± 0.00012
LnT0 [m ² /h]	2.37 ± 0.00075	2.43 ± 0.10	3.75 ± 0.027
Srmax [m]	0.025 ± 0.00014	0.0085 ± 0.0003	0.0002 ± 0.00003
Srinit [-]	0.5 ± 0.27	0.47 ± 0.27	0.48 ± 0.27
Statistical parameters			
Model variance V	1.68 ± 0.07 [mm]	0.024 ± 0.001 [log(l/s)]	0.002 ± 0.0001 [log(l/s)]
Model variance [mm]	1.68 ± 0.07	0.015 ± 0.00002	0.015 ± 0.0000014
AR parameter [-]	-	-	0.975 ± 0.006
Models efficiency			
Efficiency in calibration (non transformed data)	0.76	0.55	0.90
Efficiency in validation (non transformed data)	0.68	0.79	0.97

Table 4-3 Topmodel posterior parameter distributions (mode and standard deviation) for different statistical likelihood functions and efficiency (Nash-Sutcliffe criterion) of the considered models.

The table above presents the synthesis of the results in this case study. Analysis of these results gives evidence of the influence of the statistical corrections on the posterior distributions of TOPMODEL parameters. The modeller must be aware of the role played by the fitting criteria on the posterior parameter distributions especially when the model is used for predictive purposes. The predictive power of the above models is increasing with the complexity of the model and it is maximum when all the statistical corrections are introduced (Table 4-3).

4.3 Conclusions

One important topic in the hydrological modelling is related to the development of appropriate calibration methods in order to estimate robust parameters. Furthermore, a good calibration method should provide not only optimal parameters but should also assess the uncertainty associated with both estimated parameters and model predictions. In this context, the present chapter has focussed on a simple conceptual hydrological model, TOPMODEL and two Bayesian methods of estimating parameters. The basics of the Bayesian GLUE and Monte Carlo Markov Chain methodologies have been presented and the two approaches have been compared through an application done for the upper part of the Haute-Mentue catchment. The GLUE methodology conducted to high uncertainty in estimation of both parameters and simulated discharges. Three cases have been studied for the Monte Carlo Markov Chain method upon that statistical corrections have been used or not in order ensure that statistical hypothesis concerning the model residuals are respected:

- ❑ the case without any corrections (log-transform of the discharge series and autoregressive modelling of the simulation error);
- ❑ the case with one correction, only log-transform of the discharge series;
- ❑ the case with two corrections: log transform of the discharge data and autoregressive model for the simulation error.

Introduction of both corrections was considered necessary, as large departures from the working hypothesis concerning the model residuals have been noticed.

The results obtained for the proposed case study show that introduction of the statistical corrections (and thus introduction of two new statistical parameters) led to greater uncertainty in parameter estimation while the uncertainty due to the model structure was significantly improved. Increased predictive power of the TOPMODEL has been obtained after using both statistical corrections.

Both methodologies have been implemented in a LABVIEW[®] programming environment, which is a relatively new graphical programming language [<http://www.ni.com/>], aimed especially for data acquisition and data treatment. More details about this language program as well the front panels of TOPMODEL, GLUE and MCMC methodologies can be found in Annex 5.

4.4 References

- Aronica, G., B. Hankin and K. Beven (1998). "*Uncertainty and equifinality in calibrating distributed roughness coefficients in a flood propagation model with limited data.*" *Advances in Water Resources* 22(4): 349-365.
- Beven, K. (1989). "*Changing Ideas in Hydrology - the Case of Physically-Based Models.*" *Journal of Hydrology* 105(1-2): 157-172.
- Beven, K. (1996). "*A discussion of distributed hydrological modelling.*" *Distributed hydrological modelling*. B. A. Abbot and J. C. Refsgaard. Dordrecht/ Boston/ London, Kluwer Academic Publishers.
- Beven, K. and J. Freer (2001). "*Equifinality, data assimilation, and uncertainty estimation in mechanistic modelling of complex environmental systems using the GLUE methodology.*" *Journal of Hydrology* 249: 11-29.
- Beven, K. and M. J. Kirkby (1979). "*A physically based variable contributing area model of basin hydrology.*" *Hydrol.Sci.Bull.* 24(1): 43-69.
- Beven, K., A. Musy and C. Higy (2001). "*Tribune Libre: The uniqueness of place, action and time.*" *Revue des Sciences de l'Eau* 14(4).
- Beven, K. J. (2000). "*Uniqueness of place and process representations in hydrological modelling.*" *Hydrology and Earth System Sciences* 4(2): 203-213.
- Beven, K. J. (2001). "*Rainfall-Runoff Modelling.*" Chichester, Wiley.
- Beven, K. J. and A. M. Binley (1992). "*The future of distributed models- models calibration and uncertainty prediction.*" *Hydrological Processes* 6: 279-298.
- Blazkova, S. and K. Beven (2002). "*Flood frequency estimation by continuous simulation for a catchment treated as ungauged (with uncertainty).*" *Water Resources Research* 38(8).
- Blazkova, S., K. J. Beven and A. Kulasova (2002). "*On constraining TOPMODEL hydrograph simulations using partial saturated area information.*" *Hydrological Processes* 16(2): 441-458.

- Blöschl, G. and M. Sivapalan (1995). *"Scale issues in hydrological modelling: A review"*. Sussex, John Wiley&Sons.
- Box, G. E. P. and O. R. Cox (1964). *"The analysis of transformations."* J.R. Stat. Sc.Ser.B 26(2): 211-252.
- Boyer, E. W., G. M. Hornberger, K. E. Bencala and D. McKnight (1996). *"Overview of a simple model describing variation of dissolved organic carbon in an upland catchment."* Ecological Modelling 86(2-3): 183-188.
- Brazier, R. E., K. J. Beven, J. Freer and J. S. Rowan (2000). *"Equifinality and uncertainty in physically based soil erosion models: Application of the glue methodology to WEPP-the water erosion prediction project-for sites in the UK and USA."* Earth Surface Processes and Landforms 25(8): 825-845.
- Cameron, D., K. Beven and J. Tawn (2000). *"Modelling extreme rainfalls using a modified random pulse Bartlett-Lewis stochastic rainfall model (with uncertainty)."* Advances in Water Resources 24(2): 203-211.
- Christensen, S. (2004). *"A synthetic groundwater modelling study of the accuracy of GLUE uncertainty intervals."* Nordic Hydrology 35(1): 45-59.
- Christophersen, N., C. Neal, R. P. Hooper, R. D. Vogt and S. Andersen (1990). *"Modelling streamwater chemistry as a mixture of soilwater end-members - a step towards second generation acidification models."* Journal of Hydrology 116: 307-320.
- Cowles, M. K. and P. B. Carlin (1996). *"Markov Chain Monte Carlo Convergence Diagnostics: A Comparative Review."* Journal of American Statistical Association 91(434): 883-904.
- Duan, Q. Y., V. K. Gupta and S. Sorooshian (1993). *"Shuffled Complex Evolution Approach for Effective and Efficient Global Minimization."* Journal of Optimization Theory and Applications 76(3): 501-521.
- Engeland, K. (2002). *"Parameter estimation in regional hydrological models"*. Departement of geophysics. Oslo, University of Oslo.
- Engeland, K. and L. Gottschalk (2002). *"Bayesian estimation of parameters in a regional hydrological model."* Hydrology and Earth System Sciences 6(5): 883-898.
- Franks, S. W. and K. J. Beven (1997). *"Bayesian estimation of uncertainty in land surface-atmosphere flux predictions."* Journal of Geophysical Research-Atmospheres 102(D20): 23991-23999.
- Franks, S. W., P. Gineste, K. J. Beven and P. Merot (1998). *"On constraining the predictions of a distributed model: The incorporation of fuzzy estimates of saturated areas into the calibration process."* Water Resources Research 34(4): 787-797.
- Gelman, A., J. B. Carlin, H. S. Stern and R. D.B. (2000). *"Bayesian Data Analysis"*. Boca Raton, London, New York, Washington D.C., Chapman&Hall/CRC.
- Geman, S. and D. Geman (1984). *"Stochastic relaxation, Gibbs' distribution and Bayesian restoration of images."* IEEE Trans.,PAMI 6: 721-741.
- Geweke, J. (1992). *"Evaluating the accuracy of sampling - based approaches to calculating posterior moments (with discussion)"*. Bayesian statistics 4. A. F. M. Smith. Oxford, Clarendon Press: 169-193.
- Gupta, V. K. and S. Sorooshian (1985). *"The Automatic Calibration of Conceptual Catchment Models Using Derivative-Based Optimization Algorithms."* Water Resources Research 21(4): 473-485.
- Hastings, W. K. (1970). *"Monte Carlo methods using Markov chains and their applications."* Biometrika 57: 97-109.
- Higy, C. (2000). *"Modélisations conceptuelles et à base physique des processus hydrologiques: Application au bassin versant de la Haute-Mentue"*. Thesis EPFL, No.2148. Lausanne.

- Iorgulescu, I. (1997). *"Analyse du comportement hydrologique par une approche intégrée à l'échelle du bassin versant. Application au bassin versant de la Haute-Mentue."* Thesis EPFL, No.1613. Lausanne.
- Joerin, C. (2000). *"Etude des processus hydrologiques par l'application du traçage environnemental. Association à des mesures effectuées à l'échelle locale et analyse d'incertitude"*. Thesis EPFL, No.2165. Lausanne.
- Kirkpatrick, S., C. D. J. Gelatt and M. P. Vecchi (1983). *"Optimization by simulated annealing."* Science 220: 671-680.
- Kuczera, G. (1983). *"Improved Parameter Inference in Catchment Models .1. Evaluating Parameter Uncertainty."* Water Resources Research 19(5): 1151-1162.
- Kuczera, G. and E. Parent (1998). *"Monte Carlo assessment of parameter uncertainty in conceptual catchment models: the Metropolis algorithm."* Journal of Hydrology 211(1-4): 69-85.
- Lamb, R., K. Beven and S. Myrabo (1998). *"Use of spatially distributed water table observations to constrain uncertainty in a rainfall-runoff model."* Advances in Water Resources 22(4): 305-317.
- Metropolis, N., A. W. Rosenbluth, M. N. Rosenbluth, A. H. Teller and E. Teller (1953). *"Equation of state calculations by fast computing machines."* Journal of Chemical Physics 21(6): 1087-1092.
- Nash, J. E. and J. V. Sutcliffe (1970). *"River flow forecasting through conceptual models."* Journal of Hydrology 10: 282-290.
- Overney, O. (1997). *"Prédiction des crues par modélisation couplée stochastique et déterministe:méthode et analyse d'incertitudes"*. Thesis No.1751, EPFL. Lausanne.
- Page, T., K. J. Beven, J. Freer and A. Jenkins (2003). *"Investigating the uncertainty in predicting responses to atmospheric deposition using the model of acidification of groundwater in catchments (MAGIC) within a generalised likelihood uncertainty estimation (GLUE) framework."* Water Air and Soil Pollution 142(1-4): 71-94.
- Refsgaard, J. C. and B. Storm (1996). *"Construction, calibration and validation of hydrological models"*. Distributed hydrological modelling. B. A. Abbot and J. C. Refsgaard. Dordrecht, Kluwer Academic Publisher.
- Scanlon, T. M., J. P. Raffensperger and G. M. Hornberger (2001). *"Modeling transport of dissolved silica in a forested headwater catchment: Implications for defining the hydrochemical response of observed flow pathways."* Water Resources Research 37(4): 1071-1082.
- Scanlon, T. M., J. P. Raffensperger, G. M. Hornberger and R. B. Clapp (2000). *"Shallow subsurface storm flow in a forested headwater catchment: Observations and modeling using a modified TOPMODEL."* Water Resources Research 36(9): 2575-2586.
- Sen, S. and P. L. Stoffa (1995). *"Global optimization methods in geophysical inversion"*. Amsterdam, Elsevier.
- Sorooshian, S. (1991). *"Parameter estimation,model identification and model validation:conceptual-type models"*. Recent advances in the modelling of hydrologic systems. D. S. Bowles and P. E. O'Connell. Dordrecht, Kluwer Academic Publisher. 345.
- Sorooshian, S. and V. K. Gupta (1983). *"Automatic Calibration of Conceptual Rainfall-Runoff Models - the Question of Parameter Observability and Uniqueness."* Water Resources Research 19(1): 260-268.
- Tanner, M. H. (1992). *"Tools for statistical inference:observed data and augmentation methods"*. Lecture notes in statistics. New York, Springer-Verlag. 67.

-
- Torre, F., J. J. Boreux and E. Parent (2001). "*The Metropolis-Hastings algorithm, a handy tool for the practice of environmental model estimation: illustration with biochemical oxygen demand data.*" Cybergéo paper 187.
- Walsh, B. (2000). "*Markov Chain Monte Carlo and Gibbs sampling*". Lecture notes for EEB 596z.

5. Integrating additional information in conceptual rainfall-runoff modelling

Abstract

The present chapter introduces in the first part, two Bayesian (GLUE and MCMC) multi-calibration methodologies that have been applied with two versions of TOPMODEL in order to assess the parameter and the modelling uncertainty. Field estimated additional information, i.e. soil storage saturation deficit and stream tracers' concentrations have been used within this methodology in order to constrain model parameterizations. The multi-response calibration method was tested for a small head-catchment on the Haute-Mentue basin and the first results are presented and commented in the second part of this chapter.

Key words

multi-response Bayesian methodology, TOPMODEL, internal variable, additional information, uncertainty

In this chapter, the single and multi-response calibration methodologies will be compared and the impact of the multi response calibrating approach on model outputs and model parameters uncertainty will be assessed. First, the concept of additional information will be presented as well as those of internal variables for the modelling approach. Next, the Bayesian multi-calibration methodology is introduced and last, several examples of application of the multi-calibration approach on the Haute-Mentue catchment will be presented and the results commented.

5.1 Augmenting information in conceptual hydrological models; internal variables

The main aim of the present chapter is to assess the importance of multiple responses during the calibration of conceptual rainfall-runoff models. Before that, an introduction about the additional information that can be used in hydrological modelling will be proposed. Conceptual rainfall-runoff models have generally a representation of their internal states and they are modelling more variables (fluxes and internal states) than the streamflow alone (Engeland (2002)). For example, TOPMODEL simulates total discharge at the outlet of a catchment together with its subsurface and overland components but also distributed values of the groundwater levels or of the soil storage saturation deficits.

A good description of the internal states of a model is important when the model is used for more purposes than the single one of reproducing discharges at the outlet. Recently, internal variables of different conceptual models have been used to constrain the uncertainty of the model parameters and of the model output. Last but not least, the internal variables could strengthen the scientific value of a given model and they could contribute to precise the limits of the tested model (Engeland (2002)). In the present study, we will work with one of TOPMODEL internal variables that is the soil storage deficit and we will also consider additional information such as the chemical signal of the observed discharge in order to constrain model uncertainty and model parameters uncertainty. We will try in this study to find possible answers to questions that interest the hydrological community such as:

- is there really an equifinality problem in the identification of distributed model structures, or will it be reduced or eliminated in future by improved observational techniques?
- what types of observation have the greatest value in constraining the predictions of distributed models?
- are stochastic approaches needed either to assess the predictive uncertainty arising from model and parameter uncertainty or to search for the 'single realization' that is reality?
- what is the most effective way to spend money on measurements for constraining the uncertainties in distributed model predictions?

questions that have been selected from the introduction of a special dedicated issue of Hydrological Processes (Beven and Feyen (2002)).

5.1.1 Local saturation deficit as an internal variable: field estimation and TOPMODEL concept

The third chapter analyzed a field experiment conducted on the Haute-Mentue catchment whose aim was to study the temporal evolution of the soil moisture at different depths. This experiment was carried out on two sites chosen for their representative morphometrical and lithological characteristics. The measured values of the soil moisture at the two sites will be used in order to estimate the temporal evolution of the entire profile deficit to saturation. The formula below was used:

$$D_{field} = \int_0^z (\theta_s(z) - \theta(z)) \cdot dz \quad (5.0)$$

where D_{field} is the soil profile saturation deficit;

$\theta_s(z)$ is the saturated soil moisture

$\theta(z)$ is the soil moisture at the depth z

Figure 5-1 presents the soil storage saturation deficit and the water level height in a superficial 60 cm piezometer for the Ruzillon experimental site. Comparison of the soil moisture deficit with the water table elevation in the piezometer, helps identify humid periods where the soil profile is partially or completely saturated.

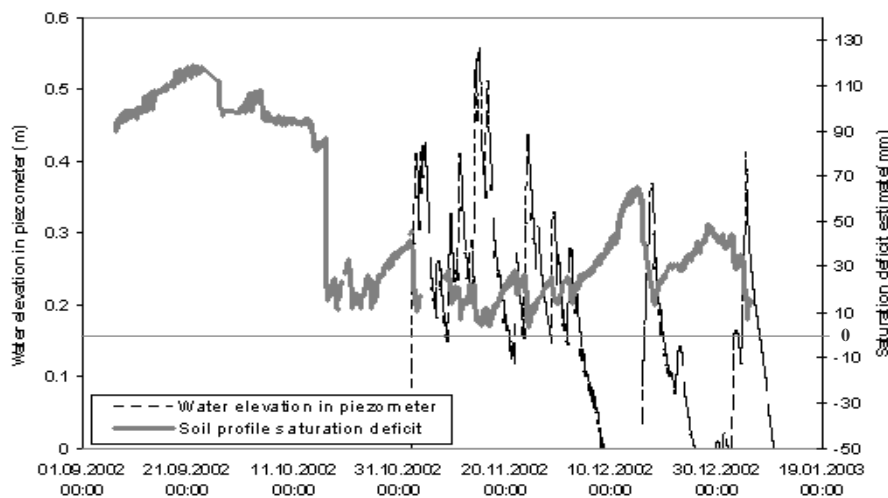


Figure 5-1 Ruzillon experimental site: water table elevation in 60 cm depth piezometer and soil profile saturation deficit.

The figure above shows clearly that during the autumn 2002 most part of the soil profile was saturated, which means that, the hydrological processes that occur at the hill slope scale are superficial and that the water table is responding very quick to the rainfall input. Even after September 2002, when little precipitation has been registered in this region, the deeper soil horizons saturated quickly and the groundwater table rose rapidly close to the ground surface. During September 2002, the real soil saturation deficit of the entire soil profile was different from those represented in the figure above, as the groundwater

table was lower than 60 cm. During this period, occasional measurements of the groundwater table in a 1.2 m deep piezometer evidenced no water meaning that the groundwater table was deeper.

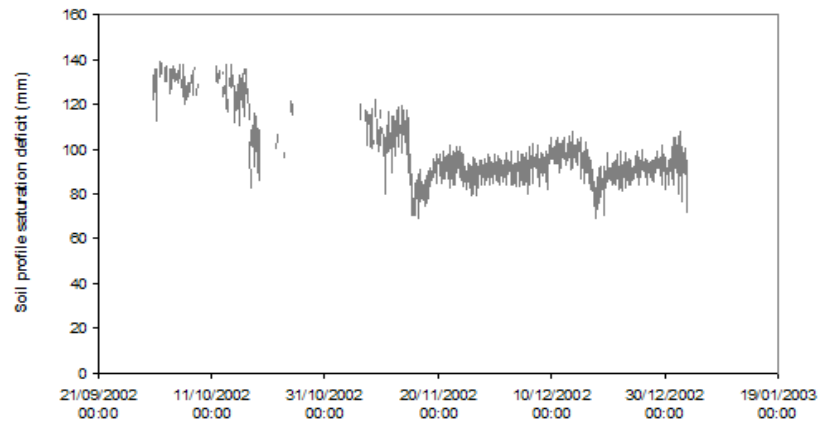


Figure 5-2 Esserts site: soil profile saturation deficit

Figure 5-2 represents the available soil profile saturation deficits for the Esserts experimental site. Comparing with the same chart for the Ruzillon experimental site, one can see that this hillslope is reacting completely different to the same rainfall input and antecedent conditions. Even after long wet periods, the soil profile remains unsaturated with small amplitude of variation of the saturation deficit. The occasional measurements that have been taken at a 1.2 m deep piezometer, installed near this site, showed very rarely water inside. Only for the strong rainfall events in the end of November 2002, did the water table reach 70 cm depth. This is evidence of a different behaviour of the hill slope with different hydrological processes that have been discussed earlier in Chapter 3.

TOPMODEL uses the notion of saturation deficit being the quantity of water to be added to the soil profile in order to bring it to complete saturation (or to bring the water table to the surface) (Higy (2000)). The figure below (Figure 5-3a) shows the concept of saturation deficit defined in TOPMODEL and compares it with those derived by field available measurements (Figure 5-3 b and c).

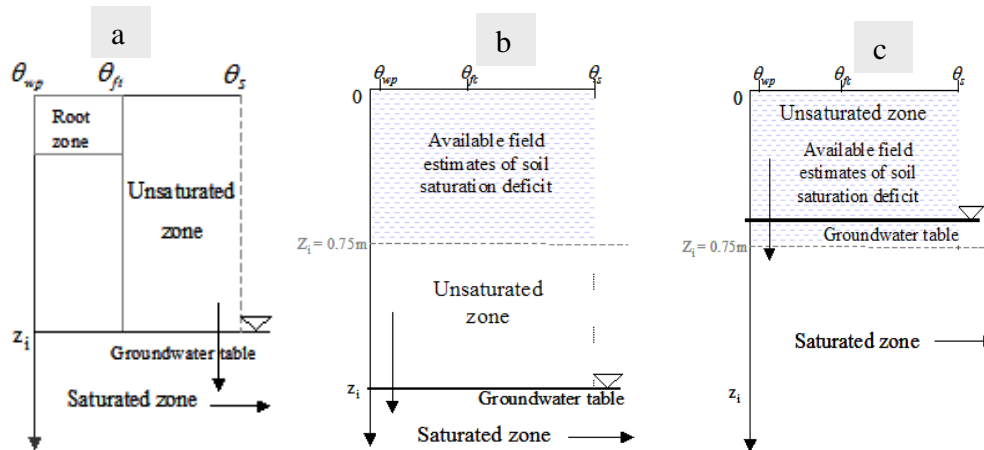


Figure 5-3 TOPMODEL saturation deficit concept (a) and comparison with the available soil saturation deficit field estimates during dry (b) and wet (c) conditions

Relative to the existent soil moisture data at the two experimental sites (Ruzillon and Esserts), TOPMODEL notion of saturation deficit is equivalent to those computed on the field for the experimental sites during wet periods when the groundwater table is no deeper than 75 cm from the ground surface and when the real evapo-transpiration is negligible. For dry periods with groundwater table depths deeper than 75 cm, the available field data are underestimating the total saturation deficit of the soil profile, which makes comparison with the model estimates rather inappropriate.

The main conclusion of this analysis is that, at least for the humid periods, the field estimated saturated deficit could be used as additional information in hydrological modelling in catchments with shallow groundwater that reacts quickly to the rainfall input.

After ensuring that the field measurements and the TOPMODEL estimates for the saturation deficit are representing equivalent features, we used the local field estimates at the Ruzillon site as an observed internal variable to constrain the TOPMODEL' uncertainty.

The literature review shows several applications where different internal variables have been used to constrain both parameter and model uncertainty. For TOPMODEL for instance, Lamb et al. (1998)) used both runoff data and individual groundwater measurements for a small Norwegian catchment in order to study their influence on the uncertainty estimation. Franks et al. (1998) conditioned parameterisation of TOPMODEL on discharges and then on fuzzy estimates of saturated areas derived from a synthetic-aperture radar (SAR) and shown that despite the uncertainty in the predictions of the saturated areas, this methodology could be useful in rejecting many previously acceptable TOPMODEL parameterisations. Blazkova et al. (2002)) realized a similar analysis for a small catchment in Czech Republic. Estimates of the saturated areas given by field observations used within GLUE methodology in order to constrain the parameter uncertainty. The results of this study shown that the TOPMODEL surface saturated

transmissivity parameter was the most influenced by this multi-calibration approach but this didn't influence much on the model output uncertainty.

In this study, instead of depths to the groundwater we worked with the saturation deficits. In the TOPMODEL concept, the two terms are almost equivalent as the saturation deficit is related to the groundwater depth by the following formula:

$$D_i = \theta_{dp} \cdot z_i \quad (5.1)$$

where θ_{dp} is the drainable porosity (the difference between the soil moisture at saturation and at the field capacity), z_i is the depth to the groundwater and D_i is the local saturation deficit. Figure 5-4 shows this correlation for the Ruzillon site, where both piezometer depth as well as soil moisture data were available for a humid period in Autumn 2002.

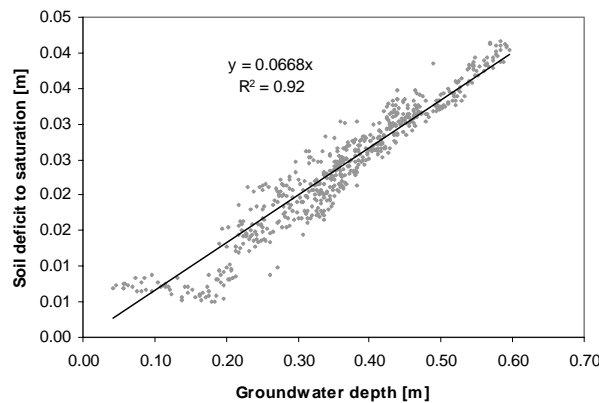


Figure 5-4 Relationship between the groundwater depth and the soil saturation deficit for Ruzillon site

5.1.2 Linking hydrological models with water quality model and using chemical information as soft data to constrain a hydrological model: a brief review

The main developments concerning the tracing modelling approach have been already presented in chapter 3. In recent years, scientific effort has been oriented toward environmental problems, which have opened the way of a number of applications in hydrology and chemical modelling. The years '80-'90 have seen a lot of hydrological model appear, which attempted to link hydrology to chemical modelling of the stream water. Attempts included both conceptual (lumped, semi-distributed and distributed) and physically based hydrological models and a brief review is presented further.

a) The classical attempt was to develop integrated hydro-chemical models to assess both hydrological and chemical fluxes. A brief presentation of these models is made in

(Arheimer and Olsson (2003)). The great majority of the models presented in this report are already operational in different parts of Europe. The report present 37 models that are being used all over the Europe, among them, nine models are presented that work at the catchment scale. The most known models are: the conceptual, semi-distributed HBV-N model (Andersson and Arheimer (1998)), which is largely used in northern Europe to model eutrophication and nitrogen transport, the conceptual process oriented MAGIC model (Cosby et al. (1985)) for acidification and nitrogen transport, the fully distributed and physically based SHETRAN and MIKE-SHE models (Abbot et al. (1986)) that describe the major flow processes of the entire land phase of the hydrological cycle and that have been used for eutrophication, pollutant and nitrogen transport and the conceptual, distributed SWAT model (Arnold et al. (1998)) that models eutrophication, pesticide control, nutrients and sediments.

b) While most of the models presented above are complex models, some attempts have also been done toward using simple conceptual models with a chemical module used rather to assess the hydrological model identifiability than to make prediction for the chemical stream water signal. Attempts in this direction have been made by Hooper et al. (1988) and they concluded that the use of the chemical information can help analysis of the hydrological models structure and of their ability to predict multiple signals.

c) Another approach was to test the ability of existing conceptual models to reproduce streamwater chemical signals. Robson et al. (1992)) used TOPMODEL and separated the base flow depth components in order to compare them to those identified by a chemical mixing model. The conclusion was encouraging as the simulated TOPMODEL components compared well with those defined by the chemical approach.

d) Some other researches have been conducted in order to take into account the advances made in the field of hydrograph separation using environmental tracing into the conceptual hydrological modelling. Uhlenbrook and Leibundgut (2000) developed a conceptual rainfall-runoff model (TAC- *Tracer Aided Catchment Model*) on the basis of the tracer hydrological investigations in the Brugga catchment. The TAC model includes the dominant runoff generation processes, which are conceptualised through several linear and non-linear reservoir concepts. Seibert and McDonnel (2002) developed a conceptual model and introduced tracing information through fuzzy measures for evaluating and validating model simulation and parameter acceptability. Weiler et al. (2003) developed a new model for hydrograph isotopic separation that integrates the instantaneous unit hydrograph and computes transfer functions for event and pre-event water that provides finally coupled representations of the transport and hydraulic functions in a New Zealand catchment.

e) The last approach presented here in order to link hydrological models to chemical ones consists in modifying existing simple conceptual models in order to make possible introduction of a chemical mixing model such as EMMA approach and to assess modelling of different hydrological processes and chemistry of the stream water. Boyer et al. (1996) used TOPMODEL and partitioned the simulated subsurface flow into a quick and a slow components in order to simulate the nitrogen concentration of the

streamwater. Scanlon et al. (2000) modified the classical version of TOPMODEL in order to introduce the stormflow component and to simulate the silica concentration of the streamwater in a small catchment in USA (Scanlon et al. (2001)).

In this work, we took into consideration this last kind of approach in order to test and to validate TOPMODEL output predictions within a Bayesian multi-calibration approach. The main TOPMODEL concepts have been presented in Chapter 4.

5.2 Parameter estimation: the case of multi-response calibration

Soon after the appearance of the first studies dedicated to the uncertainty in hydrological modelling, the interest of the modellers moved towards ways to reduce uncertainty of the parameters and of the simulated responses. Naturally, one way to do that was by considering the internal structure of hydrological models given the fact that hydrological models, conceptual or physically based, do have a representation of the internal states and they simulate more fluxes than the runoff (Engeland (2002)). The first application of these ideas have been concretised in some papers appeared in the '90s. Before that, Kuczera (1983) proposed a Bayesian methodology to combine different kinds of hydrological data in order to improve model parameter estimation and to finally reduce uncertainty in parameters fitted to runoff data. This approach was hierarchical and was tested with three levels of information (runoff data, prior information on some model parameters and soil moisture data). It demonstrated that the use of different kinds of data could be very useful to reduce parameter uncertainty and could help parameter identifiability. Hooper et al. (1988) developed and tested a multi-signal calibration methodology for the Birkenes hydrochemical model in order to better assess the identifiability of the model parameters. They calibrated runoff data and tracer data (Oxygen-18) and used simple and weighted least squares objective function and a gradient search optimisation technique in order to estimate model parameters. They concluded that the model was overparametrized and that only one store (instead of two) would be sufficient for the available data.

Mroczkowski et al. (1997) developed a methodology to calibrate a model by using several responses based on the ideas developed earlier by Kuczera in 1983. The methodology has been applied with the CATPRO hydrochemical model for a small catchment in Australia. A joint calibration on streamflow, stream chloride and average groundwater level time series was performed by considering the NLFIT nonlinear regression model with cross-correlated random errors between the three responses.

This methodology was also applied in Kuczera and Mroczkowski (1998) for the same hydrochemical model and showed that joint calibration on runoff data and groundwater levels reduced some parameter uncertainty but left unchanged the uncertainty of the poorly identified parameters. The most dramatic changes occurred when joint calibration was done on runoff and stream chloride.

During the same period the GLUE methodology gained importance in the hydrological community and a number of papers studied the effect of working with multiple responses on the parameter and simulation uncertainty. Seibert et al. (1997) tested the ability of TOPMODEL to simulate runoff and groundwater levels and concluded that the model was able to reproduce the temporal trends of the observed groundwater levels at 37 locations in a catchment in Norway but systematic bias was observed compared with measured groundwater levels. Later, Lamb et al. (1998) used GLUE methodology with jointly calibration of runoff and groundwater spatially distributed observations to constrain parameter and simulation uncertainty. They concluded that the use of groundwater data helped reducing the parameter uncertainty but the groundwater table uncertainty bounds were still wide and without reproducing the rapid temporal variation. Franks et al. (1998) analysed within a GLUE methodology the impact of introducing fuzzy estimates of the saturated areas on the parameter uncertainty. They concluded that despite the uncertainty in estimation of the saturated areas this was useful to reduce significantly the uncertainty of one model parameter as well as those of the modelled runoff for some events.

The last years some automatic procedures appeared in order to perform multi-calibration for distributed models like MIKE-SHE and MIKE-NAM (Madsen and Jacobsen (2001)) and (Madsen (2000)). Nevertheless, for these applications, the *Shuffled Complex Evolution* (SCE) algorithm (Duan et al. (1992), and Duan et al. (1994)) was applied but the objectives were not to consider uncertainty nor to work with internal variables but to consider jointly different objective functions for the runoff response.

The next chapter will assess the worth of a multi-calibration methodology of a simple conceptual model (TOPMODEL) in a Bayesian context. First the GLUE multi-calibration methodology will be presented and the further attention will be accorded to the Monte Carlo Markov Chains methods for multiple responses.

5.2.1 The Bayesian method (likelihood formulation, prior and posterior distribution)

The principles of the Bayesian methodology have been already presented in Chapter 4.2.1. Here only the aspects concerning the application of the Bayesian concepts to the case of a multi-response calibration situation will be discussed. As the final aim in this study was to assess the importance of using multiple responses on the parameter uncertainty and on the model output uncertainty, first we have to specify the prior information. In our study, this was the same as those already established in the previous chapter for the two TOPMODEL applications. Uniform prior distributions over the feasible range have been chosen, for simplicity purposes, for the hydrological model parameters as well as for the statistical parameters. As the methodology to deriving posterior distribution remains essentially the same the most important changes occur in establishing the likelihood function in such way that it includes several responses. Next

the main developments of the two Bayesian methodologies, GLUE and Monte Carlo Markov Chain in the context of multiple calibration will be shown.

5.2.2 GLUE methodology – Generalized Likelihood Estimation

The Generalized Likelihood Uncertainty Estimation was largely used in different parts of the world in order to assess parameter and model output uncertainty. In the context of working with multiple responses, the same methodology was used to assess the importance of using additional information (local groundwater tables, saturated areas) to constrain uncertainty of TOPMODEL parameters and predictions. As shown in Chapter 4, the GLUE Bayesian methodology includes two aspects: definition of the generalized likelihood function and choice of the sampling algorithm.

Generalized likelihood function

The first step in using this methodology is to choose the likelihood measure. We decided to adopt here the same subjective likelihood measure as in the paper of Lamb et al. (1998)).

$$L = \exp\left(-W \frac{\sigma_e^2}{\sigma_o^2}\right) \quad (5.2)$$

where L is the likelihood measure, W is a weighting factor, σ_e^2 is the model variance and σ_o^2 is the variance of observed data. The weights W were equal for both responses and fixed at 0.5.

The updating of the formula to include a second response in the calibration approach is done in conformity with the formula below (Lamb et al. (1998)):

$$L(\Theta_i | Y_{1,n}) \propto L(\Theta_i | Y_1) \cdot \dots \cdot L(\Theta_i | Y_n) \quad (5.3)$$

where

$L(\Theta_i | Y_1)$ is the likelihood measure for the first considered response,

..

$L(\Theta_i | Y_n)$ is the likelihood measure for the n considered response and

$L(\Theta_i | Y_{1,n})$ is the updated likelihood measure and n is the number of responses used in calibration.

Importance sampling searching algorithm

As search algorithm, we used in this work, the importance sampling, the same as in Chapter 4. The only difference is that in this case, a threshold value for the likelihood measures has been used, fixed at 0.3, under which the simulations have been considered non-behavioural (Beven and Freer (2001)). The remaining realizations have been re-ranked with the formula given in equation (4.23).

This methodology was used in order to calibrate the classical version of TOPMODEL on total stream discharges and on soil storage saturation deficit. An application example can be seen further in the present chapter.

5.2.3 Monte Carlo Markov Chain methods

In Chapter 4, we used Monte Carlo Markov Chains (MCMC) methods in order to assess the uncertainty of both parameters and model output for the case of single response calibration. Both statistical likelihood and Metropolis sampling method proved their utility for the analysis of the posterior distributions of the model estimated parameters. In this chapter, we'll apply the MCMC methods to assess parameter and model output uncertainty for the case of multiple responses calibration. First, the general aspects of the method will be treated and then this will be tested on a classical and a modified version of TOPMODEL for case of two and three responses calibration.

Simulation error modelling strategy: Statistical likelihood function generalization

As the general Bayesian concepts have already been presented, only the aspects concerning the updating of the likelihood function will be considered here. The first step in implementing the method is to choose a simulation error modelling strategy. We used for this application, a statistical likelihood function. For simplification purposes, we considered:

- i. that the simulations errors, for each of the considered response, could be modelled by a normal distribution and
- ii. that the simulations errors of the considered responses are independent and identically distributed (IID).

For n responses, these assumptions can be written as:

$$\begin{aligned}
 Y_1 &= Y_1^{sim} + \varepsilon_1; \\
 Y_2 &= Y_2^{sim} + \varepsilon_2; \\
 &\vdots \\
 &\vdots \\
 Y_n &= Y_n^{sim} + \varepsilon_n.
 \end{aligned}
 \tag{5.4}$$

where n is the number of model responses considered in the calibration, $Y_{1 \rightarrow n}^{sim}$ and $Y_{1 \rightarrow n}$ are the simulated and observed values for the same model responses and $\varepsilon_{1 \rightarrow n}$ are the simulation errors. The simulated responses, $Y_{1 \rightarrow n}^{sim} = f(I_{1 \rightarrow n}, \theta)$, are functions of observed input data (I_n) and model parameters (θ).

In order to use the properties of the normal law, the model residuals for each response should be subject to appropriate statistical corrections if assumptions of variance constancy and autocorrelation are detected. As already shown in Chapter IV, Box-Cox transformation should be applied if any departure from the above assumptions is detected.

Depending on the assumed degree of complexity of the available data and the correction needed in respect to the normality assumption, several cases can be considered for the simulation errors:

1. the simplest option would be to consider that for each model, the simulation errors follow normal distributions and they are independent such that there would be no need to take into account any error autocorrelation. This would be translated as follows:

$$\varepsilon_1 \sim N(0, \sigma_1); \varepsilon_2 \sim N(0, \sigma_2); \dots \varepsilon_n \sim N(0, \sigma_n) \quad (5.5)$$

where $\sigma_1, \sigma_2, \sigma_n$ represent the model variance for each considered response;

2. an intermediary case would be to consider that simulation errors are not independent and one should take into consideration this by introducing a constant autocorrelation for all considered responses:

$$\varepsilon_1 \sim AR(\rho, \sigma_1); \varepsilon_2 \sim AR(\rho, \sigma_2); \dots \varepsilon_n \sim AR(\rho, \sigma_n) \quad (5.6)$$

where ρ is the autoregressive parameter, constant for each of the n considered responses and $\sigma_1, \sigma_2, \sigma_n$ represent the model variance for each considered response;

3. the most complex case, is those in which autocorrelation of the simulation errors is corrected by an individual autoregressive model AR(1) for each considered response:

$$\varepsilon_1 \sim AR(\rho_1, \sigma_1); \varepsilon_2 \sim AR(\rho_2, \sigma_2); \dots \varepsilon_n \sim AR(\rho_n, \sigma_n) \quad (5.7)$$

where ρ_1, ρ_2, ρ_n are the individual autoregressive parameter for each considered response and $\sigma_1, \sigma_2, \sigma_n$ represent the model variance for each considered response.

The choice of one case or another should be subject to deep analysis, as this will determine the number of statistical parameters that should be added to the hydrological parameters during the calibration approach.

Under the assumption of multiple responses with IID errors, the combined statistical likelihood function is simply the product of the individual likelihood functions considered for each individual response:

$$L_{multiple} = \prod_{i=1}^n L_i(\theta) = \prod_{i=1}^n p(Y_i | \theta) , \quad (5.8)$$

which can be further developed as:

$$L_{multiple} = \prod_{i=1}^n L_i(\theta) = \left[\frac{1}{(\sqrt{2\pi})^{t_1} \cdot \sigma_1^{t_1}} \cdot \exp \left(-\frac{\sum_{t=1}^{t_1} (Y_1 - Y_1^{sim})^2}{2 \cdot \sigma_1^2} \right) \right] \cdot \left[\frac{1}{(\sqrt{2\pi})^{t_2} \cdot \sigma_2^{t_2}} \cdot \exp \left(-\frac{\sum_{t=1}^{t_2} (Y_2 - Y_2^{sim})^2}{2 \cdot \sigma_2^2} \right) \right] \cdot \dots \cdot \left[\frac{1}{(\sqrt{2\pi})^{t_n} \cdot \sigma_n^{t_n}} \cdot \exp \left(-\frac{\sum_{t=1}^{t_n} (Y_n - Y_n^{sim})^2}{2 \cdot \sigma_n^2} \right) \right] \quad (5.9)$$

where Y_1, \dots, Y_n are the observed responses used in the calibration, $Y_1^{sim}, \dots, Y_n^{sim}$ are the corresponding simulated responses, $\sigma_1^2, \dots, \sigma_n^2$ are the variances for the simulation error corresponding to each response and t is the number of observations available for each observed response.

In order to use this combined likelihood function, the model residuals of the considered responses should be IID otherwise more complex models including error correlation between the different responses should be taken into consideration.

Sampling methodology: Gibbs within Metropolis algorithm

In order to compute the posterior distribution of the model parameters, we used the Gibbs within Metropolis algorithm whose main developments have been presented in Chapter 4. Its use was motivated by the work with multi-normal distributions with unknown variances. As for the case of a single response, the model variances are treated as statistical model parameters together with the autoregressive parameters.

For the multiple-response case, the vector of statistical parameters will include the same number of variances as the number of responses included in calibration. Depending of the simplification assumptions, the vector of statistical parameters could also include at maximum, n autoregressive parameters where n is the number of responses used in calibration.

For all the case studies proposed here, the autoregressive model has been chosen only for the observed discharge, as the resting time series are not complete. If we compare the model that we have chosen with those presented above, we could synthesise it as follows:

$$\varepsilon_1 \sim AR(\rho, \sigma_1); \varepsilon_2 \sim N(0, \sigma_2); \dots \varepsilon_n \sim N(0, \sigma_n) \quad (5.10)$$

where ρ is the autoregressive parameter for the discharge simulation errors and $\sigma_1, \sigma_2, \sigma_n$ represent the model variance for each considered response (discharge, soil moisture deficit, calcium or silica).

We have shown in the previous chapter, that the conditional distribution of the model variance, given the other hydrological and statistical parameters, is a Gamma distribution with parameters: $\frac{n}{2}$ and S ,

$$G\left(\frac{N}{2}, S\right) \quad (5.11)$$

where n is the number of observations of the considered response and S is given by

$$S = \frac{1}{2} \cdot \sum_{i=1}^t (Y_n - Y_n^{sim})^2 \quad (5.12)$$

For each considered response and under the assumption of IID of the simulation errors of the responses used in calibration, we used these conditional distributions to sample the model variances from previously sampled hydrological parameters.

Under the same IID assumptions, it can be proved that the updated acceptance rule r for n responses, is the product of individual acceptance rule:

$$\begin{aligned} r = & \exp \left[\left(\frac{1}{\sigma_{1,old}^2} + \frac{1}{\sigma_{1,new}^2} \right) \cdot (S_{1,old} - S_{1,new}) \right] \cdot \left(\frac{S_{1,new}}{S_{1,old}} \right)^{\frac{N_1}{2}} \cdot \exp \left[\left(\frac{1}{\sigma_{2,old}^2} + \frac{1}{\sigma_{2,new}^2} \right) \cdot (S_{2,old} - S_{2,new}) \right] \cdot \left(\frac{S_{2,new}}{S_{2,old}} \right)^{\frac{N_2}{2}} \cdot \\ & \dots \exp \left[\left(\frac{1}{\sigma_{n,old}^2} + \frac{1}{\sigma_{n,new}^2} \right) \cdot (S_{n,old} - S_{n,new}) \right] \cdot \left(\frac{S_{n,new}}{S_{n,old}} \right)^{\frac{N_n}{2}} \end{aligned} \quad (5.13)$$

where $\sigma_1 \dots \sigma_n$ are the variances parameters for each response, $S_1 \dots S_n$ are the squared sum of residuals for the n responses, $N_1 \dots N_n$ are the number of observations for each considered responses. The subscript old/new makes reference to the asymmetric jump distributions (see Chapter 4, page 101).

The convergence of the algorithm was as previously determined with the test of GEWEKE (Geweke (1992)).

The above-mentioned methodology has been implemented in a LABVIEW programming environment.

5.3 Multi-response calibration for the Haute-Mentue sub-catchments with GLUE and MCMC Bayesian approaches

In this sub-chapter, we'll present the application of the above-developed methodology to different sub-basins of the Haute-Mentue catchment.

First, a two-response calibration of the classical version of TOPMODEL is proposed, the two responses being the total discharge and the local soil storage saturation deficit. Two Bayesian approaches, GLUE (Generalized Likelihood Uncertainty Estimation) and MCMC (Monte Carlo Markov Chains) methods have been used to estimate both parameters and model uncertainty.

Second, the MCMC approach has been tested for a three-response calibration of one modified version of TOPMODEL. The three responses are the total discharge, the calcium concentration of the observed discharge and the silica concentration of the same observed discharge.

The input data was represented by the rainfall data measured at the meteorological station of Chalet du Villars. The potential evapotranspiration, which is required by the hydrological models as input data, has been computed by the Penman-Monteih formula using temperature, relative humidity, global radiation and wind speed measured at the same meteorological station of Chalet du Villars on the Haute-Mentue catchment. The discharges have been measured for several sub-catchments of the Haute-Mentue catchment. The study period covers essentially the autumn-winter 2002 seasons. The hydro-meteorological context for the chosen study periods is presented in Figure 5-5.

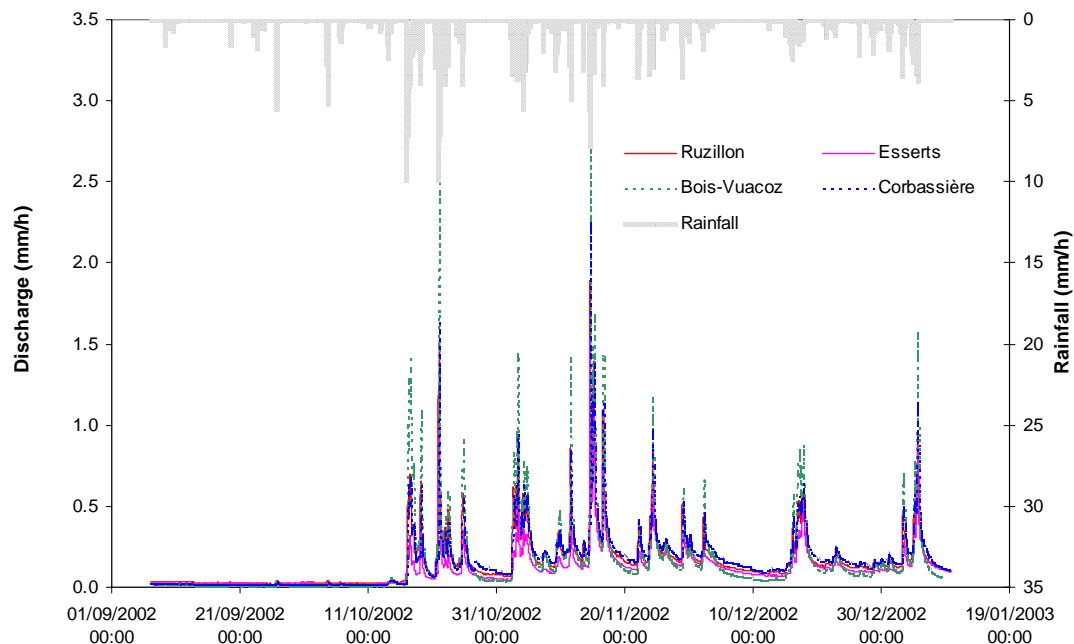


Figure 5-5 Hydro-meteorological context on the Haute-Mentue main sub-catchments: September 2002-January 2003

The evaluation of the multi-calibrating procedures has been done by using the undisturbed-catchment multiple response split-sample test proposed by Mroczkowski et al. (1997)). All considered responses are used both in model calibration and validation (Figure 5-6).

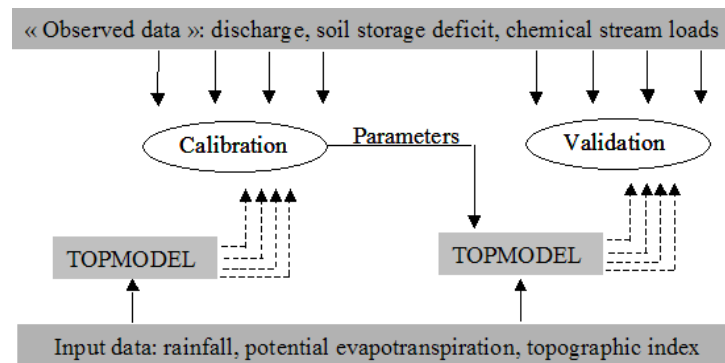


Figure 5-6 Multiple-response split-sample test (inspired from Mroczkowski et al. (1997))

5.3.1 Integrating catchment saturation deficit field estimates in rainfall-runoff modelling: classical version of TOPMODEL

To test the above methodology, we used the classical version of TOPMODEL and the field estimates of the saturation deficit in order to condition the uncertainty of the modelled discharge and of the model parameters. TOPMODEL uses the soil storage saturation deficit as an internal variable. The classical version presented in chapter 4, which has four parameters and simulates total discharges and the spatially semi-distributed storage deficits, has been used in this study.

Field estimates of saturation deficit have been obtained from local measurements effectuated within a plot of about 1m^2 . The soil moisture is punctual information, the derived values representing averages on 10 cm depth along the vertical inserted rods. In order to compare modelled “local values” of the storage deficit with those estimated from point soil moisture measurements, we had to make some scaling assumptions concerning:

- i. transposability of point information to a 25×25 m grid (the spatial unit of the DEM - Digital Elevation Model used by TOPMODEL to compute the statistical distribution of the topographical index)
- ii. transposability further to a corresponding class of a topographic index.

The topographic index uses the hydrologic similarity concept, which assumes that every point on the catchment with the same topographical conditions reacts in the same way from the hydrological point of view.

Previous research on this catchment (Talamba (1999)) showed that topographical characteristics of the Corbassière sub-catchments are intimately related to the geological characteristics. Tertiary sandstone deposits are translated in the relief by steep slopes

and more favourable conditions for the infiltration while the morainic quaternary deposits are characteristic to the gentle slopes less favourable to water infiltration. After comparing the topographic index spatial distribution (Figure 5-7 a) with the geological map of the Haute-Mentue catchment, two regions can be clearly distinguished: one corresponding to the morainic deposits with higher values of the topographic index between 8 and 10 and the other corresponding to the molassic deposits with lower values of the topographical index, between 6 and 8 (Figure 5-7 b and c). The two experimental plots for monitoring of the soil water content are each of them corresponding to the two classes defined above: the Ruzillon plot belongs to the class including morainic deposits and topographic index between 8 and 9 while the Esserts plot belongs clearly to the class including molassic deposits with values of the topographic index between 7 and 8.

In this context, we assumed that field estimated values of the soil storage deficit at the site of Ruzillon are the same as for all topographic index bins that have the same topographic index as those computed for the field site. Second, as a further extrapolation, we assumed that the field estimated soil storage deficit would be the same for all bins that are within the same class of the topographic index distribution as the considered field site. The field estimates of the soil storage deficit at the second field site, Esserts, were used only as orientative information since the real estimates are much higher than those observed up to 75 cm soil depth. Figure 5-7b presents the spatial repartition of the topographic index within the classes 6 and 8 for the Corbassière catchment. Figure 5-7c represents the spatial distribution of the topographic index within the classes 8 and 10 for the same Corbassière catchment. The two small red squares in Figure 5-7a show the site of the field plots.

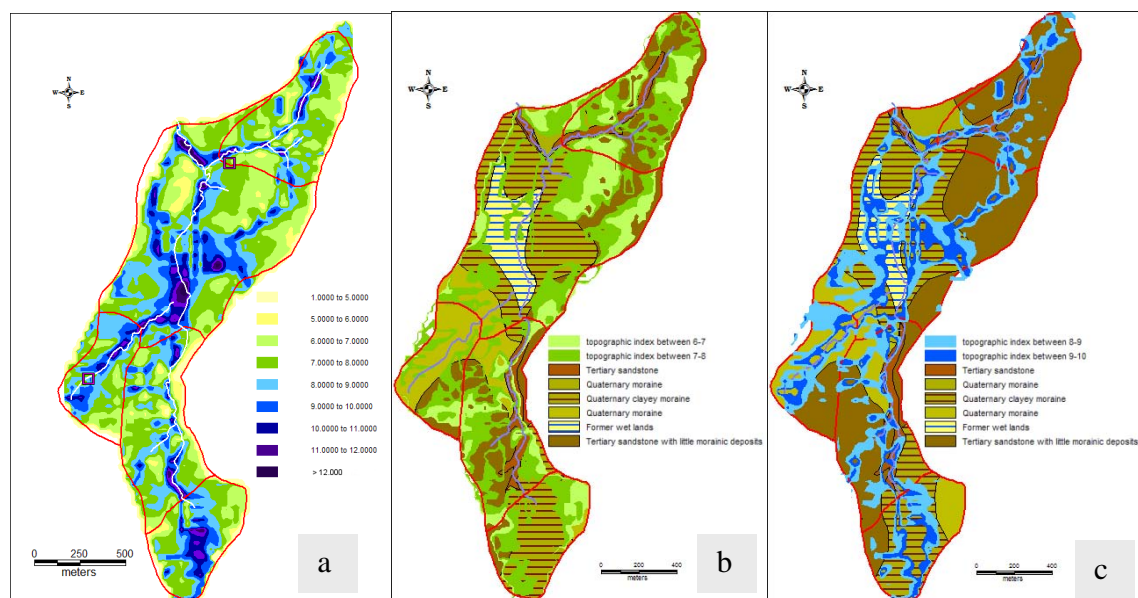


Figure 5-7 Spatial distribution of the topographic index for the Corbassière catchment as computed from a DEM at 1:25000 scale and comparison with the geological map of the same catchment.

We used the field estimated soil storage deficit as an internal variable to constrain and assess the uncertainty of TOPMODEL parameters and simulation results. In order to do that we used the multi-response calibrating methodology presented previously in this chapter.

The prior distributions of the hydrological parameters were the same as those presented in Table 1 from Chapter 4. The vector of statistical parameters included two models variances (one for the discharge and the second for the soil storage deficit response), which were sampled as already mentioned from Gamma distributions with parameters given by (5.11). Where the statistical diagnostic plots indicated as necessary, we also included the autoregressive parameter AR whose prior distribution was considered uniform on the interval 0-1. The likelihood function was given by the equation (5.9) for the case $n = 2$ where the two considered responses were the total discharge at the considered outlet and the soil storage deficit for a given class of the topographic index.

$$L_1 = \prod_{i=1}^2 L_i(\theta) = \left[\frac{1}{(\sqrt{2\pi})^{t_{discharge}} \cdot \sigma_{discharge}^{t_{discharge}}} \cdot \exp \left(\frac{\sum_{t=1}^{t_{discharge}} (Y_{discharge} - Y_{discharge}^{sim})^2}{2 \cdot \sigma_{discharge}^2} \right) \right] \cdot \left[\frac{1}{(\sqrt{2\pi})^{t_{soil_storage}} \cdot \sigma_{soil_storage}^{t_{soil_storage}}} \cdot \exp \left(\frac{\sum_{t=1}^{t_{soil_storage}} (Y_{soil_storage} - Y_{soil_storage}^{sim})^2}{2 \cdot \sigma_{soil_storage}^2} \right) \right] \quad (5.14)$$

where $Y_{discharge}$ and $Y_{soil_storage}$ are the observed discharge and soil storage saturation deficit time series; $Y_{discharge}^{sim}$ and $Y_{soil_storage}^{sim}$ are the simulated discharge and soil storage saturation deficit time series and $\sigma_{discharge}^2$ and $\sigma_{soil_storage}^2$ are the model variances parameters for the two responses.

When the residuals plots indicated violation of the constancy of the variance assumption, log-transformation of the variables was performed and the statistical likelihood function was updated to:

$$L_2 = \prod_{i=1}^2 L_i(\theta) = \left[\frac{1}{(\sqrt{2\pi})^{t_{discharge}} \cdot \sigma_{discharge}^{t_{discharge}}} \cdot \exp \left(\frac{\sum_{t=1}^{t_{discharge}} (y_{discharge} - y_{discharge}^{sim})^2}{2 \cdot \sigma_{discharge}^2} \right) \right] \cdot \left[\frac{1}{(\sqrt{2\pi})^{t_{soil_storage}} \cdot \sigma_{soil_storage}^{t_{soil_storage}}} \cdot \exp \left(\frac{\sum_{t=1}^{t_{soil_storage}} (y_{soil_storage} - y_{soil_storage}^{sim})^2}{2 \cdot \sigma_{soil_storage}^2} \right) \right] \quad (5.15)$$

where $y_{discharge}$ and $y_{soil_storage}$ are the log-transformed observed discharge and soil storage saturation deficit time series; $y_{discharge}^{sim}$ and $y_{soil_storage}^{sim}$ are the log-transformed simulated discharge and soil storage saturation deficit time series.

When statistical residuals plots indicated time dependence of the simulations errors, a simple autoregressive model has been applied for the model residuals which changed the likelihood function to:

$$L_3 = \prod_{i=1}^2 L_i(\theta) = \left[\frac{1}{(\sqrt{2\pi})^{t_{discharge}} \cdot \sigma_{discharge}^{t_{discharge}}} \cdot \exp \left(- \frac{\sum_{t=1}^{t_{discharge}} ((y_{discharge} - y_{discharge}^{sim}) - AR \cdot (y_{discharge}^{t-1} - y_{discharge}^{sim_{t-1}}))^2}{2 \cdot \sigma_{discharge}^2} \right) \right] \cdot \left[\frac{1}{(\sqrt{2\pi})^{t_{soil_storage}} \cdot \sigma_{soil_storage}^{t_{soil_storage}}} \cdot \exp \left(- \frac{\sum_{t=1}^{t_{soil_storage}} (y_{soil_storage} - y_{soil_storage}^{sim})^2}{2 \cdot \sigma_{soil_storage}^2} \right) \right] \quad (5.16)$$

where the new parameter AR represents the autoregressive parameter. Note that one single autoregressive parameter, for the discharge simulation errors, has been taken into account since the soil storage saturation deficit data are incomplete.

The multi-response calibrating methodology was tested for Ruzillon catchment and the main results are presented below.

This case study followed the same scheme as the case studies in the previous chapter:

- A. first, the multi GLUE calibrating methodology and the generalized likelihood measure were applied;
- B. second, the MCMC calibrating methodology and the statistical likelihood function were applied with several situations:
 - I. statistical likelihood function (L_1) with any log transform of the observed data and without AR(1) model for the simulation error;
 - II. statistical likelihood function (L_2) with log transform for both discharge and soil storage deficit but without AR(1) model for the simulation error;
 - III. statistical likelihood function (L_3) with log transform of the observed data and with AR(1) model for the simulation error.

As for the previous model application, the multi-calibration methodology was first applied for the end October 2002-January 2003 for the Ruzillon catchment.

A. GLUE methodology

The figures below show the simulation results and the total output uncertainty due to the parameter uncertainty after applying the GLUE methodology with the likelihood measure given by (5.3) for the single and multi-response calibration cases. The importance-sampling algorithm has been used with a threshold, to distinguish between behavioural and non-behavioural simulations, fixed at 0.3.

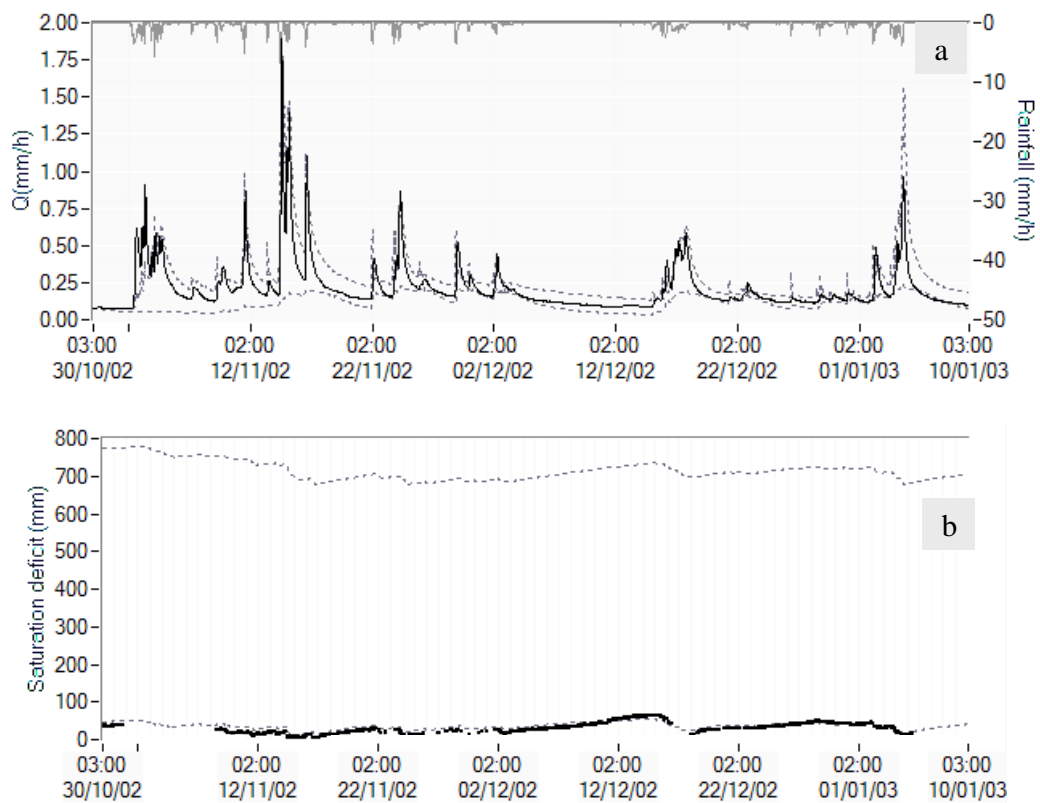


Figure 5-8 Topmodel and GLUE methodology- single calibration: Observed discharge (black line) and uncertainty bounds resulting from the parameters uncertainty (grey dotted lines) (a) and Observed soil storage deficit (black points) and uncertainty bounds resulting from the parameters uncertainty (grey dotted lines) (b)

In order to compare the single and the multi calibrating methodologies we represented the results for the two cases. Figure 5-8 (a and b) present the results of the single response GLUE calibrating methodology while Figure 5-9 presents the results of the two-responses GLUE calibrating methodology. The uncertainty bounds at 90% computed for the discharge and for the soil storage saturation deficit are resulting only from the uncertainty of the estimated parameters.

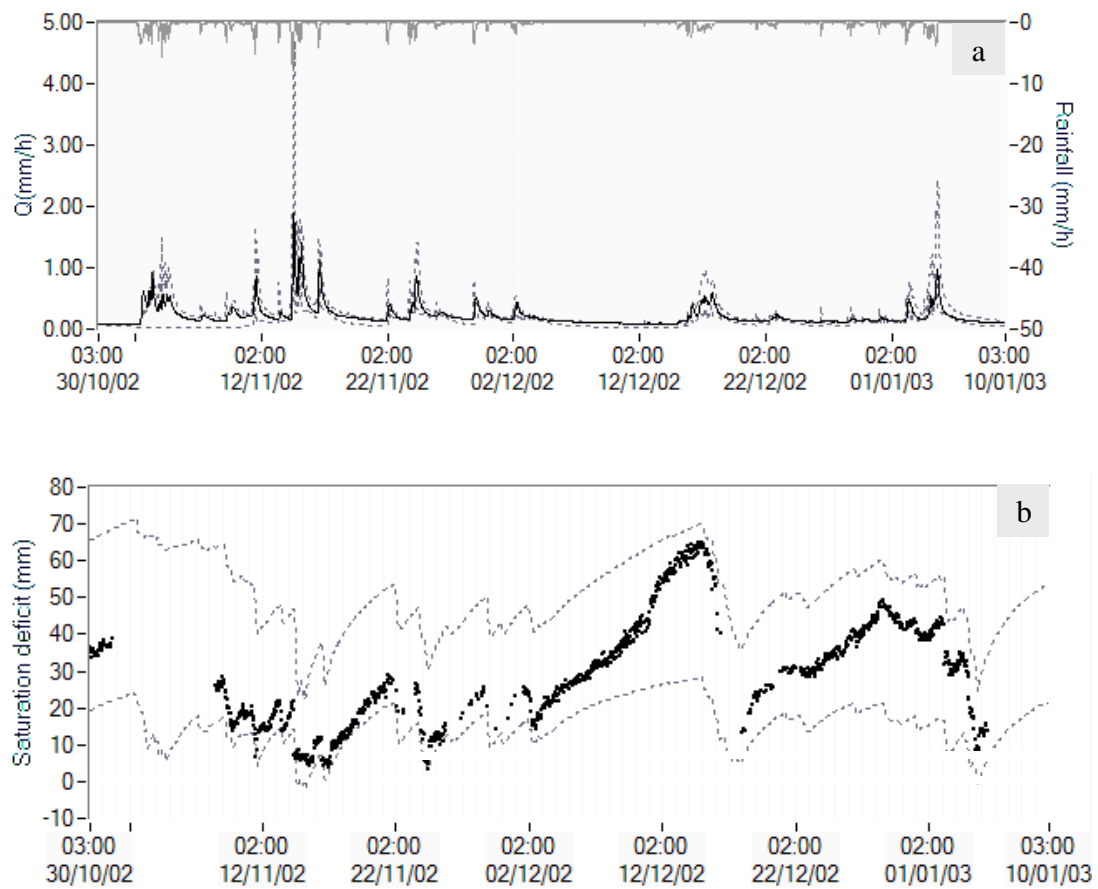


Figure 5-9 Topmodel and GLUE methodology- multi calibration: Observed discharge (black line) and uncertainty bounds resulting from the parameters uncertainty (grey dotted lines) (a) and Observed soil storage deficit (black points) and uncertainty bounds resulting from the parameters uncertainty (grey dotted lines) (b)

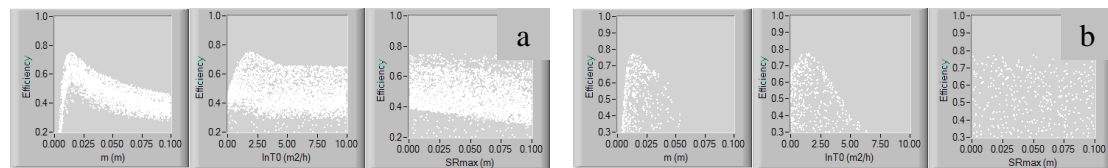


Figure 5-10 Topmodel and GLUE methodology- likelihood measure versus sampled parameters from the posterior distribution: single calibration (a) and multi-response calibration (b)

The posterior parameter distributions before (a) and after (b) the conditioning of TOPMODEL on both discharge and soil storage saturation deficit are presented in (Figure 5-10). Prior to conditioning on both observed discharges and soil storage deficit, the uncertainty bounds of the three most sensitive parameters are very large, covering almost the entire prior range of variation. These explain the large simulated uncertainty bounds for the total discharge and the storage deficit observed in Figure 5-8. Nevertheless, the simulated uncertainty bounds enclose completely the observed discharge.

Analysis of the soil storage saturation deficit after conditioning on observed discharge only shows that the general trend of the storage deficit temporal evolution is conserved while an important bias is observed between the simulation and the observed data. This observation is consistent with those of Seibert et al. (1997) who found that TOPMODEL was able to reproduce the temporal dynamics of the groundwater levels but with a systematic offset between observed and simulated values.

After conditioning on, both flow and soil storage deficit, the uncertainty of at least m and $\ln T0$ parameters is much lower. Unexpectedly, this didn't lead to a significantly decrease of the uncertainty of the estimated discharge (Figure 5-9 a) but on the contrary to an increase. The observed discharge is most of the time inside the predicted uncertainty, which is a good aspect. The multi-response calibration led to lower uncertainty bounds that reflect better than those computed with the single calibration approach, the shape of the flood hydrograph. The simulated uncertainty bounds are sensibly reduced for the storage deficit and observed series finds itself within the simulation uncertainty bounds.

These results are partially in the same line with those presented by Lamb et al. (1998) who used spatially distributed water table observations to constrain both parameters and TOPMODEL predictions. Nevertheless, they concluded that conditioning on both discharge and local groundwater tables led to larger uncertainty bounds for both model sensitive parameters and for the discharge simulated output. They also concluded that considering groundwater observations from several boreholes led to an increased uncertainty bounds for each local groundwater series. Several observations could explain these results; among these - the choice of the generalized likelihood measure and the choice of too narrow variation ranges for some of the model parameters. In our case, multi calibration and conditioning on both observed discharges and soil storage saturation deficit decreased considerably the uncertainty of the soil storage saturation deficit. Despite these results, the uncertainty remains still important for predicting purposes for both considered responses.

B. Monte Carlo Markov Chain methodology

The following examples apply the MCMC multi-calibration methodology for Ruzillon catchment and for the same study period. As a general approach we first used the single calibration approach in order to test and validate the model for another response that hasn't been previously used in calibration. After that, we introduced the additional responses during the calibration approach by using the multi-response calibrating methodology and evaluated the results.

The multiple split-sample Mroczkowski et al. (1997)) test was used and thus we separated the study period in a calibration sub-period (30 October 2002 - 21 November 2002) and a validation one (22 November 2002 – 10 January 2003).

I. Statistical likelihood function (L_I) without log-transform of the observed data and without AR (1) model for the discharge simulation error

SINGLE RESPONSE CALIBRATION: TOPMODEL was calibrated by using a single response (the observed discharge) and the resulting parameters posterior distributions were used to further validate the model for an internal variable (soil storage saturation deficit) that hasn't been used into the calibration approach. Figure 5-11 and Figure 5-12 shows the results for both responses of this kind of validation for the Ruzilon catchment.

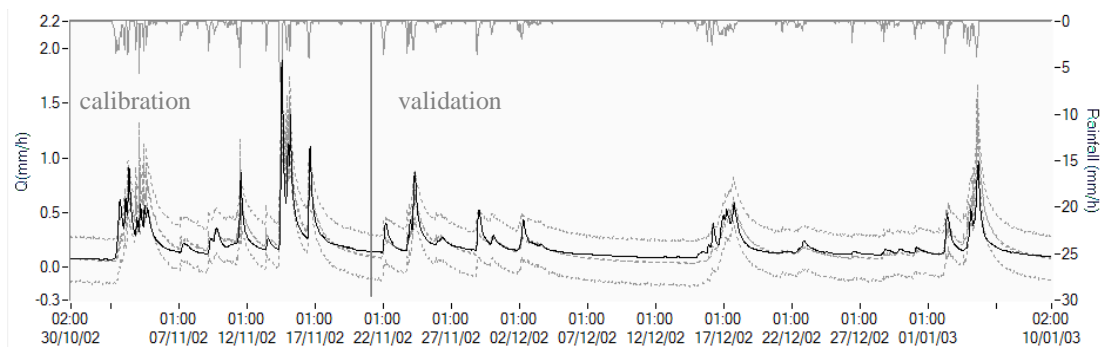


Figure 5-11 TOPMODEL and MCMC methodology- single calibration: observed discharge (black line) and uncertainty bounds from parameter uncertainty (inner bounds) and from model variance (outer bounds) at 90%

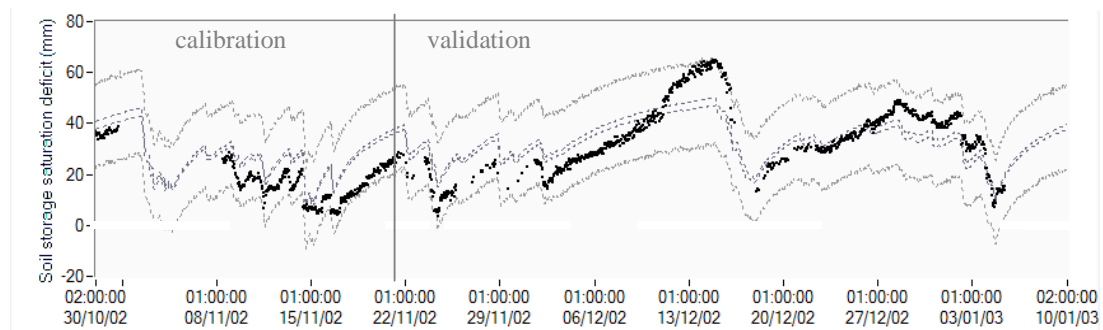


Figure 5-12 TOPMODEL and MCMC methodology- single calibration: observed soil storage saturation deficit (black points) and uncertainty bounds from parameter uncertainty (inner bounds) and from model variance (outer bounds) at 90%

Model calibration on single discharge response shows very small uncertainties for the estimated parameters (Annex VI), which induce small uncertainty for both predicted discharges (Figure 5-11) and soil storage saturation deficit (Figure 5-12). On the contrary, the total uncertainty due to the model structure and defined by the model variance parameter is very high and this explains most part of the total uncertainty of the predicted discharge and soil storage saturation deficit responses both during calibration and validation periods. Figure 5-12 shows the simulation results for the soil storage saturation deficit. Even if the model didn't include into the calibration this response, the general trend of the soil storage temporal dynamic is respected, the observations finding

themselves within the total uncertainty bounds. The same comments apply for the validation period. Nevertheless the model is rather unusable for prediction purposes for both discharges and soil storage deficit because of the important uncertainty due to the model variance.

The posterior distributions of the hydrological and statistical parameter together with the diagnostics plots of the models residuals for the simulations above are shown in Annex VI. The analysis of these plots evidences that the residuals variance is strongly varying with the simulated discharge and that these residuals are significantly correlated which could influence on the quality of the estimated parameters and on their use for periods other than those used in calibration. When violations of homoscedascity, independence or normality are detected, the interpretation of the parameter standard deviation becomes difficult and estimation of the parameters might be compromised. Too narrow or too wide uncertainty bounds are often one of the consequences of these wrong assumptions and model validation appreciation for periods others than those used in calibration becomes also a difficult task.

MULTI-RESPONSE CALIBRATION: In order to see if augmenting information will constrain parameter and model uncertainty, we used the field estimated soil deficit as an internal variable and we calibrated TOPMODEL on two responses: observed discharge and soil storage saturation deficit. Calibration was done using the statistical likelihood (L_I) as given by the equation (5.14). The model hydrological and statistical parameters have been sampled using the previous described Gibbs within Metropolis search algorithm.

Figure 5-13 and Figure 5-14 show the results for the simulated discharges and for the soil storage saturation deficit together with the uncertainty bounds at 90%.

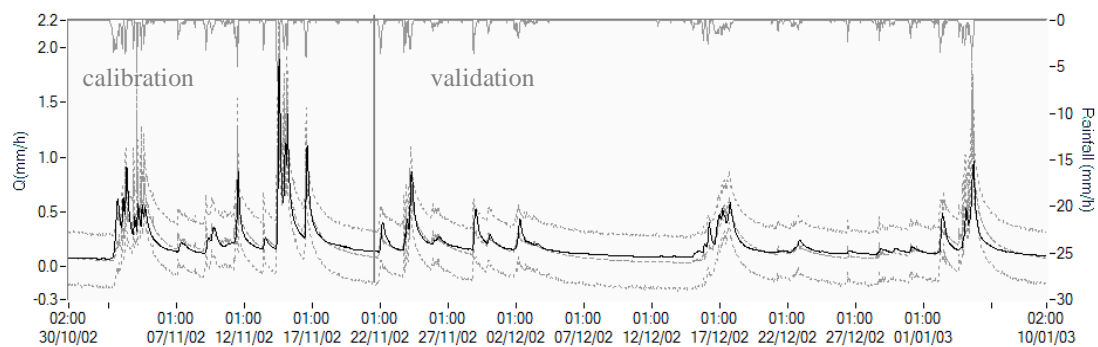


Figure 5-13 TOPMODEL and MCMC methodology- multi calibration: observed discharge (black line) and uncertainty bounds from parameter uncertainty (inner bounds) and from model variance uncertainty (outer bounds) at 90%

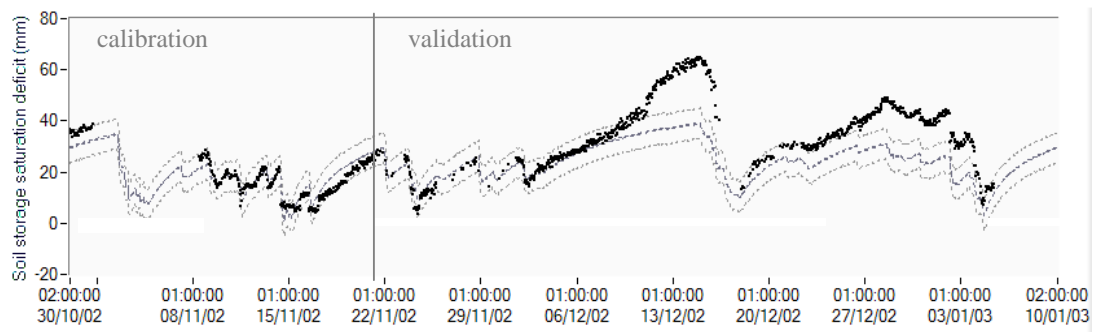


Figure 5-14 TOPMODEL and MCMC methodology- multi calibration: observed soil storage deficit (black points) and uncertainty bounds from parameter uncertainty (inner bounds) and from model variance (outer bounds) at 90%

While most part of the observed discharge and soil storage deficits observed values are within the simulated uncertainty bounds for the calibration period, for the validation period, the observed values of the soil storage deficits fall outside the simulated uncertainty bounds. This is explained by the fact that different conditions apply for the validation period with longer recession and larger values of the soil storage deficit that haven't been observed during the calibration period. Table 5-1 describes the posterior distributions of the parameters in terms of mode, mean, standard deviation and coefficient of variation. Both standard deviation and coefficient of variation are presented, as the last could be a more appropriate indicator to describe the uncertainty when the modes of the distributions change.

		Single calibration				Multi-calibration			
		Mode	Mean	SD	CV	Mode	Mean	SD	CV
Hydrological parameters	M (m)	0.011	0.011	0.0004	0.03	0.011	0.011	0.00007	0.01
	LnT0(m ² /h)	1.82	1.82	0.05	0.03	1.14	1.14	0.005	0.004
	Srmax [m]	0.009	0.009	0.0009	0.10	0.012	0.012	0.0007	0.06
	Srinit [%]	0.54	0.5	0.27	0.56	0.78	0.53	0.26	0.50
Statistical parameters	Variance-Q[mm]	0.75	0.76	0.04	0.06	1.03	1.05	0.06	0.058
	Variance-SD [mm]	99	99	10.9	0.11	13.03	12.82	1.03	0.08

Table 5-1 Parameters posterior distributions: mode and variation coefficient for the single and multi-response calibration approaches

The histograms of the posterior distributions of the hydrological and statistical parameters together with the residuals diagnostic plots and convergence criterion are all presented in Annex VI. The posterior distributions of the hydrological parameters show small variation coefficients for the multi-response calibrating methodology, which will traduce in smaller uncertainty bounds for the predicted responses. For the single-calibration approach, the two statistical parameters (Variance-Q for the discharge) and (Variance-SD for the storage deficit) show for both responses values high enough to make TOPMODEL estimates unusable for prediction purposes.

The multi-calibration approach reduced the uncertainty of model hydrological parameters but increased the uncertainty concerning the model variance for the streamflow response. In fact, the two statistical parameters tend to compensate somehow which could be interpreted as a trade-off behaviour of the two responses during the multi-calibration process.

II. Statistical likelihood function (L_2) with log-transform for both discharge and soil storage deficit but without AR (1) model for the discharge simulation error;

The diagnostic plots of the previous applied models residuals (Annex VI) indicate large departures from the hypothesis of homoscedasticity for both observed discharge and soil storage saturation deficit. In order to correct for this, we have further applied the same statistical model for the log-transformed discharge and soil storage deficit data. First, we considered the single-calibration case and tested the potential of such model to validate observed soil storage deficit data and second, we introduced this last response into the calibration approach and analysed the results.

SINGLE-RESPONSE CALIBRATION: Figure 5-15 shows the results of model calibration conditioned only on the log-discharge of observed data.

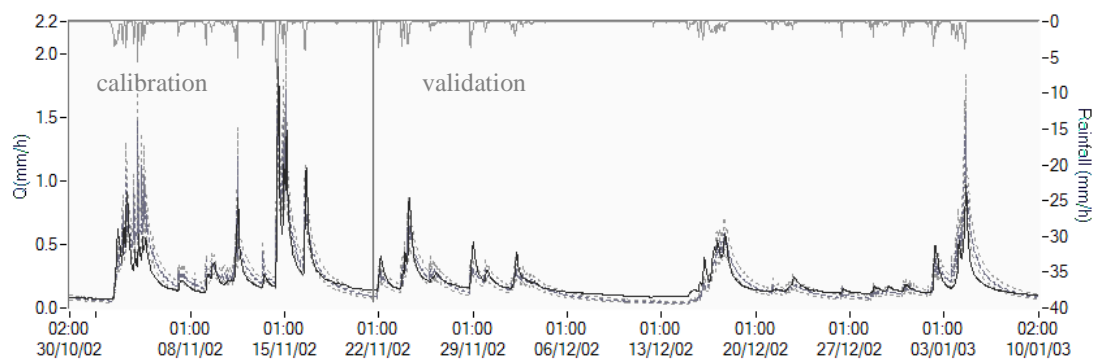


Figure 5-15 TOPMODEL and MCMC methodology- single calibration: observed discharges (dark grey line) and uncertainty bounds from parameter uncertainty (light grey dotted lines) and from model variance (darker grey dotted lines) at 90%

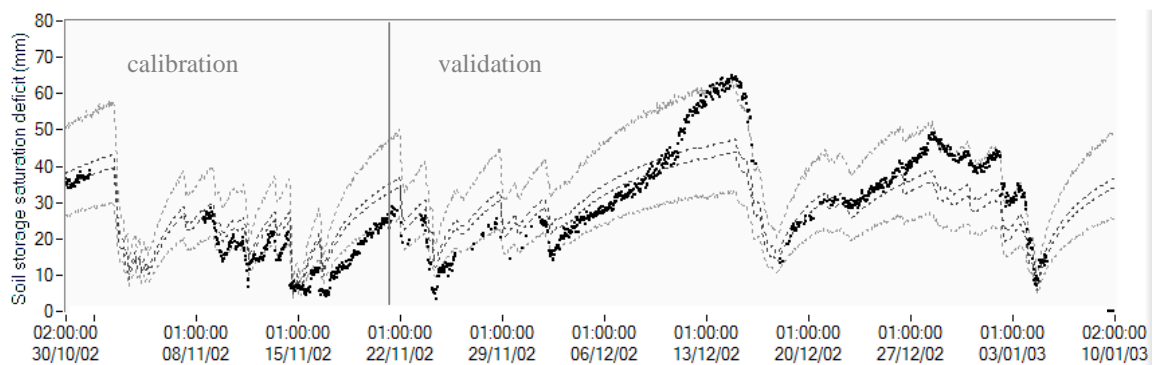


Figure 5-16 TOPMODEL and MCMC methodology- single-response: observed soil storage deficit (dark grey dotted line) and uncertainty bounds from parameter uncertainty (light grey dotted lines) and from model variance (darker grey dotted lines) at 90%

The uncertainty in predicting the discharge data is considerably reduced and this is mainly due to the decreasing of the model uncertainty (Figure 5-15). The part of uncertainty due to the parameters remained almost unchanged during calibration and validation periods. Regarding the soil storage saturation deficit response one can see that there is still a great uncertainty in estimating this response for the beginning of the period but the wetter the antecedent conditions, the narrower the uncertainty bounds become. For the validation period, the uncertainty becomes more important as new observed data are considered that haven't been used in the calibration.

MULTI-RESPONSE CALIBRATION: Figure 5-17 and Figure 5-18 show the results of the multi-calibration procedure for the same catchment and the same study period. One can see that no important changes occur for the discharge response (Figure 5-17): the model uncertainty is a little greater while the uncertainty in estimation the model hydrological parameters reduces (Annex VII and Table 5-2).

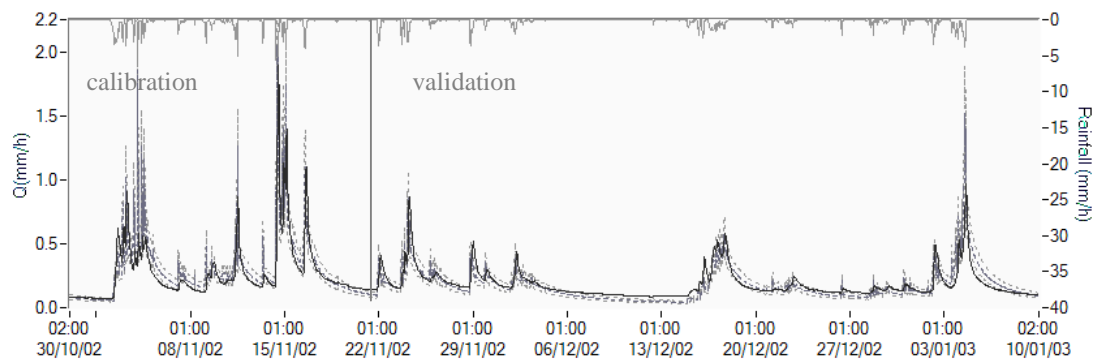


Figure 5-17 TOPMODEL and MCMC methodology- multi calibration: observed discharges (dark grey line) and uncertainty bounds from parameter uncertainty (light grey dotted lines) and from model variance (darker grey dotted lines) at 90%

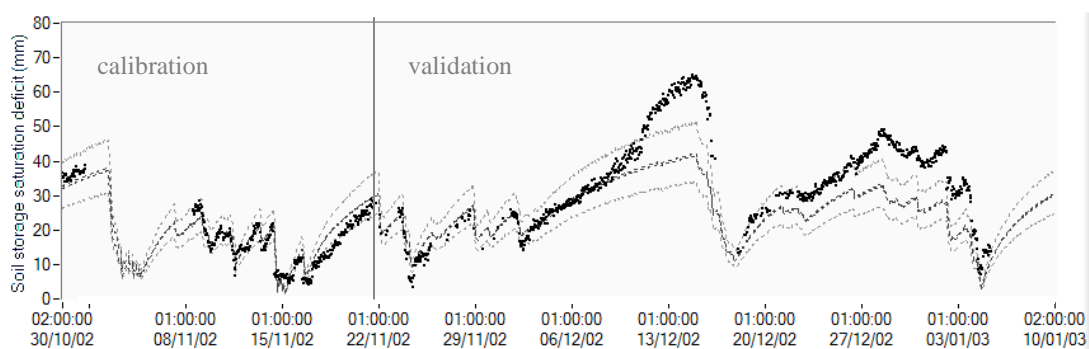


Figure 5-18 TOPMODEL and MCMC methodology- multi-response: observed soil storage deficit (dark grey dotted line) and uncertainty bounds from parameter uncertainty (light grey dotted lines) and from model variance (darker grey dotted lines) at 90%

For the second response, the soil storage saturation deficit, the uncertainty after the multi-calibration approach reduces significantly, most of the time the observed data being within the uncertainty bounds. The same conclusions apply for the validation period:

despite a little higher predictive uncertainty, the uncertainty bounds are clearly narrower than in the case where only a response has been considered.

		Single calibration				Multi-calibration			
		Mode	Mean	SD	CV	Mode	Mean	SD	CV
Hydrological parameters	M (m)	0.012	0.012	0.0004	0.03	0.013	0.013	0.00013	0.01
	LnT0(m ² /h)	1.5	1.53	0.05	0.03	0.92	0.91	0.007	0.008
	Srmax	0.0015	0.0016	0.0009	0.53	0.004	0.004	0.0016	0.4
	Srinit	0.53	0.51	0.26	0.52	0.73	0.53	0.28	0.52
Statistical parameters	Variance-Q[ln(l/s)]	0.016	0.016	0.001	0.06	0.018	0.018	0.001	0.06
	Variance-Q[mm]	0.02	0.02	0.02	1.00	0.021	0.021	0.02	0.95
	Variance-SD[mm]	0.04	0.04	0.005	0.12	0.016	0.015	0.001	0.07

Table 5-2 Parameters posterior distributions: mode, mean, standard deviation (SD) and variation coefficient (CV) for the single and multi-response calibration approaches

The residuals diagnostic plots in Annex VII show clear evidence of time dependence of the model residuals for both considered responses. In order to correct for this, a more complex statistical likelihood function was developed and the results are presented below.

III. Statistical likelihood function (L_3) with hydrological parameters vector and with log transform of the input data and with AR (1) model for the discharge simulation error

Beside the log-transform of the observed discharges and the soil storage saturation deficits, we further accounted for the previous detected residuals time-dependence by modelling the residuals with a simple autoregressive model. As we didn't dispose of complete time series of soil storage saturation deficit data, we applied an autoregressive model (AR (1)) only to the residuals of the observed discharge response.

SINGLE-RESPONSE CALIBRATION: Figure 5-19 and Figure 5-20 show the results of the single calibration approach for observed discharge and for the soil storage saturation deficit. The uncertainty in the simulated discharge shows considerably improvement: the uncertainty bounds are extremely narrow which normally would lead to a high confidence of the predicted responses. On the contrary, the uncertainty of the soil storage saturation deficit is considerably increased.

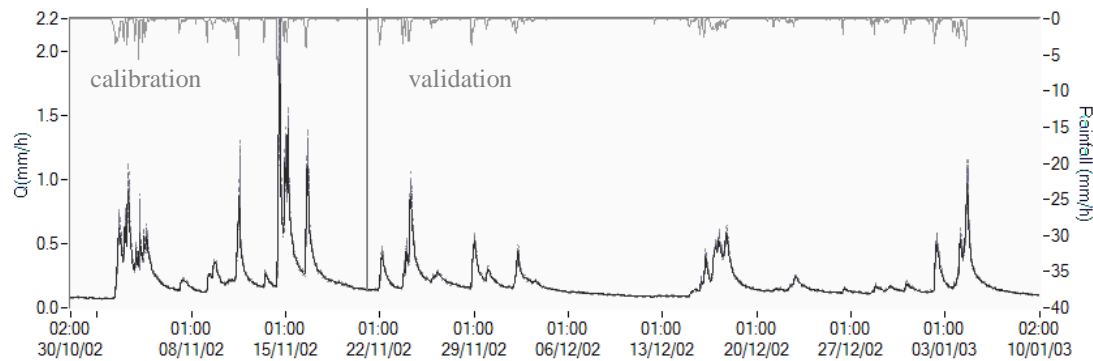


Figure 5-19 TOPMODEL and MCMC methodology- single calibration: observed discharges (dark grey line) and uncertainty bounds from parameter uncertainty (light grey dotted lines) and from model variance (darker grey dotted lines) at 90%

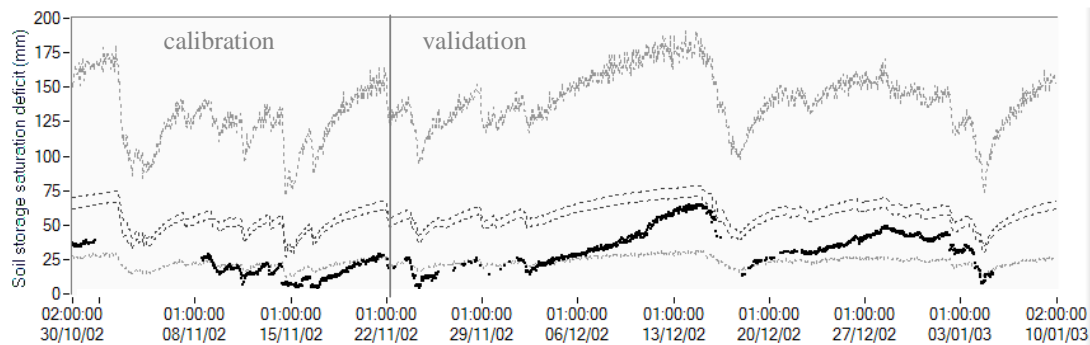


Figure 5-20 TOPMODEL and MCMC methodology- single-response: observed soil storage deficit (dark grey dotted line) and uncertainty bounds from parameter uncertainty (light grey dotted lines) and from model variance (darker grey dotted lines) at 90%

Introduction of the AR (1) model has changed significantly the posterior distribution of at least one parameter ($\ln T_0$). The figures in Annex VIII indicate that the posterior distribution for this parameter lies in a region with high values of $\ln T_0$. This had a direct consequence on the soil storage saturation deficit internal variable as high values of the $\ln T_0$ correspond to large values of the soil transmissivity, which will further favour rain infiltration and increase the soil storage saturation deficit. This behaviour is also confirmed by the high-simulated values of the soil storage saturation deficit and by the reduced temporal dynamics of the same internal variable.

The single calibration approach conducted with an autoregressive model of the discharge residuals led to a very good and high confident simulation of the discharges while the soil storage saturation deficit was systematically underestimated and with very high uncertainty bounds.

MULTI-RESPONSE CALIBRATION: In order to assess the significance of the multi-calibration approach, we present below the results concerning the predictive uncertainty for both discharge and soil storage estimates during the calibration and the validation periods as well. The results concerning the simulated discharge show a slight increase of

the uncertainty bounds due to a greater model variance without important deterioration of the total results (Figure 5-21). A relative improvement is on the contrary observed for the simulated soil storage saturation deficit for the calibration period (Figure 5-22). For the validation period, the uncertainty bounds are larger without nevertheless including all observed data (Figure 5-22). This is mainly explained by the fact that different hydrological conditions characterized this winter period with less rainfall and thus longer recession periods for which the model haven't been calibrated. The predictive capacity of this model is very high for the observed discharges but still very limited for the soil storage saturation deficit. Analysis of the residuals plots show that the soil storage saturation deficits residuals exhibit important time dependence. As time independency was detected an autoregressive model should be applied in order to correct for this problem and to improve the predictive capacity of the model.

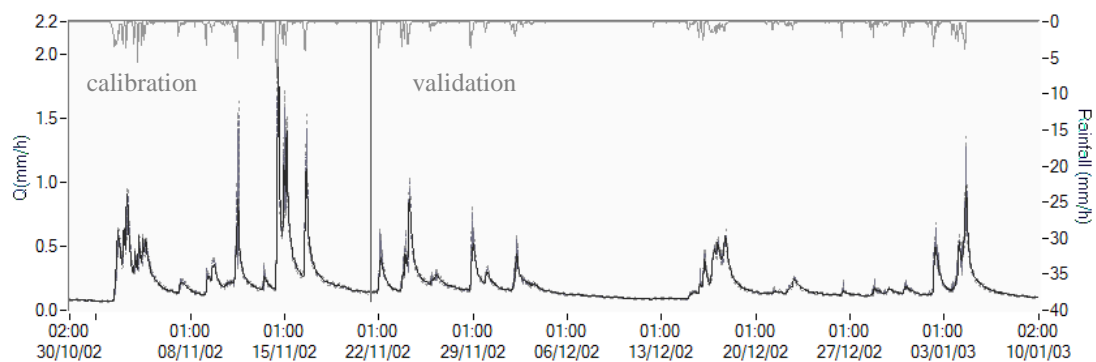


Figure 5-21 TOPMODEL and MCMC methodology- multi calibration: observed discharges (dark grey line) and uncertainty bounds from parameter uncertainty (light grey dotted lines) and from model variance (darker grey dotted lines) at 90%

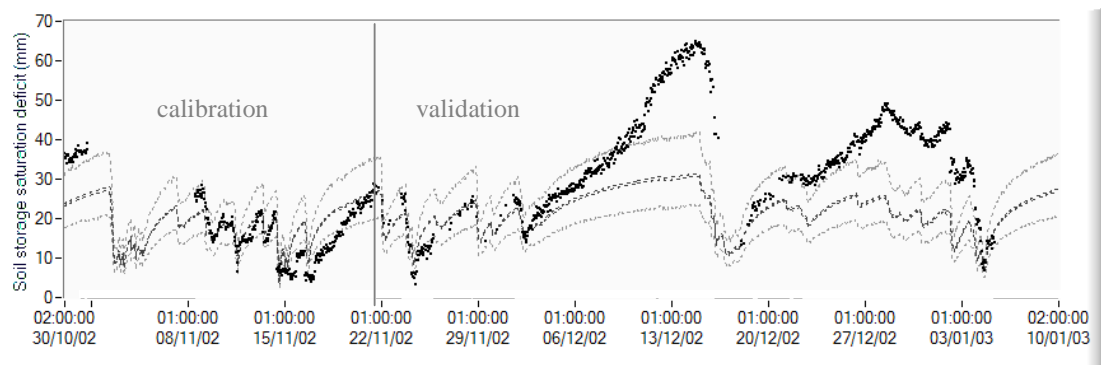


Figure 5-22 TOPMODEL and MCMC methodology- multi-response: observed soil storage deficit (dark grey dotted line) and uncertainty bounds from parameter uncertainty (light grey dotted lines) and from model variance (darker grey dotted lines) at 90%

	Single calibration				Multi-calibration			
	Mode	Mean	SD	CV	Mode	Mean	SD	CV
M (m)	0.011	0.011	0.0005	0.046	0.005	0.005	0.00005	0.01
LnT0(m ² /h)	4.1	4.1	0.053	0.013	2.98	2.98	0.012	0.004
Srmax[m]	0.0003	0.0016	0.0016	1.025	0.002	0.002	0.001	0.50
Srinit[-]	0.77	0.56	0.26	0.46	0.61	0.56	0.24	0.42
Var-Q[ln/l/s]	0.0013	0.0013	0.00008	0.064	0.002	0.002	0.0001	0.06
Variance-Q[mm]	0.02	0.02	0.02	0.99	0.02	0.02	0.02	0.99
Variance-SD [mm]	0.27	0.29	0.025	0.088	0.02	0.02	0.0016	0.07
AR	0.96	0.97	0.011	0.011	0.97	0.97	0.0026	0.002

Table 5-3 Parameters posterior distributions: mode, mean, standard deviation (SD) and variation coefficient (CV) for the single and multi-response calibration approaches

It is important to mention as well that the parameters uncertainty is significantly lower after introducing the second response (Table 5-3) but in this case the parameter uncertainty is far less important to decide the degree of uncertainty about the two considered responses. For these examples, it seems that the model variance is the parameter, which will finally decide the amplitude of the uncertainty bounds.

In conclusion, the introduction of the second response during the calibration approach deteriorated some how the uncertainty estimation for the discharge data but improved significantly the uncertainty estimation for the soil storage deficit.

Single and Multi-calibrations: comments

This analysis intended to assess the impact of augmenting information during calibration of a rainfall-runoff conceptual model on the model uncertainty and the model parameters uncertainty. In order to study this, a multi calibrating methodology has been proposed. The impact of the additional information on the resulting model parameters and output uncertainty has been studied through a comparative approach. First, the TOPMODEL has been calibrated against a single response and both kind of uncertainty assessed. Second, TOPMODEL has been calibrated against two responses (observed discharge and soil storage saturation deficit). This analysis has been conducted at three levels: first, the calibrated responses have been used without taking into account any statistical correction; second, the calibrated responses have been log-transformed in order to ensure constant residual variances and third, beside the previous log-transform, an autoregressive model (AR (1)) has been applied to model the residuals in order to remove their time dependence.

This work has shown that, in all cases, additional information:

- i. reduced the parameter uncertainty bounds;
- ii. increased slightly the model uncertainty of the discharge response due to increased corresponding model variance;
- iii. decreased significantly the model uncertainty of the soil storage saturation deficit due to a decrease of the corresponding simulated model variance;

In comparison with GLUE methodology which puts most part of the uncertainty in the parameters, the MCMC methods puts only a small part of the total uncertainty on the model parameters uncertainty, the resting uncertainty being explained as due to the model structure.

The trade-off behaviour is noticed for both methods, GLUE and MCMC, reflecting in higher uncertainty of the discharge response when the multi-calibration approach is used compared with the single calibration approach.

The multi-calibration approach, applied with GLUE and MCMC methods, reduces the uncertainty of the second calibrated response but the uncertainty bounds remains too large for the GLUE methods, rendering this method unusable for predictive purposes.

The multi-response calibrating methodology underlined the trade-off between the two considered responses. This trade-off is well evidenced in (Figure 5-23) where the right panel presents the sum of the residuals squared for both discharge and soil storage deficit responses for all sampled points during the Gibbs-Metropolis algorithm and the left one presents the same sum of the squared residuals for the sampled points after the burning-period has been removed.

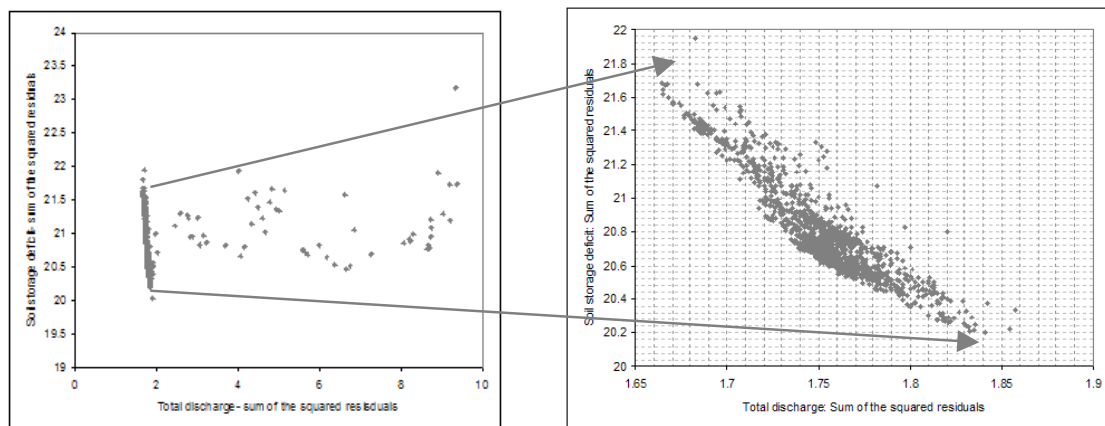


Figure 5-23 Example of “trade-off” behavior between the sum of the squared residuals for the observed discharge and the soil storage saturation deficit after performing the Gibbs-Metropolis algorithm: all iterations and iterations without the burn-in

In order to evidence the predictive power of the single and the multi-calibration methodologies, Table 5-4 below shows the model performance in terms of Nash-Sutcliffe criterion for the three kinds of models:

	Single response				Multiple responses			
	Calibration		Validation		Calibration		Validation	
	Q	SD	Q	SD	Q	SD	Q	SD
Simulation error without log-transform and without AR (1)	0.70	0.38	0.55	0.73	0.56	0.87	0.50	0.43
Simulation error with log- transform and without AR (1)	0.64	0.60	0.61	0.73	0.54	0.89	0.60	0.62
Simulation error with log- transform and with AR (1) for the discharge	0.91	-9.16	0.97	-0.84	0.74	0.70	0.84	0.02

Table 5-4 Nash-Sutcliffe efficiencies for the three considered models (the efficiency was computed for the mode values of the posterior parameter distributions); Note: Q –discharge response; SD- soil storage saturation deficit response;

One can see that, for the *single calibrating methodology*,

- ❑ the simplest tested model (without any statistical correction) led to acceptable simulation of the discharge for the calibration period. The validation efficiency is much lower instead. When the second response, the soil storage saturation deficit, was not included into the calibration approach, the performance in simulating this response is not satisfactory but in validation, a surprisingly high performance was noticed.
- ❑ The model with log-transform of both responses led to a much more stable model behaviour with acceptable efficiency in calibration and validation for both responses.
- ❑ The complete statistical model added to the hydrological one, shows excellent and stable efficiencies for the simulated discharge in both calibration and validation but the efficiency decreased drastically for the second simulated response: the soil storage saturation deficit.

For the *multi-calibrating methodology* the main conclusions are presented below:

- ❑ The first model (without statistical corrections) decreased the efficiency of the simulated discharge and increased considerably those of the soil storage saturation deficit for the calibration period. The results for the validation period show decreased efficiency for both responses.
- ❑ The model with log-transformed responses shows as expected, lower efficiency for the simulated discharge but considerably increased efficiency for the soil storage saturation deficit for the calibration period. For the validation period, stable behaviour is to be observed for both responses, with acceptable Nash-Sutcliffe efficiencies.
- ❑ The complete statistical, model exhibit mitigated results in the sense that lower efficiencies have been obtained for the simulated discharge but superior to what has been obtained previously in both calibration and validation; the second response exhibits an efficiency which is lower than those obtained in calibration and which is also much lower when compared with those obtained in validation for the two previous models. This could partially be explained by the fact that longer recession periods are to be simulated for the validation period, which was not the case for the calibration period. As the diagnostic plots indicate, the

residuals for the soil storage saturation deficit are highly correlated which would require further time introduction of an autoregressive model for this response as well. The model behaviour in validation could thus also have been improved if continuous time series would have been available for the soil storage saturation deficit as well, which would have allowed introduction of a complete statistical model for this response as well.

Concerning the multi-calibrating methodology, one observation is to be made for all the three cases concerning reproduction of the soil storage saturation deficit: the efficiency in validation depends on the particularities of the calibration period. In our case, the calibration period included only a short wet period in autumn 2002 without long recession periods. The validation period included on the contrary two periods with longer recession and reproduction of these was much more difficult as the model parameters were calibrated only for wet conditions. As the calibrated parameters seem to highly depend on the meteorological context it would be necessary for the future that longer periods be chosen as calibration periods in order for the estimated parameters to be used for longer validation periods. Otherwise, the calibrated parameters for wet conditions should be applied only for validation periods with similar meteorological conditions.

5.3.2 Integrating tracing information in rainfall-runoff modelling: modified version of TOPMODEL

In this chapter will consider the MCMC multi-calibration approach for a modified version of TOPMODEL for which the additional information is not represented by a direct calculated internal variable but by direct observations of the stream chemistry introduced into the modelling by an indirect end mixing modelling approach. We considered that, an EMMA hydrograph decomposition approach could be applied for TOPMODEL components (overland flow, shallow subsurface flow and deep flow) in order to model the temporal dynamics of the calcium and silica simulated stream flow concentrations.

The present work is in line with the approach followed by Boyer. This study uses the concept developed by Boyer et al. (1996) whose main developments have been presented earlier in the previous chapter.

The model simulates total discharge and two basic components: the overland flow, the subsurface flow, which is further decomposed into subsurface quick flow and base groundwater flow. The main hydrological processes represented here are the flow over saturated areas (overland saturated flow) and saturation from below. Field experience showed that for the Haute-Mentue catchment, for the regions covered by morainic deposits, these are the most important processes explaining most of the growth of the hydrograph. Only after dry antecedent conditions or in the presence of strong rainfall intensities at the beginning of an event a perched aquifer lasting several hours could be noticed at the limit between a sandy and a clayey soil horizon. As, at the time scales greater than 24h this becomes a secondary event with a minor contribution to the total

stream discharge we concluded that the simple modified version of TOPMODEL would be enough to capture the main mechanisms occurring on the Haute-Mentue catchment. Furthermore, the environmental tracing that was performed since several years on the Haute-Mentue catchment identifies three geographical sources contributing to the floods: rain water, soil water and groundwater. In our application we assumed that the overland flow estimated by the model would be more or less equivalent to the rainwater component estimated with the tracing approach. Further, the tracing approach identifies two other geographical pathways corresponding to the soil water and the groundwater. The distinction between the two sources is made only on the basis of their chemical composition. Here we used calcium and silica to distinguish between these two sources. Figure 2 in Chapter III shows the differences in calcium and silica content for the end-members we considered here. As one could see the main difference between the soil water and the groundwater is given essentially by the content in calcium. In fact, the water coming from deeper sources has greater calcium content, as the bedrock on the Haute-Mentue catchment is essentially formed by carbonate rocks. The soil water is diluted in this component as the infiltrating water has little contact with the carbonate bedrock. In terms of mechanisms this component is not clearly defined as it may be formed by new perched water formed within the soil horizon or by old groundwater mixed with new infiltrated water forming kind of calcium diluted groundwater. In respect to these and in order to make possible the comparison between EMMA chemical mixing model and TOPMODEL, we introduced a number of parameters that are meant to delimitate between the deep groundwater flow formed essentially by old water and the shallow groundwater flow formed by a mixture of old and new waters. These new TOPMODEL parameters are: the drainable porosity in m^3/m^3 (n), the depth of the soil reservoir in meters (Z_{up}), the total depth to the bedrock in m (Z_{tot}). Further, the TOPMODEL simulated flow components have been used within an EMMA chemical mixing model in order to predict the calcium and silica stream concentration. The mass balance (water and tracer) equations used to compute the stream calcium and silica concentrations at each time step are presented below:

$$\begin{aligned} C_{Ca\text{-stream}} &= X_{\text{groundwater}} \cdot C_{Ca\text{-groundwater}} + X_{\text{soil}} \cdot C_{Ca\text{-soil}} + X_{\text{rainfall}} \cdot C_{Ca\text{-rainfall}} \\ C_{Si\text{-stream}} &= X_{\text{groundwater}} \cdot C_{Si\text{-groundwater}} + X_{\text{soil}} \cdot C_{Si\text{-soil}} + X_{\text{rainfall}} \cdot C_{Si\text{-rainfall}} \end{aligned} \quad (5.17)$$

where $X_{\text{groundwater}} = \frac{Q_{\text{groundwater}}}{Q_{\text{total}}}$; $X_{\text{soil}} = \frac{Q_{\text{soil}}}{Q_{\text{total}}}$; $X_{\text{rainfall}} = \frac{Q_{\text{rainfall}}}{Q_{\text{total}}}$ represent the proportions of each flow component at the total flow discharge at the stream outlet. C_{Ca} and C_{Si} represent the concentrations in calcium and silica of each flow component (indexes-groundwater, soil and rainfall) and of the total discharge (index stream). The end-members that have been used in this study case are the groundwater, the soil water and the rain water and they have been assigned constant concentrations over the time and over the space within each considered catchment (Table 5-5). The chemical composition of the groundwater varies spatially from one catchment to another but the chemical definition of the other end-members is kept constant. This corresponds to the Model 3 used by Joerin et al. (2002).

	Ruzillon		Esserts	
	Ca [μeq/l]	SiO ₂ [mg/l]	Ca [μeq/l]	SiO ₂ [mg/l]
Groundwater	3000	10.75	2450	11
Soil water	450	7	450	7
Rain water	70	0.1	70	0.1

Table 5-5 Chemical definition of the end-members used by EMMA approach

The joint likelihood function that we used for this example is the same as given by the general form expressed in (5.9) for the case $N = 3$.

$$\begin{aligned}
 L_{multiple} = \prod_{i=1}^3 L_i(\theta) = & \left[\frac{1}{(\sqrt{2\pi})^{t_{discharge}} \cdot \sigma_{discharge}^{t_{discharge}}} \cdot \exp \left(-\frac{\sum_{t=1}^{t_{discharge}} (Y_{discharge} - Y_{discharge}^{sim})^2}{2 \cdot \sigma_{discharge}^2} \right) \right] \cdot \\
 & \left[\frac{1}{(\sqrt{2\pi})^{t_{calcium}} \cdot \sigma_{calcium}^{t_{calcium}}} \cdot \exp \left(-\frac{\sum_{t=1}^{t_{calcium}} (Y_{calcium} - Y_{calcium}^{sim})^2}{2 \cdot \sigma_{calcium}^2} \right) \right] \cdot \\
 & \left[\frac{1}{(\sqrt{2\pi})^{t_{silica}} \cdot \sigma_{silica}^{t_{silica}}} \cdot \exp \left(-\frac{\sum_{t=1}^{t_{silica}} (Y_{silica} - Y_{silica}^{sim})^2}{2 \cdot \sigma_{silica}^2} \right) \right]
 \end{aligned} \tag{5.18}$$

To sample from the posterior distributions of the model parameters we have used the Gibbs within Metropolis algorithm where the acceptance ratio was updated:

$$\begin{aligned}
 r = & \exp \left[\left(\frac{1}{\sigma_{1,old}^2} + \frac{1}{\sigma_{1,new}^2} \right) \cdot (S_{1,old} - S_{1,new}) \right] \cdot \left(\frac{S_{1,new}}{S_{1,old}} \right)^{\frac{N_1}{2}} \cdot \exp \left[\left(\frac{1}{\sigma_{2,old}^2} + \frac{1}{\sigma_{2,new}^2} \right) \cdot (S_{2,old} - S_{2,new}) \right] \cdot \left(\frac{S_{2,new}}{S_{2,old}} \right)^{\frac{N_2}{2}} \cdot \\
 & \dots \exp \left[\left(\frac{1}{\sigma_{3,old}^2} + \frac{1}{\sigma_{3,new}^2} \right) \cdot (S_{3,old} - S_{3,new}) \right] \cdot \left(\frac{S_{3,new}}{S_{3,old}} \right)^{\frac{N_3}{2}}
 \end{aligned} \tag{5.19}$$

where the subscripts 1, 2 and 3 make reference to the total discharge, calcium and silica responses.

The MCMC calibrating methodology and the statistical likelihood function were applied for the case of a statistical likelihood function with log- transform of the observed data and with AR (1) model for the simulation error.

The next paragraph will follow the analysis structure already introduced before. The capability of TOPMODEL to predict calcium and silica concentrations in the stream flow is initially evaluated without using directly this chemical information into the calibration approach. Second we introduce the two chemical time series into the MCMC multi-calibration approach and evaluate the results on the model parameter distributions and on the model output. The methodology has been tested with the discharge and the chemical data from the Ruzillon and Esserts catchments and the results presented here are only preliminary results. The parameter prior distributions are presented below:

	Parameter	Min	Max	Distribution
Hydrological parameters	m [m]	0.0001	0.1	uniform
	LnT0[m ² /h]	0.0001	10	uniform
	n [m ³ /m ³] Ruzillon	0.01	0.1	uniform
	n [m ³ /m ³] Esserts	0.01	0.3	uniform
	Z up [m]	0.10	1.00	uniform
	Z total [m]	1.00	5.00	uniform
Statistical parameters	Inv. Variance Vq	0	∞	uniform
	Inv. Variance Vca	0	∞	uniform
	Inv. Variance Vsi	0	∞	uniform
	AR parameter	0	1	uniform

Table 5-6 Prior distributions for the hydrological and statistical parameters

Based on previous modelling experience, that showed that the residual variance is not homoscedastic for discharge data but also for chemical data, we worked with log-transformed data. Further, a simple autoregressive model AR (1) was used to model the discharge simulation errors. Even if previous applications showed that the residuals for the chemical signals are highly correlated, we introduced the AR modelling only for the discharges, as the time series of the two chemical species are not complete and as one of the aims of this study being to test the ability of corrected TOPMODEL to predict the chemical signal of the streamflow.

The updated statistical likelihood function is as presented before:

$$\begin{aligned}
 L_{multiple} = \prod_{i=1}^3 L_i(\theta) = & \left[\frac{1}{(\sqrt{2\pi})^t \cdot V_Q^t} \cdot \exp \left(\frac{\sum ((q - q_{t-1}) - AR \cdot (q_{t-1} - q_{t-1}^{sim}))^2}{2 \cdot V_Q^2} \right) \right] \\
 & \cdot \left[\frac{1}{(\sqrt{2\pi})^t \cdot V_{Ca}^t} \cdot \exp \left(\frac{\sum (\ln(C_{Ca}) - \ln(C_{Ca}^{sim}))^2}{2 \cdot V_{Ca}^2} \right) \right] \\
 & \cdot \left[\frac{1}{(\sqrt{2\pi})^t \cdot V_{Si}^t} \cdot \exp \left(\frac{\sum (\ln(C_{Si}) - \ln(C_{Si}^{sim}))^2}{2 \cdot V_{Si}^2} \right) \right]
 \end{aligned}
 \tag{5.20}$$

Where $q = \log(Q + k)$ and $k = 0.00001$, and Q is the observed or simulated discharge data. The Gibbs within Metropolis algorithm has been applied in order to sample from the posterior distributions of the hydrological and statistical parameters. The algorithm worked with 10000 iterations from which only the last 25% have been retained for further

analysis. A thinning factor of 3 was applied to the final sample in order to reduce the correlation within the sampled parameters.

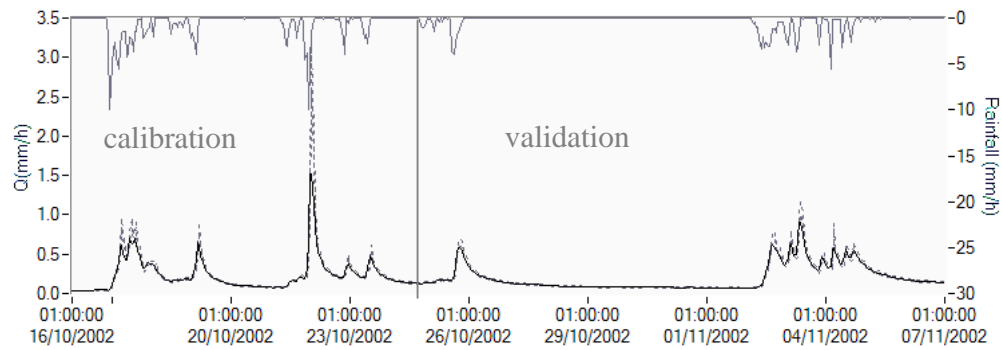


Figure 5-24 TOPMODEL and MCMC methodology: observed discharge (grey line) and uncertainty bounds (grey dotted lines) at 90%; Ruzillon catchment

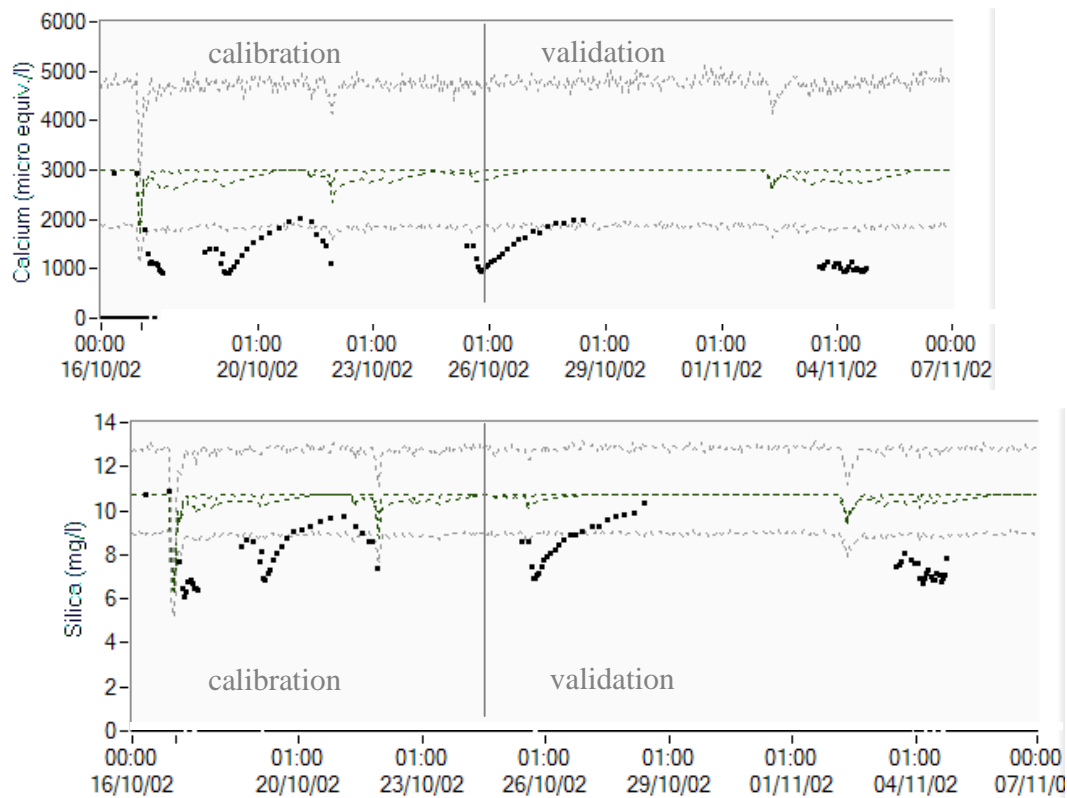


Figure 5-25 TOPMODEL and MCMC methodology: Observed calcium (dark points) -top, observed silica signal (dark points)-down, together with simulated parameter uncertainty bounds (inner bounds) and model uncertainty (outer bounds) at 90%; Ruzillon catchment

SINGLE-RESPONSE CALIBRATION: The modified version of TOPMODEL was calibrated against the observed discharge series. As the autoregressive model was considered, the simulated discharge was very well estimated and the uncertainty bounds are very narrow, limiting very closely the observed discharge (Figure 5-24). The

autoregressive coefficient is very high, which means that the statistical correction accounted for almost all the structural error of TOPMODEL. Posterior distribution of the $\ln T0$ parameter shows clearly that, when the model is conditioned only on the observed discharges, the MCMC approach converges towards high values of the soil transmissivity, which results in large contributions of the groundwater component to the total discharge and hence small variation of the calcium and silica concentrations over the time. Parameter uncertainty is low but model uncertainty is high for the simulated chemical species and the observed calcium and silica concentrations often fall outside the simulated bounds (Figure 5-25).

MULTI-RESPONSE CALIBRATION: Figure 5-26 shows the results of the simulated discharge after conditioning on discharge and both calcium and silica observed time series.

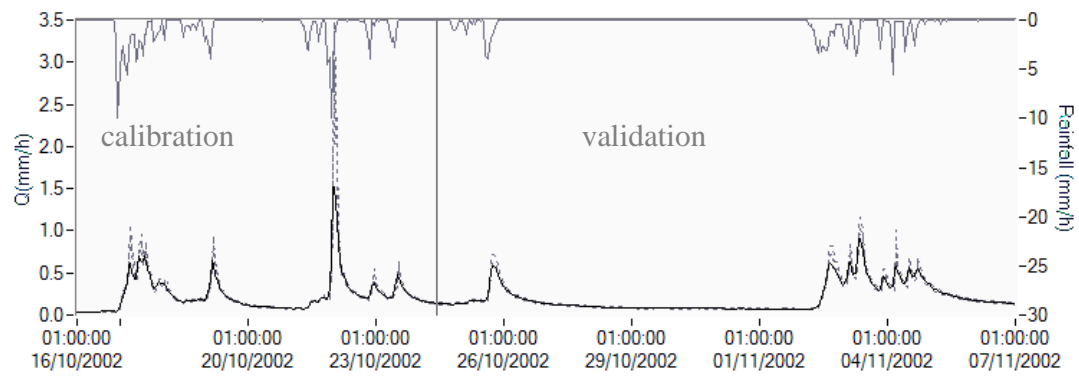


Figure 5-26 TOPMODEL and MCMC methodology: observe discharge (grey line) and uncertainty bounds (grey dotted lines) at 90%; Ruzillon catchment

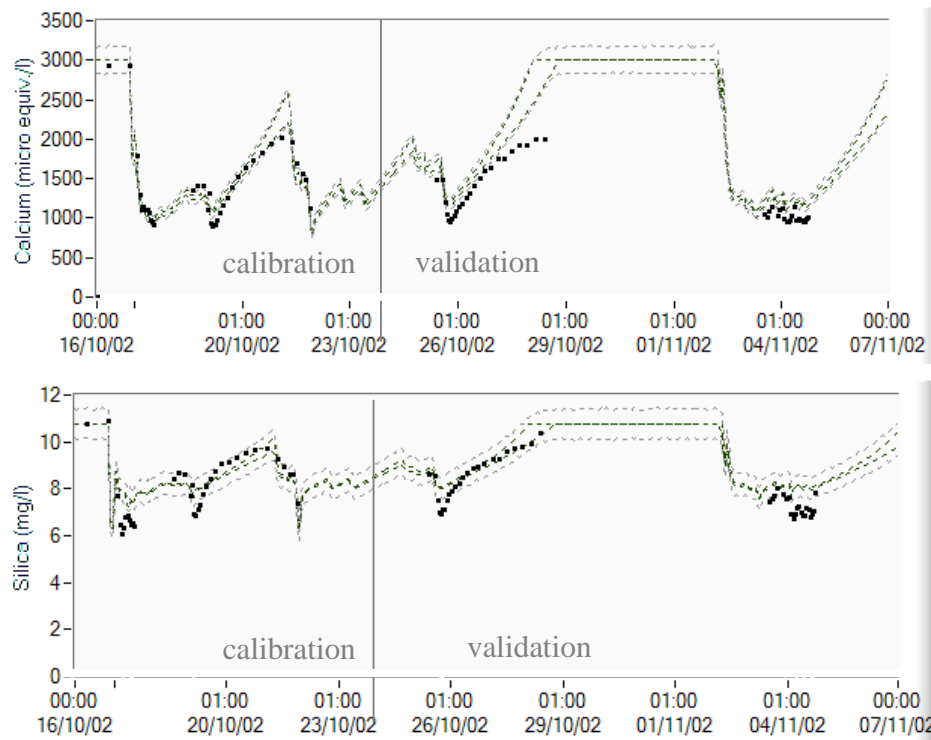


Figure 5-27 TOPMODEL and MCMC methodology: Observed calcium (dark points) -top, observed silica signal (dark points)-down, together with simulated parameter uncertainty bounds (inner bounds) and model uncertainty (outer bounds); Ruzillon catchment

		Responses used in calibration							
		Single response				Multi Response			
		Mode	Average	SD	CV	Mode	Average	SD	CV
Hydrological parameters	M (m)	0.012	0.012	0.0012	0.09	0.0091	0.0091	0.0002	0.02
	LnT0(m2/h)	4.72	4.73	0.056	0.01	4.72	4.73	0.031	0.007
	n (m3/m3)	0.04	0.05	0.023	0.46	0.049	0.05	0.0014	0.028
	Zup (m)	0.61	0.56	0.23	0.41	0.95	0.94	0.02	0.02
	Ztot (m)	3.15	3.13	1.08	0.34	1.06	1.08	0.02	0.02
Statistical parameters	Variance - Q	0.002	0.0029	0.0003	0.10	0.0027	0.0003	0.0003	0.10
	Variance - Ca	0.11	0.13	0.04	0.27	0.002	0.002	0.0005	0.25
	Variance - Si	0.016	0.02	0.006	0.30	0.002	0.0021	0.0005	0.24
	AR	0.98	0.98	0.007	0.007	0.98	0.98	0.008	0.008

Table 5-7 TOPMODEL and MCMC methodology: Single and multi-calibration approaches: posterior parameter distributions (for the case with log-transform data and AR(1,0) for the discharge residual modelling); Ruzillon catchment

Figure 5-26 and Figure 5-27 demonstrate that no further improvement for the discharge simulation of the uncertainty is noticed. Nevertheless, a slight increase of the model variance for the discharge response is to be noted. This behaviour is similar to that of the previous application when a kind of trade-off was observed between the considered objective functions. A great improvement is observed when looking to the uncertainty

bounds of the calcium and silica signals. This applies for both calibration and validation periods. The posterior hydrological parameter uncertainty exhibit different behaviours: the uncertainty of m and $\ln T0$ posterior distributions is reduced but in a smaller proportion than those of the parameters defining the partition of soil and groundwater reservoirs: n , the drainable porosity, the upper soil (Z_{up}) and total soil depths (Z_{tot}). The decreased uncertainty of the posterior hydrological parameters is reinforced by the important decrease of the uncertainty of the model variance parameters, which finally led to a reduction of the total simulated uncertainty for the two chemical signals such that we could use the model for predictive purposes for conditions that are similar to those observed during the calibration period.

The same modified version of TOPMODEL and the same statistical likelihood function were applied to Esserts catchment during the same study period. As for the previous example, only the last kind of model (including log-transformed data and AR (1) model for the simulation error) is presented here.

SINGLE-CALIBRATION RESPONSE:

Calibration of the modified version of TOPMODEL against observed discharge data for the Esserts catchment led to the following results:

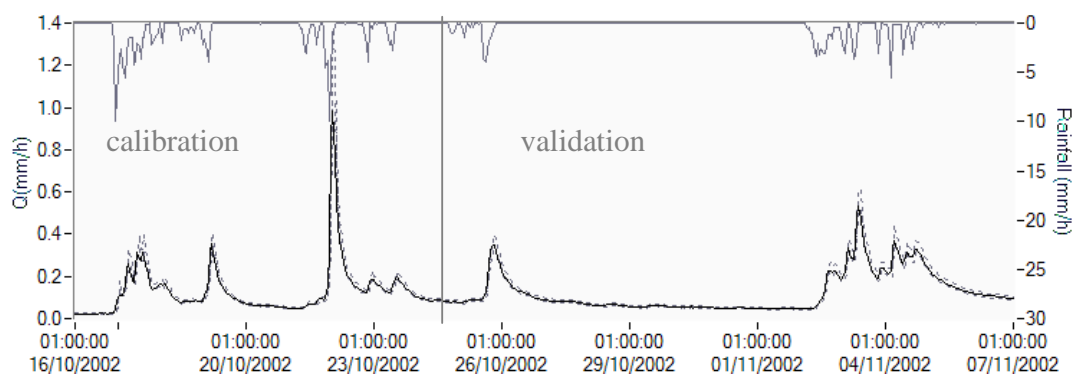


Figure 5-28 TOPMODEL and MCMC methodology: observed discharge (grey line) and uncertainty bounds (grey dotted lines) at 90%; Esserts catchment

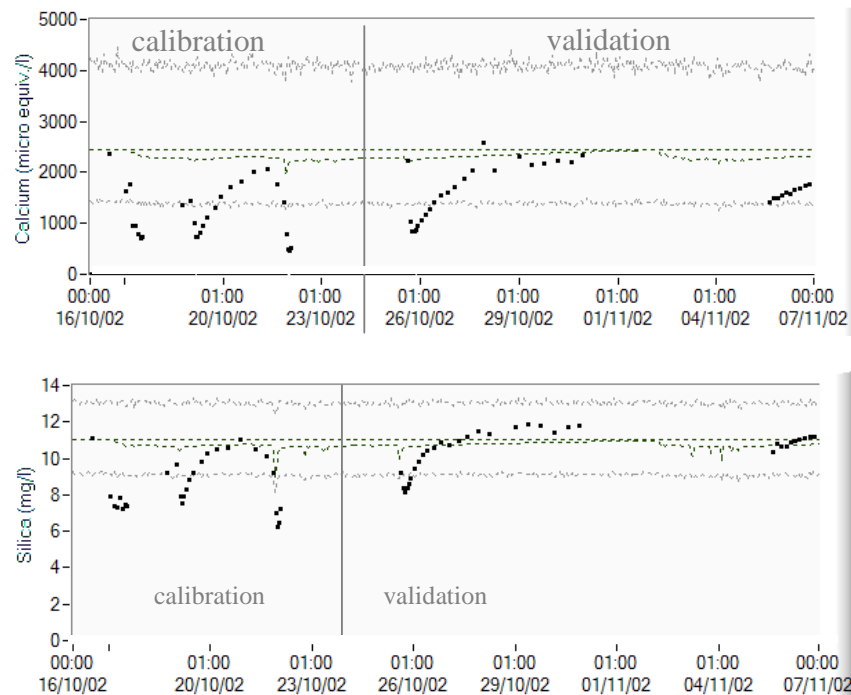


Figure 5-29 TOPMODEL and MCMC methodology: Observed calcium (dark points) -top, observed silica signal (dark points)-down, together with simulated parameter uncertainty bounds (inner bounds) and model uncertainty (outer bounds) at 90%; Esserts catchment

As for the Ruzillon catchment, the single response calibration led to a very good simulation of the discharge response, with a high predictive confidence demonstrated by the small uncertainty bounds. On the contrary, the two chemical signals are characterized by high uncertainty mainly due to the high model variances. The single-response calibration led again to high values of the $\ln TO$ transmissivity parameter, which results in discharge simulations formed essentially by the groundwater component. The dynamics of the chemical signal in the stream water is not correctly simulated. The posterior parameter distributions together with the statistical diagnostic plots and convergence tests are presented in Annex IX.

MULTI-RESPONSE CALIBRATION: In order to assess the importance of additional information on the TOPMODEL and its parameters uncertainty, a multi-response calibration was performed for Esserts catchment. The statistical likelihood function was the same as those used previous for Ruzillon catchment and the prior distributions the same as mentioned in Table 5-6. Figure 5-30 presents the results of such multi calibration for the discharge data. No important differences compared with the single calibration case are to be noticed. The simulated discharge is characterized by very narrow uncertainty bounds and a high predictive power (see the validation period).

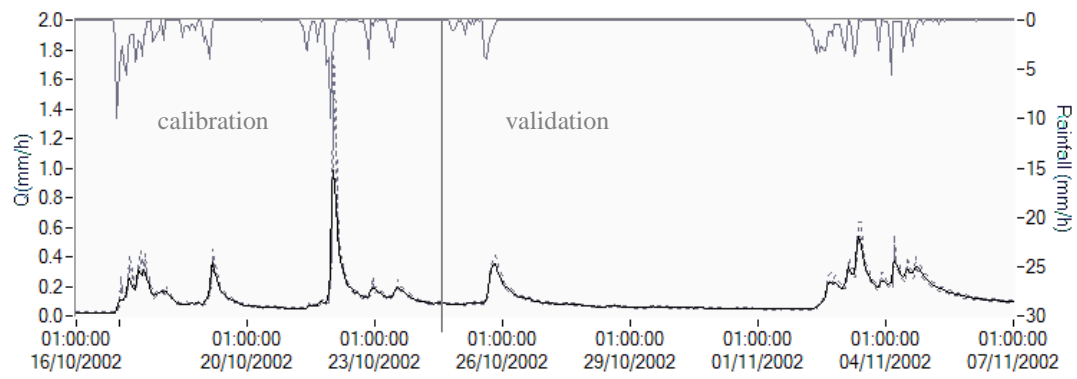


Figure 5-30 TOPMODEL and MCMC methodology: observed discharge (grey line) and uncertainty bounds (grey dotted lines) at 90%; Esserts catchment

Figure 5-31 show the results of the multi-response calibration methodology for the two chemical signals: calcium and silica concentration in the stream water. The total simulated uncertainty is considerably reduced and the simulated dynamics of the two signals is much more faithful to the observed one.

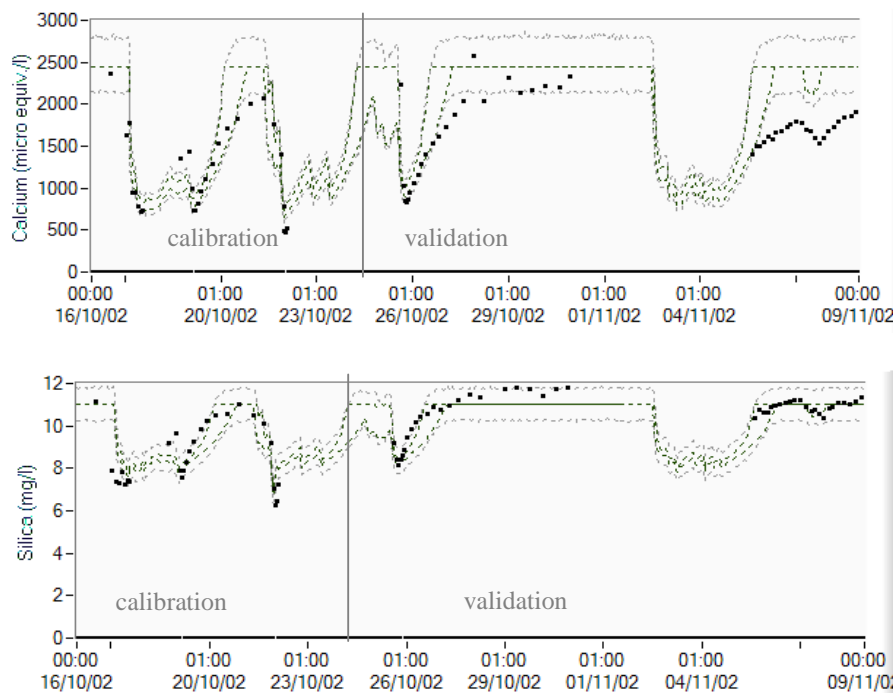


Figure 5-31 TOPMODEL and MCMC methodology: Observed calcium (dark points) -top, observed silica signal (dark points)-down, together with simulated parameter uncertainty bounds (inner bounds) and model uncertainty (outer bounds) at 90%; Esserts catchment

For both case studies (Ruzillon and Esserts) the total uncertainty during flood events is due essentially to the parameter uncertainty while during low flow periods this is mainly due to the model variance. A sensitivity study that was done on the hydrological model

parameters evidenced that the model performance was very sensitive to the choice of the hydrological parameters and among these, the most important were those parameters related to the partition between the soil and the groundwater compartments. A very small variation of these parameters led to different model performances in terms of reproduction of the observed calcium and silica data.

		Responses used in calibration							
		Single response				Multi Response			
		Mode	Average	SD	CV	Mode	Average	SD	CV
Hydrological parameters	M (m)	0.022	0.0264	0.0065	0.24	0.011	0.01	0.0005	0.04
	LnT0(m2/h)	4.77	5.90	1.66	0.28	4.84	4.84	0.09	0.02
	n (m3/m3)	0.5	0.3	0.078	0.50	0.06	0.07	0.004	0.06
	Zup (m)	0.55	0.55	0.24	0.44	0.9	0.9	0.014	0.02
	Ztot (m)	3.77	3.08	1.09	0.35	1.02	1.02	0.02	0.02
Statistical parameters	Variance - Q	0.0036	0.004	0.0004	0.10	0.0043	0.0043	0.00047	0.11
	Variance - Ca	0.13	0.17	0.048	0.28	0.0087	0.011	0.0035	0.31
	Variance - Si	0.016	0.02	0.006	0.31	0.0025	0.003	0.0009	0.28
	AR	0.99	0.99	0.006	0.006	0.99	0.99	0.0045	0.0045

Table 5-8 TOPMODEL and MCMC methodology: Single and multi-calibration approaches: posterior parameter distributions (for the case with log-transform data and AR(1) for the discharge residuals modelling); Esserts catchment

Table 5-8 shows comparatively the hydrological and statistical parameters posterior distributions. Among the hydrological parameters two categories are to be distinguished. The first one includes the parameters that define the saturated zone (exponential decreasing of the saturated transmissivity with the depth, and the saturated transmissivity at the ground surface). Multi-response calibration helps better identifying these parameters but generally does not dramatically improve their posterior distributions in terms of dispersion. The second category includes the parameters that define the separation between soil and groundwater reservoirs (drainable porosity, upper and total soil depths). For this kind of parameters, the multi-response calibration reduces significantly their uncertainty and contributes greatly to the reduction of the total simulated uncertainty. Single and multi-responses calibrations evidence two particular behaviours: the discharge model variance remains unchanged or increases slightly after introducing additional information. The calcium and silica model variances are considerably reduced after performing the multi-response calibration approach. This demonstrates once again the trade-off behaviour of the multi-calibration approach.

Introducing tracing information in conceptual rainfall-runoff models: comments

The Monte Carlo Markov Chains multi-response calibrating methodology was applied for Ruzillon and Esserts sub-catchments of the Haute-Mentue basin. This case study tested the ability of a modified version of TOPMODEL to reproduce the chemical signal of the stream flow during different flood events that occurred during the second half of October 2002.

The main conclusions that apply for this three responses calibrating methodology are the same as for the two responses calibrating methodology. Briefly, introduction of additional chemical information during the calibration approach led to:

- i. reduced hydrological and statistical parameter uncertainty bounds; As expected, among the hydrological parameters, the best identified parameters were those defining the soil and groundwater reservoirs. The same parameters were found to explain most part of the total parameter uncertainty.
- ii. almost no increase or slight increase of the model uncertainty of the discharge response due to an increased corresponding model variance;
- iii. significant decrease of the model uncertainty of the two considered chemical species (calcium and silica stream flow concentrations) due to a decrease of the corresponding simulated models' variances;

Parallel monitoring of the sum of the squared residuals for the three considered responses indicated that a particular behaviour has occurred during the Metropolis searching algorithm. This behaviour could be visualized in Figure 5-32 left and suggests the movement of the “feasible space” in a way reminding the movement of a Pareto front in multi-objectives calibration, towards regions where the minimum of the three considered responses are located. Once arrived in these regions (after the removal of the “burn-in” period), the trade-off behaviour, between the three considered responses, prevails and each of the solution points located in this 3D front represents a compromise between the global optimum of the three considered responses (Figure 5-32 right).

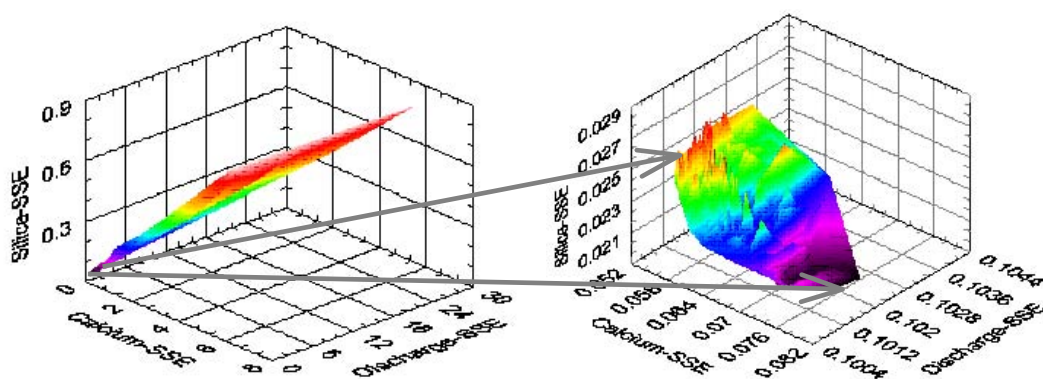


Figure 5-32 Trade-off behaviour during the Metropolis algorithm before removing the burning-in period (left) and after (right)

Ruzillon catchment	Single-response calibration			Multi-response calibration		
	Discharge	Calcium	Silica	Discharge	Calcium	Silica
Calibration	0.7	-0.8	0.8 ?	0.6	0.97	0.98
Validation	0.94	-1.65	0.8	0.93	0.96	0.97

Esserts catchment	Single-response calibration			Multi-response calibration		
	Discharge	Calcium	Silica	Discharge	Calcium	Silica
Calibration	0.8	-0.30	0.87	0.65	0.93	0.98
Validation	0.97	0.67	0.99	0.97	0.86	0.99

Table 5-9 Nash-Sutcliffe model efficiencies for the three responses for the single and multi-response calibrating methodologies

Table 5-9 indicate the model efficiencies for the three considered responses, in term of Nash-Sutcliffe criterion for the two analysed catchments during both calibration and validation periods. Analysis of the model performances show that beside the acceptable predictive performance of the simulated discharge, multi-response calibration also enabled an acceptable predictive performance of the two other responses: discharge concentrations of calcium and silica.

5.4 Conclusions

Application of the single and the Bayesian multi-calibrating methodologies led to the following general conclusions:

- despite the reproaches that could be addressed to the simplistic way in which the scale issues have been treated, this work showed that Bayesian methods (GLUE and MCMC) enabled to take into account TOPMODEL internal variables (such as soil storage saturation deficit) which contributed to reduce both parameter uncertainty and soil storage saturation simulated output uncertainty.
- while for the GLUE methodology, the total modelling uncertainty is mainly represented as parameters uncertainty, for MCMC methodology, the uncertainty due to the parameters is very small compared with the uncertainty due to the statistical model variance parameters.
- the use of the internal variable in the Bayesian calibration process has led to a trade-off behaviour concerning the total uncertainty of the two simulated responses: the uncertainty of the soil storage saturation response as well as those of the silica and calcium streamwater concentrations diminished at the expense of the increasing of the uncertainty of the discharge simulated response.
- the use of additional information (such as geo-chemical runoff concentrations) and the use of a complete statistical likelihood function allowed good reproduction of the chemical signal of the runoff for both calcium and silica tracers.

The multi-response calibrating methodology showed that internal variable and other available additional information could contribute to better identify the posterior distributions of the hydrological and statistical model parameters without major deterioration of the simulated discharge and its total uncertainty.

5.5 References

- Abbot, M. B., J. C. Bathurst, J. A. Cunge, P. E. O'Connell and J. Rasmussen (1986). "An introduction to the European Hydrological System-Système Hydrologiques Européen, "SHE", 1. History and philosophy of a physically based modelling system; 2. Structure of a physically based distributed modelling system." *Journal of Hydrology* 87: 45-77.
- Andersson, L. and B. Arheimer (1998). "Modelling nitrogen transport and retention in the catchments of Southern Sweden." *Ambio* 27(6): 471-480.
- Arheimer, B. and J. Olsson (2003). "Integration and Coupling of Hydrological Models with Water Quality Models: Applications in Europe", World Meteorological Organization.
- Arnold, J. G., R. Srinivasan, R. S. Muttiah and J. R. Williams (1998). "Large area hydrologic modelling and assessment. Part 1: Model development." *Journal of American Water Resources Association* 34: 73-89.
- Beven, K. and J. Feyen (2002). "The future of distributed modelling, Special Issue." *Hydrological Processes* 16: 169-172.
- Beven, K. and J. Freer (2001). "Equifinality, data assimilation, and uncertainty estimation in mechanistic modelling of complex environmental systems using the GLUE methodology." *Journal of Hydrology* 249: 11-29.
- Blazkova, S., K. J. Beven and A. Kulasova (2002). "On constraining TOPMODEL hydrograph simulations using partial saturated area information." *Hydrological Processes* 16(2): 441-458.
- Boyer, E. W., G. M. Hornberger, K. E. Bencala and D. McKnight (1996). "Overview of a simple model describing variation of dissolved organic carbon in an upland catchment." *Ecological Modelling* 86(2-3): 183-188.
- Cosby, B. J., G. M. Hornberger, J. N. Galloway and R. F. Wright (1985). "Modelling the effects of acid deposition: assessment of a lumped-parameter model of soil water and streamwater chemistry." *Water Resources Research* 21: 51-63.
- Duan, Q., S. Sorooshian and V. K. Gupta (1992). "Effective and efficient global optimization for conceptual rainfall-runoff models." *Water Resources Research* 28(4): 1015-1031.
- Duan, Q., S. Sorooshian and V. K. Gupta (1994). "Optimal use of the SCE-UA global optimization method for calibrating watershed models." *Journal of Hydrology* 158: 265-284.

- Engeland, K. (2002). *"Parameter estimation in Regional hydrological models"*. Geophysics Departement. Oslo, University of Oslo.
- Franks, S., P. Gineste, K. Beven and P. Merot (1998). *"On constraining the predictions of a distributed model: the incorporation of fuzzy estimates of saturated areas into the calibration process."* Water Resources Research 34(4): 787-797.
- Geweke, J. (1992). *"Evaluating the accuracy of sampling - based approaches to calculating posterior moments (with discussion)"*. Bayesian statistics 4. A. F. M. Smith. Oxford, Clarendon Press: 169-193.
- Higy, C. (2000). *"Modélisations conceptuelles et à base physique des processus hydrologiques: Application au bassin versant de la Haute-Mentue"*. Génie Rural. Lausanne, EPFL.
- Hooper, R. P., A. Stone, N. Christophersen, E. d. Grosbois and H. M. Seip (1988). *"Assessing the Birkenes model of stream acidification using a multisignal calibration methodology."* Water Resources Research 24(8): 1308-1316.
- Joerin, C., K. J. Beven, I. Iorgulescu and A. Musy (2002). *"Uncertainty in hydrograph separations based on geochemical mixing models."* Journal of Hydrology 255(1-4): 90-106.
- Kuczera, G. (1983). *"Improved Parameter Inference in Catchment Models .2. Combining Different Kinds of Hydrologic Data and Testing Their Compatibility."* Water Resources Research 19(5): 1163-1172.
- Kuczera, G. and M. Mroczkowski (1998). *"Assessment of hydrologic parameter uncertainty and the worth of multiresponse data."* Water Resources Research 34(6): 1481-1489.
- Lamb, R., K. Beven and S. Myrabo (1998). *"Use of spatially distributed water table observations to constrain uncertainty in a rainfall-runoff model."* Advances in Water Ressources 22(4): 305-317.
- Madsen, H. (2000). *"Automatic calibration of a conceptual rainfall-runoff model using multiple objectives."* Journal of Hydrology 235: 276-288.
- Madsen, H. and T. Jacobsen (2001). *"Automatic calibration of the MIKE-SHE integrated hydrological modelling system"*. 4th DHI Software Conference, Helsingor, Denmark.
- Mroczkowski, M., G. P. Raper and G. Kuczera (1997). *"The quest for more powerful validation of conceptual catchment models."* Water Resources Research 33(10): 2325-2335.
- Robson, A., K. Beven and C. Neal (1992). *"Towards identifying sources of subsurface flow: a comparison of components identified by a physically based runoff model and those determined by chemical mixing techniques."* Hydrological Processes 6: 199-214.
- Scanlon, T. M., J. P. Raffensperger and G. M. Hornberger (2001). *"Modeling transport of dissolved silica in a forested headwater catchment: Implications for defining the hydrochemical response of observed flow pathways."* Water Resources Research 37(4): 1071-1082.
- Scanlon, T. M., J. P. Raffensperger, G. M. Hornberger and R. B. Clapp (2000). *"Shallow subsurface storm flow in a forested headwater catchment: Observations and modeling using a modified TOPMODEL."* Water Resources Research 36(9): 2575-2586.

- Seibert, J., K. H. Bishop and L. Nyberg (1997). "*A test of TOPMODEL's ability to predict spatially distributed groundwater levels.*" *Hydrological Processes* 11(9): 1131-1144.
- Seibert, J. and J. McDonnell (2002). "*On the dialog between experimentalist and modeler in catchment hydrology: Use of soft data for multicriteria model validation.*" *Water Resources Research* 38(11): 1241.
- Talamba, D. (1999). "*Study of the hydrological processes by a comparative approach at the catchment scale: Application to the Haute-Mentue catchment*". Lausanne, EPFL.
- Uhlenbrook, S. and C. Leibundgut (2000). "*Development and validation of a process oriented catchment model based on dominating runoff generation processes.*" *Phys.Chem.Earth(B)* 25(7-8): 653-657.
- Weiler, M., B. L. McGlynn, K. J. McGuire and J. McDonnell (2003). "*How does rainfall become runoff? A combined tracer and runoff transfer function approach.*" *Water Resources Research* 39(11).

6. Conclusions and Perspectives

Conclusions – main achievements of this research

□ “Catchment hydrology at a cross – roads”?

The present work is related to the recent research topics in hydrology devoted to the integration of additional information into the hydrological modelling. Seibert and McDonnell (2002) stated that complex descriptions of the age, origin and pathway of subsurface storm flow abound in the literature but most of the catchment modelling studies do not fully use this information for model development, calibration and testing. As a consequence, process hydrological studies of dominant runoff producing processes and model studies of runoff generation are often poorly linked.

□ The experimental approach revisited

The first part of the present research has been devoted to the experimental work on the upper part of the Haute-Mentue catchment. Two different techniques (environmental tracing and TDR soil moisture monitoring) have been applied whose association proved profitable to retrieve the main processes and mechanisms responsible for the flood runoff generation.

- *Environmental tracing*: when the hypothesis don't change the conclusions do the same (confirmation of past researches results)

The long previous field experience allowed the environmental tracing to become a routine application on the Haute-Mentue catchment. It was also previously demonstrated that on this catchment, *silica* and *calcium* are appropriate tracers for hydrograph separation, as they allow clearly distinguishing between rain water, soil water and groundwater components of the floods. Two intensive field campaigns have been conducted in year 2002 in order to apply environmental tracing in four Haute-Mentue sub-catchments. The results that have been obtained confirm those obtained previously by Iorgulescu (1997) and Joerin (2000). In wet antecedent conditions, an increased contribution of the soil water was noticed for all the catchments except Corbassière while in dry conditions, in all catchments except Bois-Vuacoz and Ruzillon, the groundwater was the most important contributor to the flood. During strong storm events, the four catchments reacted similarly,

the runoff being formed essentially by rainwater and groundwater. The two main lithological formations (moraine and molasse) and the resulting soil textural characteristics explain the main differences that have been observed for the Haute-Mentue sub-catchments.

- *Soil moisture monitoring*: a necessary step towards identifying runoff mechanisms

The environmental tracing, as a catchment scale technique, allowed identification of the main water pathways during the runoff events. Despite this precious information, the environmental tracing does not allow identification of the hydrological mechanisms involved in runoff generation. Hence, the necessity of the association with other experimental approaches is obvious. In this work, implementation, on two experimental sites (with two different geological and pedological conditions) of a multiple TDR device allowed continuous monitoring of the soil moisture at different depths across the contributive part of the hillslopes. Different behaviours have been noticed upon we refer to the “morainic” or “molassic” experimental sites. The particularities of the wetting front depend on the antecedent humidity conditions and on the rainfall characteristics (duration and intensity). Vertical infiltration in superficial horizons was noticed for both sites under low rainfall intensities and in dry antecedent conditions. Soil saturation occurred for the superficial soil horizons under high rainfall intensities, in dry antecedent conditions; progressive groundwater rise was characteristic under low rainfall intensities but wet conditions while deep soil saturation for the “molassic” site and complete saturation of soil profile has been observed under high rainfall intensities and wet conditions for the “morainic” site.

- *Environmental tracing + soil moisture monitoring....*

Environmental tracing previous and present results together with the soil water monitoring results helped completing the knowledge concerning the conceptual model of two catchments: Ruzillon and Esserts. Briefly, dependent on the antecedent humidity conditions and on the rainfall characteristics the following cases have been identified:

- I. dry antecedent conditions and low rainfall intensities: vertical infiltration in superficial horizons prevails for both considered sites; the contributing areas are reduced and limited to the riparian zone; limited mixing of the old groundwater with the new rain water occur which finally explain why the groundwater component is the most important contributor to the streams;
- II. dry antecedent conditions and high rainfall intensities: soil saturation occurs in superficial soil horizons which makes possible rapid initiation of a preferential flow above soil textural discordances; rapid infiltration does not favour water contact with the soil matrix and explain why the rain water is one of the most important contributor to

the flood. As a consequence of the high rainfall intensities, groundwater ridging could occur and deliver pre-event water to the stream, which would explain why groundwater is the other component of the storm flood.

- III. Wet antecedent conditions and low rainfall intensities: The contributing area is larger; vertical infiltration has been noticed through a wet and well homogenized soil moisture profile which determine groundwater to rise slowly and hence favour a longer contact of the pre-event water with the soil matrix. The groundwater is mixed with the new rainwater causing dilution of the calcium and it enriches in silica becoming thus soil water and explaining the high-observed contribution of this component to the total flood runoff.
- IV. Wet antecedent conditions and high rainfall intensities: The contributing area reaches the greatest extent; for the morainic site, the soil profile is completely saturated and lateral flow downslope is activated; the soil water is the most important component of the floods as mixing of the already enriched in silica groundwater occur with the rainwater.

□ The modelling approach revisited: conceptual and physically based hydrological modelling, which one to choose?

After having gathered new information and having built the conceptual hydrological model of the Haute-Mentue catchment, one other important step of this work was the hydrological modelling of the same catchment. It was already stated that two modelling approaches have been privileged by previous researches: simple conceptual and complex physically based. Which one to choose in order to better represent the catchment hydrological response? It was stated that “recently there has been a tendency away from fully-distributed, physically-based models back to conceptual models due to concerns overparameterisation, parameter uncertainty and model output uncertainty” (Seibert and McDonnell (2002)). In our case, we first compared the results obtained by previous modelling researches on the Haute-Mentue catchment. It seemed that either conceptual (TOPMODEL) or physically based (SHETRAN) models have led to similar results for the Haute-Mentue catchment. Furthermore, one of the main conclusions concerning the physically based approach was the demanding management of the input database as well as the lack of control in explaining one result or another because of the many parameters and parameters interactions. From the practical point of view, we wanted to test a parametrisation methodology in order to integrate new field available information so the use of a simple but physically based model (TOPMODEL) was the choice of predilection.

□ LABVIEW – could be really a tool for the hydrologists?

Once the hydrological model has been chosen, in order to control it and to have the freedom of modifying and opening it to a new calibrating methodology, the necessity to

choose a programming environment was obvious. There are many available implementations of TOPMODEL from the original FORTRAN (Beven and Kirkby (1979)) to the newer MATLAB (Romanowicz (1997)) computer programs. Nevertheless we have chosen here to work with LABVIEW, a relatively recent graphical programming environment developed by National Instruments. Despite the fact that it was initially conceived for data acquisition from physics and electronic devices, present LABVIEW[®] versions have proven to be an easy to debug, powerful simulation tool, user friendly and enabling real-time control of the parameters during the model calibration process.

□ **Bayesian approach, a way to link field reality to modelling theory!**

The second objective of the present study was to develop a new parametrization methodology in order to integrate different sources of information into the process of calibration of the hydrological model. Here, we have chosen a stochastic Bayesian approach, as by definition, Bayesian statistics is the science of combining information. Bayesian methods are using a probability model to fit a set of data and to summarize the results. The use of Bayesian statistics helps combining previous views about parameters with new information, enabling the creation of adaptive models. In the context of the present research, the first step in implementing the Bayesian theory was to assign, based on existing knowledge, the prior distributions of the TOPMODEL parameters. The second step was to condition the prior parameters distributions to the available field observed data (discharges, soil storage saturation deficits, calcium and silica stream water concentrations) through the “likelihood function” and the third step was the updating of the TOPMODEL parameters posterior distribution after that the field data has been observed.

□ **Parameter estimation and uncertainty in hydrological modelling: GLUE (Generalized Likelihood Uncertainty Estimation) or MCMC (Monte Carlo Markov Chain)**

Two Bayesian techniques of estimating parameters have been privileged in this research not only because of their updating ability but also because they are able to quantify the uncertainty of the estimated parameters and of the model simulated outputs. The first technique includes the well-known GLUE method developed by Beven and Binley (1992) which uses a subjectively chosen generalized likelihood function to describe the simulation error and importance sampling algorithm as searching method. The second technique includes the more recently developed MCMC methods (Kuczera and Parent (1998)), which use a statistical likelihood function for the simulation error and the Gibbs within Metropolis algorithm as the searching method. Both techniques have been used in this work, in single and multi-response calibrating modes to estimate the parameters of two versions of TOPMODEL. The main conclusions concerning parameter estimation and parameter uncertainty with the two techniques are given below:

- in both single and multi response calibration modes, the GLUE methodology led to larger parameter and model output uncertainty; most of the total modelling uncertainty is thus explained by the model parameters uncertainty, the other sources of errors being ignored;

- the use of the statistical likelihood function in the MCMC approach led to the introduction in the calibration approach, beside the hydrological vector of parameters, of a sub-vector of statistical parameters (i.e. simulation error variances for discharge, soil storage saturation deficits, calcium and silica stream concentrations responses, autoregressive parameter for the discharge simulation error);
- in both single and multi-response calibration modes, the MCMC methodology led to smaller parameter uncertainty, the total modelling uncertainty being mainly explained by the model structure and less by the model parameters uncertainty.
- the use of the statistical likelihood function in MCMC techniques required that statistical assumptions (of normality, constant variance and time independence of the simulation errors) be respected. As departures from these assumptions have been noticed, a more complex statistical likelihood function has been tested that takes into account appropriate corrections (Box-Cox transformations and autoregressive modelling of the simulation error).
- Comparison between statistical likelihood function without and with corrections showed that the posterior distributions of the hydrological parameter change and that the predictive power of the model increases when corrections are accounted for.

One important observation has to be made concerning the two techniques. There are no major differences between GLUE and MCMC methods, both belonging to the class of statistical Monte Carlo Bayesian stochastic methods. Two steps could differentiate these methodologies: one is the choice of the searching algorithms and the second is the choice of the likelihood function.

□ Are internal variables useful in hydrological modelling?

The first application of the multi-calibrating Bayesian methodology that has been proposed in this work studied the role of the internal variable to constrain the total modelling uncertainty. The classical version of TOPMODEL has been used in this application to simulate the total runoff of a small head catchment on the Haute-Mentue basin during a humid period in 2002. As TOPMODEL simulates more fluxes than the total runoff at the catchment outlet, we tried in this work to apply a Bayesian multi calibrating methodology in order to include the soil storage saturation deficit into the calibration approach and to assess the role of this internal variable in the total modelling uncertainty. Field estimation of the soil storage saturation deficit has been available due to the implementation, on a representative site, of a TDR set-up to monitor the soil moisture variations at different depths. A simple hydrological similarity concept was two times used in order to (i) transpose the local estimated soil storage saturation deficit to the model grid scale and (ii) further to transpose the grid estimated soil storage deficit to the corresponding class of topographical index such as computed by TOPMODEL methodology.

The main results obtained in this work are presented below:

- for both GLUE and MCMC methods, the use of the soil storage saturation deficit internal variable has led to smaller parameters uncertainty than in the case when only the discharge has been used in the calibration;

- for GLUE methodology, despite the reduced parameters uncertainty, the uncertainty of the simulated discharge was a greater after introduction of the soil storage saturation deficit response; this behaviour was already noticed in literature and could be explained by the interactions between the model parameters.
- for both GLUE and MCMC methodologies, the uncertainty of the soil storage saturation deficit was considerably reduced with the multi-calibrating methodology.
- for the MCMC methodology, the total uncertainty of the simulated discharge was higher than in the single-response calibrating case; this is mainly explained by greater model variances due to greater discharge simulation errors.
- a compensation or “trade-off” behaviour has been noticed for both GLUE and MCMC methods: the total uncertainty of the simulated discharge was higher in the multi-response calibration case than obtained in the single-response calibration case while the total uncertainty of the soil storage saturation deficits considerably reduced.
- the GLUE methodology revealed some inquiries related to the subjective nature of its implementation procedure as the final conclusions are highly dependent on the choice of the so-called behavioural parameters.

❑ **Are simple conceptual hydrological models able to reproduce the stream water chemistry?**

The second application of the multi calibrating methodology tested the ability of a modified version of TOPMODEL to reproduce the chemical signal of the stream water. In the international context, the interest in the geochemical dimensions of the streamflow modelling increases, and thus conceptual hydrological modelling approaches that explicitly treat volume-based mixing and water (and ultimately tracer) mass balance become increasingly useful (Seibert and McDonnell (2002)).

Here a simple approach has been considered: to the existing parameters of the classical TOPMODEL version three more parameters were added in order to separate the subsurface flow into groundwater and soil water components. An EMMA approach has further been considered in order to compute silica and calcium concentrations of the simulated runoff. The model has been tested for two head sub-catchments of the Haute-Mentue basin in autumn 2002. Application of the multi-response Bayesian calibrating methodology with a full statistical likelihood function that took into account both type of statistical corrections (Box-Cox transformation and autoregressive modelling of the discharge simulation errors) has led to:

- i. reduced hydrological and statistical parameter uncertainty bounds; among the hydrological parameters, the best identified parameters were the new introduced ones defining the soil and groundwater reservoirs. The same parameters were found to explain most part of the total parameter uncertainty.
- ii. almost no increase or slightly increase of the model uncertainty of the discharge response due to an increased corresponding model variance;
- iii. significantly decrease of the model uncertainty of the two considered chemical species (calcium and silica stream flow concentrations) due to a decrease of the corresponding simulated models’ variances;

□ Was the gap between reality and theory bridged?

In the context of the international research and in line with those initiated at the HYDRAM Institute, this research aimed to contribute at reducing the gap between the field experimentalist and the modeler to the benefit of the hydrological science. One of the main achievements of this research is that field knowledge, through statistical Bayesian methods, could contribute to reduce the uncertainty of both estimated parameters and model output uncertainty.

The present research evidenced that introducing additional information into the calibration process has led to a compensation or trade-off behavior, which worsen the simulation efficiencies for the discharge response but increase the efficiency for the other responses. In parallel the uncertainty associated with the discharge response was increased following to the multi-response calibration approach while those of the new introduced responses was considerably reduced. This model behavior reminds one statement that has been made by Klemes (1986) some years ago. We consider that field knowledge makes a model maybe to be "less right, for the right reasons" but we also consider that this would be more suitable than a model being "right for the wrong reasons".

Nevertheless, the complete answer to this question is far from being found. What seems to be obvious is that in order to bridge the gap between hydrology field evidence and model problems, stronger collaboration will be needed between not only hydrologists (experimentalists and modelers) but also between them and other participants to the general applied scientific effort such as statisticians, geologists, geometers. We hope that in the future this collaboration will not only have bridged the gap between reality and theory but also will contribute to build models that should "*be right, for the right reasons*".

Perspectives

□ How to go on with the field experimental approach... and which would be the most effective way to spend money on measurements for constraining the uncertainties in distributed model predictions?

The present research followed to a long field experience that conducted to a better understanding of the hydrological behaviour of the Haute-Mentue catchment. Both global and local field techniques have been used and association of their results proved to be very profitable to the comprehension of the hydrological mechanisms responsible for the flood generation. Environmental tracing is a global technique that still could be profitable for modelling studies that are being done at the same scale. Local techniques despite the important information that might bring often require important efforts and materials and

often suffer of the lack of spatial representativity. The scale issue or how to take into account plot or point measurements when distributed models are working at larger grid scales? remains one of the main interest topic in hydrology. One intermediary solution for the small catchments that have been proposed in this study might be the identification through intensive mapping and use of all previous available information of uniform topo-geo-hydro-climatic “representative areas” towards which more field intensive and monitoring efforts be concentrated.

If most of the classical measurements are destructive, new insights concerning the mechanisms that govern the runoff generation would be possible through the rapid development of geophysical techniques, which, still despite their cost, their apparent heaviness and the need of specialists, represent an integrative non-intrusive method able to provide a 3D almost “ real-time” tomography of the stream-hillslope near subsurface environment. For the Haute-Mentue catchment, an answer in this direction will maybe be given in the near future by an on-going research at the Geophysical Institute of Lausanne in collaboration with Hydram Laboratory.

□ ... and with the hydrological modelling ?

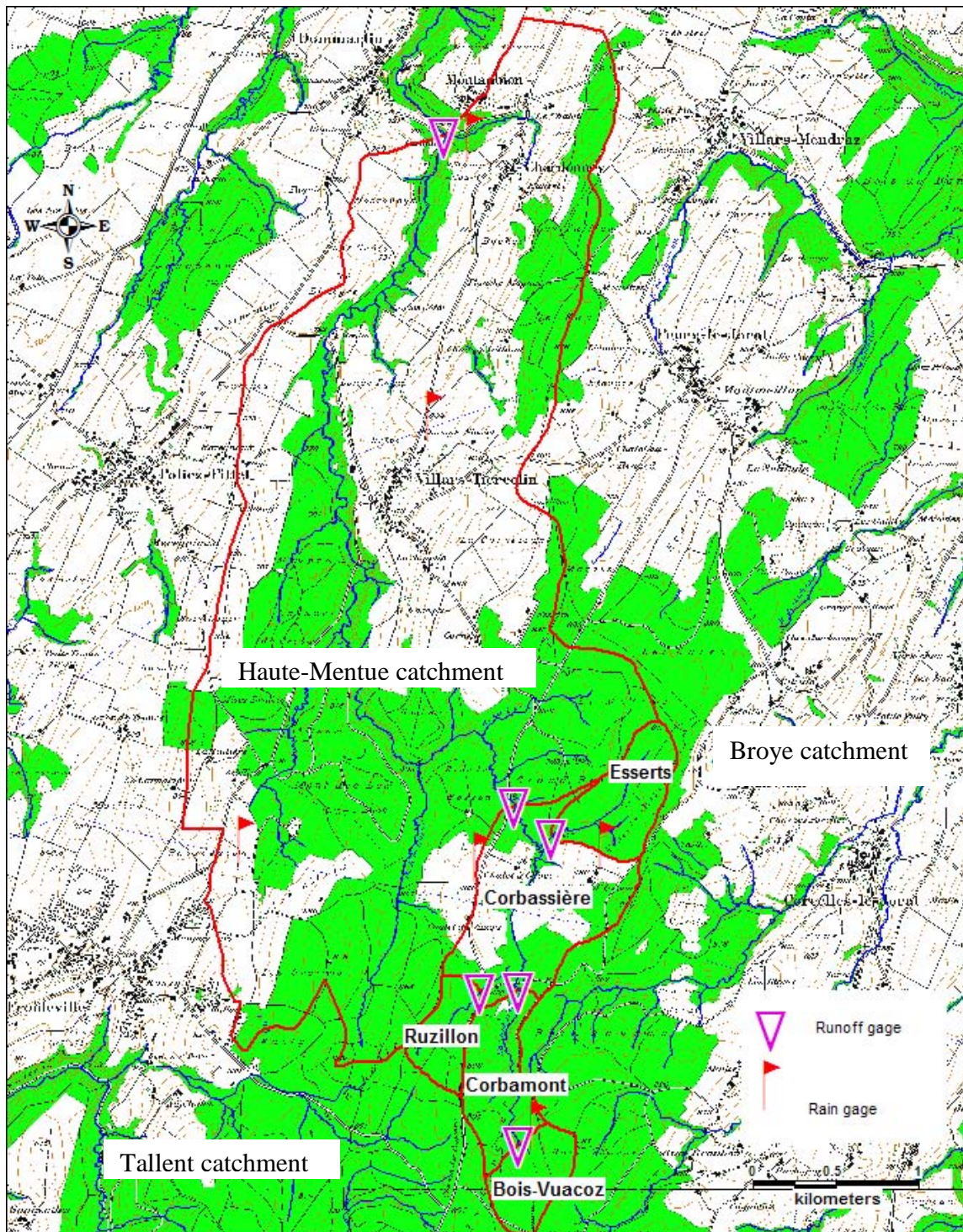
This research showed that the actual state of art of the hydrological modelling finds itself at a cross - roads. The high present qualitative understanding of the hydrological behaviour should form the starting point to the development of new process-oriented hydrological models that would take fully benefit of the field knowledge through Bayesian approaches. The scale issues should be accounted for in the hydrological modelling and in this context, the updating nature of the Bayesian methods could prove useful in the development of a joint multi-site parameter estimation technique using the Haute-Mentue nested catchment integrative measurements.

References

- Beven, K. and M. J. Kirkby (1979). "A physically based variable contributing area model of basin hydrology." *Hydrol.Sci.Bull.* 24(1): 43-69.
- Beven, K. J. and A. M. Binley (1992). "The future of distributed models- models calibration and uncertainty prediction." *Hydrological Processes* 6: 279-298.
- Iorgulescu, I. (1997). "Analyse du comportement hydrologique par une approche intégrée à l'échelle du bassin versant. Application au bassin versant de la Haute-Mentue." Thesis EPFL, No.1613. Lausanne.
- Joerin, C. (2000). "Etude des processus hydrologiques par l'application du traçage environnemental. Association à des mesures effectuées à l'échelle locale et analyse d'incertitude". Thesis EPFL, No.2165. Lausanne.
- Klemes, V. (1986). "Operational testing of hydrological simulation models." *Hydrological Sciences Journal-Journal Des Sciences Hydrologiques* 31: 13-24.

- Kuczera, G. and E. Parent (1998). "*Monte Carlo assessment of parameter uncertainty in conceptual catchment models: the Metropolis algorithm.*" *Journal of Hydrology* 211(1-4): 69-85.
- Romanowicz, R. (1997). "*A MATLAB implementation of TOPMODEL.*" *Hydrological Processes* 11(9): 1115-1129.
- Seibert, J. and J. McDonnell (2002). "*On the dialog between experimentalist and modeler in catchment hydrology: Use of soft data for multicriteria model validation.*" *Water Resources Research* 38(11): 1241.

ANNEXES

Haute-Mentue catchment topographical map and permanent equipment

Mineral Soils conditioned by Limited Age: Cambisols

From: “Lectures notes on the major soils of the world”

Edited by: Paul Driessen, Wageningen Agricultural University, International Institute for Aerospace Survey and Earth Sciences (ITC), Jozef Deckers, Catholic University of Leuven Otto Spaargaren, International Soil Reference and Information Centre Freddy Nachtergaele, FAO (<http://www.fao.org/DOCREP/003/Y1899E/y1899e00.htm#toc>)

The Reference Soil Group of the Cambisols holds soils with incipient soil formation. Beginning transformation of soil material is evident from weak, mostly brownish discolouration and/or structure formation below the surface horizon. Early soil classification systems referred to these 'brown soils' as 'Braunerde' (Germany), 'Sols bruns' (France), 'Brown soils'/'Brown Forest soils' (USA), or 'Brunizems' (Russia). FAO coined the name 'Cambisols'; USDA Soil Taxonomy classifies these soils as 'Inceptisols'.

Definition of Cambisols : Soils having

- a *cambic*[@] horizon; or
- a *mollic*[@] horizon overlying subsoil with low base saturation within 100 cm depth; or
- one of the following:
- an *andic*[@], *vertic*[@] or *vitric*[@] horizon starting between 25 and 100 cm below the surface; or
- a *plinthic*[@], *petroplinthic*[@] or *salic*[@] or *sulfuric*[@] horizon starting between 50 and 100 cm below the soil surface, in the absence of loamy sand or coarser material above these horizons.

Summary description of Cambisols

Connotation: soils with beginning horizon differentiation evident from changes in colour, structure or carbonate content; from L. *cambiare*, to change.

Parent material: medium and fine-textured materials derived from a wide range of rocks, mostly in colluvial, alluvial or aeolian deposits.

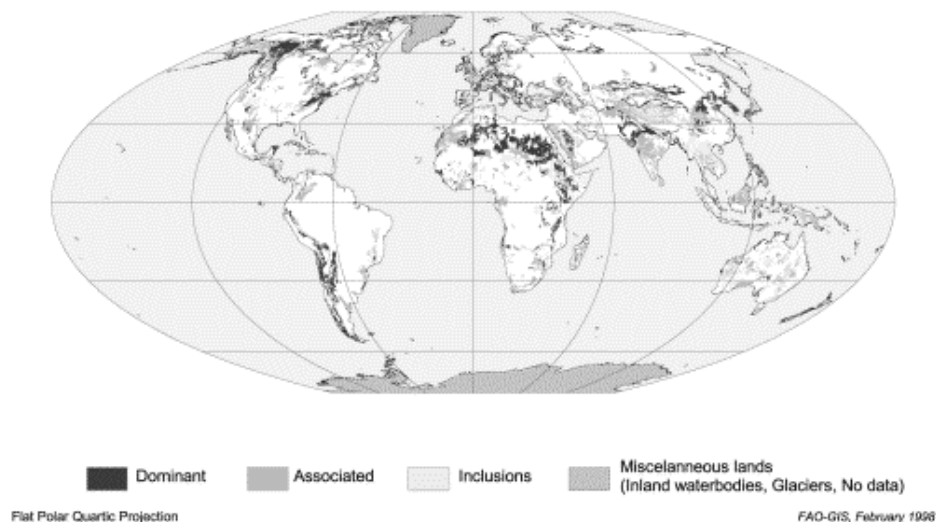
Profile development: ABC profiles. Cambisols are characterized by slight or moderate weathering of parent material and by absence of appreciable quantities of illuviated clay, organic matter, aluminium and/or iron compounds.

Environment: level to mountainous terrain in all climates and under a wide range of vegetation types.

Regional distribution of Cambisols

Cambisols cover an estimated 1.5 billion hectares worldwide. This Reference Soil Group is particularly well represented in temperate and boreal regions that were under the influence of glaciation during the Pleistocene, partly because the soil's parent material is still young but also because soil formation is comparatively slow in the cool, northern regions. Erosion and deposition cycles account for the widespread occurrence of Cambisols in mountain regions. Cambisols are less common in the tropics and subtropics. The (young) alluvial plains and terraces of the Ganges-Brahmaputra system are probably the largest continuous surface of Cambisols in the tropics. Cambisols are also common in areas with active geologic erosion where they may occur in association with mature tropical soils. Figure 1 shows the world-wide occurrence of Cambisols.

Figure 1 Cambisols world-wide



Use: a wide variety of agricultural uses; climate, topography, shallowness, stoniness, or low base status may pose restrictions on land use. In steep lands mainly used for grazing and/or forestry.

Associations with other Reference Soil Groups

Cambisols in cool regions are particularly common in alluvial, colluvial and aeolian deposits. Cambisols in wetlands are associated with *Gleysols* and *Fluvisols*.

Genesis of Cambisols

Most (not all) Cambisols are soils with beginning horizon differentiation; they are in a transitional stage of development, from a young soil to a mature soil with an argic, natric, spodic, or ferralic B-horizon. The first step in this development is the formation of a *cambic* subsurface horizon that is to be regarded as a 'minimum B-horizon'. Nonetheless, a cambic horizon can be quite stable, viz. where pedogenetic development is slow because of low temperatures, low precipitation, impeded drainage, highly calcareous or weathering-resistant parent materials, or where slow but continuous erosion is in equilibrium with weathering processes.

In practice, a cambic horizon is any section of a soil profile situated between an A-horizon and a relatively unaltered C-horizon, that has soil structure rather than rock structure and a colour that differs from that of the C-horizon.

Note that a cambic horizon can also occur in other Reference Soil Groups for which it is not a differentiating characteristic because other properties have higher priority. The fact that Cambisols key out late in the taxonomic hierarchy of Reference Soil Groups implies that this group includes many soils that just missed out on one or more requirements for other Reference Soil Groups.

Appreciable quantities of weatherable minerals and absence of any signs of *advanced* pedogenesis evidence the fact that Cambisols are in an early stage of soil formation. There are, however, signs of *incipient* weathering/transformation of primary minerals in a situation of free internal and external drainage. Hydrolysis of iron-containing minerals (biotite, olivine, pyroxenes, amphiboles, etc) in a weakly acid environment produces ferrous iron that is oxidized to ferric oxides and hydroxides (e.g. goethite, haematite). This '*free iron*' coats sand and silt particles, and cements clay, silt and sand to aggregates. The soil becomes structured and yellowish

brown to reddish in colour. Aluminium oxides and hydroxides, and silicate clays are formed in addition to ferric oxides. There may be some leaching of bases but no clear migration of Fe, Al, organic matter or clay. This oxidative weathering process is not limited to the cambic horizon; it occurs just as well in the A-horizon and may even be stronger there, but the dark colour of accumulated soil organic matter obscures its signs.

The processes that lead to formation of a cambic subsurface horizon are fundamentally the same in all climate zones but the intensities of chemical and biological transformations are considerably greater in the (humid) tropics than elsewhere. Cambisols in the humid tropics can form in a few years time. Those in cool and/or dry regions require more time, *inter alia* because soil formation is halted for shorter or longer periods.

Characteristics of Cambisols

Morphological characteristics

The 'typical' Cambisol profile has an ABC horizon sequence with an ochric, mollic or umbric A-horizon over a cambic B-horizon that has normally a yellowish-brown colour but that may also be an intense red. Cambisols in poorly drained terrain positions may show '*redoximorphic*' features. The soil texture is loamy to clayey. Signs of beginning clay illuviation may be detectable in the cambic horizon but the clay content is normally (still) highest in the A-horizon.

Mineralogical, physical and chemical characteristics

It is not well possible to sum up all mineralogical, physical and chemical characteristics of Cambisols in one generalised account because Cambisols occur in such widely differing environments. However:

- most Cambisols *contain at least some weatherable minerals* in the silt and sand fractions.
- most Cambisols *occur in regions with a precipitation surplus* but in *terrain positions that permit surficial discharge of excess water*.
- most Cambisols *are medium-textured* and have a *good structural stability, a high porosity, a good water holding capacity and good internal drainage*.
- most Cambisols have a *neutral to weakly acid soil reaction*, a satisfactory chemical fertility and an active soil fauna.

Note that there are numerous exceptions to the above generalisations!

Management and use of Cambisols

By and large, Cambisols make good agricultural land and are intensively used. The Eutric Cambisols of the Temperate Zone are among the most productive soils on earth. The Dystric Cambisols, though less fertile, are used for (mixed) arable farming and as grazing land. Cambisols on steep slopes are best kept under forest; this is particularly true for Cambisols in highlands.

Vertic and Calcaric Cambisols in (irrigated) alluvial plains in the dry zone are intensively used for production of food and oil crops. Eutric, Calcaric and Chromic Cambisols in undulating or hilly (mainly colluvial) terrain are planted to a variety of annual and perennial crops or are used as grazing land.

Dystric and Ferralic Cambisols in the humid tropics are poor in nutrients but still richer than associated Acrisols or Ferralsols and they have a greater cation exchange capacity. Many Gleyic Cambisols in alluvial plains make productive 'paddy soils'.

Haute-Mentue catchment

- ⇒ Preferential flow at the soil-bedrock interface (Esserts catchments- Figures 1, 2; Corbassière catchment – Figure 3; Ruzillon catchment- Figure 4)
- ⇒ Overland flow (Bois-Vuacoz catchment – Figure 5)
- ⇒ Baseflow (Corbamont catchment – Figure 6)



Figure 1



Figure 2



Figure 3



Figure 4

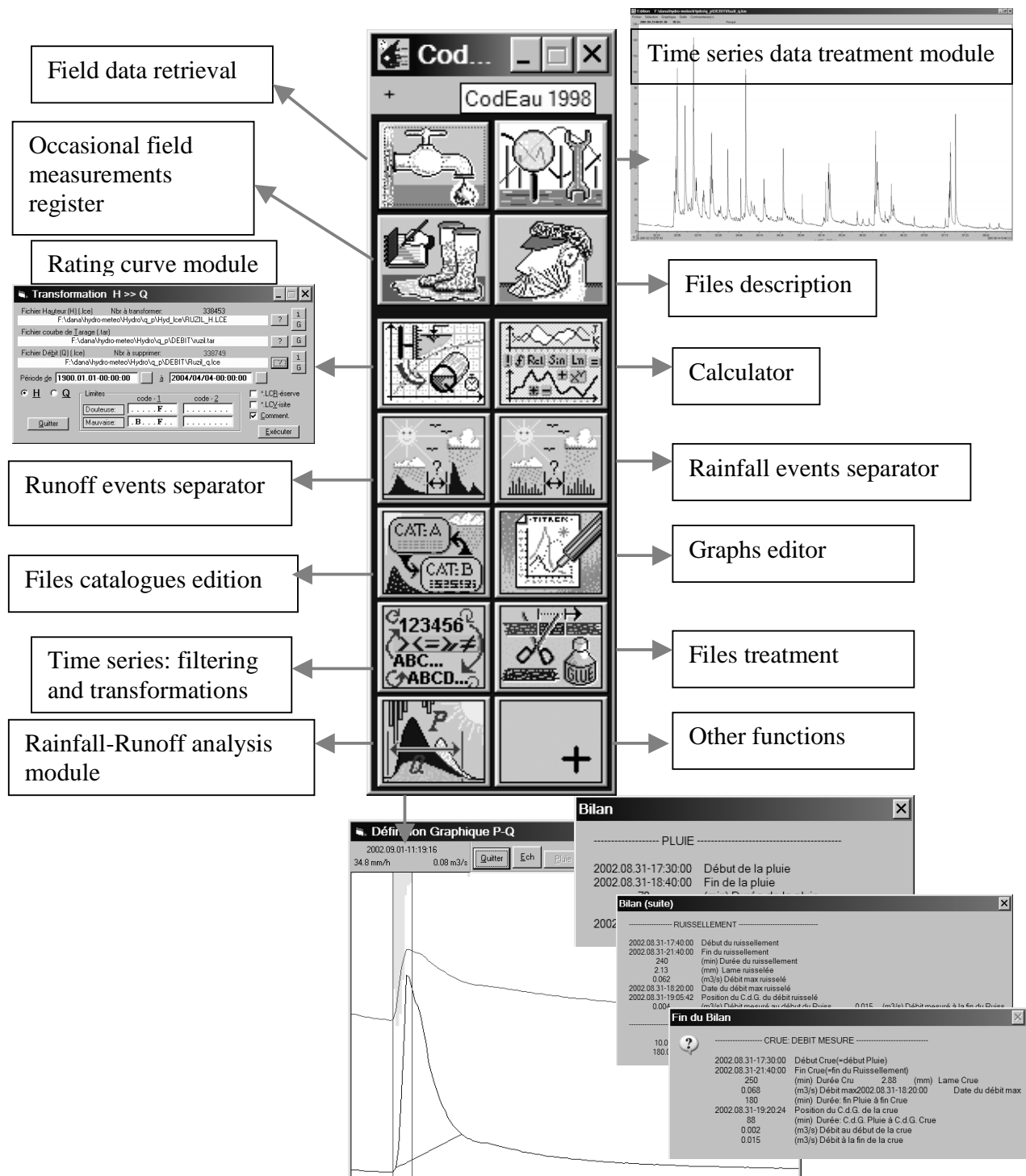


Figure 5



Figure 6

CODEAU – Hydrological data treatment computer program



LABVIEW implementation of TOPMODEL

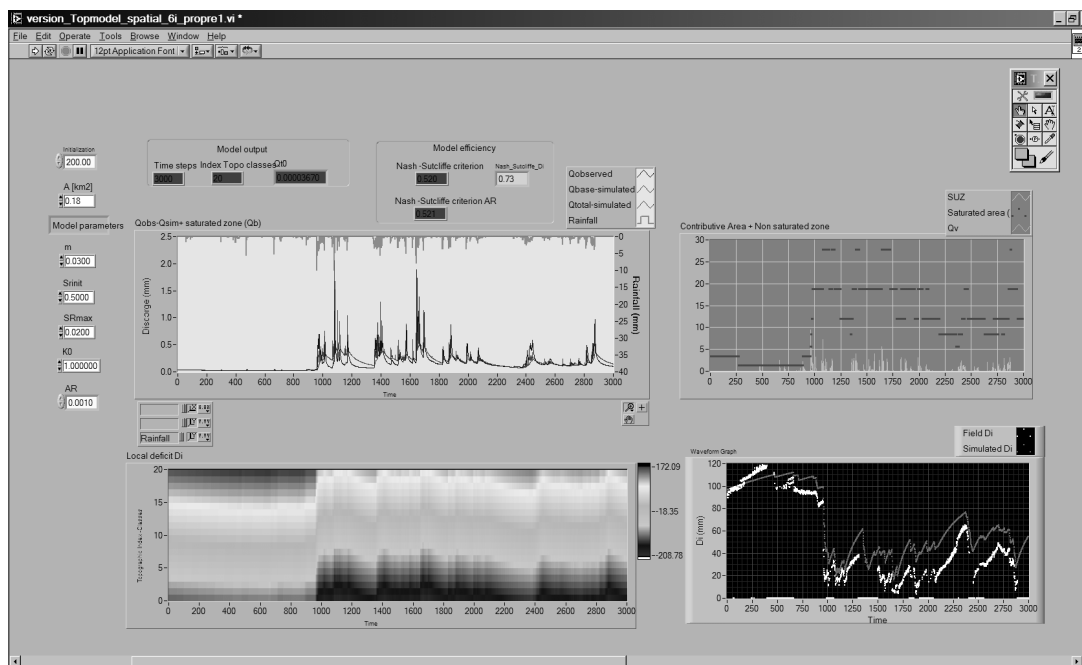


Figure 1 LABVIEW front panel and TOPMODEL user interface

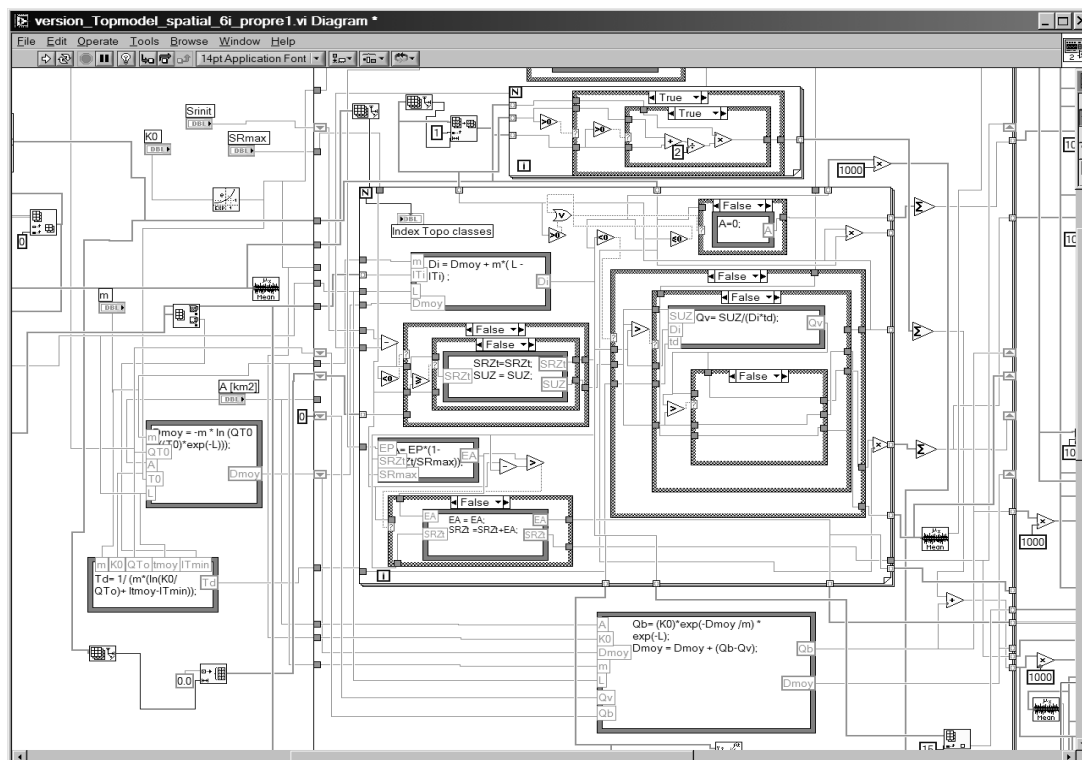


Figure 2 LABVIEW wiring diagram

LABVIEW implementation of GLUE

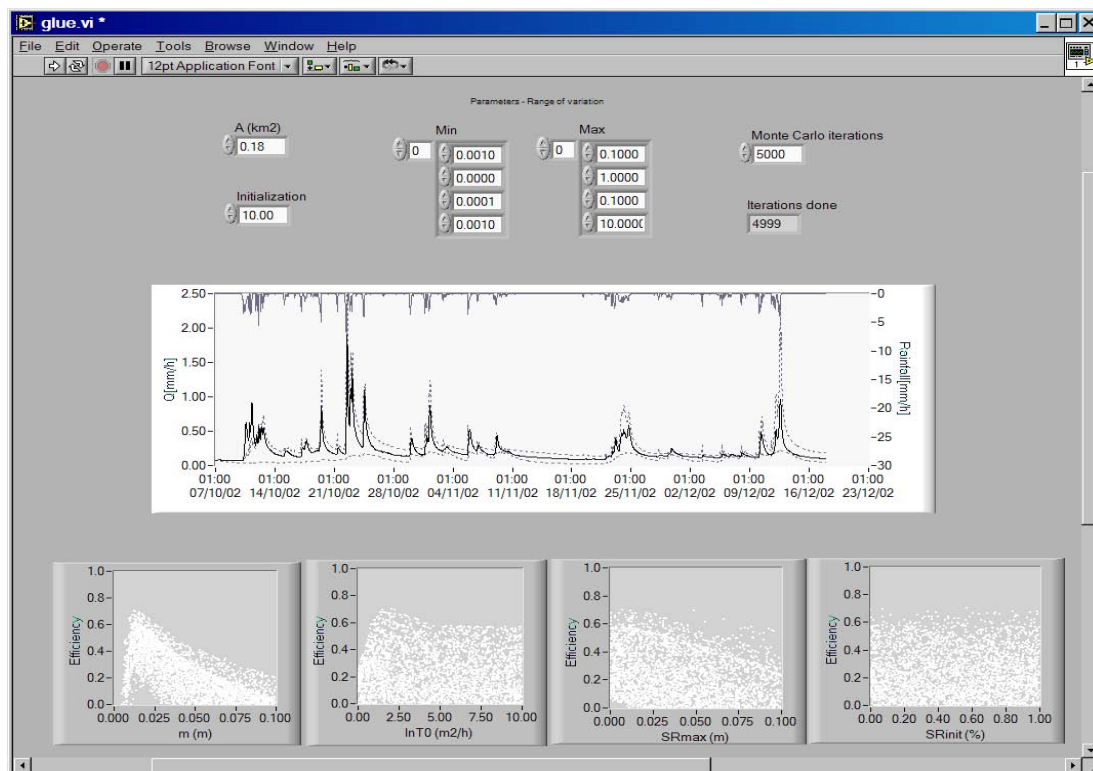


Figure 1 LABVIEW front panel and GLUE user interface

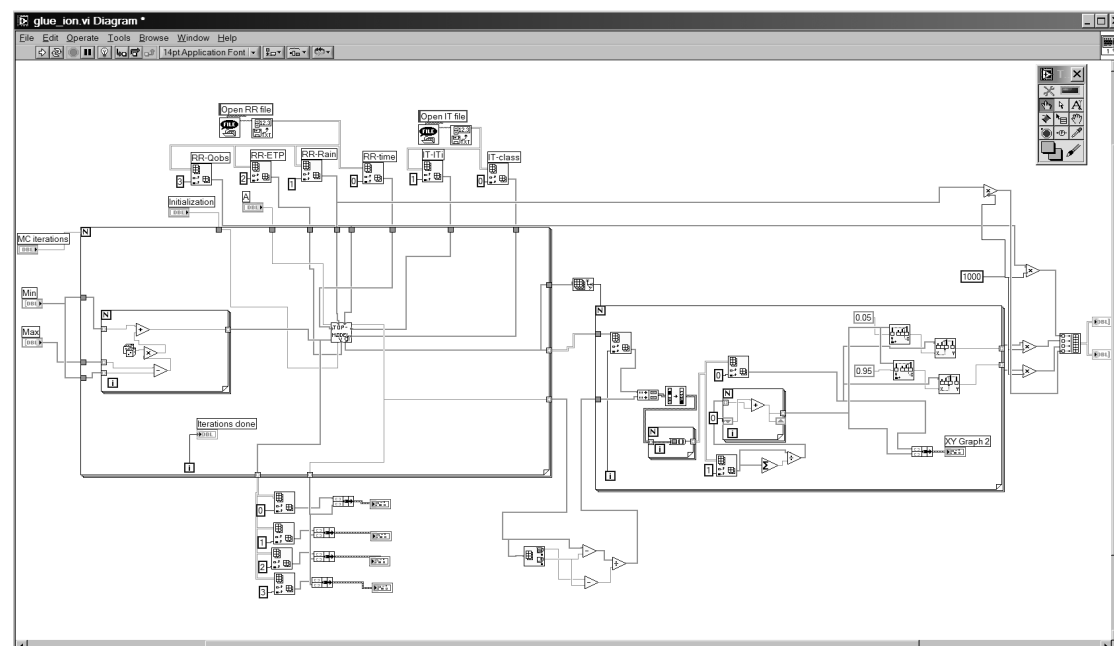


Figure 2 LABVIEW wiring diagram

LABVIEW implementation of MCMC methodology

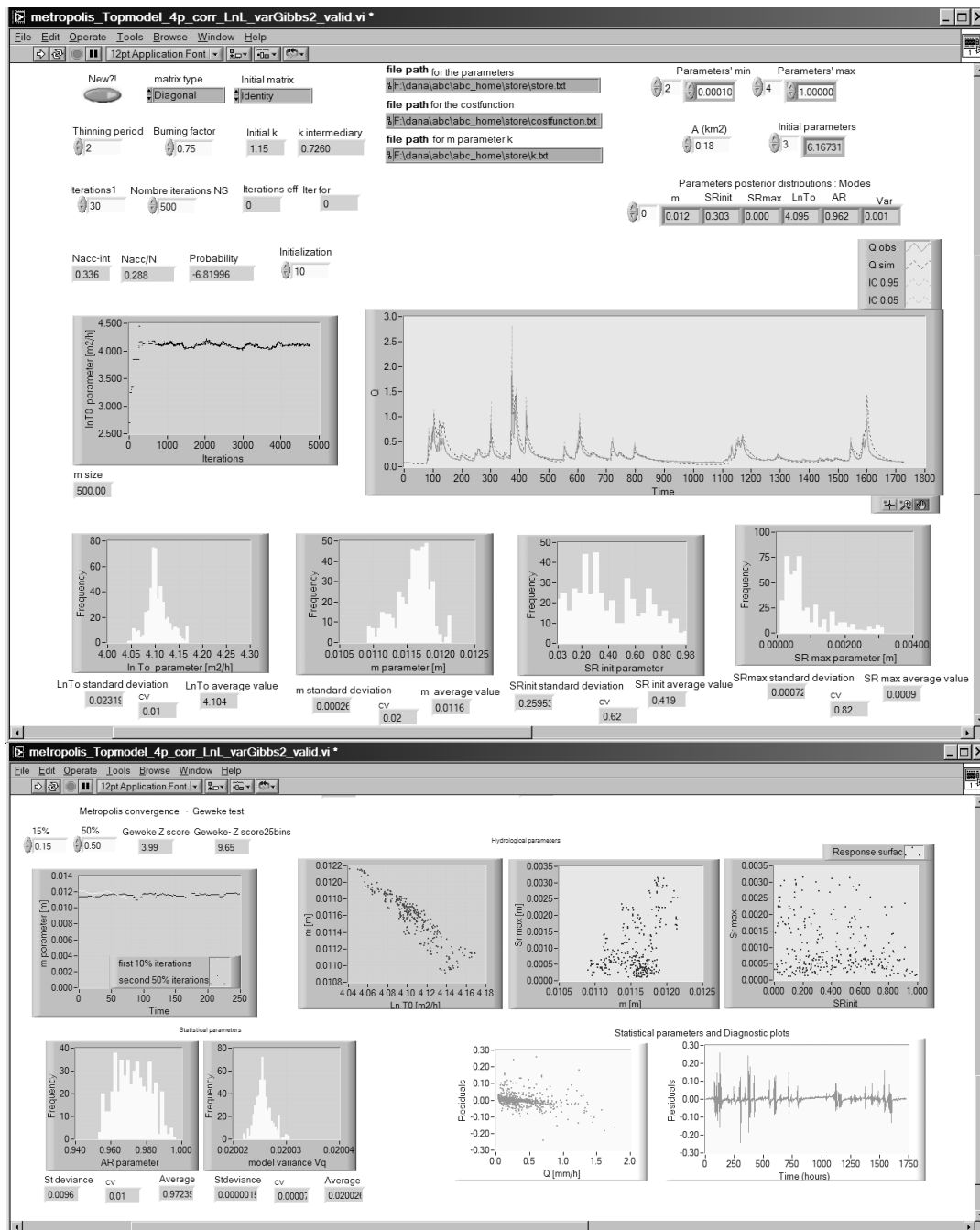


Figure 1 LABVIEW front panel and MCMC user interface

LABVIEW implementation of GLUE multi-response calibrating methodology

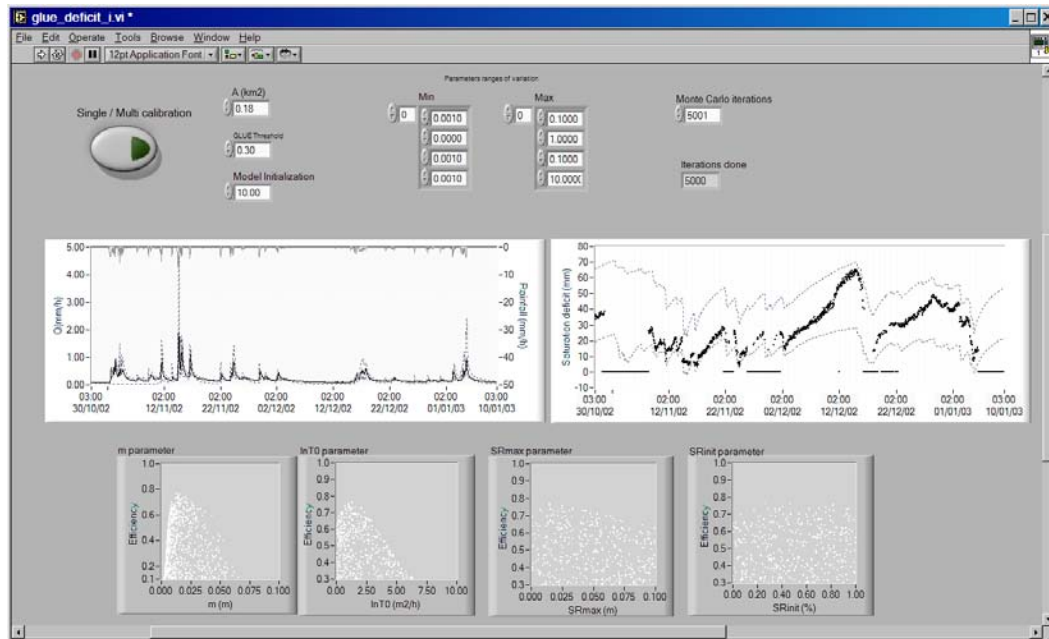


Figure 1 LABVIEW front panel and GLUE user interface

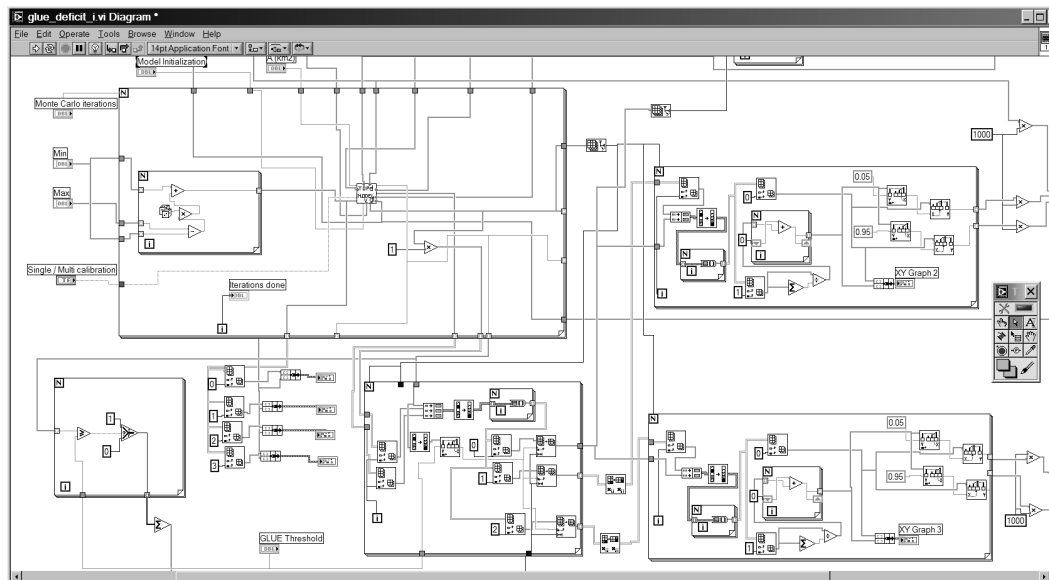
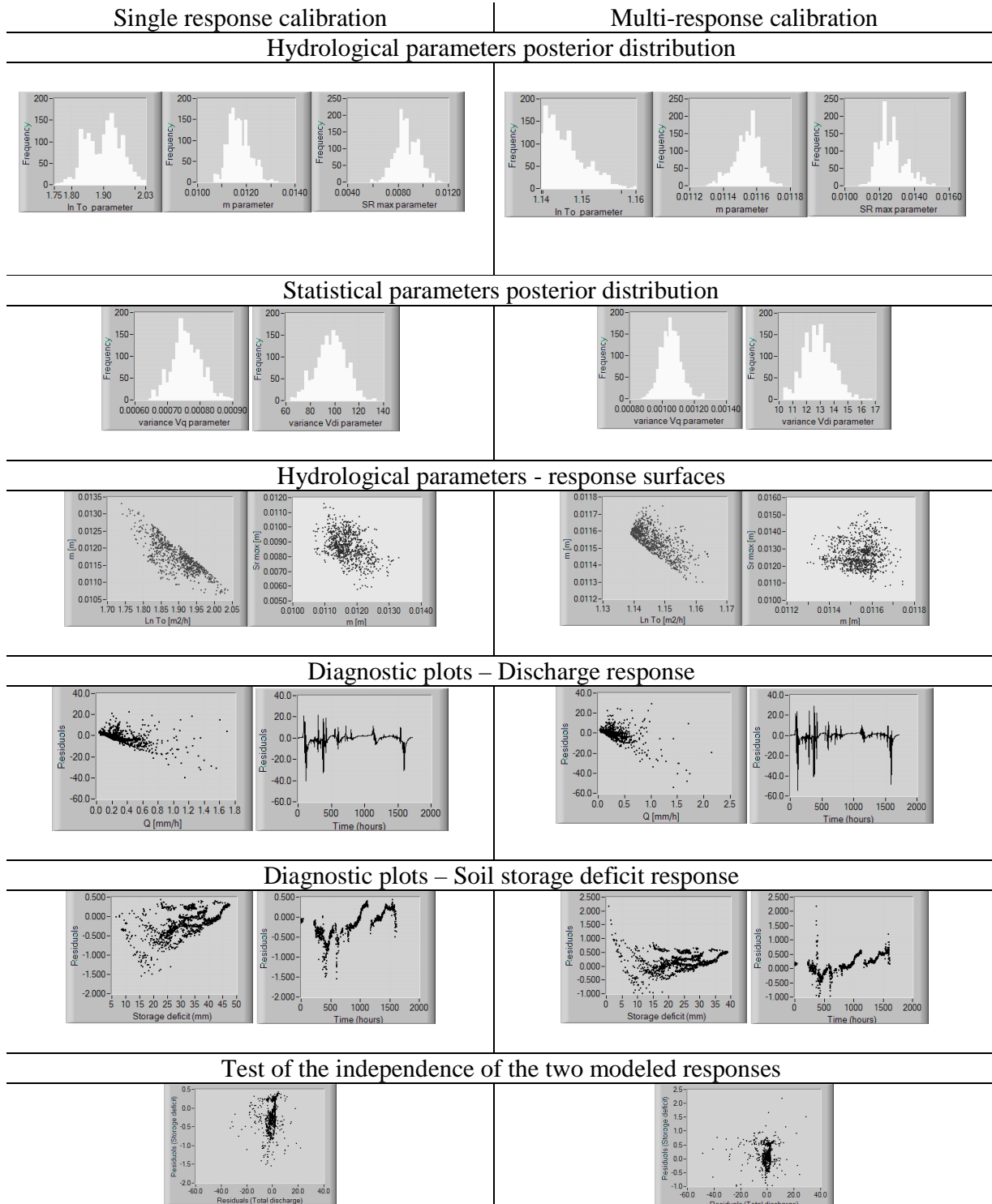


Figure 2 LABVIEW wire diagram

MCMC methodology with L1 likelihood function (without statistical corrections)

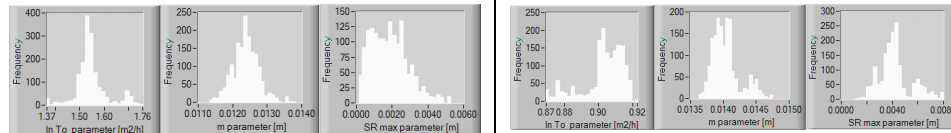


MCMC methodology with L2 likelihood function (without AR (1) model)

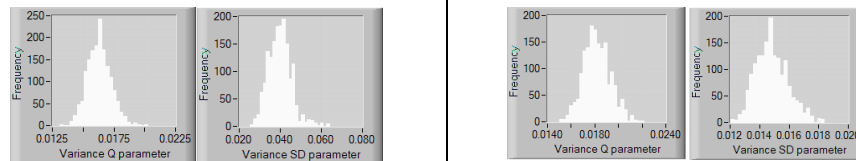
Single response calibration

Multi-response calibration

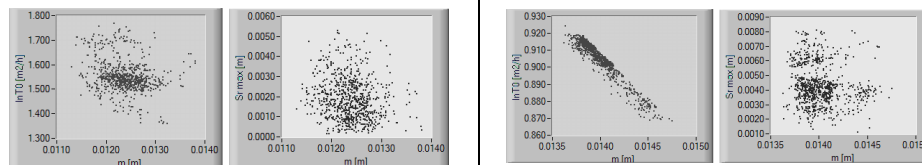
Hydrological parameters posterior distribution



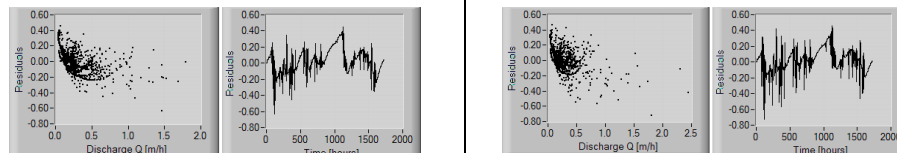
Statistical parameters posterior distribution



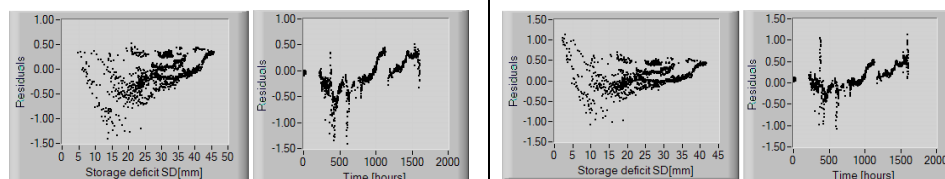
Hydrological parameters - response surfaces



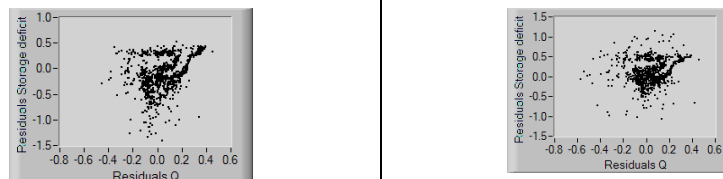
Diagnostic plots – Discharge response



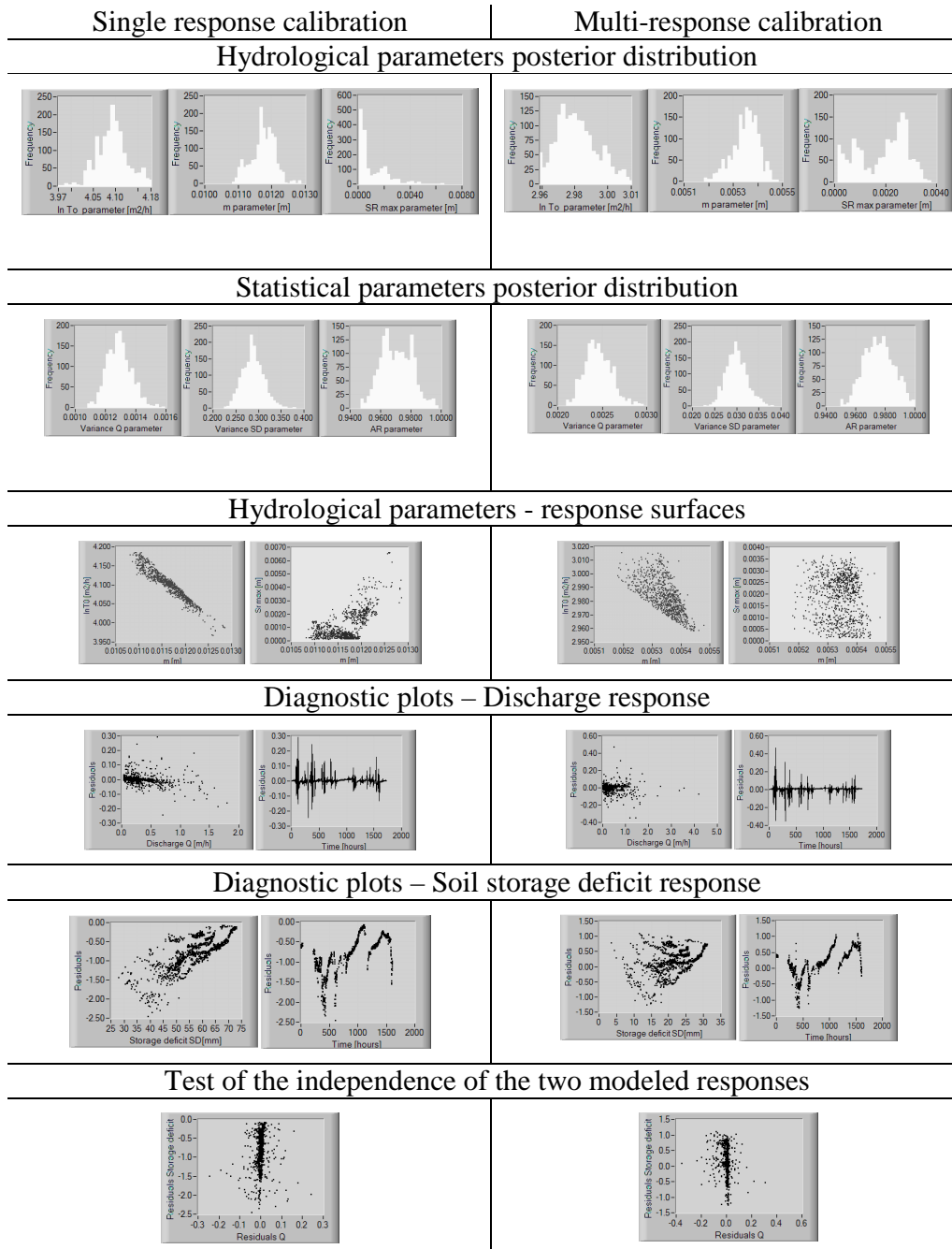
Diagnostic plots – Soil storage deficit response



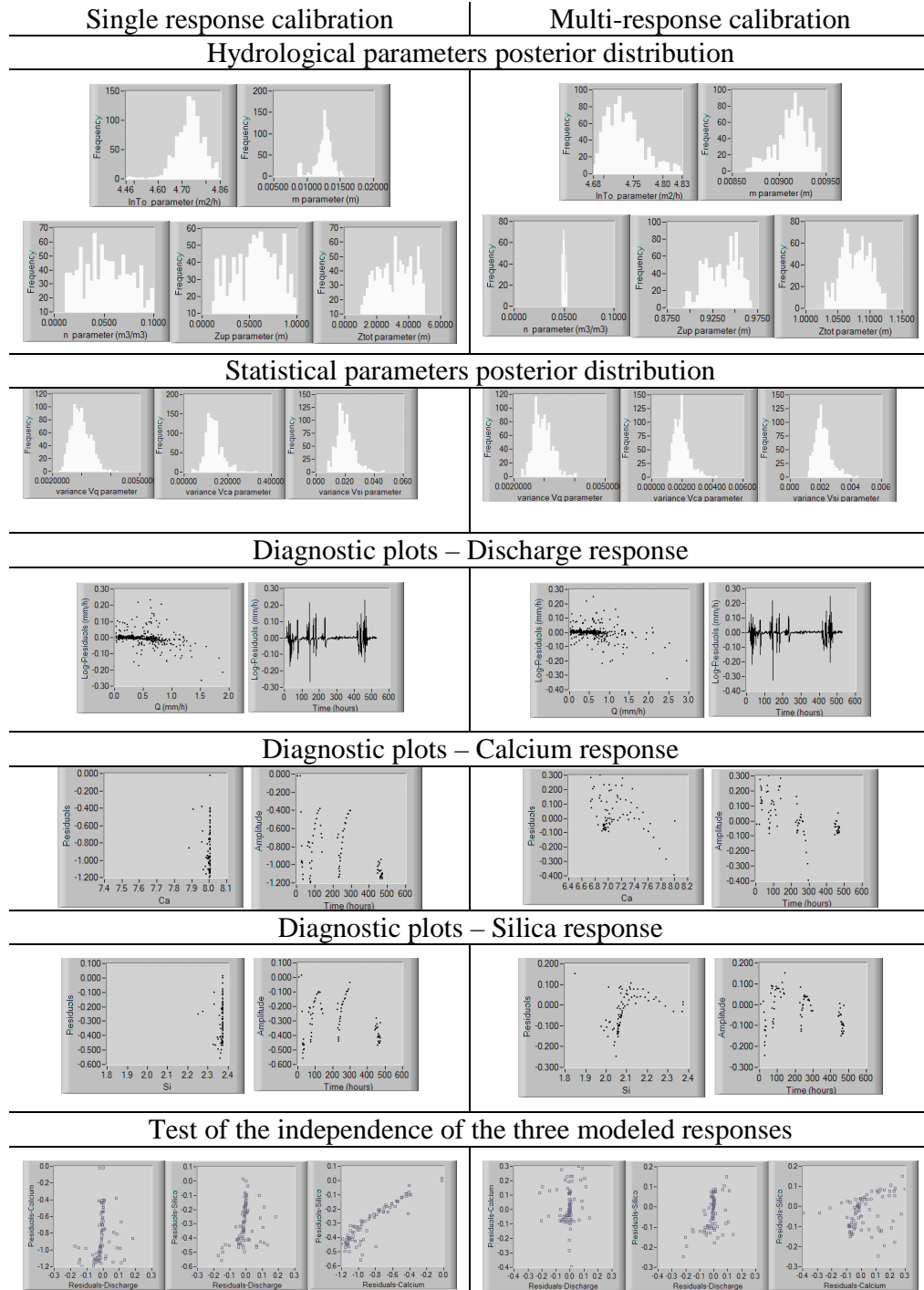
Test of the independence of the two modeled responses



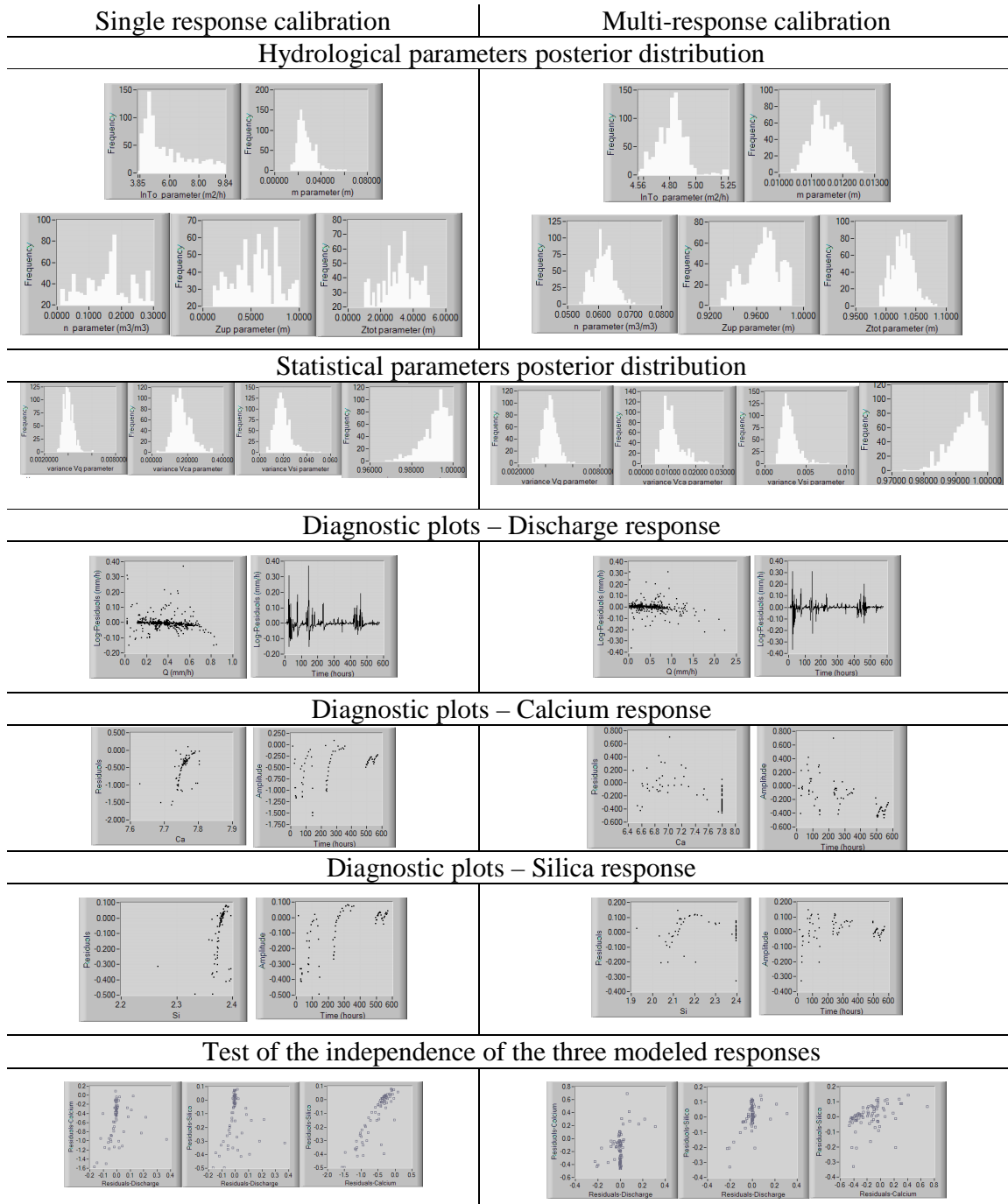
MCMC methodology with L3 likelihood function (with statistical corrections)



Ruzillon catchment: Single and 3-response calibrating methodology with L3 statistical function



Esserts catchment: Single and 3-response calibrating methodology with L3 statistical function



Daniela Balin
Ch. Des Pyramides, 1007, Lausanne
Tel. 021 /625 89 62
E-mail: daniela.talamba@epfl.ch

15 mars 1970
Romanian, married



Professional experience

- Hydrology and Land Improvement Institute, EPFL, Switzerland since 2000
 - assistant
 - GESREAU Vaud Canton project / implementation of a methodology of flood estimation for small catchments
 - WRINCLE European Project: climatic changes impact on the hydrologic regime / parameters regionalization of a rainfall-runoff model
 - ESPACE FNS Project / study of the hydrological behaviour through experimental and modelling approaches
- Geography Faculty, Iasi University, Romania 1996-1998
 - assistant
 - development of the « History of material civilizations » course and corresponding seminars (in French)
 - coordination of practical works in hydrology and geomorphology
- College « C.Negruzzi », Iasi, Romania 1993-1996
 - teacher
 - teaching in geography

Education

- PhD Thesis, HYDRAM Laboratory, EPFL, Lausanne, Switzerland 2001-2004
- Postgraduate certificate in hydrology, EPFL, Lausanne, Switzerland 1999
- Licence in geography (physical geography and French), Romania 1993
- Bachelor in mathematic-physics, Romania 1988

Languages

Romanian – mother tongue

French – fluent (read, spoken, written)

English – TOEFL certificate (1998), good (read, written, spoken)

German – average level (read, written, spoken)

Informatics

Microsoft Word, Excel, Power Point, S-Plus, SIG (MapInfo), LABVIEW, professional computers (CODEAU), web design (Macromedia - Dreamweaver)

Leisure

Walking, ride, ski

Volunteer in the ski camp for foreign students in Engelberg, Switzerland

Publications

Peer reviewed

Talamba D., Joerin C., Musy A., Balin I., 2000. *Study of the subsurface flow using environmental and artificial tracers: the Haute-Mentue case, Switzerland*, in “Tracers and Modelling in Hydrogeology”, IAHS Publication, No. 262, pages 559-564.

Niggli M., Talamba D., Hingray B., Musy A., 2001. Estimation des debits de pointe pour des bassins versants non jaugés: Application à la Suisse Occidentale, Wasser, Energie, Luft. No. 9-10

Talamba D., Joerin C., Musy A., Balin I., 2003., *Monitoring and statistical modelling of the surface and subsurface flow at different scales*, in “Monitoring and modelling catchment water quality and quantity”, IHP-VI, Technical Documents in Hydrology, No.66, pg.97-103, UNESCO, Paris

Balin Talamba, D., Joerin C., Higy C., Musy A., 2003. *Use of environmental tracing to constrain a rainfall-runoff model. Application to the Haute-Mentue catchment*. Journal of Hydrology and Hydromechanics, 51, No 3, pg.187-195

Joerin C., Beven K.J., Musy A., Balin Talamba D., Accepted, *Study of hydrological processes by the combination of environmental tracing and hillslope measurements: application on the Haute-Mentue catchment*. Hydrological Processes.

Other

Talamba D., Higy C., Musy A., 2001. *A new methodology to study runoff generation mechanisms at different scales using physically based models*. Geophysical Research Abstracts, Vol. 3

Niggli M., Talamba D., Hingray B., Musy A., 2001. *Regionalization of annual flood - a methodology of combination of different methods*. Geophysical Research Abstracts, Vol. 3

Balin Talamba D., Higy C., Joerin C., Musy A., 2002. *Hydrological modelling and sensitivity analysis using TOPMODEL and simulated annealing techniques. Application to the Haute-Mentue catchment*. Geophysical Research Abstracts, Vol.4

Niggli M., Talamba D., Hingray B., Musy A., *Regionalization of Annual Floods – An Adaptive Method to Errors and Data Uncertainties (AMED)*. International Conference on Flood Estimation, Proceedings, 499-406, Bern.

Participation to international conferences

- ⇒ 5-èmes Rencontres Hydrologiques Franco-Roumaines, Lyon, France, September 1999, oral presentation: « *Traitement des données hydro-pluviométriques en vue de l'analyse des processus hydrologiques sur le bassin de la Haute-Mentue* »
- ⇒ International Conference on Tracers and modelling in Hydrogeology, Liège, Belgium, May 2000, poster presentation: “*Study of the subsurface flow using environmental and artificial tracers: the Haute-Mentue case, Switzerland*”
- ⇒ International Conference on Monitoring and Modelling catchment water quality and quantity, Ghent, Belgium, September 2000, oral presentation: “*Monitoring and statistical modelling of the surface and subsurface flow at different scales*”
- ⇒ European Geophysical Assembly held in Nice, France, March 2001,
 - oral presentation: “*A new methodology to study runoff generation mechanisms at different scales using physically based models*”
 - oral presentation: “*Regionalization of annual flood - a methodology of combination of different methods*”
- ⇒ European Geophysical Assembly, Nice, France, April 2002, oral presentation: “*Hydrological modelling and sensitivity analysis using TOPMODEL and Simulated Annealing techniques. Application to the Haute-Mentue catchment*”
- ⇒ International Conference on Elementary Representative Basins (ERB), “Interdisciplinary Approaches in Small Catchment Hydrology Monitoring and Research” held at Liptovski Mikulas in Slovakia, September 2002, oral presentation: “*Use of environmental tracing to constrain a rainfall-runoff model. Application to the Haute-Mentue catchment*”

